Nonlinear study of a one-dimensional structure under loading

Marwan Hariz

DOCTORAT BRETAGNE LOIRE / MATHSTIC

UNIVERSITÉ DE RENNES 1

THÈSE DE DOCTORAT DE

L'UNIVERSITÉ DE RENNES 1

ÉCOLE DOCTORALE N° 601
Mathématiques et Sciences et Technologies de l'Information et de la Communication
Spécialité : *Mathématiques et leurs interactions*

Par
Marwan HARIZ

Étude non-linéaire d'une structure unidimensionnelle sous chargement

Thèse présentée et soutenue à Rennes, le 06 Décembre 2021
Unité de recherche : IRMAR, UMR CNRS 6625 Institut de Recherche Mathématique de Rennes

Rapporteurs avant soutenance :

Sébastien NEUKIRCH	Directeur de recherche CNRS, Université Pierre et Marie Curie
Francesco DELL'ISOLA	Full Professor, Università degli Studi dell'Aquila

Composition du Jury :

Président :	Noël CHALLAMEL	Professeur des universités, Université Bretagne Sud
Examinateurs :	Nicolas BIDEAU	Maître de conférences, Université de Rennes 2
	Christelle COMBESCURE	Maître de conférences, Écoles de saint Cyr Coëtquidan
	Francesco DELL'ISOLA	Full Professor, Università degli Studi dell'Aquila
	Sébastien NEUKIRCH	Directeur de recherche CNRS, Université Pierre et Marie Curie
Dir. de thèse :	Loïc LE MARREC	Maître de conférences, Université de Rennes 1
Co-dir. de thèse :	Jean LERBET	Professeur Des Universités, Université d'Evry-Val d'Essonne

Acknowledgement

During the past three years I have received a great deal of support and assistance.

I would first like to thank my supervisors, Professor Loïc Le Marrec and Professor Jean Lerbet, whose expertise was invaluable in formulating the research questions and methodology. Your insightful feedback pushed me to sharpen my thinking and brought my work to a higher level.

Also, I would especially like to show my deepest thanks for Lalaonirina Rakotomanana and Guy Casale for sharing their enormous experiences, valuable comments and suggestions. I am really grateful for their precious advice and help.

I am also grateful to the members of the jury who were more than generous with their expertise and precious time. A special thanks to Prof. Sébastien Neukirch and Prof. Francesco dell'Isola for their countless hours of reflecting, reading, and most of all patience throughout the entire process. Thank you Dr. Christelle Combescure, Dr. Nicolas Bideau and Prof. Noël Challamel for agreeing to invest time for reading this work and providing interesting and constructive feedback which was much appreciated.

To the member of thesis committee, Françoise Dal'Bo and François Maucourant, thank you for your time and support.

I want to express my heartfelt gratitude to the funding received towards my PhD from Henri Lebesgue Center, IRMAR and Université de Rennes 1. I am also grateful to the funding received through the Walid Joumblatt Foundation For University Studies to undertake my PhD.

I would like to thank all the secretaries of the IRMAR and Université de Rennes 1, especially Marie-Aude Verger for her kindness, her availability, and her efficiency to solve my problems.

I would also like to thank all my tutors for their valuable guidance throughout my studies. You provided me with the tools that I needed to choose the right direction and successfully complete my dissertation.

I gratefully acknowledge the effort of Larry Page and Sergey Brin and all Google employees who facilitated my research and my life.

I could not have completed this dissertation without the support of my friends, who provided stimulating discussions as well as happy distractions to rest my mind outside of my research.

In addition, I would like to thank my parents for their wise counsel and sympathetic ear. You are always there for me and I am who I am today thanks to you.

Finally, my dearest thoughts go to my lovely partner Farah who has accompanied and supported me these last years and with whom I share pleasant moments. I am beyond lucky to have you in my life.

Abstract

In this thesis, we discuss an elastic, isotropic and homogeneous straight Timoshenko beam with linear constitutive laws subjected to external forces and moments, and surrounded eventually by foundations.

On one hand, we are interested in analyzing the effect of Winkler foundation on a Timoshenko beam. We show the influence of wall rigidity in a dynamical way where modal analyses are conducted for a rigid wall and dispersion relations are discussed for an elastic wall. Furthermore, we expose buckling solutions of a plane, quasi-static Timoshenko beam with small transformation subjected to a longitudinal force and surrounded by an elastic wall modeled by two-parameter Winkler foundation. A non-dimensional analysis of associated Haringx and Engesser model is performed where buckling stress and shape are exposed analytically. Relations for rigidity of the wall and buckling solutions are made for different regimes and for both models using an asymptotic approach. Introducing the yield limit gives a simple criterion in terms of stiffness foundation and slenderness ratio for which buckling or irreversible transformation occurs. A more detailed study of plasticity behaviour could improve our approach.

On the other hand, we expose solutions of a quasi-static but large transformation of a Timoshenko beam. We offer analytical post-buckling solutions for different regimes driven explicitly by two invariants of the problem. Firstly, we establish the planar problem for which a Cauchy initial value problem was found, where load (force and moment) is prescribed at one end and kinematics (translation, rotation) at the other. With such formalism, solutions are explicit for any load and existence, uniqueness and regularity of the solution are detailed. Therefore, analytical post-buckling solutions are found with different regimes. This approach presents how these solutions of a Cauchy initial value problem may help tackle (i) boundary problems, where physical quantities (of load, position or section orientation) are prescribed at both ends and (ii) problems of quasi-static instabilities. In particular, several problems of bifurcation are explicitly formulated in case of buckling or catastrophe. A more detailed study of energy function property and a dynamic approach could ameliorate our understanding of planar elastic beam.

In the non-planar case, we impose moment only at the boundary, this approach converts a Timoshenko beam into a Kirchhoff rod. Invariants in this case are moments and energy per unit length. These invariants dictate the existence of the solutions and impose four regimes depending on the thickness of the cross-section. Explicit solutions are given in terms of Jacobian elliptic functions. Rod shapes are given for different cases and a detailed approach for the influence of each control parameter was introduced. We apply this approach to present the equilibrium of the Möbius strip and the Torus knots. Our study can be further extended to investigate DNA shapes and chromatin condensation.

RÉSUMÉ

Les poutres sont des structures elancées qui résistent aux charges longitudinales, aux forces de cisaillement, aux moments de flexion et torsion.
L'histoire de l'étude d'une poutre remonte au XVe siècle. En 1493, Leonardo da Vinci a présenté une poutre soumise à une charge à l'extrémité. Plus tard, Galileo Galilei a essayé d'améliorer le travail de Léonard de Vinci dans sa célèbre publication "Discorsi e dimostrazioni matematiche" en 1638.
Cependant, la première théorie complète de la poutre, connue sous le nom de poutre d'Euler-Bernoulli, a été développée par Leonhard Euler et Daniel Bernoulli au XVIIIe siècle. Cette poutre est soumise à une contrainte cinématique: les sections restent planes et perpendiculaires à l'axe neutre après déformation. Pour généraliser la poutre d'Euler-Bernoulli, Timoshenko a assoupli cette contrainte en ajoutant l'effet du cisaillement.
Nous discutons dans cette thèse d'une poutre de Timoshenko élastique, isotrope, homogène et droite avec des lois de comportements linéaires, soumise à des forces et moments extérieurs et entourée éventuellement par des fondations.

Cinématique d'une poutre

Notre approche est basée sur la théorie de Timoshenko suivant le point de vue de Cosserat. La poutre est constituée d'une courbe qui définie l'ensemble des centres de masse de la section, appelée fibre moyenne $\mathcal{C}$, telle que, à chacun de ses points est liée une base vectorielle orthonormale $(\mathbf{d_1}, \mathbf{d_2}, \mathbf{d_3})$ nommée base de directeurs de la poutre. Par convention, $(\mathbf{d_1}, \mathbf{d_2})$ sont liées à la section de la poutre et $\mathbf{d_3}$ est normale à la section. La position de tout point M de la poutre dans la courbe déformée est définie par:

$$(\xi_1, \xi_2, S, t) \longrightarrow \mathbf{OM}(S,t) = \boldsymbol{\varphi}(S,t) + \sum_{\alpha=1}^{2} \xi_\alpha \mathbf{d}_\alpha(S,t). \tag{1}$$

A chaque instant t, il existe un tenseur de rotation $\mathbf{R}(S,t)$, qui relie la base initiale $(\mathbf{e_1}, \mathbf{e_2}, \mathbf{e_3})$ avec la base déformée: $\mathbf{d_i} = \mathbf{R}(S,t)\mathbf{e_i}$. Ainsi la courbure et la vitesse de rotation des directeurs sont définies par:

$$\frac{\partial \mathbf{d_i}}{\partial S} = \boldsymbol{\kappa} \times \mathbf{d_i}, \qquad \boldsymbol{\kappa} = \text{vect}(\frac{\partial \mathbf{R}}{\partial S}\mathbf{R}^T); \qquad \frac{\partial \mathbf{d_i}}{\partial t} = \boldsymbol{\omega} \times \mathbf{d_i}, \qquad \boldsymbol{\omega} = \text{vect}(\frac{\partial \mathbf{R}}{\partial t}\mathbf{R}^T). \tag{2}$$

La déformation de la poutre est présentée par le tenseur de Green-Lagrange:

$$\mathbf{E} = \sum_{i=1}^{3} \Big((\widetilde{\boldsymbol{\varepsilon}} + \boldsymbol{\kappa} \times \mathbf{GM}) \cdot \mathbf{d_i} \Big) \frac{\mathbf{e_i} \otimes \mathbf{e}_3 + \mathbf{e}_3 \otimes \mathbf{e_i}}{2} + \frac{1}{2} \left\| \widetilde{\boldsymbol{\varepsilon}} + \boldsymbol{\kappa} \times \mathbf{GM} \right\|^2 \mathbf{e}_3 \otimes \mathbf{e}_3. \tag{3}$$

Ainsi la déformation est entièrement déterminée par $\boldsymbol{\varepsilon} = \dfrac{\partial \boldsymbol{\varphi}}{\partial S}$ et $\boldsymbol{\kappa}$.

Equations dynamiques des poutres

En appliquant le principe de travail virtuel, on obtient les équations d'équilibres:

$$\frac{\partial \mathbf{N}}{\partial S} + \mathbf{q} = \rho_0 A \, \frac{\partial^2 \boldsymbol{\varphi}}{\partial t^2}, \qquad \frac{\partial \mathbf{M}}{\partial S} + \frac{\partial \boldsymbol{\varphi}}{\partial S} \times \mathbf{N} + \mathbf{m} = \rho_0 \frac{\partial (\mathbb{I}\,\boldsymbol{\omega})}{\partial t}. \tag{4}$$

Où $\mathbf{N}$ et $\mathbf{M}$ sont les forces et moments internes, $\mathbf{q}$ et $\mathbf{m}$ sont la densité linéique de force extérieure et le couple linéique, respectivement.

Energie, forces et moments

On applique le modèle d'hyperélasticité de Saint Venant-Kirchhoff où l'énergie linéique est définie d'une manière adimensionelle par:

$$\Psi = \frac{1}{2}\Big(\varepsilon_1^2 + \varepsilon_2^2 + g(\varepsilon_3 - 1)^2 + \frac{eg}{1+e}\kappa_1^2 + \frac{g}{1+e}\kappa_2^2 + \kappa_3^2\Big). \tag{5}$$

Où g précise le matériel de la poutre et e dépend de la géométrie de la section. Par conséquent:

$$\begin{array}{lll} N_1 = \varepsilon_1, \quad N_2 = \varepsilon_2, & & \text{forces de cisaillement.} \\ N_3 = \varepsilon_3 - 1, & & \text{force normale.} \\ M_1 = \dfrac{eg}{1+e}\kappa_1, \quad M_2 = \dfrac{g}{1+e}\kappa_2, & & \text{moments de flexion.} \\ M_3 = \kappa_3, & & \text{moment de torsion.} \end{array} \tag{6}$$

Poutre plane

Dans le cas des poutres planes, la dynamique est donnée par:

$$\begin{aligned} \varepsilon_1' + g(\varepsilon_3 - 1)\kappa_2 + q_1 &= \ddot{\varphi}_1 + 2\dot{\varphi}_3\dot{\theta}_2 - \varphi_1\dot{\theta}^2 + \varphi_3\ddot{\theta}, \\ g\varepsilon_3' - \varepsilon_1\kappa_2 + q_3 &= \ddot{\varphi}_3 - 2\dot{\varphi}_1\dot{\theta} - \varphi_3\dot{\theta}^2 - \varphi_1\ddot{\theta}, \\ g\kappa_2' + \varepsilon_1\varepsilon_3 - g\varepsilon_1(\varepsilon_3 - 1) + m_2 &= \ddot{\theta}. \end{aligned} \tag{7}$$

Poutre Timoshenko et fondation de Winkler

Nous nous intéressons dans cette partie à l'analyse de l'effet des fondations de Winkler qui exercent une contrainte transversale sur une poutre plane de Timoshenko. Donc on se restreint à l'hypothèse de petite perturbation où les déformations sont données par:

$$\varepsilon_1 = u_1' - \theta, \qquad \varepsilon_3 = u_3', \qquad \kappa = \theta'.$$

Avec $\mathbf{u} = u_1\mathbf{d_1} + u_3\mathbf{d_3}$ est le déplacement de la poutre.
Dans le cas d'un mur rigide; on a $\mathbf{u} = 0, q_3 = m_2 = 0$ et $q_1 = \theta'$, alors, En imposant des conditions initiales de type Dirac (choc ponctuel à une extremité), on obtient:

$$\theta(s,t) = 2\Omega_0 \sum_n \frac{(-1)^n}{\omega_n} \sin(k_n s) \sin(\omega_n t). \tag{8}$$

Les variables dynamiques sont garanties en utilisant (6).
Ensuite, nous nous intéressons au flambage d'une poutre entourée d'une fondation de Winkler à deux paramètres. Plus précisement, nous imposons une force longitudinale qui aboutit à réécrire l'équilibre statique sous la forme de l'équilibre de Haringx:

$$u'' - g\kappa_1 u - (1+g\epsilon)\theta' = 0, \qquad g\theta'' + (1+g\epsilon)u' - (1+g\epsilon+g\kappa_2)\theta = 0. \tag{9}$$

Un autre modèle largement utilisé pour le flambement est proposé par Engesser pour lequel les relations d'équilibre sont :

$$(1-g\epsilon)u'' - g\kappa_1 u - \theta' = 0, \qquad g\theta'' + u' - (1+g\kappa_2)\theta = 0. \tag{10}$$

Pour les deux modèles, l'analyse de flambement est effectuée en étudiant, d'une manière analytique, la relation entre la charge critique de flambement et le nombre d'onde des modes de flambement, en fonction des paramètres de la fondation. De plus, l'introduction de la limite d'élasticité du matériel de la poutre nous conduit à conclure que dans le régime de flambage, les modèles d'Engesser et de Haringx convergent vers la même estimation de la contrainte critique de flambage, où les modes de flambage ont sensiblement le même comportement.

Analyse explicite de la grande transformation d'une poutre de Timoshenko

Dans cette partie, nous analysons la transformation post-flambée d'une poutre plane de Timoshenko soumise à des charges et des moments externes avec $\mathbf{q} = \mathbf{m} = 0$. En étudiant l'équilibre statique de (4), nous remarquons que $\mathbf{N}(s)$ est uniforme tout au long de la section, mais l'orientation de la section n'est pas fixe. Cela nous motive à introduire l'angle $\phi(s)$. Ensuite, les déformations peuvent être écrites en termes de ϕ:

$$\varepsilon_1(s) = N_\ell \sin(\phi(s)), \qquad \varepsilon_3(s) = 1 + \frac{N_\ell}{g}\cos(\phi(s)), \qquad \kappa_2(s) = -\phi'(s). \tag{11}$$

En conséquent, l'équilibre statique (7) est donné par:

$$(g\phi')^2 + 2gN_\ell\cos(\phi) - (g-1)N_\ell^2\cos^2(\phi) = M_\ell^2 + 2gN_\ell\cos(\phi_\ell) - (g-1)N_\ell^2\cos^2(\phi_\ell). \tag{12}$$

Cet équilibre n'est qu'un problème de Cauchy dependant de conditions initiales en $(N_\ell, \phi_\ell, M_\ell)$.
La solution de l'équation (12) est donnée sous forme de fonctions de Jacobi.
Vu que notre approache aboutit à des équations exactes, nous examinons le comportement d'une

poutre soumise à une force suiveuse. Un rapport de taille indépendant du matériel et des propriétés géométriques de la poutre est obtenu.
Pour le contrôle cinématique d'une poutre supportant une charge morte, le phénomène de catastrophe est observé d'une manière directe et explicite.

Comportement d'une tige de Kirchhoff chargée par un moment pur

Dans cette partie, une analyse quasi-statique d'une poutre de Timoshenko soumise à un moment à l'éxtremité est présenté. Plus précisement, en regardant l'équilibre statique (4), on constate que $\mathbf{N}$ est une constante qui depend de la force exercée à l'extremité. on peut donc supposer que cette force est nulle c'est à dire le comportement de cette poutre est contrôlée uniquement par un moment. Dans cette condition une poutre est exactement une tige de Kirchhoff où l'equilibre vectoriel est donné par $\mathbf{M}' = 0$. Ceci aboutit après projection:

$$r_1\,\kappa_1'(s) - (r_2 - 1)\,\kappa_2(s)\kappa_3(s) = 0, \quad r_2\,\kappa_2'(s) + (r_1 - 1)\,\kappa_1(s)\kappa_3(s) = 0, \quad \kappa_3'(s) + (r_2 - r_1)\,\kappa_1(s)\kappa_2(s) = 0. \tag{13}$$

Avec $r_1 = \dfrac{eg}{1+e}$ et $r_2 = \dfrac{g}{1+e}$. On remarque que (13) dépend du matériel g et essentiellement de la forme des sections e.
De cet équilibre on déduit les deux invariants le moment M et l'énergie linéique Ψ:

$$M^2 = M_1^2 + M_2^2 + M_3^2, \qquad \Psi = \frac{1}{2}\Big(\frac{M_1^2}{r_1} + \frac{M_2^2}{r_2} + M_3^2\Big). \tag{14}$$

Dans l'espace de configuration (M_1, M_2, M_3), ces deux invariants correspondent à une sphère et une ellipsoïde. Donc leurs intersections donnent une condition nécessaire de l'existence des solutions de (13). D'où l'existence de 4 régimes differents qui dépendent de e. De plus, les solutions exactes de (13) sont sous la forme de $\kappa_i = \overline{\kappa_i} pq\Big(\lambda(s+s_0), m\Big)$, où, pq est une fonction de Jacobi et $\overline{\kappa_i}, \lambda, s_0, m$ dépendent de $\mu := \sqrt{2\psi}$ et $\eta = M/\mu$. En conclusion, la déformation de la tige est contrôlée par un paramètre géométrique et un autre matériel. Elle est aussi contrôlée par μ, le paramètre d'échelle qui contrôle la taille du motif et par η qui décrit la forme du motif. Ces résultats peuvent être appliqués pour étudier les noeuds toriques et les rubans de Möbius.

Conclusion et perspectives

Nous discutons dans cette thèse une poutre de Timoshenko soumise à des forces et moments extérieurs et entourée éventuellement par des fondations. Plus précisément, nous nous intéressons d'une part à l'analyse de l'effet des fondations de Winkler sur une poutre de Timoshenko où une relation entre la rigidité de la paroi et les solutions de flambement a été établi. Une étude plus détaillée du comportement de plasticité pourrait élargir notre analyse.
D'autre part, nous exposons les solutions quasi-statiques d'une poutre de Timoshenko en grande déformation. Dans le cas d'une poutre plane, nous discutons le problème de Cauchy et de bifurcation. L'instabilité dynamique est l'une des questions intéressantes qui peut être potentiellement abordée en étendant le présent travail. Dans le cas non-plan, nous présentons explicitiment les solutions du problème ainsi que l'équilibre des noeuds toriques et de ruban de Möbius.

List of publications and conferences

International journals

Hariz, M., Le Marrec, L. & Lerbet, J. Explicit analysis of large transformation of a Timoshenko beam: post-buckling solution, bifurcation, and catastrophes. **Acta Mech** (*2021*). https://doi.org/10.1007/s00707-021-02993-8

Hariz, M., Le Marrec, L. & Lerbet, J. Buckling of Timoshenko beam under two-parameters Winkler foundations. **submitted in** 'International Journal of Solids and Structures' (*2021*).

Hariz, M., Le Marrec, L. & Lerbet, J. Behaviour of a Kirchhoff rod loaded by a pure moment. Under submission.

Proceedings

Hariz, M., Le Marrec, L., Lerbet, J. & Casale, G. Timoshenko beam under Winkler foundation. **CFM** (*2019*). https://cfm2019.sciencesconf.org/254870/document

International conference

Hariz M. Non-linear pre and post buckling behaviour of a Timoshenko beam, 25^{th} International Congress of Theoretical and Applied Mechanics (*2021*).

National conferences

Hariz M. Behaviour of a Kirchhoff rod loaded by a pure moment, Congrès des Jeunes Chercheurs en Mécanique - Méca-J (*2021*).

Hariz M. Bending of Timoshenko beam and its applications, Rencontre GDR-GDM, La Rochelle (*2021*).

Hariz M. Explicit Analysis of Large Transformation of a Timoshenko Beam, From PhD to PhD: A Conference Mapping the Network of Lebanese Mathematics (*2021*).

Hariz M. Explicit analysis of catastrophe on a Timoshenko beam, Rencontre du Non-Linéaire, Géométrie et Elasticité (*2021*).

Hariz M. Analytical solutions of plane Timoshenko beam under large transformation, Rencontre GDR-GDM, Paris (*2020*).

Hariz M. Timoshenko beam under Winkler foundation, Congrès Français de Mécanique, Brest (*2019*).

Internal seminar

Hariz M. Comportement d'une tige de Kirchhoff chargée par un moment pur, séminaire Landau,IRMAR, Rennes (*2021*) .

Table of Contents

INTRODUCTION

Logic is the foundation of the certainty of all the knowledge we acquire

Leonhard Euler

Beam theories

Beams are slender structures resisting to vertical loads, shear forces, bending moments and torsion and are widely used in civil, mechanical, aerospace engineering.
Many scientists aimed to study beam behaviour, including Leonardo da Vinci who, in 1493, introduced a beam subjected to end load. Later on, Galileo Galilei tried to enhance da Vinci's work in his famous publication "Discorsi e dimostrazioni matematiche" in 1638. However, the first complete beam theory known as Euler-Bernoulli beam was developed by Leonhard Euler and Daniel Bernoulli in the Eighteenth-Century [Eul51]. This theory introduced an equation that gives the relationship between deflection of the beam and the applied load:

$$EI\frac{d^4u}{dS^4} = q(S). \tag{15}$$

The curve $u(S)$ describes the deflection of the beam in the z direction. q is a distributed load, E is the Young modulus and I is the second moment of area of beam cross-section. This model uses *kinematical hypotheses*: cross-section remaining normal to the center-line and sometimes inextensibility of the center-line as seen in figure (1).
This theory led to vast sort of applications specifically in construction of the Eiffel Tower and

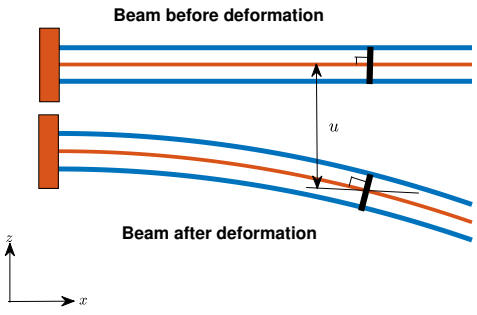

Figure 1 – *Deformation of Euler Bernoulli beam.*

Ferris Wheel. It also provides reasonable approximations for many problems especially for slender

structure. However, it overestimates the natural frequencies and kinematical hypotheses are not easily justified under such transformations. Additional Lagrange multipliers may increase the difficulty to formulate the non-linear problem [Del+16].
In order to correct the overestimation of natural frequencies in Euler-Bernoulli beam, Rayleigh provided his own beam theory and implicated the effect of rotary inertia [CY62]. Attempting to improve upon the Euler-Bernoulli model, a shear distortion was added [PB82].
Later on, Timoshenko relaxed the *kinematical hypotheses* by adding the effect of shear and rotation to the Euler-Bernoulli beam given by a shear angle $\gamma = \frac{du}{dS} - \theta$ [Tim21]. This idea is illustrated in figure (2) where we can remark that without shear ($\gamma = 0$) we retrieve exactly the Euler Bernoulli model. Timoshenko also introduced stress-strain relations for all degrees of freedom [Tim22; TG09].

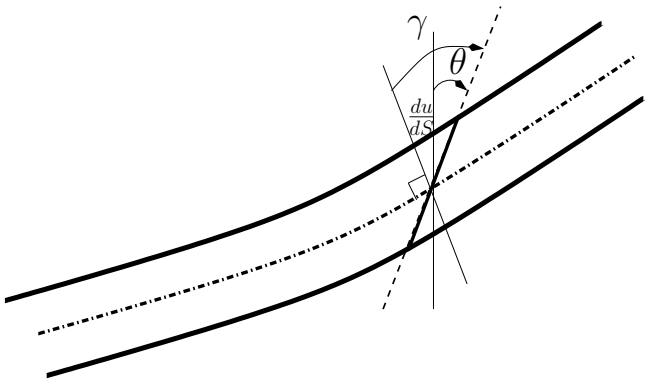

Figure 2 – *Deformation of a Timoshenko beam. The normal rotates by an amount* $\theta \neq \frac{du}{dS}$.

In the linear case, the Timoshenko model allows the consideration of shorter beam and less-standard material [Eli20]. Moreover it provides an adapted formulation for large transformation where non-linear coupling between several strains intervenes.
The governing equation of this model is given by:

$$EI\frac{d^4u}{dS^4} = q(S) - \frac{EI}{AG}\frac{d^2q}{dS^2}. \tag{16}$$

It is clear that an additional term was added to Euler's equation (1). This term represents the shear effect with G as a shear modulus that includes a shear correction factor and A as the cross section area.

Buckling

Several studies where conducted regarding these beam theories. Among others, a significant study, is the deflection of a beam caused by a longitudinal compressive external load. Many scientists investigated deflections on a beam, specifically the sudden change in shape of a structural component under load known as beam buckling analysis. One can search the critical load needed for sudden large deformation of structure known as buckling load, where this load is influenced by

the material and geometrical beam form.
One of the first attempt to study buckling was made by Euler, who considered a pin-ended column loaded by an axial load P [Eul44], bending moment in this case is given by $M = -Pu$ and the differential equation of bending is given by $M = EI\dfrac{d^2\,u}{d\,S^2}$, so, an ordinary linear differantial equation was obtained

$$\frac{d^2\,u}{d\,S^2} + k^2 u = 0, \qquad \text{with} \qquad k^2 = \frac{P}{EI}.$$

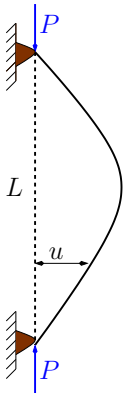

Figure 3 – *Euler column submitted to axial load.*

For pin-ended beam (fig.(3)), boundary conditions are given by $u(0) = u(L) = 0$, therefore, the critical loads for nonzero deflection is given by $P_{crn} = (\dfrac{n\pi}{L})^2 EI$, the lowest critical load is given for $n = 1$ and it is called the Euler load:

$$P_E = \frac{\pi^2}{L^2} EI. \tag{17}$$

A while after, scientists aimed to generalize Euler load for a "non Euler-Bernoulli beam". J.A Haringx proposed a theory for helical springs [Har42] in which he explained the fact that springs of small slenderness do not buckle. Whereas, F. Engesser proposed another theory that consider the influence of shear on the buckling loads of straight bars [Eng91]. These two theories differ regarding how the normal and shear forces are defined with respect to the non-deformed or deformed cross section. In Haringx's approach, the normal force is chosen normal to the deformed cross section in the state after loading, whereas in Engesser's theory, the normal force is chosen parallel to the beam axis in the loaded state.
During the last decades, many researchers investigated beam behaviour and its relation in micro-structure, some of them supported the Engesser approach while others adapted Haringx strategy. So far, no accord has yet been reached.
Nanni [VN71] studied the effect of shear forces on the buckling load of simply supported members with narrow rectangular cross section and of elliptic cross section and concluded that Engesser's approach was superior. While Reissner [Rei72] computed one-dimensional large strain beam theory for plane beams and noticed that Haringx theory provided better agreement. Ziegler [Zie82] for-

mulated a one-dimensional formulation for bars, and concluded that Engesser approach is superior to Haringx's for columns and can still be improved if axial shortening is taken into account, while Haringx's is more appropriate for helical springs. These conclusions were, shortly afterwards, refused by Reissner [Rei58], who again supported Haringx's formulation, finding that both theories can be obtained by different forms of the one-dimensional stress-strain relations. Then, Bažant derived Engesser formula from the theoretical analysis of the problem [Ced+10] and performed some theoretical considerations on the buckling behaviour of weak-in shear columns. He, despite some correspondence between Engesser and Haringx formulations, concluded that Haringx formula gave better results [Baz03]. He reinforced his idea in [BB04] and invented a finite element studies of homogeneous orthotropic columns using a constant shear modulus for an elastic material in small strain, which corresponds to Engesser-type theory [BB04]. Blaauwendraad [Bla08] agreed with Bažant and advised to avoid the Haringx model in building construction and civil engineering and to rather choose Engesser's hypothesis. These results were rebutted by Aristizabal [AO07] who studied static and dynamic stability of uniform shear beam-columns under generalized boundary conditions and employed Haringx's model. Allen [All69] studied the buckling behaviour of sandwich structures and derived the Engesser formula while Kardomateas *et al.* [Kar+02] made theoretical predictions and FEM analysis of buckling loads for sandwich columns with metallic laminated facings and foam or honeycomb cores under uniform axial compression, and noticed that Haringx formula was closer to their results.
Attard [Att03] computed an internal strain energy density for isotropic hyperelastic Hookean materials and showed that this formulation leads to a buckling load formula that agrees with Haringx's. Simo and Kelly [SK84] performed a two-dimensional buckling analysis of multilayer elastomeric bearings, and concluded that, as long as the beam theory assumptions hold, their formulation was in closer agreement with the Haringx theory. After a while, Banerjee and Williams [BW94] analyzed shear-deformable uniform columns, derived the Engesser formula and buckling curves for the most common supporting conditions. Coming after, Pedro Dias Simao [Sim17] studied the influence of shear deformations on the buckling of columns using the Generalized Beam Theory (GBT) and energy principles. He deduced that Engesser load agrees much better with the results arising from the GBT analysis. Later, Xiang-Fang Li *et al.*. [LL18] studied the effects of Engesser's and Haringx's hypotheses on buckling of Timoshenko and higher-order shear deformable columns and they concluded that for shorter columns with weak shear rigidity Engesser beam theory gives the lowest estimate of the critical load, and it is more conservative.

Large transformation

For large transformation, an adequate approach is to consider Timoshenko beam as a one-dimensional Cosserat body [CC09]. Following this approach, it is possible to extend the Timoshenko initially linearized theory to large transformations [EH20]. Among others, Mohyeddin and Fereidoon [MF14] offered analytical solutions for the large deflection of a simply supported Timoshenko beam. Li [LL16] investigated a closed problem both analytically and numerically. Accord-

ingly Antman [Ant05] developed non-linear theory of elastic bodies such as strings, rods, beams. Reissner adopted the same formulation to give the principle of virtual work leading to constitutive and equilibrium equations [Rei72]. Following the same approach, Simo examined a numerical formulation of a finite strain beam theory and gave a stress-strain relation [Sim85]. Later on, these results where expanded by Rakotomanana who regarded waves and vibrations of strings, beams and shells [Rak09]. Henceforth, Le Marrec *et al.* gave an exact theory of Timoshenko beam undergoing three-dimensional finite transformation and subjected to dynamical perturbations [LMLR18] .
Stability of the equilibrium solutions is of crucial importance under such large transformations (*e.g.* [Big12]). Buckling of straight beam was extended to ring by Reissner [Rei82]. Bažant and Cedolic investigated the stability of elastic structures using energy methods [Ced+10]. The link with incremental equilibrium equations was investigated in [Baz71] where an example of flexure and shear of a Timoshenko beam was presented. However, energetic approach is not the unique approach. For example the numerical solutions of the extensible Timoshenko beam model under distributed load performed in [Del+19] motivates Corte *et al.* to identify sequences of equilibria among which two at most are stable [DC+19].
In the previous mentioned studies, analytical expression of a solution is not the main objective. In practice such analytical solutions mainly invoque Jacobian elliptic functions. These functions appear as solutions of many important problems in classical mechanics. Mathematical background can be found, among others, in [Mey01; BB12] and fundamental relations are reported in [Olv+10]. Ohtsuki [OHT86] gave analytical and numerical solutions for large deflections of a symmetric three point bending of a simply supported beam subjected to a central concentrated load. Chucheespakul *et al.* [Chu+99] set up Euler-Bernoulli elastica for pinned-pinned beam. Whereas Magnusson *et al.* provided the behaviour of the extensible elastica solution for an Euler-Bernoulli beam [MRL01]. The Timoshenko beam was treated by Humer who adapted Reissner's beam approach and gave buckling and postbuckling solutions for cantilever beam subjected to follower force [Hum13; HP19]. In pursuit, Batista specified analytical solutions of cantilever beam [Bat13; Bat14]. Other boundary conditions were presented in [Bat16a] but no general formulation was presented for general boundary conditions.

Elastic beam on a foundation

Knowing that beam behaviour is also related to what it surrounds, many researchers examined beams supported on elastic foundation and their applications in modern engineering, such as soil foundation, strip foundation, foundation of the buildings as well as such structure of underpass bridges. To describe the interactions of the beam and foundation as most appropriately as possible, scientists have proposed various kinds of foundation models. One of the first attempt to study elastic beam on deformable foundation was made by Emil Winkler in 1867 [Win67]. This model known by Winkler foundation (*e.g* figure (4)) consists of a beam on elastic foundation which assumes linear

force-deflection relationship. Namely,

$$q(S) = K_W u(S). \tag{18}$$

Where K_W is the Winkler spring stiffness. Pasternak [Pas54] generalized the Winkler model and

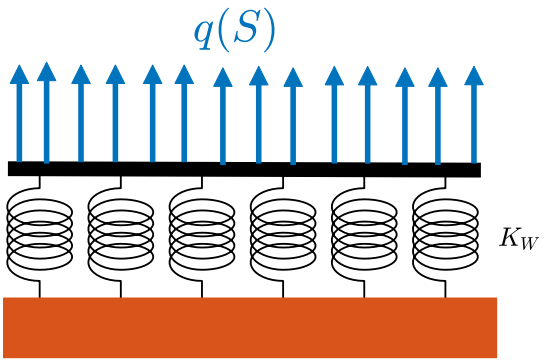

Figure 4 – *Winkler foundation on an elastic beam.*

assumed existence of shear interactions between the spring elements illustrated in figure (5) left with the following relation:

$$q(S) = K_W u(S) - K_P \frac{d^2\, u(S)}{d\, S^2}. \tag{19}$$

With K_P is the shear stiffness of the shear layer . A possible generalization of Pasternak model is Reissner model [Rei58] that has been analyzed by Kerr [Ker64]:

$$q(S) - K_R \frac{d^2\, q(S)}{d\, S^2} = K_W u(S) - K_P \frac{d^2\, u(S)}{d\, S^2}. \tag{20}$$

Where K_R is a function of the two linear elastic spring layers and shear layer. This model is illustrated at the right part of figure (5).

Many results were obtained using these models. As an example, Hetenyi discussed the behaviour of beams on elastic foundation [HH46]. Zhang *et al.*.[ZM05] investigated the secondary bifurcations and tertiary states of a beam resting on nonlinear foundation. In addition, Guo-Ping [XZ09] found a numerical method for critical buckling load for a beam on elastic foundation. In the same spirit, Challamel studied the buckling of elastic beam using Reissner model, and he also investigated the buckling of generic higher-order shear beam with elastic connections using local and nonlocal formulation [CMB10]. Moreover, Rajesh [RS17] examined the free vibration of uniform Timoshenko beams on Pasternak foundation using coupled displacement field method. In the same manner, Rana *et al.* [RH16] investigated the exact solution of post-buckled non linear beam on elastic foundation

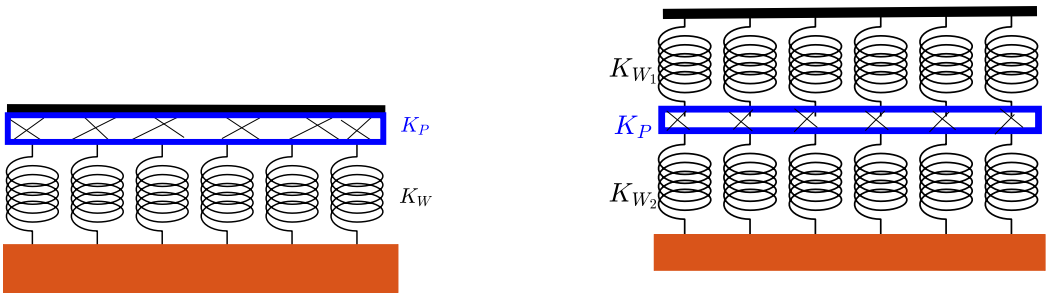

Pasternak foundation. *Reissner foundation.*

Figure 5 – *Elastic foundations.*

and showed that the foundation stiffness is greatly influenced by the buckling force of the beam with an internal hinge. Furthermore, Mercan *et al.* [Akg+16] found a static analysis of beams on elastic foundation by the method of discrete singular convolution.

Manuscript organization

All along the manuscript we will focus on an elastic, isotropic, homogeneous straight Timoshenko beam with linear constitutive laws. In the first chapter, we give some preliminaries that are essential to study beam behaviour. We use the Principle of Virtual Power to establish beam equilibrium under large transformation written in a non-dimensional form. This equilibrium is a first order non-linear partial differential system of equations with respect to strains and a second order with respect to kinematical variables.
The second chapter investigates a planar Timoshenko beam subjected to Winkler foundations. For rigid foundations, exact solutions were obtained using Sturm-Liouville criterion and by imposing an initial choc type condition. This is not the case for elastic foundations where equilibrium is written as a coupled wave equations. In this case, dispersion curves are discussed using harmonic vibrations. To investigate bifurcation, we discuss buckling solutions of a plane, Timoshenko beam with quasi-static small transformation subjected to a longitudinal force and surrounded by an elastic wall modeled by two-parameters Winkler foundation. A non-dimensional analysis of associated Haringx and Engesser model is performed and buckling stress and shape are exposed analytically. Relations for rigidity of the wall and buckling solutions were made for different regime and for both models using asymptotic approach. Introducing the yield limit gives a simple criterion in terms of stiffness foundation and slenderness ratio for which buckling or irreversible transformation occur.
The third chapter describes the plane transformation of straight Timoshenko beam subjected to load at the boundaries. In order to embrace wide applications, the situations for quasi-static follower or dead load are examined and the domain of variation of each dimensionless parameters

is examined. By series of mathematical transformations, we transform the non-linear equilibrium system into a scalar equation seen as a Cauchy initial problem on contrary to most previously conducted studies (based on boundary value problem). This imposes a meticulous analysis (values, variation domain) of each component of the problem. Two invariants of the problem are exhibited. Existence and uniqueness of the solution for a prescribed load is addressed. Explicit and analytical solutions of the problem for any given load (force and moment) at one end is given by means of Jacobian elliptic functions. The problem of regularity of these solutions in regards to a smooth (and quasi-static) evolution of the load at one end is tackled through a deep analysis of the analytical expressions. After an illustrating example, the problem of a pure-shear follower load is presented and shows how asymptotic solutions can be recovered through Taylor expansion of the attainable expression. Also, the problem of quasi-static stability is addressed as a driven parametric oscillator in a general situation. The last section shows how the proposed approach is able to face problem of quasi-static instability more general than bifurcation (buckling) as catastrophe. These instabilities are widely used in mechanics, especially in structural design and construction.

The fourth chapter analyzes the behaviour of a straight Timoshenko subjected to pure moment, this approach leads to a model similar to Kirchhoff rod model without an external force. Domains of variation of each dimensionless parameter is examined. Furthermore, two invariants that depend on moments and energy density govern the problem. Four regimes model arise that depends on the thickness of the cross section. Solutions were found in an analytical way (in terms of Jacobian elliptic functions). A detailed study is given on rod shapes to give a better understanding on the load parameters. Later on, a connection between our theoretical study and the physical world was made, specifically we first analyzed a Möbius strip obtained by a deformation of a straight beam where we obtained exact solutions for symmetric cross-section. Then we implicated our exact approach into the study of Torus knots where interesting results were obtained regarding the shape of these knots.

We will end the manuscript with a conclusion which englobes our research and open several perspectives for future work in this field.

Chapter 1

Problem statement

In this chapter we present the general formulation of the problem that will be used all along the manuscript.

1.1 Mathematical background

Let $\mathcal{V}$ be the set of all vectors, $\mathcal{V}$ has the structure of a real vector space [GS08]:

$$\mathbf{a}+\mathbf{b}\in\mathcal{V}\quad\forall\,\mathbf{a},\mathbf{b}\in\mathcal{V}\qquad\text{and}\qquad\alpha\mathbf{a}\in\mathcal{V}\quad\forall\alpha\in\mathbb{R},\ \ \mathbf{a}\in\mathcal{V}. \tag{1.1}$$

Einstein summation: All along this manuscript whenever an index occurs twice in a term a sum is implied over that index.
Conventional summation: We abbreviate the arguments in functions depending on the three components (a_1,a_2,a_3) or merely on the first two components (a_1,a_2) of a vector $\mathbf{a}\in\mathcal{V}$ by a_i or a_α, respectively.
Euclidean scalar product of two vector $\mathbf{a}$ and $\mathbf{b}$ is:

$$\mathbf{a}\cdot\mathbf{b}:=a_ib_i.$$

Vector product of two vector $\mathbf{a}$ and $\mathbf{b}$ is denoted by:

$$\mathbf{a}\times\mathbf{b},$$

where $(\mathbf{a}\times\mathbf{b})_k=a_ib_j\epsilon_{ijk}$ with $\epsilon_{ijk}=\begin{cases}1, & \text{if } ijk=123,\ 231 \text{ or } 312,\\ -1, & \text{if } ijk=321,\ 213 \text{ or } 132,\\ 0, & \text{otherwise (repeated index).}\end{cases}$.

Triple scalar product is given by:

$$(\mathbf{a}\times\mathbf{b})\cdot\mathbf{c}=\det(\mathbf{a},\mathbf{b},\mathbf{c}), \tag{1.2}$$

where $(\mathbf{a},\mathbf{b},\mathbf{c})$ is the 3×3 matrix with columns $\mathbf{a},\mathbf{b}$ and $\mathbf{c}$. By properties of the permutation symbol under cyclic permutation of its indices:

$$(\mathbf{a}\times\mathbf{b})\cdot\mathbf{c}=(\mathbf{b}\times\mathbf{c})\cdot\mathbf{a}=(\mathbf{c}\times\mathbf{a})\cdot\mathbf{b}. \tag{1.3}$$

The triple vector product is given by:

$$\mathbf{a} \times (\mathbf{b} \times \mathbf{c}) = (\mathbf{a} \cdot \mathbf{c})\mathbf{b} - (\mathbf{a} \cdot \mathbf{b})\mathbf{c}. \tag{1.4}$$

A second-order tensor $\mathbf{T}$ on the vector space $\mathcal{V}$ is a linear mapping $\mathbf{T} : \mathcal{V} \longrightarrow \mathcal{V}$. The set of second-order tensors is denoted by $\mathcal{V}^2$.
The dyadic product of two vectors $\mathbf{a}$ and $\mathbf{b}$ is the second-order tensor $\mathbf{a} \otimes \mathbf{b}$ defined by:

$$(\mathbf{a} \otimes \mathbf{b})\mathbf{v} = (\mathbf{b} \cdot \mathbf{v})\mathbf{a}, \qquad \forall\, \mathbf{v} \in \mathcal{V},$$

having the following property:

$$(\mathbf{a} \otimes \mathbf{b})(\mathbf{c} \otimes \mathbf{d}) = (\mathbf{b} \cdot \mathbf{c})\mathbf{a} \otimes \mathbf{d}. \tag{1.5}$$

Hence any second order tensor $\mathbf{T}$ could be represented using dyadic product as

$$\mathbf{T} = T_{ij}\mathbf{e_i} \otimes \mathbf{e_j},$$

with the Cartesian frame $\mathbf{e} = (\mathbf{e_1}, \mathbf{e_2}, \mathbf{e_3})$.
To any tensor $\mathbf{S}$ we associate a transpose $\mathbf{S}^T$, which is the unique tensor with the property

$$\mathbf{Su} \cdot \mathbf{v} = \mathbf{u} \cdot \mathbf{S}^T\mathbf{v}, \qquad \forall \mathbf{u}, \mathbf{v} \in \mathcal{V}.$$

$\mathbf{S}$ is symmetric if $\mathbf{S} = \mathbf{S}^T$ and $\mathbf{S}$ is skew-symmetric if $\mathbf{S} = -\mathbf{S}^T$.
Trace of a tensor $\mathbf{S}$ is a scalar function denoted by $tr(\mathbf{S})$ and given by

$$tr(\mathbf{S}) = S_{ii},$$

with the following properties

$$tr(\mathbf{T} + \mathbf{S}) = tr(\mathbf{T}) + tr(\mathbf{S}), \qquad \forall\ \mathbf{T}, \mathbf{S} \in \mathcal{V}^2. \tag{1.6}$$

$$tr(\alpha\mathbf{T}) = \alpha\, tr(\mathbf{T}), \qquad \forall\ \alpha \in \mathbb{R}, \forall\ \mathbf{T} \in \mathcal{V}^2. \tag{1.7}$$

$$tr(\mathbf{T}^T) = tr(\mathbf{T}), \qquad \forall\ \mathbf{S} \in \mathcal{V}^2. \tag{1.8}$$

$$tr(\mathbf{TS}) = tr(\mathbf{ST}), \qquad \forall\ \mathbf{T}, \mathbf{S} \in \mathcal{V}^2. \tag{1.9}$$

Theorem 1.1.1. Given any skew-symmetric tensor $\mathbf{W}$ there is a unique vector $\mathbf{w}$ such that

$$\mathbf{Wv} = \mathbf{w} \times \mathbf{v}, \qquad \forall \mathbf{v} \in \mathcal{V}.$$

Analogous to the scalar product for vectors, we define an inner scalar product for second-order tensors by

$$\mathbf{S} : \mathbf{D} = tr(\mathbf{S}^T\mathbf{D}). \tag{1.10}$$

1.2 Beam model

This section is based on the work done by Le Marrec *et. al.* in [LMLR18].
In this manuscript, we aim to study a straight, elastic, isotropic and homogenous Timoshenko

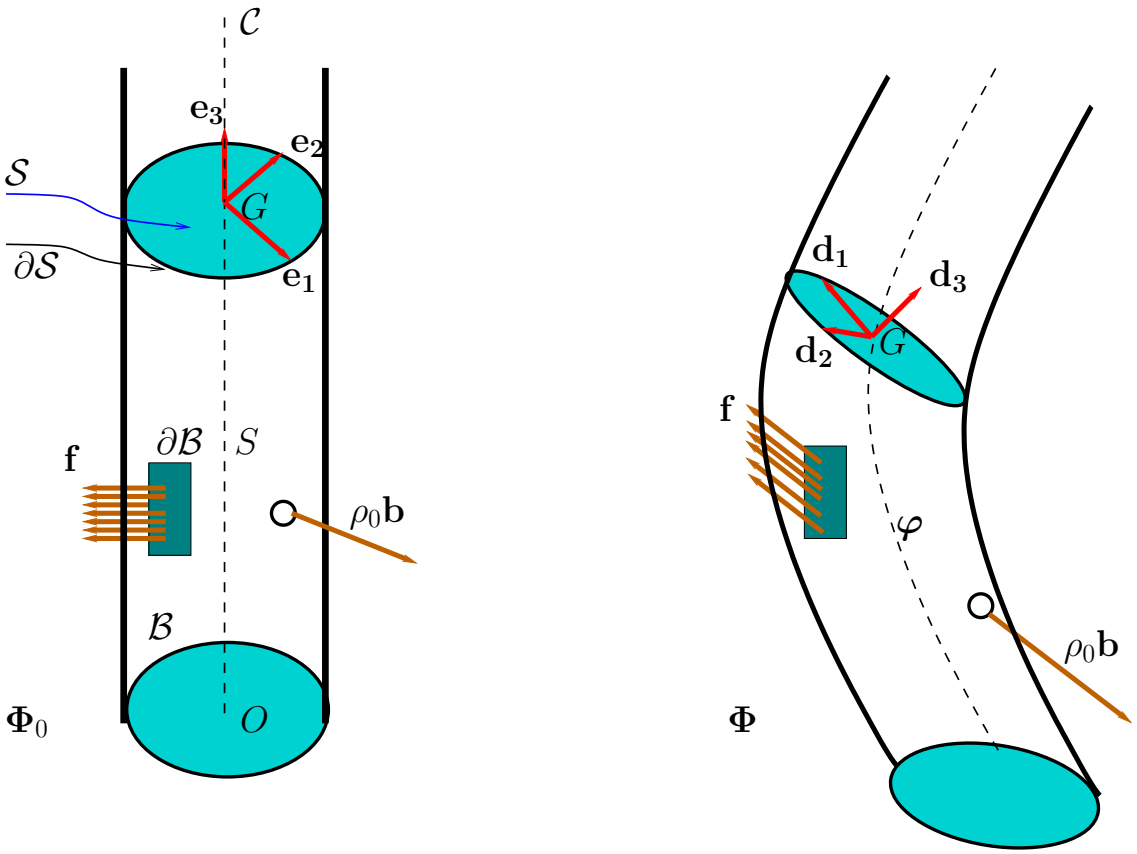

Figure 1.1 – *Reference configuration* $\mathbf{\Phi}_0$ *(left) and current configuration* $\mathbf{\Phi}$*. A priori the force densities may change along the transformation. The cross-section is normal to the centerline* $\mathcal{C}$ *in the reference configuration but not necessarily in the current configuration :* $\mathbf{d_3}$ *is not tangent to* $\mathcal{C}$*.*

beam. A suitable way to model this beam is to consider it as a bounded material body $\mathcal{B}$. Its reference configuration $\mathbf{\Phi}_0$ is defined as the configuration where the body is at rest (stress-free) in absence of external load. Let $\partial\mathcal{B}$ be the surface boundary of $\mathcal{B}$ where traction $\mathbf{f}$ is eventually prescribed (per unit initial area of the reference configuration). The body is subjected to a body force field $\rho_0\mathbf{b}$, where ρ_0 is the mass density in the reference configuration (see figure 1.1).

Cosserat continuum

Given the fact that beams are slender structures, so it is considered as one dimensional Cosserat body [CC09] with two degree of freedom: one that controls the position of the centerline and another that governs orientation of the section. Namely, we define a spatial material curve $\mathcal{C}$. Practically the curve corresponds to the positions of the section center of mass G. In the reference configuration ($t = 0$) the beam is straight, so this curves is a straight segment of length L. A fixed origin O and a Cartesian frame $(\mathbf{e_1}, \mathbf{e_2}, \mathbf{e_3})$ is chosen in such a way that $\mathbf{OG} = S\mathbf{e_3}$ in the initial configuration. Here $S \in [0, L]$ is a material curvilinear coordinate of $\mathcal{C}$. At each time t, the placement of G is defined by

$$\boxed{(S,t) \in [0,L] \times [0,+\infty[\longrightarrow \boldsymbol{\varphi}(S,t) := \mathbf{OG}(S,t).}$$

Lastly, as S is a material coordinate it always belongs to $[0, L]$, G spans the center line $\mathcal{C}$ even if the true length of $\mathcal{C}$ is modified in the actual configuration.
Sections of the beam $\mathcal{S}$ are supposed to be rigid and normal to the spatial curve in the reference configuration. Hereafter, the section is supposed to be uniform all along the fiber.
For such a Cosserat-like structure it is justified to use a moving director frame basis $(\mathbf{d_1}, \mathbf{d_2}, \mathbf{d_3})$ for which this basis is a principal basis and $\mathbf{d_3}$ is always normal to the cross-section. In reference configuration $(\mathbf{d_1}, \mathbf{d_2}, \mathbf{d_3})$ coincides with the Cartesian frame. After transformation, as the orientation of the section is not necessarily uniform, this basis depends on the curvilinear abscissa S of the beam and on time. In contrary to Euler-Bernoulli model $\mathbf{d_3}$ is not necessarily tangent to the center line. However, this basis is always orthonormal $\mathbf{d_3} = \mathbf{d_1} \times \mathbf{d_2}$.
We define (ξ_1, ξ_2) as the local coordinates of any point M of the cross-section:

$$\mathbf{GM} = \xi_1 \mathbf{d_1} + \xi_2 \mathbf{d_2} := \xi_\alpha \mathbf{d}_\alpha. \tag{1.11}$$

The position of any material point M of the beam in the deformed configuration is defined by [Rak09]:

$$\mathbf{OM}(\xi_1, \xi_2, S, t) = \boldsymbol{\varphi}(S,t) + \xi_\alpha \mathbf{d}_\alpha(S,t). \tag{1.12}$$

Displacement of M is given by

$$\mathbf{u} = \mathbf{OM} - \mathbf{OM_0}, \tag{1.13}$$

whereas $\mathbf{OM_0} = \varphi_\mathbf{0} + \mathbf{G_0M_0} = S\mathbf{e_3} + \xi_\alpha \mathbf{e}_\alpha$ is the position in the reference configuration.

1.2.1 Curvature and spin

By construction, a rotation tensor $\mathbf{R}(S,t)$ is intrinsically defined along the curve $\mathcal{C}$ of the beam at rest and relates each director to the reference one: $\mathbf{d_i}(S,t) = \mathbf{R}(S,t)\mathbf{e_i}$ then $\mathbf{e_i} = \mathbf{R}^T(S,t)\mathbf{d_i}(S,t)$. The rotation determines the twist and spin of directors.

Twist

As $\mathbf{e_i} = \mathbf{R}^T\mathbf{d_i}$, spatial derivation of directors writes :

$$\frac{\partial \mathbf{d_i}}{\partial S} = \frac{\partial \mathbf{R}}{\partial S}\mathbf{R}^T\mathbf{d_i}, \tag{1.14}$$

where $\frac{\partial \mathbf{R}}{\partial S}\mathbf{R}^T$ is a skew-symmetric tensor. Its axial vector $\boldsymbol{\kappa}$ is defined as the twist vector or *generalized curvature*. Accordingly, spatial derivation of directors can be obtained by

$$\frac{\partial \mathbf{d_i}}{\partial S} = \boldsymbol{\kappa} \times \mathbf{d_i}. \tag{1.15}$$

We can write (1.15) as

$$\frac{\partial \mathbf{d}_i}{\partial S} = \mathbf{K}\mathbf{d}_i, \qquad \text{where} \qquad \mathbf{K} = \begin{pmatrix} 0 & \kappa_3 & -\kappa_2 \\ -\kappa_3 & 0 & \kappa_1 \\ \kappa_2 & -\kappa_1 & 0 \end{pmatrix}. \tag{1.16}$$

Therefore, we obtain the following non linear first order system of nine partial differential equations with respect to $\mathbf{d}_i$:

$$\begin{aligned} \frac{\partial \mathbf{d}_1}{\partial S} &= \kappa_3(S,t)\mathbf{d}_2(S,t) - \kappa_2(S,t)\mathbf{d}_3(S,t), \\ \frac{\partial \mathbf{d}_2}{\partial S} &= \kappa_1(S,t)\mathbf{d}_3(S,t) - \kappa_3(S,t)\mathbf{d}_1(S,t), \\ \frac{\partial \mathbf{d}_3}{\partial S} &= \kappa_2(S,t)\mathbf{d}_1(S,t) - \kappa_1(S,t)\mathbf{d}_2(S,t). \end{aligned} \tag{1.17}$$

Where κ_1 and κ_2 are curvatures with respect to $(\mathbf{d}_1, \mathbf{d}_2)$ and κ_3 is twist vector that defines the amount of rotation of the local basis $(\mathbf{d}_1, \mathbf{d}_2, \mathbf{d}_3)$ around $\mathbf{d}_3$ as S increases.

Spin

The same procedure is performed for time derivation:

$$\frac{\partial \mathbf{d_i}}{\partial t} = \frac{\partial \mathbf{R}}{\partial t}\mathbf{R}^T\mathbf{d_i}, \tag{1.18}$$

and spin $\boldsymbol{\omega}$ is the axial vector associated with the skew-symmetric tensor of $\frac{\partial \mathbf{R}}{\partial t}\mathbf{R}^T$. Then

$$\frac{\partial \mathbf{d_i}}{\partial t} = \boldsymbol{\omega} \times \mathbf{d_i}. \tag{1.19}$$

So, by letting $\mathbf{W} = \begin{pmatrix} 0 & \omega_3 & -\omega_2 \\ -\omega_3 & 0 & \omega_1 \\ \omega_2 & -\omega_1 & 0 \end{pmatrix}$ we obtain:

$$\begin{aligned} \frac{\partial \mathbf{d_1}}{\partial t} &= \omega_3(S,t)\mathbf{d}_2(S,t) - \omega_2(S,t)\mathbf{d}_3(S,t), \\ \frac{\partial \mathbf{d_2}}{\partial t} &= \omega_1(S,t)\mathbf{d}_3(S,t) - \omega_3(S,t)\mathbf{d}_1(S,t), \\ \frac{\partial \mathbf{d_3}}{\partial t} &= \omega_2(S,t)\mathbf{d}_1(S,t) - \omega_1(S,t)\mathbf{d}_2(S,t). \end{aligned} \tag{1.20}$$

Remark. $\boldsymbol{\omega}$ and $\boldsymbol{\kappa}$ are related due to the Maurer-Cartan form [Nak03]:

$$\frac{\partial \boldsymbol{\kappa}}{\partial t} - \boldsymbol{\omega} \times \boldsymbol{\kappa} = \frac{\partial \boldsymbol{\omega}}{\partial S} \ . \tag{1.21}$$

1.2.2 Deformation and strains

Strain is the local stretching of a body caused by a deformation. Beam is considered as a 3D-body, so using the standard continuous mechanics model, a natural way to quantify strain is the deformation gradient given by $\mathbf{F} = \nabla_X \mathbf{OM}$ where $X = (\xi_1, \xi_2, S)$ is the material coordinates, therefore

$$\mathbf{F} = \mathbf{d_1} \otimes \mathbf{e_1} + \mathbf{d_2} \otimes \mathbf{e_2} + (\xi_1 \frac{\partial \mathbf{d_1}}{\partial S} + \xi_2 \frac{\partial \mathbf{d_2}}{\partial S} + \frac{\partial \boldsymbol{\varphi}}{\partial S}) \otimes \mathbf{e_3}. \tag{1.22}$$

Using (1.11) $\mathbf{F}$ is written as:

$$\mathbf{F} = \mathbf{d}_\alpha \otimes \mathbf{e}_\alpha + (\boldsymbol{\kappa} \times \mathbf{GM} + \frac{\partial \boldsymbol{\varphi}}{\partial S}) \otimes \mathbf{e_3}. \tag{1.23}$$

Since $\boldsymbol{\kappa} \times \mathbf{GM} + \frac{\partial \boldsymbol{\varphi}}{\partial S} = \Big(\big(\boldsymbol{\kappa} \times \mathbf{GM} + \frac{\partial \boldsymbol{\varphi}}{\partial S} \big) \cdot \mathbf{d_i} \Big) \mathbf{d_i}$, so, we can rewrite $\mathbf{F}$ as:

$$\begin{aligned} \mathbf{F} = \mathbf{d_i} \otimes \mathbf{e_i} + \Big((\boldsymbol{\kappa} \times \mathbf{GM} + \frac{\partial \boldsymbol{\varphi}}{\partial S}) \cdot \mathbf{d_1} \Big) \mathbf{d_1} \otimes \mathbf{e_3} + \Big((\boldsymbol{\kappa} \times \mathbf{GM} + \frac{\partial \boldsymbol{\varphi}}{\partial S}) \cdot \mathbf{d_2} \Big) \mathbf{d_2} \otimes \mathbf{e_3} + \\ \Big((\boldsymbol{\kappa} \times \mathbf{GM} + \frac{\partial \boldsymbol{\varphi}}{\partial S}) \cdot \mathbf{d_3} - 1 \Big) \mathbf{d_3} \otimes \mathbf{e_3}. \end{aligned} \tag{1.24}$$

This motivates us to write $\mathbf{F} := \mathbf{R}(\mathbf{I} + \mathbf{H})$ where, $\mathbf{R} = \mathbf{d_i} \otimes \mathbf{e_i}$ and $\mathbf{H}$ is a tensor given by:

$$\mathbf{H} = \Big((\boldsymbol{\kappa} \times \mathbf{GM} + \frac{\partial \boldsymbol{\varphi}}{\partial S}) \cdot \mathbf{d_1} \Big) \mathbf{e_1} \otimes \mathbf{e_3} + \Big((\boldsymbol{\kappa} \times \mathbf{GM} + \frac{\partial \boldsymbol{\varphi}}{\partial S}) \cdot \mathbf{d_2} \Big) \mathbf{e_2} \otimes \mathbf{e_3} + \Big((\boldsymbol{\kappa} \times \mathbf{GM} + \frac{\partial \boldsymbol{\varphi}}{\partial S}) \cdot \mathbf{d_3} - 1 \Big) \mathbf{e_3} \otimes \mathbf{e_3}. \tag{1.25}$$

It should be mentioned that $\mathbf{F}$ provides local information of the deformation and it is not symmetric in general, this motivates us to introduce the right Green-Cauchy strain tensor $\mathbf{C} = \mathbf{F}^T\mathbf{F}$. Notice that $\mathbf{C}$ is symmetric but $\mathbf{C}$ doesn't vanish at rest, therefore, Green-Lagrange strain tensor

$$\mathbf{E} := \frac{1}{2}(\mathbf{C} - \mathbf{I}), \tag{1.26}$$

is a better way to define strain for finite transformation.
According to [Sim85] generalized strain is given by:

$$\widetilde{\boldsymbol{\varepsilon}}(S,t) := \frac{\partial \boldsymbol{\varphi}}{\partial S} - \mathbf{d_3}. \tag{1.27}$$

The component of this strain in the frame of directors have to be clearly distinguished as they have two distinct physical meaning :

$$\begin{aligned} \widetilde{\boldsymbol{\varepsilon}} \cdot \mathbf{d_1} &\quad : \text{shear strain}, \\ \widetilde{\boldsymbol{\varepsilon}} \cdot \mathbf{d_2} &\quad : \text{shear strain}, \\ \widetilde{\boldsymbol{\varepsilon}} \cdot \mathbf{d_3} &\quad : \text{longitudinal strain}. \end{aligned} \tag{1.28}$$

Using the fact that $\mathbf{F} := \mathbf{R}(\mathbf{I} + \mathbf{H})$, therefore:

$$\begin{aligned} \mathbf{E} &= \frac{1}{2}\Big((\mathbf{R}(\mathbf{I}+\mathbf{H}))^T(\mathbf{R}(\mathbf{I}+\mathbf{H})) - \mathbf{I}\Big), \\ \mathbf{E} &= \frac{1}{2}\Big(\mathbf{H} + \mathbf{H}^T + \mathbf{H}^T\mathbf{H}\Big). \end{aligned} \tag{1.29}$$

Hence $\mathbf{E}$ takes the form of an anti-plane tensor [Rak09]:

$$\mathbf{E} = \sum_{i=1}^{3} \Big((\widetilde{\boldsymbol{\varepsilon}} + \boldsymbol{\kappa} \times \mathbf{GM}) \cdot \mathbf{d_i}\Big) \frac{\mathbf{e_i} \otimes \mathbf{e}_3 + \mathbf{e}_3 \otimes \mathbf{e_i}}{2} + \frac{1}{2} \left\| \widetilde{\boldsymbol{\varepsilon}} + \boldsymbol{\kappa} \times \mathbf{GM} \right\|^2 \mathbf{e}_3 \otimes \mathbf{e}_3. \tag{1.30}$$

And deformations are defined entirely with respect to $\boldsymbol{\kappa}$ and $\widetilde{\boldsymbol{\varepsilon}}$.

Remark. *By observing (1.30), we can remark that the relation between the Green-Lagrange deformation tensor E and the uni-dimensional deformations $\widetilde{\varepsilon}$ as well as κ is not linear, so these deformations do not obey the same laws: a linear constitutive law in terms of E is not necessary linear with respect to κ and $\widetilde{\varepsilon}$. To ensure linearity, an additional condition should be guaranteed, this idea will be illustrated in section (1.3.2).*

1.2.3 Stress, forces and moments

Stress is the internal resistance to external loads. An intuitive way to describe combined stresses is the cauchy stress tensor σ. This tensor expresses the stress relative to the deformed configuration. One can also define a stress tensor with respect to the reference configuration known as the first Piola-Kirchhoff stress $\mathbf{P} := \det\mathbf{F}\sigma\mathbf{F}^{-T}$. $\mathbf{P}$ is not symmetric in general, hence in order to associate a stress to the Green-Lagrange strain, the second Piola-Kirchhoff is introduced:

$$\mathbf{P} = \mathbf{FS}. \tag{1.31}$$

Law of angular momentum imposes $\mathbf{PF}^T = \mathbf{FP}^T$. As a consequence, $\mathbf{S}$ is symmetric.

Forces and moments

Beam dynamics requires the definition of associated internal forces and moments. The resultant force $\mathbf{N}$ and the moment $\mathbf{M}$ per unit reference length acting on the section $\mathcal{S}$ are given in terms of the nominal Piola-Kirchhoff stress tensor:

$$\begin{aligned} \mathbf{N} &:= \int_{\mathcal{S}} \mathbf{P}(\mathbf{e_3}) dA = N_i \mathbf{d_i}, \\ \mathbf{M} &:= \int_{\mathcal{S}} \mathbf{GM} \times \mathbf{P}(\mathbf{e_3}) dA = M_i \mathbf{d_i}. \end{aligned} \tag{1.32}$$

1.2.4 Principle of virtual work

The principle of virtual work forms the foundation for the variational principles of mechanics and it could be used to find the fundamental laws of motion (equilibrium equations). A virtual displacement is an infinitesimal displacement of any point of a mechanical system that may or may not take place but that is compatible with the constraints of the system and a virtual work is the work done by a real force acting through a virtual displacement, or a virtual force acting through a real displacement.
The principle of virtual work states that:

$$\int_{\mathcal{B}} \rho_0 \mathbf{b} \cdot \delta\mathbf{u} \, \mathrm{d}V + \int_{\partial\mathcal{B}} \mathbf{f} \cdot \delta\mathbf{u} \, \mathrm{d}A = \int_{\mathcal{B}} \rho_0 \frac{\partial^2 \mathbf{u}}{\partial t^2} \cdot \delta\mathbf{u} \, \mathrm{d}V + \int_{\mathcal{B}} \mathbf{P} : \delta\mathbf{F} \, \mathrm{d}V, \quad \forall \ \delta\mathbf{u} \in \mathbf{W}. \tag{1.33}$$

Where $\mathbf{u}$ is the displacement of any point of the three-dimensional body and $\mathbf{W}$ is the space of kinematically compatible virtual displacement, usually called the space of variation of the continuum. The various terms in the preceding equation are:

$$\begin{aligned} \mathcal{P}_{acc}(\mathbf{\Phi}, \delta\mathbf{\Phi}) &= \int_{\mathcal{B}} \rho_0 \frac{\partial^2 \mathbf{u}}{\partial t^2} \cdot \delta\mathbf{u} \, \mathrm{d}V. && \text{Virtual work of acceleration,} \\ \mathcal{P}_{e}(\mathbf{\Phi}, \delta\mathbf{\Phi}) &= \int_{\mathcal{B}} \rho_0 \mathbf{b} \cdot \delta\mathbf{u} \, \mathrm{d}V + \int_{\partial\mathcal{B}} \mathbf{f} \cdot \delta\mathbf{u} \, \mathrm{d}A. && \text{Virtual work of external loading,} \\ \mathcal{P}_{i}(\mathbf{\Phi}, \delta\mathbf{\Phi}) &= \int_{\mathcal{B}} \mathbf{P} : \delta\mathbf{F} \, \mathrm{d}V. && \text{Virtual internal work,} \end{aligned} \tag{1.34}$$

for which

$$\begin{aligned} \mathbf{\Phi}(S) &= \big(\boldsymbol{\varphi}(\boldsymbol{S}), \mathbf{Q}(S)\big), && \in \mathbb{R}^3 \times \mathcal{SO}(3), \\ \delta\mathbf{\Phi}(S) &= \big(\delta\boldsymbol{\varphi}(\boldsymbol{S}), \tilde{\mathbf{Q}}(S)\big), && \in \mathbb{R}^3 \times \mathcal{SO}(3). \end{aligned} \tag{1.35}$$

For a beam-structure the kinematics of any point is constrained by the rigid motion of the section. In particular, the displacement $\mathbf{u}$ (respectively $\delta\mathbf{u}$) may be written in terms of $\boldsymbol{\varphi}$ and $\mathbf{Q}$ (respectively $\delta\boldsymbol{\varphi}$ and $\tilde{\mathbf{Q}}$) as $\mathbf{u} = \boldsymbol{\varphi} - \boldsymbol{\varphi_0} + (\mathbf{Q} - \mathbf{I})\mathbf{G_0M_0}$. Small variations with respect to the kinematics is given by

$$\delta\mathbf{u} = \delta\boldsymbol{\varphi} + \delta\boldsymbol{\omega} \times \mathbf{GM}. \tag{1.36}$$

Where $\delta\boldsymbol{\omega}$ is the axial vector associated to the skew-symmetric tensor $\tilde{\mathbf{Q}}$.
Time differentiation of the beam structure gives:

$$\begin{aligned}\frac{\partial^2\mathbf{u}}{\partial t^2} &= \frac{\partial}{\partial t}\Big(\frac{\partial\boldsymbol{\varphi}}{\partial t}+\frac{\partial\mathbf{GM}}{\partial t}\Big),\\ &= \frac{\partial}{\partial t}\Big(\frac{\partial\boldsymbol{\varphi}}{\partial t}+\boldsymbol{\omega}\times\mathbf{GM}\Big).\end{aligned} \tag{1.37}$$

It should be mentioned that another formulation of the internal virtual work may be obtained according to the dual tensor $\mathbf{S}$ and $\mathbf{E}$. In fact, since $\mathbf{P}=\mathbf{FS}$, so, on one hand

$$\begin{aligned}\mathbf{P}:\delta\mathbf{F} &= tr(\mathbf{P}^T\delta\mathbf{F}),\\ &= tr((\mathbf{FS})^T\delta\mathbf{F}),\\ &= tr(\mathbf{S}^T\mathbf{F}^T\delta\mathbf{F}),\end{aligned} \tag{1.38}$$

and on the other

$$\begin{aligned}\delta\mathbf{E} &= \frac{1}{2}\delta\Big((\mathbf{F})^T\mathbf{F}-\mathbf{I}\Big),\\ &= \frac{1}{2}\Big((\delta\mathbf{F})^T\mathbf{F}+\mathbf{F}^T\delta\mathbf{F}\Big),\end{aligned} \tag{1.39}$$

therefore:

$$\begin{aligned}\mathbf{S}:\delta\mathbf{E}=tr(\mathbf{S}^T\delta\mathbf{E})=tr(\mathbf{S}\delta\mathbf{E}) &\overset{(1.7)}{=} \frac{1}{2}\Big(tr(\mathbf{S}\delta\mathbf{F}^T\mathbf{F}+\mathbf{S}\mathbf{F}^T\delta\mathbf{F})\Big),\\ &\overset{(1.6)}{=} \frac{1}{2}\Big(tr(\mathbf{S}\delta\mathbf{F}^T\mathbf{F})+tr(\mathbf{S}\mathbf{F}^T\delta\mathbf{F})\Big),\\ &\overset{(1.8)}{=} \frac{1}{2}\Big(tr\Big((\mathbf{S}\delta\mathbf{F}^T\mathbf{F})^T\Big)+tr(\mathbf{S}\mathbf{F}^T\delta\mathbf{F})\Big),\\ &\overset{(1.8)}{=} \frac{1}{2}\Big(tr(\mathbf{F}^T\delta\mathbf{F}\mathbf{S})+tr(\mathbf{S}\mathbf{F}^T\delta\mathbf{F})\Big),\\ &\overset{(1.9)}{=} \frac{1}{2}\Big(tr(\mathbf{S}\mathbf{F}^T\delta\mathbf{F})+tr(\mathbf{S}\mathbf{F}^T\delta\mathbf{F})\Big)=\mathbf{P}:\delta\mathbf{F}.\end{aligned} \tag{1.40}$$

Virtual work of acceleration

According to the kinematical variables, the virtual work of acceleration takes the following form:

$$\begin{aligned}
\mathcal{P}_{acc}(\Phi,\delta\Phi) &= \int_{\mathcal{C}}\int_{\mathcal{S}} \rho_0 \frac{\partial}{\partial t}\left(\frac{\partial \boldsymbol{\varphi}}{\partial t} + \boldsymbol{\omega}\times\mathbf{GM}\right)\cdot\Big(\delta\boldsymbol{\varphi} + \delta\boldsymbol{\omega}\times\mathbf{GM}\Big)\,\mathrm{d}A\,\mathrm{d}S,\\
&= \int_{\mathcal{C}}\int_{\mathcal{S}} \rho_0 \left(\frac{\partial \boldsymbol{\varphi}^2}{\partial t^2} + \frac{\partial \boldsymbol{\omega}}{\partial t}\times\mathbf{GM} + \boldsymbol{\omega}\times\frac{\partial \mathbf{GM}}{\partial t}\right)\cdot\Big(\delta\boldsymbol{\varphi} + \delta\boldsymbol{\omega}\times\mathbf{GM}\Big)\,\mathrm{d}A\,\mathrm{d}S,\\
&= \int_{\mathcal{C}}\int_{\mathcal{S}} \rho_0 \left(\frac{\partial \boldsymbol{\varphi}^2}{\partial t^2} + \frac{\partial \boldsymbol{\omega}}{\partial t}\times\mathbf{GM} + \boldsymbol{\omega}\times(\boldsymbol{\omega}\times\mathbf{GM})\right)\cdot\Big(\delta\boldsymbol{\varphi} + \delta\boldsymbol{\omega}\times\mathbf{GM}\Big)\,\mathrm{d}A\,\mathrm{d}S,\\
&= \int_{\mathcal{C}}\int_{\mathcal{S}} \rho_0 \Big(\frac{\partial \boldsymbol{\varphi}^2}{\partial t^2}\cdot\delta\boldsymbol{\varphi} + \frac{\partial \boldsymbol{\varphi}^2}{\partial t^2}\cdot\Big(\delta\boldsymbol{\omega}\times\mathbf{GM}\Big) + \Big(\frac{\partial \boldsymbol{\omega}}{\partial t}\times\mathbf{GM}\Big)\cdot\delta\boldsymbol{\varphi} +\\
&\quad \Big(\frac{\partial \boldsymbol{\omega}}{\partial t}\times\mathbf{GM}\Big)\cdot\Big(\delta\boldsymbol{\omega}\times\mathbf{GM}\Big) + \boldsymbol{\omega}\times(\boldsymbol{\omega}\times\mathbf{GM})\cdot\delta\boldsymbol{\varphi} +\\
&\quad \Big(\boldsymbol{\omega}\times(\boldsymbol{\omega}\times\mathbf{GM})\Big)\cdot(\delta\boldsymbol{\omega}\times\mathbf{GM})\Big)\,\mathrm{d}A\,\mathrm{d}S.
\end{aligned} \tag{1.41}$$

However, $\int_{\mathcal{S}} \mathbf{GM}\,\mathrm{d}A = \mathbf{0}$, therefore,

$$\begin{aligned}
&\int_{\mathcal{C}}\int_{\mathcal{S}} \rho_0 \Big(\frac{\partial \boldsymbol{\varphi}^2}{\partial t^2}\cdot\Big(\delta\boldsymbol{\omega}\times\mathbf{GM}\Big) + \Big(\frac{\partial \boldsymbol{\omega}}{\partial t}\times\mathbf{GM} + \boldsymbol{\omega}\times(\boldsymbol{\omega}\times\mathbf{GM})\Big)\cdot\delta\boldsymbol{\varphi}\Big)\,\mathrm{d}A\,\mathrm{d}S =\\
&\int_{\mathcal{C}} \rho_0 \Big(\frac{\partial \boldsymbol{\varphi}^2}{\partial t^2}\cdot\Big(\delta\boldsymbol{\omega}\times\int_{\mathcal{S}}\mathbf{GM}\,\mathrm{d}A\Big) + \Big(\frac{\partial \boldsymbol{\omega}}{\partial t}\times\int_{\mathcal{S}}\mathbf{GM}\,\mathrm{d}A + \boldsymbol{\omega}\times(\boldsymbol{\omega}\times\int_{\mathcal{S}}\mathbf{GM}\,\mathrm{d}A)\Big)\cdot\delta\boldsymbol{\varphi}\Big)\,\mathrm{d}S = 0.
\end{aligned} \tag{1.42}$$

Moreover, in order to simplify computation, we consider uniform cross-section, then $\int_{\mathcal{S}} \rho_0 \mathrm{d}A = \rho_0 A$ and using the relation of triple product $(\mathbf{a}\times\mathbf{b})\cdot\mathbf{c} = (\mathbf{b}\times\mathbf{c})\cdot\mathbf{a}$ to obtain

$$\mathcal{P}_{acc}(\Phi,\delta\Phi) = \int_{\mathcal{C}} \rho_0 A\,\frac{\partial^2\boldsymbol{\varphi}}{\partial t^2}\cdot\delta\boldsymbol{\varphi} + \int_{\mathcal{S}} \rho_0 \Big(\mathbf{GM}\times\Big(\frac{\partial\boldsymbol{\omega}}{\partial t}\times\mathbf{GM}\Big) + \mathbf{GM}\times\Big(\boldsymbol{\omega}\times(\boldsymbol{\omega}\times\mathbf{GM})\Big)\Big)\mathrm{d}A\cdot\delta\boldsymbol{\omega}\,\mathrm{d}S\ .$$

Hence,

$$\mathcal{P}_{acc}(\Phi,\delta\Phi) = \int_{\mathcal{C}} \rho_0 A\,\frac{\partial^2\boldsymbol{\varphi}}{\partial t^2}\cdot\delta\boldsymbol{\varphi} + \int_{\mathcal{S}} \rho_0 \frac{\partial}{\partial t}\Big(\mathbf{GM}\times\Big(\boldsymbol{\omega}\times\mathbf{GM}\Big)\Big)\mathrm{d}A\cdot\delta\boldsymbol{\omega}\,\mathrm{d}S\ . \tag{1.43}$$

Introducing $\mathbb{I}$, the tensor of quadratic moment of the section, we have for any vector $\mathbf{a}$

$$\int_{\mathcal{S}} \mathbf{GM}\times\Big(\mathbf{a}\times\mathbf{GM}\Big)\,\mathrm{d}A = \mathbb{I}\,\mathbf{a}.$$

For uniform mass density in the section, the virtual work of acceleration becomes:

$$\mathcal{P}_{acc}(\Phi,\delta\Phi) = \int_{\mathcal{C}}\ \rho_0 A\,\frac{\partial^2\boldsymbol{\varphi}}{\partial t^2}\cdot\delta\boldsymbol{\varphi} + \rho_0\Big(\frac{\partial(\mathbb{I}\,\boldsymbol{\omega})}{\partial t}\Big)\cdot\delta\boldsymbol{\omega}\,\mathrm{d}\,S. \tag{1.44}$$

Keeping in mind that $\{\mathbf{d_i}\}$ is the principal basis of the section, the tensor of quadratic moment is

diagonal $\mathbb{I} = I_i \mathbf{d_i} \otimes \mathbf{d_i}$, written in matrix form as

$$\mathbb{I} = \begin{pmatrix} I_1 & 0 & 0 \\ 0 & I_2 & 0 \\ 0 & 0 & I_3 \end{pmatrix}, \tag{1.45}$$

with

$$I_1 = \int_{\mathcal{S}} \xi_2^2 \, \mathrm{d}A, \qquad I_2 = \int_{\mathcal{S}} \xi_1^2 \, \mathrm{d}A, \qquad I_3 = \int_{\mathcal{S}} \xi_1^2 + \xi_2^2 \, \mathrm{d}A.$$

External virtual work

Now considering the external virtual work using the kinematics of rigid body of any section:

$$\mathcal{P}_e(\Phi, \delta\Phi) = \int_{\mathcal{B}} \rho_0 \mathbf{b} \cdot (\delta\boldsymbol{\varphi} + \delta\boldsymbol{\omega} \times \mathbf{GM}) \, \mathrm{d}V + \int_{\partial\mathcal{B}} \mathbf{f} \cdot (\delta\boldsymbol{\varphi} + \delta\boldsymbol{\omega} \times \mathbf{GM}) \, \mathrm{d}A. \tag{1.46}$$

Using invariance of the scalar triple product under a circular shift we obtain:

$$\mathcal{P}_e(\Phi, \delta\Phi) = \int_{\mathcal{B}} \delta\boldsymbol{\varphi} \cdot \rho_0 \mathbf{b} + \delta\boldsymbol{\omega} \cdot (\mathbf{GM} \times \rho_0 \mathbf{b}) \, \mathrm{d}V + \int_{\partial\mathcal{B}} \delta\boldsymbol{\varphi} \cdot \mathbf{f} + \delta\boldsymbol{\omega} \cdot (\mathbf{GM} \times \mathbf{f}) \, \mathrm{d}A. \tag{1.47}$$

Keeping in mind that $\int_{\mathcal{B}} \mathrm{d}V = \int_{\mathcal{C}} \int_{\mathcal{S}} \mathrm{d}A\mathrm{d}S$ and $\int_{\partial\mathcal{B}} \mathrm{d}A = \int_{\mathcal{C}} \int_{\partial\mathcal{S}} \mathrm{d}L\mathrm{d}S$, therefore,

$$\mathcal{P}_e(\Phi, \delta\Phi) = \int_{\mathcal{C}} \int_{\mathcal{S}} \delta\boldsymbol{\varphi} \cdot \rho_0 \mathbf{b} + \delta\boldsymbol{\omega} \cdot (\mathbf{GM} \times \rho_0 \mathbf{b}) \, \mathrm{d}A\mathrm{d}S + \int_{\mathcal{C}} \int_{\partial\mathcal{S}} \delta\boldsymbol{\varphi} \cdot \mathbf{f} + \delta\boldsymbol{\omega} \cdot (\mathbf{GM} \times \mathbf{f}) \, \mathrm{d}L\mathrm{d}S. \tag{1.48}$$

However, $\delta\boldsymbol{\varphi}$ and $\delta\boldsymbol{\omega}$ are independent of the local coordinates (ξ_1, ξ_2) of the section, they are not affected by the integration over $\mathcal{S}$. Hence:

$$\mathcal{P}_e(\Phi, \delta\Phi) = \int_{\mathcal{C}} \mathbf{q} \cdot \delta\boldsymbol{\varphi} + \mathbf{m} \cdot \delta\boldsymbol{\omega} \, \mathrm{d}S, \tag{1.49}$$

for which the external applied force $\mathbf{q}(S, t)$ per unit length is:

$$\mathbf{q} := \int_{\mathcal{S}} \rho_0 \mathbf{b} \, \mathrm{d}A + \int_{\partial\mathcal{S}} \mathbf{f} \, \mathrm{d}L, \tag{1.50}$$

and the external applied couple $\mathbf{m}(S, t)$ per unit reference length is:

$$\mathbf{m} := \int_{\mathcal{S}} \mathbf{GM} \times \rho_0 \mathbf{b} \, \mathrm{d}A + \int_{\partial\mathcal{S}} \mathbf{GM} \times \mathbf{f} \, \mathrm{d}L. \tag{1.51}$$

Internal virtual work

The local increment of the deformation is given by:

$$\begin{aligned}\delta\mathbf{F} &= \delta\Big(\mathbf{d}_\alpha\otimes\mathbf{e}_\alpha+(\frac{\partial\boldsymbol{\varphi}}{\partial S}+\boldsymbol{\kappa}\times\mathbf{GM})\otimes\mathbf{e_3}\Big),\\ &= \delta\mathbf{d}_\alpha\otimes\mathbf{e}_\alpha+\delta(\frac{\partial\boldsymbol{\varphi}}{\partial S}+\frac{\partial\mathbf{GM}}{\partial S})\otimes\mathbf{e_3},\\ &= \delta\mathbf{d}_\alpha\otimes\mathbf{e}_\alpha+\delta(\frac{\partial\boldsymbol{\varphi}}{\partial S}+\xi_\alpha\frac{\partial\mathbf{d}_\alpha}{\partial S})\otimes\mathbf{e_3}.\end{aligned}\tag{1.52}$$

Keeping in mind that δ and $\dfrac{\partial}{\partial S}$ commute, we obtain

$$\delta\mathbf{F}=(\delta\boldsymbol{\omega}\times\mathbf{d}_\alpha)\otimes\mathbf{e}_\alpha+\Big(\frac{\partial}{\partial S}(\delta\boldsymbol{\varphi}+\delta\boldsymbol{\omega}\times\mathbf{GM})\Big)\otimes\mathbf{e_3}.\tag{1.53}$$

In order to simplify notations, we introduce $\mathbf{p_i}$ such that $\mathbf{p_i}=\mathbf{P}(\mathbf{e_i})$ then $\mathbf{P}=\mathbf{p_i}\otimes\mathbf{e_i}$. Hence density of virtual work becomes:

$$\begin{aligned}\mathbf{P}:\delta\mathbf{F} &= \mathbf{p}_\alpha\cdot(\delta\boldsymbol{\omega}\times\mathbf{d}_\alpha)+\mathbf{p_3}\cdot\Big(\frac{\partial}{\partial S}(\delta\boldsymbol{\varphi}+\delta\boldsymbol{\omega}\times\mathbf{GM})\Big),\\ &\overset{(1.3)}{=} \delta\boldsymbol{\omega}\cdot(\mathbf{d}_\alpha\times\mathbf{p}_\alpha)+\mathbf{p_3}\cdot\Big(\frac{\partial}{\partial S}(\delta\boldsymbol{\varphi}+\delta\boldsymbol{\omega}\times\mathbf{GM})\Big).\end{aligned}\tag{1.54}$$

At this stage, no specific information is explicitly given on $\mathbf{p}_\alpha$. However, symmetry of second Piola-Kirchhoff stress tensor imposes $\mathbf{FP}^T-\mathbf{PF}^T=\mathbf{0}$. This can be written explicitly as:

$$\Big(\mathbf{d}_\alpha\otimes\mathbf{e}_\alpha+(\frac{\partial\boldsymbol{\varphi}}{\partial S}+\boldsymbol{\kappa}\times\mathbf{GM})\otimes\mathbf{e_3}\Big)\Big(\mathbf{e_i}\otimes\mathbf{p_i}\Big)-\Big(\mathbf{e}_\alpha\otimes\mathbf{d}_\alpha+\mathbf{e_3}\otimes(\frac{\partial\boldsymbol{\varphi}}{\partial S}+\boldsymbol{\kappa}\times\mathbf{GM})\Big)\Big(\mathbf{p_i}\otimes\mathbf{e_i}\Big)=0.\tag{1.55}$$

Using (1.5) to obtain:

$$\mathbf{d}_\alpha\otimes\mathbf{p}_\alpha-\mathbf{p}_\alpha\otimes\mathbf{d}_\alpha+\Big(\tfrac{\partial\boldsymbol{\varphi}}{\partial S}+\boldsymbol{\kappa}\times\mathbf{GM}\Big)\otimes\mathbf{p_3}-\mathbf{p_3}\otimes\Big(\tfrac{\partial\boldsymbol{\varphi}}{\partial S}+\boldsymbol{\kappa}\times\mathbf{GM}\Big)=\mathbf{0}\ .\tag{1.56}$$

However, a zero tensor is a skew-symmetric tensor. So (1.56) is equivalent to :

$$\mathbf{p}_\alpha\times\mathbf{d}_\alpha+\mathbf{p_3}\times\left(\frac{\partial\boldsymbol{\varphi}}{\partial S}+\boldsymbol{\kappa}\times\mathbf{GM}\right)=\mathbf{0}\ ,$$

that gives a relation between $\mathbf{p}_\alpha$ and $\mathbf{p_3}$ imposed by the angular momentum conservation law. Introducing this relation in the virtual internal work density (1.54):

$$\mathbf{P}:\delta\mathbf{F}=\delta\boldsymbol{\omega}\cdot\left(\mathbf{p_3}\times\Big(\frac{\partial\boldsymbol{\varphi}}{\partial S}+\boldsymbol{\kappa}\times\mathbf{GM}\Big)\right)+\mathbf{p_3}\cdot\left(\frac{\partial}{\partial S}(\delta\boldsymbol{\varphi}+\delta\boldsymbol{\omega}\times\mathbf{GM})\right)\ .$$

Expanding each term, we obtain:

$$\begin{aligned}\mathbf{P} : \delta\mathbf{F} &= \delta\boldsymbol{\omega} \cdot \mathbf{p_3} \times \tfrac{\partial \boldsymbol{\varphi}}{\partial S} + \delta\boldsymbol{\omega} \cdot \Big(\mathbf{p_3} \times \big(\boldsymbol{\kappa} \times \mathbf{GM}\big)\Big) + \mathbf{p_3} \cdot \tfrac{\partial \delta\boldsymbol{\varphi}}{\partial S} + \mathbf{p_3} \cdot \tfrac{\partial \delta\boldsymbol{\omega}}{\partial S} \times \mathbf{GM} + \mathbf{p_3} \cdot \delta\boldsymbol{\omega} \times \tfrac{\partial \mathbf{GM}}{\partial S} \\ &\overset{(1.3)}{=} \mathbf{p_3} \cdot (\tfrac{\partial \delta\boldsymbol{\varphi}}{\partial S} - \delta\boldsymbol{\omega} \times \tfrac{\partial \boldsymbol{\varphi}}{\partial S}) - \mathbf{p_3} \cdot \Big(\delta\boldsymbol{\omega} \times (\boldsymbol{\kappa} \times \mathbf{GM})\Big) + \mathbf{p_3} \cdot \delta\boldsymbol{\omega} \times \boldsymbol{\kappa} \times \mathbf{GM} \\ &+ (\mathbf{GM} \times \mathbf{p_3}) \cdot \tfrac{\partial\, \delta\boldsymbol{\omega}}{\partial S}\end{aligned} \tag{1.57}$$

Therefore,

$$\mathbf{P} : \delta\mathbf{F} = \mathbf{p_3} \cdot \left(\frac{\partial\, \delta\boldsymbol{\varphi}}{\partial S} - \delta\boldsymbol{\omega} \times \frac{\partial \boldsymbol{\varphi}}{\partial S}\right) + (\mathbf{GM} \times \mathbf{p_3}) \cdot \frac{\partial\, \delta\boldsymbol{\omega}}{\partial S}\ . \tag{1.58}$$

Keeping in mind that variation of strain is frame-indifferent (*e.g.*[CJ99]), corotational variation must be prescribed. For any vector $\mathbf{a} = a_i \mathbf{d_i}$ this variation is:

$$\delta^R \mathbf{a} := \delta\mathbf{a} - \delta\boldsymbol{\omega} \times \mathbf{a} = (\delta a_i)\ \mathbf{d_i}\ .$$

These corotational variations are well defined in (1.58) and closely related to Maurer-Cartan form, according to (1.27)

$$\begin{aligned}\delta^R \widetilde{\boldsymbol{\varepsilon}} &= \delta\Big(\frac{\partial \boldsymbol{\varphi}}{\partial S} - \mathbf{d_3}\Big) - \delta\boldsymbol{\omega} \times \Big(\frac{\partial \boldsymbol{\varphi}}{\partial S} - \mathbf{d_3}\Big), \\ &= \frac{\partial \delta\boldsymbol{\varphi}}{\partial S} - \delta\mathbf{d_3} - \delta\boldsymbol{\omega} \times \frac{\partial \boldsymbol{\varphi}}{\partial S} + \delta\boldsymbol{\omega} \times \mathbf{d_3}, \\ &= \frac{\partial \delta\boldsymbol{\varphi}}{\partial S} - \delta\boldsymbol{\omega} \times \mathbf{d_3} - \delta\boldsymbol{\omega} \times \frac{\partial \boldsymbol{\varphi}}{\partial S} + \delta\boldsymbol{\omega} \times \mathbf{d_3}, \\ &= \frac{\partial\, \delta\boldsymbol{\varphi}}{\partial S} - \delta\boldsymbol{\omega} \times \frac{\partial \boldsymbol{\varphi}}{\partial S}.\end{aligned} \tag{1.59}$$

And according to (1.21):

$$\delta^R \boldsymbol{\kappa} = \delta\boldsymbol{\kappa} - \delta\boldsymbol{\omega} \times \boldsymbol{\kappa} = \frac{\partial\, \delta\boldsymbol{\omega}}{\partial S}. \tag{1.60}$$

These corotational variations are uniform along the beam-section and are not affected by integration over the beam section. Hence, according to 1.32 (with $\mathbf{P}(\mathbf{e_3}) = \mathbf{p_3}$) this integration make appears the force and torque per unit length. Then, virtual internal work becomes [Sim85]:

$$\mathcal{P}_i(\Phi, \delta\Phi) = \int_{\mathcal{C}} \mathbf{N} \cdot \delta^R \boldsymbol{\varepsilon} + \mathbf{M} \cdot \delta^R \boldsymbol{\kappa}\, \mathrm{d}S\ . \tag{1.61}$$

In other words, for beam structures the dual quantities associated to forces and torques per unit length are corotational deformation and curvature, respectively.

1.2.5 Equilibrium relations

The Principle of Virtual work gives us the variational equation of a beam:

$$\mathcal{P}_{acc}(\Phi, \delta\Phi) + \mathcal{P}_i(\Phi, \delta\Phi) = \mathcal{P}_e(\Phi, \delta\Phi). \tag{1.62}$$

Considering a bounded beam of length L, we have after integrating by parts:

$$\mathcal{P}_i(\Phi, \delta\Phi) = \Big[\mathbf{N}\cdot\delta\boldsymbol{\varphi} + \mathbf{M}\cdot\delta\boldsymbol{\omega}\Big]_0^L - \int_{\mathcal{C}} \frac{\partial \mathbf{N}}{\partial S}\cdot\delta\boldsymbol{\varphi} + \left(\frac{\partial \boldsymbol{\varphi}}{\partial S}\times\mathbf{N} + \frac{\partial \mathbf{M}}{\partial S}\right)\cdot\delta\boldsymbol{\omega}\,\mathrm{d}S.$$

Using the previous results, we obtain $\forall\ (\delta\boldsymbol{\varphi}, \delta\boldsymbol{\omega}) \in \mathbf{W}$:

$$\Big[\mathbf{N}\cdot\delta\boldsymbol{\varphi} + \mathbf{M}\cdot\delta\boldsymbol{\omega}\Big]_0^L = \int_{\mathcal{C}} \left(\frac{\partial \mathbf{N}}{\partial S} + \mathbf{q} - \rho_0 A\,\frac{\partial^2\boldsymbol{\varphi}}{\partial t^2}\right)\cdot\delta\boldsymbol{\varphi}\,\mathrm{d}S \tag{1.63}$$

$$+ \int_{\mathcal{C}} \left(\frac{\partial \mathbf{M}}{\partial S} + \frac{\partial \boldsymbol{\varphi}}{\partial S}\times\mathbf{N} + \mathbf{m} - \rho_0\frac{\partial(\mathbb{I}\,\boldsymbol{\omega})}{\partial t}\right)\cdot\delta\boldsymbol{\omega}\,\mathrm{d}S. \tag{1.64}$$

This equation may help to obtain the strong formulation of dynamic equation of the beam-structure under finite transformation. Since (1.63) is valid for any motion $(\delta\boldsymbol{\varphi}, \delta\boldsymbol{\omega})$, therefore:

$$\begin{aligned} \frac{\partial \mathbf{N}}{\partial S} + \mathbf{q} &= \rho_0 A\,\frac{\partial^2\boldsymbol{\varphi}}{\partial t^2}, \\ \frac{\partial \mathbf{M}}{\partial S} + \frac{\partial \boldsymbol{\varphi}}{\partial S}\times\mathbf{N} + \mathbf{m} &= \rho_0\frac{\partial(\mathbb{I}\,\boldsymbol{\omega})}{\partial t}. \end{aligned} \tag{1.65}$$

With the boundary conditions

$$\begin{aligned} \mathbf{N}(0,t) &= \mathbf{N}_0(t), \quad \text{or} \quad \frac{\partial\boldsymbol{\varphi}}{\partial S}(0,t) = 0, \\ \mathbf{M}(0,t) &= \mathbf{M}_0(t), \quad \text{or} \quad \boldsymbol{\omega}(0,t) = 0, \\ \mathbf{N}(L,t) &= \mathbf{N}_L(t), \quad \text{or} \quad \frac{\partial\boldsymbol{\varphi}}{\partial S}(L,t) = 0, \\ \mathbf{M}(L,t) &= \mathbf{M}_L(t), \quad \text{or} \quad \boldsymbol{\omega}(L,t) = 0. \end{aligned} \tag{1.66}$$

In the following and for the sake of brevity, $\mathbf{q}$ and $\mathbf{m}$ are set to zero, unless stated otherwise.

Remark. Our approach is written as a Lagrangian problem where a coordinate material (ξ_1, ξ_2, S) was introduced. In addition, kinematical and dynamical variables were written in the material basis $(\mathbf{d_1}, \mathbf{d_2}, \mathbf{d_3})$.
One can adapt an Eulerian mechanical approach where we can describe the fiber in the Cartesian mechanics, also one can solve the problem of a beam subjected to dead load using Eulerian formulation.

Scalar equilibrium

Keeping in mind that we have a moving director frame, so, the derivative of any vector function $\mathbf{f}(S,t)$ is written in the director frame as $\mathbf{f}(S,t) = f_i(S,t)\mathbf{d_i}(S,t)$ is:

$$\frac{\partial \mathbf{f}}{\partial S} = \frac{\partial f_i}{\partial S}\mathbf{d_i} + f_i\frac{\partial \mathbf{d_i}}{\partial S}. \tag{1.67}$$

However, $\dfrac{\partial \mathbf{d_i}}{\partial S}$ is given by (1.17), therefore,

$$\begin{aligned}
\frac{\partial \mathbf{f}}{\partial S}\cdot\mathbf{d_1} &= \frac{\partial f_1}{\partial S} - f_2\kappa_3 + f_3\kappa_2,\\
\frac{\partial \mathbf{f}}{\partial S}\cdot\mathbf{d_2} &= \frac{\partial f_2}{\partial S} - f_3\kappa_1 + f_1\kappa_3,\\
\frac{\partial \mathbf{f}}{\partial S}\cdot\mathbf{d_3} &= \frac{\partial f_3}{\partial S} - f_1\kappa_2 + f_2\kappa_2.
\end{aligned} \tag{1.68}$$

Repeating the same procedure for the time variable t, one obtains:

$$\begin{aligned}
\frac{\partial \mathbf{f}}{\partial t}\cdot\mathbf{d_1} &= \frac{\partial f_1}{\partial t} - f_2\kappa_3 + f_3\kappa_2,\\
\frac{\partial \mathbf{f}}{\partial t}\cdot\mathbf{d_2} &= \frac{\partial f_2}{\partial t} - f_3\kappa_1 + f_1\kappa_3,\\
\frac{\partial \mathbf{f}}{\partial t}\cdot\mathbf{d_3} &= \frac{\partial f_3}{\partial t} - f_1\kappa_2 + f_2\kappa_2.
\end{aligned} \tag{1.69}$$

So first, we observe that

$$\begin{aligned}
\frac{\partial \boldsymbol{\kappa}}{\partial t} = \frac{\partial \kappa_i}{\partial t}\mathbf{d_i} + \kappa_i\frac{\partial \mathbf{d_i}}{\partial t} &\overset{(1.15)}{=} \frac{\partial \kappa_i}{\partial t}\mathbf{d_i},\\
\frac{\partial \boldsymbol{\omega}}{\partial t} = \frac{\partial \omega_i}{\partial t}\mathbf{d_i} + \omega_i\frac{\partial \mathbf{d_i}}{\partial t} &\overset{(1.19)}{=} \frac{\partial \omega_i}{\partial t}\mathbf{d_i}.
\end{aligned} \tag{1.70}$$

Furthermore, variables in (1.65) could be written after projection as

$$\frac{\partial \mathbf{N}}{\partial S} = \begin{cases} \dfrac{\partial N_1}{\partial S} - N_2\kappa_3 + N_3\kappa_2,\\ \dfrac{\partial N_2}{\partial S} - N_3\kappa_1 + N_1\kappa_3,\\ \dfrac{\partial N_3}{\partial S} - N_1\kappa_2 + N_2\kappa_1. \end{cases} \qquad \frac{\partial \mathbf{M}}{\partial S} + \Big(\widetilde{\boldsymbol{\varepsilon}} + \mathbf{d_3}\Big)\times\mathbf{N} = \begin{cases} \dfrac{\partial M_1}{\partial S} - M_2\kappa_3 + M_3\kappa_2 - N_2\Big(\widetilde{\varepsilon}_3 + 1\Big) + N_3\widetilde{\varepsilon}_2,\\ \dfrac{\partial M_2}{\partial S} - M_3\kappa_1 + M_1\kappa_3 - N_3\widetilde{\varepsilon}_1 + N_1\Big(\widetilde{\varepsilon}_3 + 1\Big),\\ \dfrac{\partial M_3}{\partial S} - M_1\kappa_2 + M_2\kappa_1 - N_1\widetilde{\varepsilon}_2 + N_2\widetilde{\varepsilon}_1. \end{cases} \tag{1.71}$$

$$\frac{\partial^2 \boldsymbol{\varphi}}{\partial t^2} = \begin{cases} \dfrac{\partial^2 \varphi_1}{\partial t^2} - 2\dfrac{\partial \varphi_2}{\partial t}\omega_3 + 2\dfrac{\partial \varphi_3}{\partial t}\omega_2 - \varphi_1(\omega_2^2 + \omega_3^2) + \varphi_2(\omega_1\omega_2 - \dfrac{\partial \omega_3}{\partial t}) + \varphi_3(\omega_1\omega_3 + \dfrac{\partial \omega_2}{\partial t}), \\ \dfrac{\partial^2 \varphi_2}{\partial t^2} + 2\dfrac{\partial \varphi_1}{\partial t}\omega_3 - 2\dfrac{\partial \varphi_3}{\partial t}\omega_1 + \varphi_1(\omega_1\omega_2 + \dfrac{\partial \omega_3}{\partial t}) - \varphi_2(\omega_1^2 + \omega_3^2) + \varphi_3(\omega_2\omega_3 - \dfrac{\partial \omega_1}{\partial t}), \\ \dfrac{\partial^2 \varphi_3}{\partial t^2} - 2\dfrac{\partial \varphi_1}{\partial t}\omega_2 + 2\dfrac{\partial \varphi_2}{\partial t}\omega_1 + \varphi_1(\omega_1\omega_3 - \dfrac{\partial \omega_2}{\partial t}) + \varphi_2(\omega_2\omega_3 + \dfrac{\partial \omega_1}{\partial t}) - \varphi_3(\omega_1^2 + \omega_2^2). \end{cases} \tag{1.72}$$

$$\frac{\partial(\mathbb{I}\,\boldsymbol{\omega})}{\partial t} = \begin{cases} I_1\dfrac{\partial \omega_1}{\partial t} + (I_3 - I_2)\omega_2\omega_3, \\ I_2\dfrac{\partial \omega_2}{\partial t} + (I_1 - I_3)\omega_1\omega_3, \\ I_3\dfrac{\partial \omega_3}{\partial t} + (I_2 - I_1)\omega_1\omega_2. \end{cases} \tag{1.73}$$

Where (1.27) has been used. Equilibrium equations written in a scalar form will be:

$$\begin{aligned} \frac{\partial N_1}{\partial S} - N_2\kappa_3 + N_3\kappa_2 &= \rho_0 A\Big(\frac{\partial^2 \varphi_1}{\partial t^2} - 2\frac{\partial \varphi_2}{\partial t}\omega_3 + 2\frac{\partial \varphi_3}{\partial t}\omega_2 - \varphi_1(\omega_2^2 + \omega_3^2) + \varphi_2(\omega_1\omega_2 - \frac{\partial \omega_3}{\partial t}) + \varphi_3(\omega_1\omega_3 + \frac{\partial \omega_2}{\partial t})\Big), \\ \frac{\partial N_2}{\partial S} - N_3\kappa_1 + N_1\kappa_3 &= \rho_0 A\Big(\frac{\partial^2 \varphi_2}{\partial t^2} + 2\frac{\partial \varphi_1}{\partial t}\omega_3 - 2\frac{\partial \varphi_3}{\partial t}\omega_1 + \varphi_1(\omega_1\omega_2 + \frac{\partial \omega_3}{\partial t}) - \varphi_2(\omega_1^2 + \omega_3^2) + \varphi_3(\omega_2\omega_3 - \frac{\partial \omega_1}{\partial t})\Big), \\ \frac{\partial N_3}{\partial S} - N_1\kappa_2 + N_2\kappa_1 &= \rho_0 A\Big(\frac{\partial^2 \varphi_3}{\partial t^2} - 2\frac{\partial \varphi_1}{\partial t}\omega_2 + 2\frac{\partial \varphi_2}{\partial t}\omega_1 + \varphi_1(\omega_1\omega_3 - \frac{\partial \omega_2}{\partial t}) + \varphi_2(\omega_2\omega_3 + \frac{\partial \omega_1}{\partial t}) - \varphi_3(\omega_1^2 + \omega_2^2)\Big). \end{aligned} \tag{1.74}$$

$$\begin{aligned} \frac{\partial M_1}{\partial S} - M_2\kappa_3 + M_3\kappa_2 - N_2\Big(\widetilde{\varepsilon}_3 + 1\Big) + N_3\widetilde{\varepsilon}_2 &= \rho_0\Big(I_1\frac{\partial \omega_1}{\partial t} + (I_3 - I_2)\omega_2\omega_3\Big), \\ \frac{\partial M_2}{\partial S} - M_3\kappa_1 + M_1\kappa_3 - N_3\widetilde{\varepsilon}_1 + N_1\Big(\widetilde{\varepsilon}_3 + 1\Big) &= \rho_0\Big(I_2\frac{\partial \omega_2}{\partial t} + (I_1 - I_3)\omega_1\omega_3\Big), \\ \frac{\partial M_3}{\partial S} - M_1\kappa_2 + M_2\kappa_1 - N_1\widetilde{\varepsilon}_2 + N_2\widetilde{\varepsilon}_1 &= \rho_0\Big(I_3\frac{\partial \omega_3}{\partial t} + (I_2 - I_1)\omega_1\omega_2\Big). \end{aligned} \tag{1.75}$$

1.2.6 Hyperelastic materials

For elastic material stress is related to strain by a constant elasticity tensor C:

$$\mathbf{S} = C\mathbf{E}, \qquad \text{where} \qquad C = \frac{\partial \mathbf{S}}{\partial \mathbf{E}}. \tag{1.76}$$

Since we are interested in large transformation, we adapt hyper-elastic material with an energy density function that relates stress and strain known as Helmotz free energy $\psi(E)$, stress in this case is given by $\mathbf{S} = \dfrac{\partial \psi}{\partial \mathbf{E}}$. Furthermore, C has a major symmetry $C_{IJKL} = C_{KLIJ}$. Then

$$\delta E_{IJ} = \frac{\partial E_{IJ}}{\partial \widetilde{\varepsilon}_l}\delta\widetilde{\varepsilon}_l + \frac{\partial E_{IJ}}{\partial \kappa_l}\delta\kappa_l.$$

Where κ_i and $\widetilde{\varepsilon}_i$ are components of the strain vectors in the current configuration: $\boldsymbol{\kappa} = \kappa_i \mathbf{d_i}$ and $\widetilde{\boldsymbol{\varepsilon}} = \widetilde{\varepsilon}_i \mathbf{d_i}$.

Keeping in mind that $\mathbf{P} : \delta\mathbf{F} = \mathbf{S} : \delta\mathbf{E}$, so, computation of virtual work gives:

$$\mathcal{P}_i(\Phi, \delta\Phi) = \int_{\mathcal{B}} \mathbf{S} : \delta\mathbf{E} \, \mathrm{d}V = \int_{\mathcal{C}} \int_{\mathcal{S}} \frac{\partial \psi}{\partial \widetilde{\varepsilon}_i} \delta\widetilde{\varepsilon}_i + \frac{\partial \psi}{\partial \kappa_i} \delta\kappa_i \, \mathrm{d}A\mathrm{d}S. \tag{1.77}$$

Direct identification with Eq.1.61 gives the components on the $\{\mathbf{d_i}\}$-basis:

$$N_i = \int_{\mathcal{S}} \frac{\partial \psi}{\partial \widetilde{\varepsilon}_i} \, \mathrm{d}A, \qquad M_i = \int_{\mathcal{S}} \frac{\partial \psi}{\partial \kappa_i} \, \mathrm{d}A. \tag{1.78}$$

Because, $\widetilde{\varepsilon}_i$ and κ_i are uniform on the section $\mathcal{S}$, the integration and derivation may be switched to give:

$$\mathbf{N} = \frac{\partial \Psi}{\partial \widetilde{\varepsilon}_i} \mathbf{d_i}, \qquad \mathbf{M} = \frac{\partial \Psi}{\partial \kappa_i} \mathbf{d_i}, \tag{1.79}$$

where Ψ is the free energy density per unit length of the beam-structure:

$$\Psi := \int_{\mathcal{S}} \psi \, \mathrm{d}A.$$

This formulation is valid for any hyperelastic model.

A large variety of hyperelastic models is possible (*e.g.*[GS08]) such as:

— St. Venant-Kirchhoff model:

$$\psi(\mathbf{E}) = \frac{\lambda}{2}(Tr(\mathbf{E}))^2 + \mu(Tr(\mathbf{E}^2)), \tag{1.80}$$

with the standard Lamé coefficients $\lambda, \mu > 0$.

— Neo-Hookean model:

$$\psi(\mathbf{C}) = a(Tr(\mathbf{C})) + \Gamma(\sqrt{det\mathbf{C}}), \tag{1.81}$$

with $\mathbf{C} = \mathbf{F}^T\mathbf{F}, \Gamma(x) = cx^2 - d\,ln(x)$ and $a, c, d > 0$.

— Mooney-Rivlin model:

$$\psi(\mathbf{C}) = a(Tr(\mathbf{C})) + b\,Tr(det(\mathbf{C})\mathbf{C}^{-1})) + \Gamma(\sqrt{det\mathbf{C}}), \tag{1.82}$$

with $a, b, c, d > 0$.

For example, St. Venant-Kirchhoff model is applied for metalic material and Neo-Hookean and Mooney-Rivlin model are mainly used for rubber-like material.

Remark. *Our main objective is to study elastic behaviour, so it seems convenient to focus only on St. Venant-Kirchhoff model for which stress is given linearly in terms of E:*

$$\mathbf{S} = \lambda tr(\mathbf{E})I + 2\mu\mathbf{E}. \tag{1.83}$$

1.2.7 Energy, internal forces and moments

The aim of this section is to find internal forces and moments, hence it is essential to calculate $\Psi(\mathbf{E})$. Knowing that

$$\mathbf{E} = \frac{1}{2}\begin{pmatrix} 0 & 0 & Z_1 \\ 0 & 0 & Z_2 \\ Z_1 & Z_2 & Z_1^2 + Z_2^2 + 2Z_3 + Z_3^2 \end{pmatrix}. \tag{1.84}$$

With $\mathbf{Z} = Z_1\mathbf{d_1} + Z_2\mathbf{d_2} + Z_3\mathbf{d}_3 := \widetilde{\boldsymbol{\varepsilon}} + \boldsymbol{\kappa} \times \mathbf{GM}$, therefore, by (1.80) energy is given by:

$$\psi(E) = \frac{1}{8}\Big(\lambda(Z_1^2 + Z_2^2 + 2Z_3 + Z_3^2)^2 + 2\mu\Big(2Z_1^2 + 2Z_2^2 + (Z_1^2 + Z_2^2 + 2Z_3 + Z_3^2)^2\Big)\Big). \tag{1.85}$$

Noting the fact that:

$$\begin{aligned} Z_1 &= \widetilde{\varepsilon}_1 - \kappa_3\xi_2, \\ Z_2 &= \widetilde{\varepsilon}_2 + \kappa_3\xi_1, \\ Z_3 &= \widetilde{\varepsilon}_3 + \kappa_1\xi_2 - \kappa_2\xi_1. \end{aligned} \tag{1.86}$$

We rewrite the volumic density of energy at any point (S, ξ_1, ξ_2) of the beam with respect to $(\kappa_i, \widetilde{\varepsilon}_i)$:

$$\psi(\widetilde{\boldsymbol{\varepsilon}}, \boldsymbol{\kappa}) = \frac{1}{2}\mu(\widetilde{\varepsilon}_1^2 + \widetilde{\varepsilon}_2^2) + \frac{1}{2}(\lambda + 2\mu)\widetilde{\varepsilon}_3^2 + \frac{1}{2}(\lambda + 2\mu)(\kappa_1^2\xi_2^2 + \kappa_2^2\xi_1^2) + \frac{1}{2}\mu(\xi_1^2 + \xi_2^2)\kappa_3 + \Psi^*(\widetilde{\boldsymbol{\varepsilon}}, \boldsymbol{\kappa}). \tag{1.87}$$

Integrating (1.87) on the section we obtain the energy density per unit length of the beam-structure:

$$\Psi(\widetilde{\boldsymbol{\varepsilon}}, \boldsymbol{\kappa}) = \frac{1}{2}\mu(A\widetilde{\varepsilon}_1^2 + A\widetilde{\varepsilon}_2^2) + \frac{1}{2}(\lambda + 2\mu)A\widetilde{\varepsilon}_3^2 + \frac{1}{2}(\lambda + 2\mu)(I_1\kappa_1^2 + I_2\kappa_2^2) + \frac{1}{2}\mu I_3\kappa_3^2 + \int_{\mathcal{S}} \Psi^* d\mathcal{S}. \tag{1.88}$$

Where $\int_{\mathcal{S}} \Psi^* d\mathcal{S}$ is a higher order polynomial that depends highly on the shape of the section, $\mathcal{S}$ is the cross-section, A is the area of the cross-section and I_1, I_2 and I_3 are the quadratic moments of acceleration. Note that we model our problem by assuming that the sections are rigid, this leads to $I_3 = I_1 + I_2$. This is not true in the general case (*e.g.* [Lur05]).
Keeping in mind that forces and moments are given by:

$$N_i = \frac{\partial \Psi}{\partial \widetilde{\varepsilon}_i}, \qquad M_i = \frac{\partial \Psi}{\partial \kappa_i}, \tag{1.89}$$

therefore,

$$\begin{aligned}
N_1 &= \mu A\widetilde{\varepsilon}_1 + \int_{\mathcal{S}} \frac{\partial \Psi^*}{\partial \widetilde{\varepsilon}_1} d\mathcal{S} \qquad N_2 = \mu A\widetilde{\varepsilon}_2 + \int_{\mathcal{S}} \frac{\partial \Psi^*}{\partial \widetilde{\varepsilon}_2} d\mathcal{S}, && \text{shear forces.} \\
N_3 &= (\lambda + 2\mu) A\widetilde{\varepsilon}_3 + \int_{\mathcal{S}} \frac{\partial \Psi^*}{\partial \widetilde{\varepsilon}_3} d\mathcal{S}, && \text{normal force.} \\
M_1 &= (\lambda + 2\mu) I_1 \kappa_1 + \int_{\mathcal{S}} \frac{\partial \Psi^*}{\partial \kappa_1} d\mathcal{S} \qquad M_2 = (\lambda + 2\mu) I_1 \kappa_2 + \int_{\mathcal{S}} \frac{\partial \Psi^*}{\partial \kappa_2} d\mathcal{S}, && \text{bending moments.} \\
M_3 &= \mu I_3 \kappa_3 + \int_{\mathcal{S}} \frac{\partial \Psi^*}{\partial \kappa_3} d\mathcal{S}, && \text{torsional moment.}
\end{aligned} \tag{1.90}$$

1.3 Dimensionless procedure

We introduce a non-dimensional formulation of the problem thanks to the gyration radius and Timoshenko cutoff frequency:

$$\varrho = \sqrt{\frac{I_1 + I_2}{A}}, \qquad \omega_c = \frac{1}{\varrho}\sqrt{\frac{\mu}{\rho_0}}. \tag{1.91}$$

A non-dimensional bulk-shear ratio is introduced too:

$$g := \frac{\lambda + 2\mu}{\mu}.$$

In term of magnitude $\varrho = \mathcal{O}(R)$, where R is a typical size of the cross-section. In the same spirit, ω_c around the frequency of a elastic shear wave (celerity $\sim \sqrt{\mu/\rho_0}$) having for wavelength ϱ. It is worthy to mention the relation between Lamé constants, Poisson's ration ν, Young modulus E and the shear modulus $G := \mu$ (including eventually a shear correction factor [Tim21]). In fact

$$\begin{aligned}
\lambda &= \frac{E\nu}{(1+\nu)(1-2\nu)}, & 2(1+\nu) &= \frac{E}{\mu}. \\
E &= \mu\frac{3\lambda + 2\mu}{\lambda + \mu}, & \nu &= \frac{\lambda}{2(\lambda+\mu)}.
\end{aligned} \tag{1.92}$$

Hence, $g \simeq 2(1+\nu)$, in addition:

$$\boxed{2 \lesssim g \lesssim 3.}$$

Regarding the geometrical shape of the cross-section and without loss of generality, we suppose that $I_1 \leq I_2 < I_3$, therefore, a cross-section parameter e is eventually introduced [For+16], satisfying:

$$e = \frac{I_1}{I_2} \tag{1.93}$$

In which e measures the slenderness of the section shape, we have:

$$\boxed{0 < e \leq 1}.$$

1.3.1 Non-dimensional variables and relations

The non dimensional length (slenderness ratio), abscissa and time are:

$$\ell = \frac{L}{\varrho}, \quad s = \frac{S}{\varrho}, \quad t = \omega_c \underline{t}.$$

where $\underline{t}$ is the physical time and the notation t is now used for the non-dimensional time. With the same convention, for any physical variables $\underline{v}(S, \underline{t})$ previously mentioned, we can associate a non-dimensional companion $v(s, t)$ as follows:

$$\begin{gathered} \widetilde{\varepsilon}_i(s,t) = \underline{\widetilde{\varepsilon}}_i(S,\underline{t}), \qquad \kappa_i(s,t) = \varrho\, \underline{\kappa}_i(S,\underline{t}), \qquad \omega_i(s,t) = \frac{1}{\omega_c}\, \underline{\omega}_i(S,\underline{t}), \\ \varphi_i(s,t) = \frac{1}{\varrho}\, \underline{\varphi}_i(S,\underline{t}), \qquad \theta_i(s,t) = \underline{\theta}_i(S,\underline{t}). \end{gathered} \tag{1.94}$$

1.3.2 Non-dimensional forces, moments and energy density

It is interesting to observe that physical force and moment $\underline{\mathbf{N}}(S, \underline{t})$ and $\underline{\mathbf{M}}(S, \underline{t})$ have also non-dimensional form $\mathbf{N}(s, t)$ and $\mathbf{M}(s, t)$ related by

$$\mathbf{N} = \frac{1}{GA}\underline{\mathbf{N}}, \qquad \mathbf{M} = \frac{1}{\varrho}\frac{1}{GA}\underline{\mathbf{M}}.$$

Remark. *In addition to linear material constitutive laws, we consider all along this manuscript linear constitutive laws in terms of $\boldsymbol{\kappa}$ and $\widetilde{\boldsymbol{\varepsilon}}$, so, it seems convenient to impose $\Psi^* = 0$.*

In this case $\lambda + 2\mu \simeq E$ and

$$g := \frac{E}{G}.$$

For later convenience, let us introduce

$$\boldsymbol{\varepsilon} := \frac{\partial \boldsymbol{\varphi}}{\partial S} = \widetilde{\boldsymbol{\varepsilon}} + \mathbf{d_3}. \tag{1.95}$$

Hence, non-dimensional quadratic density energy per unit length is given by:

$$\boxed{\Psi = \frac{1}{2}\Big(\varepsilon_1^2 + \varepsilon_2^2 + g(\varepsilon_3 - 1)^2 + \frac{eg}{1+e}\kappa_1^2 + \frac{g}{1+e}\kappa_2^2 + \kappa_3^2\Big).} \tag{1.96}$$

And, non-dimensional dynamical components will be:

$$\boxed{\begin{array}{lcll} N_1 & = & \varepsilon_1, & M_1 = \dfrac{ge}{1+e}\kappa_1. \\ N_2 & = & \varepsilon_2, & M_2 = \dfrac{g}{1+e}\kappa_2. \\ N_3 & = & g(\varepsilon_3 - 1), & M_3 = \kappa_3. \end{array}} \tag{1.97}$$

It should be mentioned that our approach is general, therefore, we can also adapt a non-linear

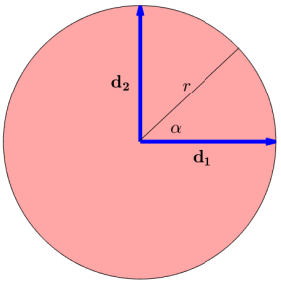

Figure 1.2 – *Circular cross-section.*

constitutive laws. As an example, we consider a beam with circular cross-section

for which $I_1 = I_2$, therefore, $e = 1$. So, by taking the polar coordinates we define ξ as:

$$\begin{array}{rcl} \xi_1 & = & r\cos\alpha, \\ \xi_1 & = & r\sin\alpha. \end{array} \tag{1.98}$$

Where $0 \leq r \leq R$ and $0 \leq \alpha \leq 2\pi$ (Figure 1.2). Straight forward calculation gives

$$\begin{aligned} N_1 &= \frac{1}{4}\left(\varepsilon_1\left(g\left(\kappa_1^2+\kappa_2^2+4\kappa_3^2+2\varepsilon_2^2+2(\varepsilon_3^2-1)\right)+4\right)-2g\varepsilon_3\kappa_1\kappa_3+2g\varepsilon_1^3\right), \\ N_2 &= \frac{1}{4}\left(\varepsilon_2\left(g\left(\kappa_1^2+\kappa_2^2+4\kappa_3^2+2\varepsilon_1^2+2(\varepsilon_3^2-1)\right)+4\right)-2g\kappa_2\kappa_3\varepsilon_3+2g\varepsilon_2^3\right), \\ N_3 &= \frac{1}{4}g\varepsilon_3\left(2\kappa_3^2-2\kappa_3\left(\kappa_1\varepsilon_1+\kappa_2\varepsilon_2\right)+\varepsilon_3\left(3\left(\kappa_1^2+\kappa_2^2\right)+2\varepsilon_1^2+2\varepsilon_2^2+2\left(\varepsilon_3^2-1\right)\right)\right), \\ M_1 &= \frac{1}{12}g\left(3\kappa_1^3+\kappa_1\left(4\kappa_3^2+3\left(\kappa_2^2+\varepsilon_1^2+\varepsilon_2^2+3\varepsilon_3^2-1\right)\right)-6\kappa_3\varepsilon_1\varepsilon_3\right), \\ M_2 &= \frac{1}{12}g\left(3\kappa_2^3+\kappa_2\left(4\kappa_3^2+3\left(\kappa_1^2+\varepsilon_1^2+\varepsilon_2^2+3\varepsilon_3^2-1\right)\right)-6\kappa_3\varepsilon_2\varepsilon_3\right), \\ M_3 &= \frac{1}{6}\left(4g\kappa_3^3+\kappa_3\left(g\left(2\left(\kappa_1^2+\kappa_2^2\right)+6\varepsilon_1^2+6\varepsilon_2^2+3\left(\varepsilon_3^2-1\right)\right)+6\right)-3g\varepsilon_3\left(\kappa_1\varepsilon_1+\kappa_2\varepsilon_2\right)\right). \end{aligned} \tag{1.99}$$

This is out of our scope and from now on, we focus only on linear constitutive laws.

1.3.3 Non-dimensional equilibrium equations

Using the fact that $\frac{\partial f}{\partial S} = \frac{1}{\varrho}\frac{\partial f}{\partial s}$ and $\frac{\partial f}{\partial \underline{t}} = \omega_c \frac{\partial f}{\partial t}$ for any function $f(s,t)$ and by injecting (1.94) into (1.74)-(1.75) one obtains:

$$\frac{GA}{\varrho}(\varepsilon_1' - \varepsilon_2\kappa_3) + \frac{EA}{\varrho}(-1+\varepsilon_3)\kappa_2 = \rho_0 A\omega_c^2\varrho\Big(\ddot{\varphi}_1 - 2\dot{\varphi}_2\omega_3 + 2\dot{\varphi}_3\omega_2 - \varphi_1(\omega_2^2+\omega_3^2) + \varphi_2(\omega_1\omega_2 - \dot{\omega}_3) + \varphi_3(\omega_1\omega_3 + \dot{\omega}_2)\Big),$$

$$\frac{GA}{\varrho}(\varepsilon_2' + \varepsilon_1\kappa_3) + \frac{EA}{\varrho}(-1+\varepsilon_3)\kappa_1 = \rho_0 A\omega_c^2\varrho\Big(\ddot{\varphi}_2 + 2\dot{\varphi}_1\omega_3 - 2\dot{\varphi}_3\omega_1 + \varphi_1(\omega_1\omega_2 + \dot{\omega}_3) - \varphi_2(\omega_1^2+\omega_3^2) + \varphi_3(\omega_2\omega_3 - \dot{\omega}_1)\Big),$$

$$\frac{EA}{\varrho}\varepsilon_3' + \frac{GA}{\varrho}(\varepsilon_2\kappa_1 - \varepsilon_1\kappa_2) = \rho_0 A\omega_c^2\varrho\Big(\ddot{\varphi}_3 - 2\dot{\varphi}_1\omega_2 + 2\dot{\varphi}_2\omega_1 + \varphi_1(\omega_1\omega_3 - \dot{\omega}_2) + \varphi_2(\omega_2\omega_3 + \dot{\omega}_1) - \varphi_3(\omega_1^2+\omega_2^2)\Big). \quad (1.100)$$

$$\frac{EI_1}{\varrho^2}\kappa_1' + EA\varepsilon_2(\varepsilon_3 - 1) - GA\varepsilon_2\varepsilon_3 + \frac{EI_3}{\varrho^2}\kappa_2\kappa_3 - \frac{EI_2}{\varrho^2}\kappa_2\kappa_3 = \rho_0\omega_c^2\Big(I_1\dot{\omega}_1 + (I_3 - I_2)\omega_2\omega_3\Big),$$

$$\frac{EI_2}{\varrho^2}\kappa_2' - EA\varepsilon_1(\varepsilon_3 - 1) + GA\varepsilon_1\varepsilon_3 - \frac{EI_3}{\varrho^2}\kappa_1\kappa_3 + \frac{EI_1}{\varrho^2}\kappa_1\kappa_3 = \rho_0\omega_c^2\Big(I_2\dot{\omega}_2 + (I_1 - I_3)\omega_1\omega_3\Big),$$

$$GA\kappa_3' + EAI_2\kappa_1\kappa_2 - EAI_1\kappa_1\kappa_2 = \rho_0\omega_c^2\Big(I_3\dot{\omega}_3 + (I_2 - I_1)\omega_1\omega_2\Big).$$

where the conventions $\frac{\partial f}{\partial s} \equiv f'$ and $\frac{\partial f}{\partial t} \equiv \dot{f}$ are used.
Now multiplying the first three equations by $\frac{\varrho}{GA}$ we obtain:

$$\varepsilon_1' - \varepsilon_2\kappa_3 + g(-1+\varepsilon_3)\kappa_2 = \ddot{\varphi}_1 - 2\dot{\varphi}_2\omega_3 + 2\dot{\varphi}_3\omega_2 - \varphi_1(\omega_2^2+\omega_3^2) + \varphi_2(\omega_1\omega_2 - \dot{\omega}_3) + \varphi_3(\omega_1\omega_3 + \dot{\omega}_2),$$

$$\varepsilon_2' + \varepsilon_1\kappa_3 - g(-1+\varepsilon_3)\kappa_1 = \ddot{\varphi}_2 + 2\dot{\varphi}_1\omega_3 - 2\dot{\varphi}_3\omega_1 + \varphi_1(\omega_1\omega_2 + \dot{\omega}_3) - \varphi_2(\omega_1^2+\omega_3^2) + \varphi_3(\omega_2\omega_3 - \dot{\omega}_1),$$

$$g\varepsilon_3' + \varepsilon_2\kappa_1 - \varepsilon_1\kappa_2 = \ddot{\varphi}_3 - 2\dot{\varphi}_1\omega_2 + 2\dot{\varphi}_2\omega_1 + \varphi_1(\omega_1\omega_3 - \dot{\omega}_2) + \varphi_2(\omega_2\omega_3 + \dot{\omega}_1) - \varphi_3(\omega_1^2+\omega_2^2). \quad (1.101)$$

Multiplying the last three equations by $\frac{1}{GA}$ and taking into consideration that $I_1 = \frac{eA\varrho^2}{1+e}$, $I_2 = \frac{A\varrho^2}{1+e}$, $I_3 = A\varrho^2$ and $\frac{\rho_0\omega_c^2\varrho^2}{G} = 1$ to get:

$$\begin{aligned}
\frac{ge}{1+e}\kappa_1' + g\varepsilon_2(\varepsilon_3 - 1) - \varepsilon_2\varepsilon_3 + \frac{1+e-g}{1+e}\kappa_2\kappa_3 &= \frac{e}{1+e}\Big(\dot{\omega}_1 - \omega_2\omega_3\Big),\\
\frac{g}{1+e}\kappa_2' - g\varepsilon_1(\varepsilon_3 - 1) + \varepsilon_1\varepsilon_3 + \frac{e(g-1)-1}{1+e}\kappa_1\kappa_3 &= \frac{1}{1+e}\Big(\dot{\omega}_2 - \omega_1\omega_3\Big),\\
\kappa_3' + \frac{g(1-e)}{1+e}\kappa_1\kappa_2 &= \dot{\omega}_3 - \frac{1-e}{1+e}\omega_1\omega_2.
\end{aligned} \tag{1.102}$$

Remark. We can rewrite (1.101) and (1.102) in terms of φ_i and ω_i by using the fact that (1.95) in a non-dimensional form is:

$$\begin{aligned}
\varepsilon_1 &= \varphi_1' + \varphi_3\kappa_2 - \varphi_2\kappa_3,\\
\varepsilon_2 &= \varphi_2' + \varphi_1\kappa_3 - \varphi_3\kappa_1,\\
\varepsilon_3 &= \varphi_3' + \varphi_2\kappa_2 - \varphi_1\kappa_2.
\end{aligned} \tag{1.103}$$

Remark. As seen in (1.101) and(1.102), static equilibrium is a first order differential system with respect to strains, so this equilibrium is controlled only by κ_i and ε_i, this idea will be essential in our analysis in Chapter three and four.

1.3.4 Planar case

For motion in the plane $(\mathbf{d_1}, \mathbf{d_3})$, the kinematics of the beam is governed by the placement

$$\underline{\boldsymbol{\varphi}}(S, \underline{t}) = \underline{\varphi_1}\mathbf{d_1} + \underline{\varphi_3}\mathbf{d_3}. \tag{1.104}$$

And a rotation tensor, that is controlled by a unique scalar angle $\underline{\theta}(S, \underline{t})$ measuring the rotation of the section around $\mathbf{d_2}$ (in a trigonometric way). Hence, $\mathbf{R}(S, \underline{t})$ is

$$\mathbf{R} = \begin{pmatrix} \cos\underline{\theta} & 0 & \sin\underline{\theta} \\ 0 & 1 & 0 \\ -\sin\underline{\theta} & 0 & \cos\underline{\theta} \end{pmatrix}. \tag{1.105}$$

Therefore,

$$\frac{\partial \mathbf{R}}{\partial S}\mathbf{R}^T = \begin{pmatrix} 0 & 0 & \frac{\partial\underline{\theta}}{\partial S} \\ 0 & 0 & 0 \\ -\frac{\partial\underline{\theta}}{\partial S} & 0 & 0 \end{pmatrix}, \qquad \frac{\partial \mathbf{R}}{\partial t}\mathbf{R}^T = \begin{pmatrix} 0 & 0 & \frac{\partial\underline{\theta}}{\partial t} \\ 0 & 0 & 0 \\ -\frac{\partial\underline{\theta}}{\partial t} & 0 & 0 \end{pmatrix}. \tag{1.106}$$

In consequence, spin and twist may be expressed as :

$$\begin{aligned} \underline{\boldsymbol{\kappa}}(S,\underline{t}) &= \underline{\kappa_2}\mathbf{d_2}, \qquad \text{with} \quad \underline{\kappa_2}(S,\underline{t}) = \frac{\partial \underline{\theta}}{\partial S}. \\ \underline{\boldsymbol{\omega}}(S,\underline{t}) &= \underline{\omega_2}\mathbf{d_2}, \qquad \text{with} \quad \underline{\omega_2}(S,\underline{t}) = \frac{\partial \underline{\theta}}{\partial t}. \end{aligned} \tag{1.107}$$

Note that for this plane motion $\mathbf{d_2} = \mathbf{e_y}$ is neither time nor space dependent.
Straight forward computations show that for large transformation, the components of $\boldsymbol{\varepsilon}$ in the moving directors frame are:

$$\underline{\varepsilon_1}(S,\underline{t}) = \frac{\partial \underline{\varphi_1}}{\partial S} + \underline{\varphi_3}\underline{\kappa_2}, \qquad \underline{\varepsilon_2}(S,\underline{t}) = 0, \qquad \underline{\varepsilon_3}(S,\underline{t}) = \frac{\partial \underline{\varphi_3}}{\partial S} - \underline{\varphi_1}\underline{\kappa_2}. \tag{1.108}$$

Internal energy, forces and moments, equilibrium relations

Keeping in mind that a Kirchhoff-Saint Venant model of isotropic material is used for which the Helmholtz free energy per unit length is quadratic with regard to strain measures:

$$\Psi = \frac{1}{2}AG\underline{\varepsilon_1}^2 + \frac{1}{2}AE(\underline{\varepsilon_3} - 1)^2 + \frac{1}{2}EI_2\underline{\kappa_2}^2. \tag{1.109}$$

Hence, the stress resultants depend linearly on the conjugate strains:

$$\begin{aligned} \underline{N_1} &= GA\,\underline{\varepsilon_1}, && \text{shear force.} \\ \underline{N_3} &= EA\,(\underline{\varepsilon_3} - 1), && \text{normal force.} \\ \underline{M_2} &= EI_2\,\underline{\kappa_2} && \text{bending moment.} \end{aligned} \tag{1.110}$$

In the directors frame, force and moment vectors are:

$$\underline{\mathbf{N}}(S,\underline{t}) = \underline{N_1}\mathbf{d_1} + \underline{N_3}\mathbf{d_3}, \qquad \underline{\mathbf{M}}(S,\underline{t}) = \underline{M_2}\mathbf{d_2}.$$

Equilibrium relations are (*e.g.* [LMLR18]):

$$\begin{aligned} \frac{\partial \underline{\mathbf{N}}}{\partial S} + \underline{\boldsymbol{q}} &= \rho_0 A\,\frac{\partial^2 \underline{\boldsymbol{\varphi}}}{\partial \underline{t}^2}, \\ \frac{\partial \underline{\mathbf{M}}}{\partial S} + \underline{\boldsymbol{\varepsilon}} \times \underline{\mathbf{N}} + \underline{\boldsymbol{m}} &= \rho_0 I_2\,\frac{\partial^2 \theta}{\partial \underline{t}^2}. \end{aligned} \tag{1.111}$$

Using (1.15) and projecting the first equation onto $\mathbf{d_1}$ and $\mathbf{d_3}$ and the second onto $\mathbf{d_2}$ one obtains respectively:

$$\begin{aligned} GA\frac{\partial \underline{\varepsilon_1}}{\partial S} + EA(\underline{\varepsilon_3}-1)\underline{\kappa_2} + \underline{q_1} &= \rho_0 A\Big(\frac{\partial^2 \underline{\varphi_1}}{\partial \underline{t}^2} + 2\frac{\partial \underline{\varphi_3}}{\partial \underline{t}}\frac{\partial \underline{\theta}}{\partial \underline{t}} - \underline{\varphi_1}\frac{\partial \underline{\theta}}{\partial \underline{t}}^2 + \underline{\varphi_3}\frac{\partial^2 \underline{\theta}}{\partial \underline{t}^2}\Big), \\ EA\frac{\partial \underline{\varepsilon_3}}{\partial S} - GA\underline{\varepsilon_1}\underline{\kappa_2} + \underline{q_3} &= \rho_0 A\Big(\frac{\partial^2 \underline{\varphi_3}}{\partial \underline{t}^2} - 2\frac{\partial \underline{\varphi_1}}{\partial \underline{t}}\frac{\partial \underline{\theta}}{\partial \underline{t}} - \underline{\varphi_3}\frac{\partial \underline{\theta}}{\partial \underline{t}}^2 - \underline{\varphi_1}\frac{\partial^2 \underline{\theta}}{\partial \underline{t}^2}\Big), \\ EI\frac{\partial \underline{\kappa_2}}{\partial S} - EA\underline{\varepsilon_1}(\underline{\varepsilon_3}-1) + GA\underline{\varepsilon_1}\underline{\varepsilon_3} + \underline{m_2} &= \rho_0 I_2\frac{\partial^2 \underline{\theta}}{\partial \underline{t}^2}. \end{aligned} \tag{1.112}$$

where (1.110) has been used.

Dimensionless form

In this case one choose $\varrho = \sqrt{\dfrac{I_2}{A}}$ and $e = 0$, therefore, dimensionless equilibrium (1.112) will be:

$$\boxed{\begin{aligned} \varepsilon_1' + g(\varepsilon_3-1)\kappa_2 + q_1 &= \ddot{\varphi_1} + 2\dot{\varphi_3}\dot{\theta} - \varphi_1\dot{\theta}^2 + \varphi_3\ddot{\theta}, \\ g\varepsilon_3' - \varepsilon_1\kappa_2 + q_3 &= \ddot{\varphi_3} - 2\dot{\varphi_1}\dot{\theta} - \varphi_3\dot{\theta}^2 - \varphi_1\ddot{\theta}, \\ g\kappa_2' + \varepsilon_1\varepsilon_3 - g\varepsilon_1(\varepsilon_3-1) + m_2 &= \ddot{\theta}. \end{aligned}} \tag{1.113}$$

Note that $\mathbf{q}$ and $\mathbf{m}$ will play an essential role in the next chapter.

1.4 Conclusion

In this chapter, we gave the general formulation of our problem in a dimensionless way, equilibrium equations of a Timoshenko beam was obtained by using the principal of virtual work. This equilibrium is given for hyperelastic material by using the Saint Venant Kirchhoff model.

Chapter 2

Timoshenko beam and Winkler foundation

The most common model for the elastic foundation is the Winkler model [Win67], which regards the foundation as a series of separated springs without coupling effects between each other. Many scientists aimed to study this foundation. Among them, Lee [Lee98] conducted the dynamic response of a Timoshenko beam on a Winkler foundation subjected to a moving mass. He found that the separation of the mass from the beam may be avoided by the presence of an Elastic foundation of large stiffness. Later on, Ergüven and Gedikli [EG03] presented a fast and accurate finite element method for Timoshenko beam on winkler foundation. A while later, Ruge and Birk [RB07] compared infinite Timoshenko and Euler–Bernoulli beam models on Winkler foundation in the frequency- and time-domain and concluded that Timoshenko beam is more advantage when dealing with transient dynamic problems in unbounded domains. Latter, Ghannadiasl and Mofid [GM15] conducted vibration of elastically restrained Timoshenko beam on a partially Winkler by the mean of dynamic green function where numerical examples are shown to illustrate the efficiency and simplicity of the new formulation based on the Green function.

In this chapter, we consider planar Timoshenko beam with linear constitutive laws and linear geometrical stress-strain relations that lie on Winkler foundation.
We start by studying in a dynamical way the impact of the rigid wall on a Timoshenko beam where exact solutions were found by applying the modal analysis and by imposing choc type boundary conditions. Then we deduce the dispersion relation when this wall is elastic, this relation will depend highly on the wall rigidity. Later, a finite longitudinal load is imposed at the boundary but the beam is surrounded by *two-parameters* foundations. In many practical case this foundation have to increase the critical buckling stress. Furthermore, this foundation exerts an external force and moment per unit length (for example by means of springs that act on the boundary of the cross-section) in order to control displacement and rotation behaviour of the cross-section [DR95; RS91]. Geometrical general problem under these hypotheses is presented in a dimensionless form that leads to Haringx approach in the first section. The Engesser model is presented in a dimensional form and for the same two-parameter foundation too. A comparison between the two problems is performed where buckling loads and buckling modes are exhibited in a general way first and for pinned-pinned boundary conditions in a second time. A finest analysis of buckling load was introduced where both values of the foundation stiffness and slenderness ratio are involved. This discussion is enriched by incorporating the yield limit of the material constituent of the beam. It leads to a simple criterion

that may be exploited by engineering analysis.

2.1 General ingredients

The kinematics of the beam is governed by the displacement $\underline{\mathbf{u}}(S,\underline{t}) = \underline{u}_1(S,\underline{t})\mathbf{d_1}(S,\underline{t}) + \underline{u}_3(S,\underline{t})\mathbf{d_3}(S,\underline{t})$ of any point of the center-line and rotation $\underline{\theta}(S,\underline{t})$ of the section around $\mathbf{d_2}$. With the same formalism, the internal force acting on the beam is of the form $\underline{\mathbf{N}}(S,\underline{t}) = \underline{N}_1\mathbf{d_1} + \underline{N}_3\mathbf{d_3}$ where $\underline{N}_1(S,\underline{t})$ is the shear force and $\underline{N}_3(S,\underline{t})$ is the normal force and the moment $\underline{\mathbf{M}}(S,\underline{t}) = \underline{M}_2\mathbf{d_2}$ where $\underline{M}_2(S,\underline{t})$ is the bending moment. Linear constitutive laws and geometrical relations are assumed:

$$\underline{N}_1 = GA(\frac{\partial \underline{u}_1}{\partial S} - \underline{\theta}), \qquad \underline{N}_3 = EA\frac{\partial \underline{u}_3}{\partial S}, \qquad \underline{M}_2 = EI\frac{\partial \underline{\theta}}{\partial S}. \tag{2.1}$$

2.1.1 Equilibrium relations

Reminding that equilibrium relations states :

$$\frac{\partial \underline{\mathbf{N}}}{\partial S} + \underline{\mathbf{q}} = \rho_0 A\ \frac{\partial^2 \underline{\mathbf{u}}}{\partial \underline{t}^2}, \qquad \frac{\partial \underline{\mathbf{M}}}{\partial S} + \frac{\partial \underline{\boldsymbol{\varphi}}}{\partial S} \times \underline{\mathbf{N}} + \underline{\mathbf{m}} = \rho_0 I_2\ \frac{\partial^2 \theta}{\partial \underline{t}^2},$$

where, according to [HLML21]:

$$\frac{\partial \underline{\boldsymbol{\varphi}}}{\partial S} = \underline{\widetilde{\boldsymbol{\varepsilon}}} + \mathbf{d_3}\ ,$$

and for which $\underline{\widetilde{\boldsymbol{\varepsilon}}} = \underline{\widetilde{\varepsilon}}_1\mathbf{d_1} + \underline{\widetilde{\varepsilon}}_3\mathbf{d_3}$, where $\underline{\widetilde{\varepsilon}}_1(S,\underline{t}) = \frac{\partial \underline{u}_1}{\partial S} - \underline{\theta}$ is the shear strain and $\underline{\widetilde{\varepsilon}}_3(S,\underline{t}) = \frac{\partial \underline{u}_3}{\partial S}$ is the longitudinal strain. So projecting along directors, one obtains the following system:

$$\begin{aligned}
\frac{\partial \underline{N}_1}{\partial S} + \frac{\partial \underline{\theta}}{\partial S}\underline{N}_3 + \underline{q_1} &= \rho_0 A\Big(\frac{\partial^2 \underline{u}_1}{\partial \underline{t}^2} + 2\frac{\partial \underline{u}_3}{\partial \underline{t}}\frac{\partial \underline{\theta}}{\partial \underline{t}} + \underline{u}_3\frac{\partial^2 \underline{\theta}}{\partial \underline{t}^2} - \underline{u}_1\frac{\partial \underline{\theta}}{\partial \underline{t}}^2\Big),\\
\frac{\partial \underline{N}_3}{\partial S} - \frac{\partial \underline{\theta}}{\partial S}\underline{N}_1 + \underline{q_3} &= \rho_0 A\Big(\frac{\partial^2 \underline{u}_3}{\partial \underline{t}^2} - 2\frac{\partial \underline{u}_1}{\partial \underline{t}}\frac{\partial \underline{\theta}}{\partial \underline{t}} - \underline{u}_1\frac{\partial^2 \underline{\theta}}{\partial \underline{t}^2} - \underline{u}_3\frac{\partial \underline{\theta}}{\partial \underline{t}}^2\Big),\\
\frac{\partial \underline{M}_2}{\partial S} + (1+\underline{\widetilde{\varepsilon}}_3)\underline{N}_1 - \underline{\widetilde{\varepsilon}}_1\underline{N}_3 + \underline{m_2} &= \rho_0 I_2\frac{\partial^2 \underline{\theta}}{\partial \underline{t}^2}.
\end{aligned} \tag{2.2}$$

The present analysis concerns an infinitesimal perturbation, so, in this case $\underline{u}_1$, $\underline{\widetilde{\varepsilon}}_1$, $\underline{\theta}$ and their derivatives are infinitesimal quantities. Neglecting $\underline{\widetilde{\varepsilon}}_3\underline{N}_1$ in (2.2) is usually interpreted as an *inextensible* approximation. Accordingly, a linearized version of (2.2) is obtained:

$$\begin{aligned}
GA\Big(\frac{\partial^2 \underline{u}_1}{\partial S^2} - \frac{\partial \underline{\theta}}{\partial S}\Big) + \underline{q_1} &= \rho_0 A\frac{\partial^2 \underline{u}_1}{\partial \underline{t}^2},\\
EA\frac{\partial^2 \underline{u}_3}{\partial S^2} + \underline{q_3} &= \rho_0 A\frac{\partial^2 \underline{u}_3}{\partial \underline{t}^2},\\
EI_2\frac{\partial^2 \underline{\theta}}{\partial S^2} + GA(\frac{\partial \underline{u}_1}{\partial S} - \underline{\theta}) + \underline{m_2} &= \rho_0 I_2\frac{\partial^2 \underline{\theta}}{\partial \underline{t}^2}.
\end{aligned} \tag{2.3}$$

The dimensionless form of (2.3) is given by

$$\begin{aligned} u_1'' - \theta' + q_1 &= \ddot{u}_1, \\ g u_3'' + q_3 &= \ddot{u}_3, \\ g\theta'' - \theta + u_1' + m_2 &= \ddot{\theta}. \end{aligned} \tag{2.4}$$

Where the fact that $u_i(s,t) = \dfrac{\underline{u_i}(S,\underline{t})}{\varrho}, q_1 = \dfrac{\varrho \underline{q_1}}{GA}, q_3 = \dfrac{\varrho \underline{q_3}}{EA}$ and $m_2 = \dfrac{\underline{m_2}}{GA}$ have been used.

2.2 Rigid wall

In this section we study in a dynamical way, a Timoshenko beam surrounded by a rigid wall that exerts a kinematical constraint. Noticing that the equation satisfied by u_3 is a scalar autonomous equation, we focus hereafter on the coupled system (u_1, θ). Therefore, orientation of the section is the only degree of freedom in this case, this will lead to a scalar problem that depends uniquely on one variable. The force exerted by the wall on the beam could be expressed in terms of this variable. In order to solve this dynamical problem, we are interested first in the modal analysis given for a specific boundary conditions that respects Sturm-Liouville criterion. For these boundary conditions, eigenmodes are given in an analytical way. By imposing a choc type initial value condition, we deduce the temporal solutions.

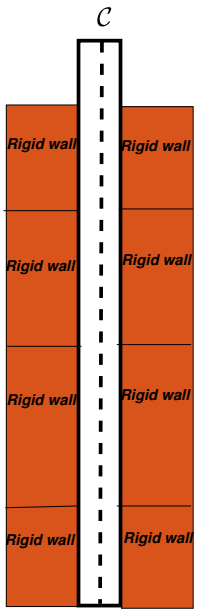

Figure 2.1 – *Beam surrounded by a rigid wall.*

2.2.1 Problem statement

The rigid wall exerts a transverse constraint on the beam (figure (2.1)) that is given by:

$$u_1(s,t) = m_2(s,t) = 0, \qquad \forall s \in [0,\ell], \qquad \forall t \in \mathbb{R}^+. \tag{2.5}$$

We deduce directly from (2.5) that $q_1 = \theta'$ and:

$$\boxed{g\theta'' - \theta = \ddot{\theta}.} \tag{2.6}$$

By using the separation of variable and letting $\theta(s,t) = \Phi(s)T(t)$ we can deduce that differential equations satisfying by $\Phi(s)$ and $T(t)$ are given by:

$$\begin{cases} g\dfrac{\Phi''}{\Phi} - 1 = -\omega^2, \\ \ddot{T} + \omega^2 T = 0. \end{cases} \tag{2.7}$$

Looking at the spatial equation we can remark that the equation is of the form:

$$\Phi''(s) + \frac{1}{g}(\omega^2 - 1)\Phi(s) = 0. \tag{2.8}$$

Therefore, our solution will be of the form

$$\Phi(s) = C_1 e^{ks} + C_2 e^{-ks} \qquad \text{If} \quad \omega^2 < 1 \quad \text{where} \quad k^2 = \frac{1}{g}(1-\omega^2) > 0, \tag{2.9}$$

and

$$\Phi(s) = C_3\cos(ks) + C_4\sin(ks) \qquad \text{If} \quad \omega^2 > 1 \quad \text{where} \quad k^2 = \frac{1}{g}(\omega^2 - 1) > 0. \tag{2.10}$$

2.2.2 Modal decomposition: Sturm-Liouville criterion

In this section we introduce a modal decomposition method to solve the problem without any numerical approach. This modal has an orthogonal character given by Sturm-Liouville criterion. To do so, let us introduce first the scalar product defined by

$$< \Phi, \Gamma >= \int_0^\ell \Phi\Gamma ds.$$

We will consider a basis mode $\{\Phi_n, \omega_n\}$ where each mode is a solution of:

$$\Phi_n'' + \frac{1}{g}(\omega_n^2 - 1)\Phi_n = 0. \tag{2.11}$$

We can apply Sturm-Liouville criterion and after multiplying by Φ_m and integrating we get

$$\int_0^\ell \Phi_n'' \Phi_m ds + \frac{1}{g}(\omega_n^2 - 1) \int_0^\ell \Phi_n \Phi_m ds = 0, \tag{2.12}$$

and by integration by part we get

$$-\int_0^\ell \Phi_n' \Phi_m' ds + \frac{1}{g}(\omega_n^2 - 1) \int_0^\ell \Phi_n \Phi_m ds = -\Big[\Phi_n' \Phi_m\Big]_0^\ell. \tag{2.13}$$

Repeating the procedure with Φ_m we get

$$-\int_0^\ell \Phi_n' \Phi_m' ds + \frac{1}{g}(\omega_m^2 - 1) \int_0^\ell \Phi_n \Phi_m ds = -\Big[\Phi_m' \Phi_n\Big]_0^\ell. \tag{2.14}$$

When subtracting (2.13) and (2.14) we get

$$(\omega_n^2 - \omega_m^2) < \Phi_n, \Phi_m >= g\Big[\Phi_m' \Phi_n - \Phi_n' \Phi_m\Big]_0^\ell. \tag{2.15}$$

To ensure the orthogonality basis, we should impose some boundary conditions (for example, for glued beam $\Phi = 0$ and for free beam $\Phi' = 0$).

2.2.3 Discussion

The solution of (2.11) is given by $\Phi_n(s) = a\cosh(k_n s) + b\sinh(k_n s)$ if $0 < \omega_n^2 < 1$ (low frequency domain) and $\Phi_n(s) = c\cos(k_n s) + d\sin(k_n s)$ if $\omega_n^2 > 1$ (high frequency domain). Where $k_n = \pm\sqrt{\dfrac{\omega_n^2 - 1}{g}}$ for high frequency and $k_n = \pm\sqrt{\dfrac{1 - \omega_n^2}{g}}$ for low frequency.
To ensure orthogonality, we impose the boundary condition

$$\theta(0,t) = 0 \qquad M_2(\ell,t) = 0 \qquad \forall t. \tag{2.16}$$

We can remark that the low frequency case is impossible. In fact $\theta(0,t) = \Phi(0)T(t) = 0$ implies $a = 0$, therefore, $\Phi_n(s) = b\sinh(k_n s)$. Now $M_2(\ell,t) = g\Phi'(\ell) = 0$ gives $k_n b\cosh(k_n s) = 0$ but $\cosh(k_n s)$ and k_n are different from zero, hence, $b = 0$ so, $\Phi_n(s) = 0, \qquad \forall n$.
Repeating the same procedure for high frequency case we deduce that $c = 0$ and $kd\cos(k\ell) = 0$.

- If $d = 0$ therefore, $\Phi_n = 0$.
- If $k = 0$ so, $\omega = 1$ and $\Phi''(s) = 0$ so, $\Phi(s) = as + b$ and since $\Phi(0) = 0$ and $\Phi_n'(\ell) = 0$ so, $\Phi_n(s) = 0$

Therefore, $d \neq 0$ and it is supposed $d = 1$ hereafter, and $k \neq 0$, so

$$\Phi_n(s) = \sin(k_n s), \qquad \text{where} \qquad k_n = \frac{(2n+1)\pi}{2\ell} = \pm\sqrt{\frac{\omega_n^2 - 1}{g}}. \tag{2.17}$$

We know that our temporal solution is given by $T_n(t) = a_n cos(\omega_n t) + b_n sin(\omega_n t)$ so

$$\theta(s,t) = \sum_n \Phi_n(s) T_n(t) = \sum_n \sin(k_n s)(a_n \cos(\omega_n t) + b_n sin(\omega_n t)). \tag{2.18}$$

2.2.4 Dynamics after a choc

We impose a choc type initial conditions

$$\theta(s,0) = 0, \qquad \dot{\theta}(s,0) = \Omega_0 \ell \delta(s-\ell) \qquad \forall t. \tag{2.19}$$

Where Ω_0 is constant and δ is the dirac function. We notice first that $\theta(s,0) = 0$ implies $\sum_n a_n \Phi_n(s) = 0$, therefore,

$$< \sum_n a_n \Phi_n(s), \Phi_m >= 0, \qquad \text{for an arbitrary m,} \tag{2.20}$$

where $< ., . >$ is the dot product.
By using Sturm-Liouville and the boundary conditions we can remark that our basis is orthogonal and therefore, we get $a_n = 0\ \forall n$, hence $\theta(s,t) = \sum_n b_n \Phi_n(s) \sin(\omega_n t)$.
By time derivation $\dot{\theta}(s,t) = \sum_n b_n \Phi_n(s) \omega_n \cos(\omega_n t)$, so, using now (2.19) and projecting along modal basis, we have

$$\begin{aligned} < \dot{\theta}(s,0), \Phi_m > &= < \sum_n b_n \Phi_n \omega_n, \Phi_m >, \\ \int_0^\ell \Omega_0 \ell \delta(s-\ell) \sin(k_n s) ds &= \sum_n b_n \omega_n \int_0^\ell \phi_n \phi_m ds. \end{aligned} \tag{2.21}$$

Keeping in mind that Φ_n is an orthogonal basis:

$$\int_0^\ell \Omega_0 \ell \delta(s-\ell) \sin(k_n s) ds = b_n \omega_n \int_0^\ell \sin(k_n s)^2 ds. \tag{2.22}$$

Using the fact that $\int_0^\ell \sin(k_n s)^2 ds = \frac{\ell}{2}(1 - \frac{\sin(2k_n \ell)}{2k_n \ell}) = \frac{\ell}{2}$, we obtain:

$$b_n = \frac{2\Omega_0}{\omega_n} \sin(\frac{(2n+1)\pi}{2}). \tag{2.23}$$

Therefore, the general form of the solution will be

$$\theta(s,t) = 2\Omega_0 \sum_n \frac{(-1)^n}{\omega_n} \sin(k_n s) \sin(\omega_n t). \tag{2.24}$$

This solutions is illustrated in figure (2.2).
It should be mentioned that the dimensionless dynamical variables are given by

$$N_1 = u_1' - \theta, \qquad N_3 = g u_3', \qquad M_2 = g\theta'. \tag{2.25}$$

So using (2.24) and the fact that $u_1 = 0$ we obtain:

$$\begin{aligned} N_1(s,t) &= 2\Omega_0 \sum_n \frac{(-1)^{n-1}}{\omega_n} \sin(k_n s)\sin(\omega_n t), \\ M_2(s,t) &= 2g\Omega_0 \sum_n \frac{(-1)^{n}}{\omega_n} k_n \cos(k_n s)\sin(\omega_n t), \\ q_1(s,t) &= 2\Omega_0 \sum_n \frac{(-1)^{n}}{\omega_n} k_n \cos(k_n s)\sin(\omega_n t). \end{aligned} \tag{2.26}$$

We conclude that load supported by the rigid wall is explicitly obtained

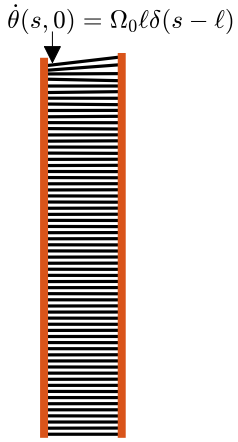

Figure 2.2 – *Influence of the boundary condition on the orientation* $\theta(s,t)$.

Remark. Euler-Bernoulli beam model have the kinematical constraint $u_1' = \theta$, so, our approach for rigid wall is not valid for this model because $u_1' = 0 \Longrightarrow \theta = 0$ and we obtain zero solution in this case.

2.3 Elastic wall

We suppose now that this beam is surrounded by an elastic wall that controls the transversal displacement. This relaxation will lead to two degrees of freedom in terms of displacement and orientation of the section. Therefore, we obtain a coupled system in terms of u_1 and θ and a wave equation for u_3. By re-writting the system as an eigenvalue problem, we find, in an analytical way the dispersion relation, we also present a criterion of solutions that depends on the rigidity of the wall and on the material of the beam.

Kinematical constraint will be in this case (in a dimensional form):

$$\underline{q_1}(S,\underline{t}) = -K\underline{u_1}(S,\underline{t}), \qquad \underline{q_3} = \underline{m_2} = 0. \tag{2.27}$$

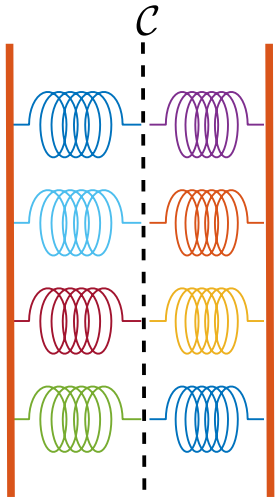

Figure 2.3 – *Beam surrounded by an elastic wall that controls the displacement.*

Where K is the translational stiffness. So we write (2.4) as:

$$\begin{aligned} u_1'' - \theta' - g\kappa u_1 &= \ddot{u}_1, \\ g u_3'' &= \ddot{u}_3, \\ g\theta'' - \theta + u_1' &= \ddot{\theta}, \end{aligned} \tag{2.28}$$

Where $\kappa = \dfrac{KI}{EA^2}$ is the dimensionless stiffness. To solve $gu_3'' = \ddot{u}_3$, we impose the change of variable:

$$v = s - gt, \qquad w = s + gt. \tag{2.29}$$

That changes the equation into:

$$\frac{\partial^2 u_3}{\partial v \partial w} = 0, \tag{2.30}$$

Therefore, general equation is given by

$$u_3(s,t) = F(s - gt) + G(s + gt). \tag{2.31}$$

In other words, solutions are sums of a right traveling function F and a left traveling function G ("Traveling" means that the shape of these individual arbitrary functions with respect to s stays constant), however, the functions are translated left and right with time at the speed g.
Now we aim to solve the coupled equation

$$\begin{aligned} u_1'' - \theta' - g\kappa u_1 &= \ddot{u}_1, \\ g\theta'' - \theta + u_1' &= \ddot{\theta}. \end{aligned} \tag{2.32}$$

Since we are interested in harmonic vibrations, solutions of the previous system are defined by

$$u_1 = Ue^{i(ks-\omega t)},\ \theta = \Theta e^{i(ks-\omega t)},$$

where U, Θ are constant and $k \in \mathbb{C}$ and $\omega \in \mathbb{R}^+$ are wavenumber and angular frequency. Therefore, space(resp. time) derivation gives a factor ik(resp. $-i\omega$). The system becomes of the form

$$(\mathbb{K} - \omega^2\mathbb{M})\mathbf{U} = 0, \tag{2.33}$$

where

$$\mathbb{K} = \begin{pmatrix} k^2 + g\kappa & ik \\ -ik & 1 + gk^2 \end{pmatrix}, \qquad \mathbb{M} = \begin{pmatrix} 1 & 0 \\ 0 & 1 \end{pmatrix}, \tag{2.34}$$

are the rigidity matrix and the mass matrix and $\mathbf{U} = (Ue^{i(ks-\omega t)}, \Theta e^{i(ks-\omega t)})$.
Since we are searching for non trivial $\mathbf{U}$ so, first we need to solve the dispersion relation $\mathcal{P}(k^2, \omega^2) = 0$, where

$$\mathcal{P}(k^2, \omega^2) = det(\mathbb{K} - \omega^2\mathbb{M}) = gk^4 + \Big(g^2\kappa - (g+1)\omega^2\Big)k^2 + \omega^4 - (g\kappa + 1)\omega^2 + g\kappa. \tag{2.35}$$

Hence for $W = \omega^2$ fixed we get a second degree polynomial with respect to $K = k^2$ where the discriminant of this polynomial is given by:

$$\Delta = (g-1)^2W^2 + 2g\Big(2 - g\kappa(g-1)\Big)W + g^2\kappa(g^2\kappa - 4). \tag{2.36}$$

Solving $\Delta = 0$ with respect to W we notice that:

$$\begin{aligned} W_1 &= \frac{g\Big((g-1)g\kappa - 2\Big) - 2\sqrt{g^2(\kappa + 1 - g\kappa)}}{(g-1)^2}, \\ W_2 &= \frac{g\Big((g-1)g\kappa - 2\Big) + 2\sqrt{g^2(\kappa + 1 - g\kappa)}}{(g-1)^2}. \end{aligned} \tag{2.37}$$

So, by using (2.37) and plotting the dispersion curve in fig.(2.4) we remark that:

- For free motion i.e. $\kappa = 0$ we have 2 distinct real roots of opposite signs.
- For $0 < \kappa \leq \dfrac{4}{g^2}$ we obtain complex solutions.
- For $\kappa > \dfrac{4}{g^2}$ we re-observe two distinct real roots.

Indeed this approach needs potentially more investigation.

2.4 Buckling of Timoshenko beam under two-parameters Winkler foundations

We aim in this section to expose buckling solutions of a plane, quasi-static Timoshenko beam with small transformation subjected to a longitudinal force and surrounded by an elastic wall mod-

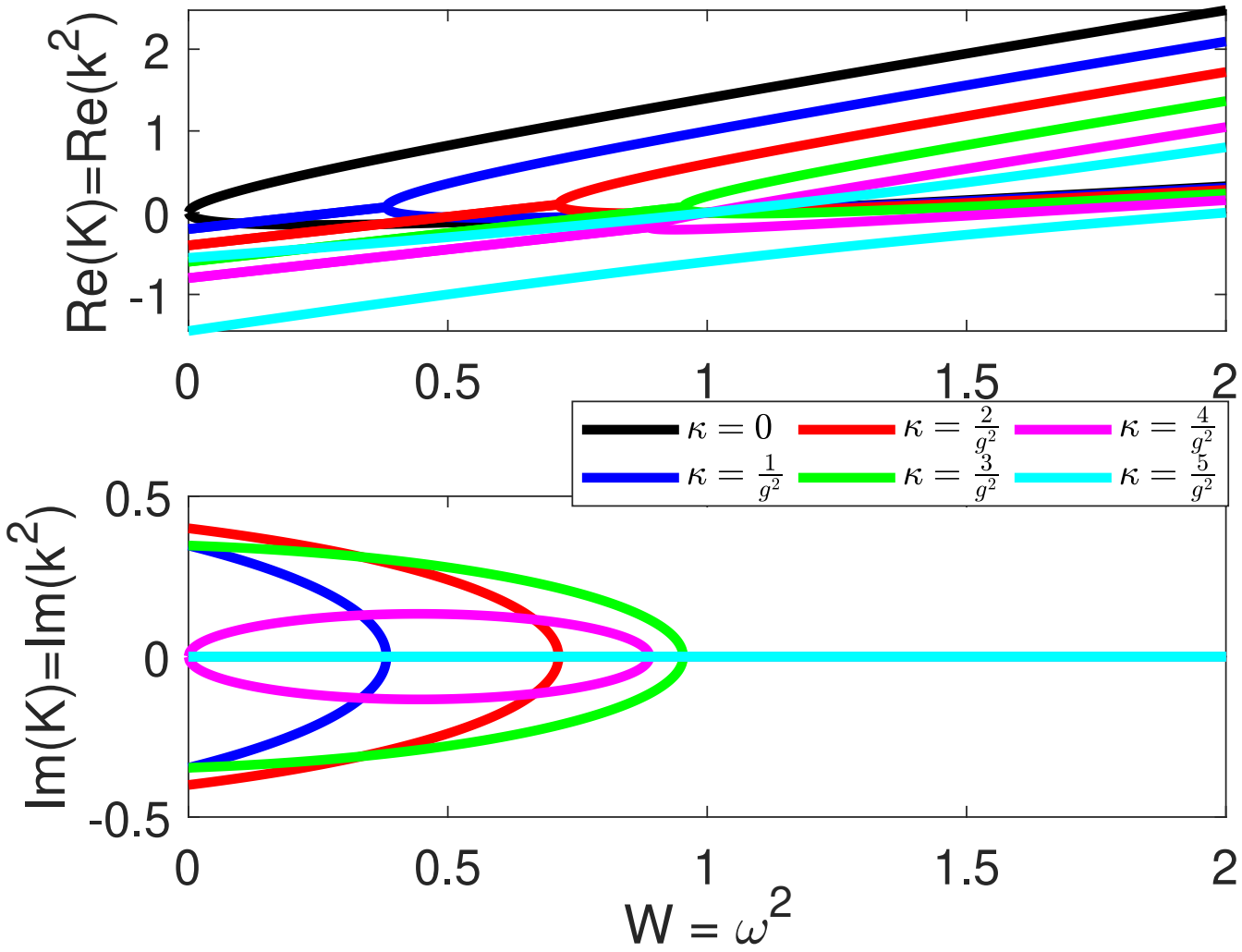

Figure 2.4 – *Dispersion curves for various κ.*

eled by two-parameters Winkler foundation. To do so, we impose a finite longitudinal compression load:

$$\mathbf{P} = -P\mathbf{d_3}, \qquad P \geq 0 \ .$$

This load causes the buckling of the beam. This is countered by the foundations. For elastic foundation, the external applied force per unit length and external applied moment per unit length are respectively:

$$\mathbf{q}(S) = -K_1 \underline{u}_1 \mathbf{d_1}, \qquad \mathbf{m}(S) = -K_2 \underline{\theta}\, \mathbf{d_2} \ ,$$

where K_1 and K_2 are translational and rotational stiffness [CP88; WXK91]. The motivation of the applied moment $\mathbf{m}(S)$ may be surprising. In Fig.2.5 a discrete construction of such external load is justified. If the distance between each rigid transversal bar is small enough, a continuous modeling leads to incorporate $\mathbf{m}(S) = -K_2\underline{\theta}\,\mathbf{d_2}$ in the model. This stiffness can be caused by the tension in an elastic membrane connecting the ends of the Winkler springs (Filonenko-Borodich model), or

as the shear stiffness of a shear layer (Pasternak model) [DR95]. Such load may be observed in real life as for auger blade embedded into the soil.

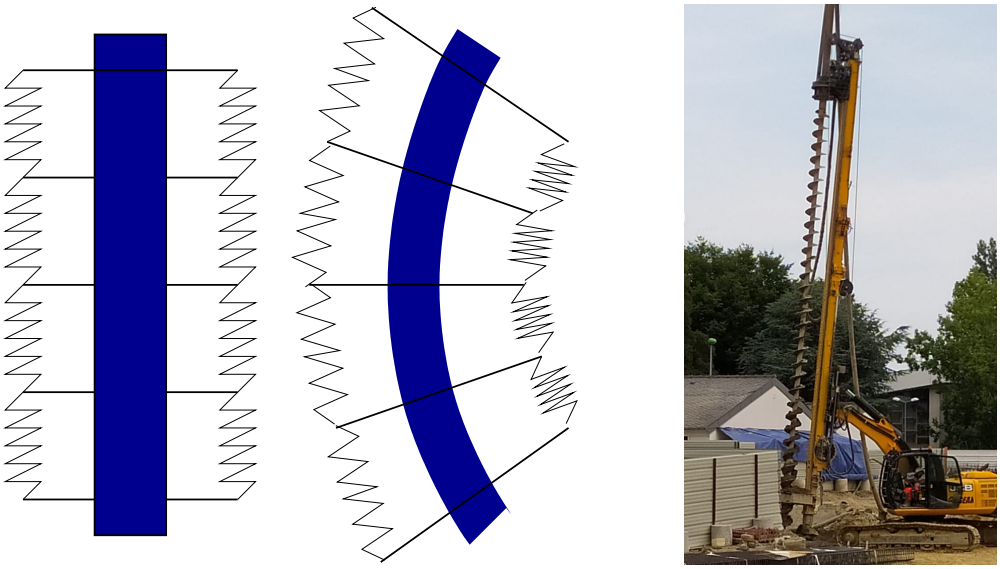

Figure 2.5 – *Motivation for the rotational reaction of the soil. Left: a beam structure in blue with glued rigid transversal blades embedded in an elastic media is modeled by a discrete system of springs. Right: an auger blade (Photo courtesy of N.Belhabchi.)*

2.4.1 Equilibrium relations

Static equilibrium in this case is given by:

$$\begin{aligned} \frac{\partial \underline{N}_3}{\partial S} - \frac{\partial \underline{\theta}}{\partial S}\underline{N}_1 = 0 \ , \\ \frac{\partial \underline{N}_1}{\partial S} + \frac{\partial \underline{\theta}}{\partial S}\underline{N}_3 - K_1\underline{u}_1 = 0 \ , \\ \frac{\partial \underline{M}_2}{\partial S} + (1+\widetilde{\varepsilon}_3)\underline{N}_1 - \widetilde{\varepsilon}_1\underline{N}_3 - K_2\underline{\theta} = 0 \ . \end{aligned} \tag{2.38}$$

The present analysis concerns an infinitesimal perturbation superimposed on a finite longitudinal compression induced by a finite force $\mathbf{P}$. So repeating the same linearisation stated before, a linearized version of (2.38) is obtained:

$$\begin{aligned} GA(\frac{\partial^2 \underline{u}_1}{\partial S^2} - \frac{\partial \underline{\theta}}{\partial S}) - \frac{\partial \underline{\theta}}{\partial S}P - K_1\underline{u}_1 = 0, \\ EI\frac{\partial^2 \underline{\theta}}{\partial S^2} + (\frac{\partial \underline{u}_1}{\partial S} - \underline{\theta})(GA+P) - K_2\underline{\theta} = 0, \end{aligned} \tag{2.39}$$

this corresponds to the application of Haringx model for Winkler foundation [Ced+10; Cha+13]. More precisely, if P is set to zero we recover the model from [DR95] in its static version.

2.4.2 Non-dimensionalization procedure

Non-dimensional formulation of the problem (2.39) is introduced thanks to the following variables:

$$\varrho = \sqrt{\frac{I}{A}}, \quad g = \frac{E}{G}, \quad \kappa_1 = \frac{K_1}{E}\frac{I}{A^2}, \quad \kappa_2 = \frac{K_2}{EA}, \quad \epsilon = \frac{P}{EA}. \tag{2.40}$$

For compression in the elastic regime $0 < \epsilon < \epsilon_{yield}$ where ϵ_{yield} is nothing else than the strain limit for which irreversible transformation occurs. For translational and rotational stiffness κ_i, $\kappa_i = 0$ in absence of foundation and $\kappa_i = \infty$ for a rigid foundation. This section focuses on the cases for which $\kappa_i < 1$ that corresponds to foundations softer than the structures.
Note that $\varrho = R/2$ for circular cross-section of radius R therefore ℓ is twice the standard slenderness ratio. More generally, beam model is justified for $\ell \gtrsim 20$. The terminology *slender beam* is used if $\ell \gtrsim 40$ whereas $20 \lesssim \ell \lesssim 40$ characterizes a *thick beam*.
Therefore (2.39) takes the form:

$$\boxed{\begin{aligned} u'' - g\kappa_1 u - (1+g\epsilon)\theta' &= 0, \\ g\theta'' + (1+g\epsilon)u' - (1+g\epsilon+g\kappa_2)\theta &= 0, \end{aligned}} \tag{2.41}$$

Another model widely used for buckling is proposed by Engesser [Eng91] for which the non-dimensional equilibrium relations are in case of two-parameter foundations:

$$\boxed{\begin{aligned} (1-g\epsilon)u'' - g\kappa_1 u - \theta' &= 0, \\ g\theta'' + u' - (1+g\kappa_2)\theta &= 0. \end{aligned}} \tag{2.42}$$

Figure (2.6) represents the difference between Haringx and Engesser's hypothesis for beam deformation where it is clear that these two hypotheses are identical for Euler Bernoulli's beam.

Figure 2.6 – *Left, the assumption for the normal force in the Engesser beam–column model. The normal force is parallel to the beam axis. Right, the assumption for the normal and shear forces in the Haringx beam–column model. The normal force is parallel to the normal of the deformed cross-section.*

2.4.3 Buckling modes

Secular relations and eigenfunctions

For harmonic solution $u(s) = Ue^{iks}$ and $\theta(s) = \Theta e^{iks}$, the linear differential system becomes $\mathbb{K}\boldsymbol{V} = 0$ where $\boldsymbol{V} = (U, \Theta)^T$ and the (hermitian) rigidity matrix is, for (2.41) and (2.42) respec-

tively:

$$\begin{aligned}\mathbb{K}^H &= \begin{pmatrix} k^2+g\kappa_1 & ik(1+g\epsilon) \\ -ik(1+g\epsilon) & 1+g(k^2+\epsilon+\kappa_2)\end{pmatrix},\\ \mathbb{K}^E &= \begin{pmatrix} k^2(1-g\epsilon)+g\kappa_1 & ik \\ -ik & 1+g(k^2+\kappa_2)\end{pmatrix}.\end{aligned} \tag{2.43}$$

Non-trivial solutions arise if $\det(\mathbb{K}) = 0$ what may be written as a secular equation:

$$\begin{aligned}\mathcal{P}^H(\epsilon,k) &= g\left(k^2\left(\kappa_2+k^2-\epsilon(g\epsilon+1)\right)+\kappa_1\left(g\kappa_2+g\left(\epsilon+k^2\right)+1\right)\right),\\ \mathcal{P}^E(\epsilon,k) &= g\left(k^2\left(\kappa_2(1-g\epsilon)-\epsilon\left(gk^2+1\right)+k^2\right)+\kappa_1\left(g\kappa_2+gk^2+1\right)\right).\end{aligned} \tag{2.44}$$

By solving $\mathcal{P}(\epsilon) = 0$ (for a fixed k), one finds a polynomial with respect to ϵ whose real positive roots are

$$\begin{aligned}\epsilon^H &= \frac{g\kappa_1+\sqrt{(g\kappa_1+k^2)\left(g\kappa_1+(1+4g\kappa_2)k^2+4gk^4\right)}-k^2}{2gk^2},\\ \epsilon^E &= \frac{\kappa_2+k^2}{1+g(\kappa_2+k^2)}+\frac{\kappa_1}{k^2}.\end{aligned} \tag{2.45}$$

Hence explicit expressions of the critical strain are obtained for a given structure (the material parameter g and the stiffnesses κ_i of the foundations) and a given wavenumber k. This latter will be fixed by boundary conditions. Without foundation the Euler critical load is $\underline{k}^2EI/L^2$, where $\underline{k} = k/\varrho$ is the dimensional wavenumber. In a non-dimensional form the critical strain associated to Euler critical load is $\epsilon^{eu} = k^2$. By taking $\kappa_1 = \kappa_2 = 0$ and applying Taylor expansion to (2.45) for small k and taking first approximation one gets:

$$\epsilon = k^2 + \mathcal{O}(k^4), \tag{2.46}$$

for both models. Hence the two models are in first approximation equal to Euler's critical load if no foundation is present and if $k \ll 1$.

Figure 2.7 presents the variation of ϵ^H and ϵ^E for various stiffnesses ; the non-dimensional Euler's critical strain $\epsilon^{eu} = k^2$ is presented too. For $k \ll 1$ Haringx and Engesser's models give the same estimation of critical strain ϵ. Of course, this estimation is sensible to the stiffnesses κ_i. On the other hand, for $1 \lesssim k$, the Haringx and Engesser's models gives distinct estimations of ϵ but curiously these estimations are in first approximation independent of the stiffness of the foundation. Note that $\epsilon^E < \epsilon^H$ in this regime as mentioned in [LL18].

Conversely, for fixed ϵ, $\mathcal{P}$ is a second degree polynomial with respect to k^2. Hence $u(s)$ and $\theta(s)$

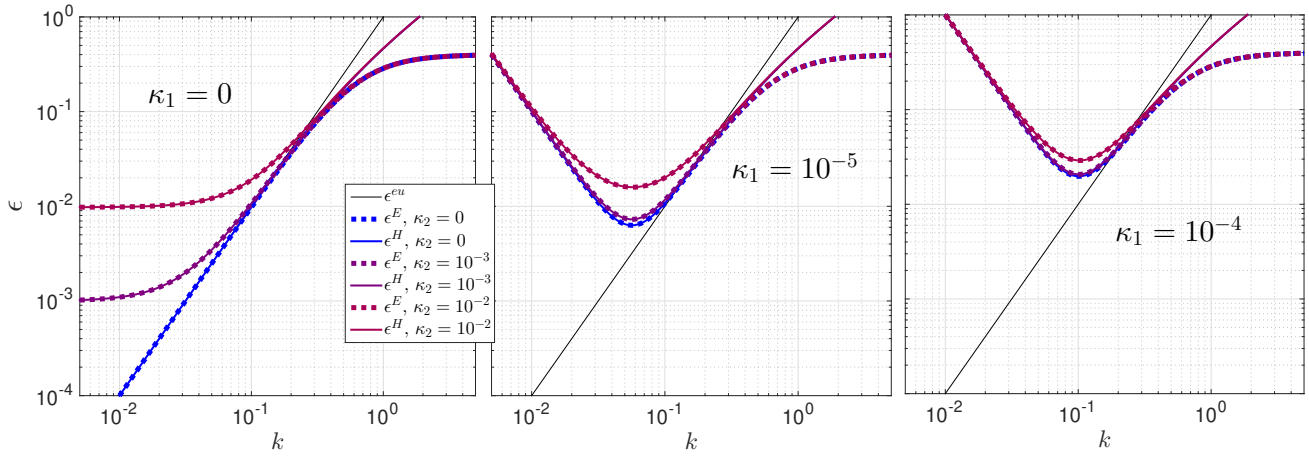

Figure 2.7 – *Variation of the buckling load* $\epsilon = \dfrac{P}{EA}$ *with respect to the wavenumber* k *for various* κ_1 *and* κ_2 *where* $g = 5/2$.

have the general form:

$$\begin{aligned} u(s) &= ae^{ik_1 s} + be^{-ik_1 s} + ce^{ik_2 s} + de^{-ik_2 s}, \\ \theta(s) &= \Xi(k_1)(ae^{ik_1 s} - be^{-ik_1 s}) + \Xi(k_2)(ce^{ik_2 s} - de^{-ik_2 s}), \end{aligned} \tag{2.47}$$

where a, b, c and d will be defined by boundary conditions. Here, $(k_1)^2$ and $(k_2)^2$ are the two roots of $\mathcal{P}(k^2) = 0$. The expression of $\theta(s)$ is obtained by solving $\mathbb{K}_{11}U + \mathbb{K}_{12}\Theta = 0$ therefore $\Theta = i\Xi U$ where $i\Xi = -\mathbb{K}_{11}/\mathbb{K}_{12}$. In details:

$$\Xi^H = k\frac{1}{1+g\epsilon} + \frac{g\kappa_1}{k}\frac{1}{1+g\epsilon}, \qquad \Xi^E = k(1-g\epsilon) + \frac{g\kappa_1}{k}. \tag{2.48}$$

Taylor expansion in terms of ϵ gives:

$$\Xi^H = \Xi^E + \mathcal{O}(\frac{\kappa_1\epsilon}{k}, k\epsilon^2). \tag{2.49}$$

By construction κ_2 is not explicit in Ξ but intervenes implicitly through ϵ.

Pinned-pinned beam

Without loss of generality, we consider a pinned-pinned beam for which (non-dimensional) boundary conditions are in terms of kinematical variables $u(s) = 0$, $\theta'(s) = 0$ at $s = 0$ and $s = \ell$. This forms a set of four linear equations in terms of $X = (a, b, c, d)^T$ that may be written

algebraically as $\mathbb{M}X = 0$ with

$$\mathbb{M} = \begin{pmatrix} 1 & 1 & 1 & 1 \\ k_1\Xi(k_1) & k_1\Xi(k_1) & k_2\Xi(k_2) & k_2\Xi(k_2) \\ e^{ik_1\ell} & e^{-ik_1\ell} & e^{ik_2\ell} & e^{-ik_2\ell} \\ k_1\Xi(k_1)e^{ik_1\ell} & k_1\Xi(k_1)e^{-ik_1\ell} & k_2\Xi(k_2)e^{ik_2\ell} & k_2\Xi(k_2)e^{-ik_2\ell} \end{pmatrix}. \tag{2.50}$$

Again, non trivial solutions exist if $\det(\mathbb{M}) = 0$ that gives the following relation:

$$\Big(k_1\Xi(k_1) - k_2\Xi(k_2)\Big)^2 \sin(k_1\ell)\sin(k_2\ell) = 0. \tag{2.51}$$

Direct computation shows that $k_1\Xi(k_1) \neq k_2\Xi(k_2)$. First it is observed that k_1 and k_2 play a similar role therefore one focuses on $k \equiv k_1$ in the following. According to (2.51) non-trivial solutions exist only if $\sin(k\ell) = 0$, this implies that k must be chosen among an infinite countable set of values, more precisely:

$$k_n = \frac{n\pi}{\ell}, \qquad n \in \mathbb{N}^*. \tag{2.52}$$

One should note that in order to respect beam hypotheses the dimensional wavelength $\underline{\lambda}$ has to satisfy $\underline{\lambda} > 2R = 4\varrho$ for circular cross-sections, or in a non-dimensional way $\lambda = \underline{\lambda}/\varrho > 4$ and since $\lambda_n = 2\pi/k_n > 4$ so the following conditions are obtained:

$$\boxed{n < \frac{\ell}{2}, \qquad k_n \leq 1\ .} \tag{2.53}$$

From this information, it means that even for a thick beam, k must be explored in a variation domain $]0,\ 1]$. According to equation (2.50), the modal amplitude may be obtained up to an arbitrary constant, by solving:

$$\mathbb{A}Y = -aZ, \qquad \text{where} \qquad Y = (b, c, d)^T,$$

with $\mathbb{A}_{ij} = \mathbb{M}_{ij}$ and $Z_i = \mathbb{M}_{i1}$ for $1 \leq i \leq 3$ and $2 \leq j \leq 4$. Fixing $a = 1$ and $k_n = n\pi/\ell$ one obtains:

$$\begin{aligned} u(s) &= \sin(\frac{n\pi}{\ell}s), \\ \theta(s) &= \Xi(\frac{n\pi}{\ell})\cos(\frac{n\pi}{\ell}s). \end{aligned} \tag{2.54}$$

Hence ϵ and κ_i intervenes in the modes chapes only through the parameter $\Xi(k, \epsilon, \kappa)$. In other words, the general shape of the eigenmode is not qualitatively modified by the loads ϵ and the stiffnesses κ_i of the foundations. As Ξ is distinct for Haringx and Engesser models, the mode shapes may differ for the two models even if the value of critical load obtained for each model is similar.

General case

For a general boundary conditions k could still be organized as an increasing countable sequence $\{k_n\}_n$ where $k_n = \mathcal{O}(\frac{n}{\ell})$. In the following, it is considered that the variation domain $]0,1]$ of k, obtained for pinned-pinned boundary conditions, is valid for other boundary conditions. From Fig.2.7, it is observed that in this domain, the estimation $\epsilon(k)$ mainly coincides for Engesser and Haringx models.
The expression of the eigenmodes still refers to (2.47) but the detailed expression may be less clear than (2.54). However, the general methodology explained above (2.54) holds.

2.4.4 Buckling limit

Till now the buckling mode is not fixed. As this latter must respect the boundary conditions, the buckling mode is associated to a wavenumber k_b among the list $\{k_n\}$. Even if $\{k_n\}$ is an increasingly sorted list, k_b is not a priori k_1. Indeed, as k_b prescribes the *first* buckling mode, it must be chosen in such a way that it corresponds to the minimal critical strain:

$$\epsilon_b := \epsilon(k_b) = \min_n(\epsilon(k_n)) \ . \tag{2.55}$$

Continuous approximation of the critical strain

Solving (2.55) consists on a discrete optimisation. In order to have a first overview of the solution, the problem is here explored in its continuous version. Indeed, from Fig.2.7, $\epsilon(k)$ is a strictly convex function for any model (and for fixed κ_i). This ensures the existence and uniqueness of a global minimum of $\epsilon(k)$.
Finding in $\mathbb{R}^{*+}$ such position k_{min} of the minimum leads to calculate $\frac{\partial \epsilon}{\partial k}\Big|_{k_{min}} = 0$. According to (2.45) one obtains for Haringx and Engesser respectively:

$$\begin{aligned}
\frac{\partial \epsilon^H}{\partial k} &= \frac{2k^6 - \kappa_1\left(g\kappa_1 + 2g\kappa_2 k^2 + \sqrt{\left(g\kappa_1 + k^2\right)\left(g\kappa_1 + 4gk^4 + 4g\kappa_2 k^2 + k^2\right)} + k^2\right)}{k^3\sqrt{\left(g\kappa_1 + k^2\right)\left(g\kappa_1 + k^2\left(4g\kappa_2 + 4gk^2 + 1\right)\right)}} = 0, \\
\frac{\partial \epsilon^E}{\partial k} &= \frac{2k}{\left(g\kappa_2 + gk^2 + 1\right)^2} - \frac{2\kappa_1}{k^3} = 0 \ .
\end{aligned} \tag{2.56}$$

Knowing that $g > 0, \kappa_1 > 0$ and $\kappa_2 > 0$, we deduce the solution of (2.56)

$$\begin{aligned}
k^H_{min} &= \sqrt{\frac{1}{2}\sqrt{\kappa_1}\left(1 + \sqrt{1 + 4g\left(\kappa_2 + \sqrt{\kappa_1}\right)}\right)}, \\
k^E_{min} &= \sqrt{\frac{\sqrt{\kappa_1}\left(1 + g\kappa_2\right)}{1 - g\sqrt{\kappa_1}}}.
\end{aligned} \tag{2.57}$$

As $\kappa_i < 1$, leading terms approximation with respect to κ_1 and κ_2 gives, for both models:

$$\boxed{k_{min} \sim \kappa_1^{1/4}}. \tag{2.58}$$

This behaviour of k_{min} is illustrated in Figure (2.8).

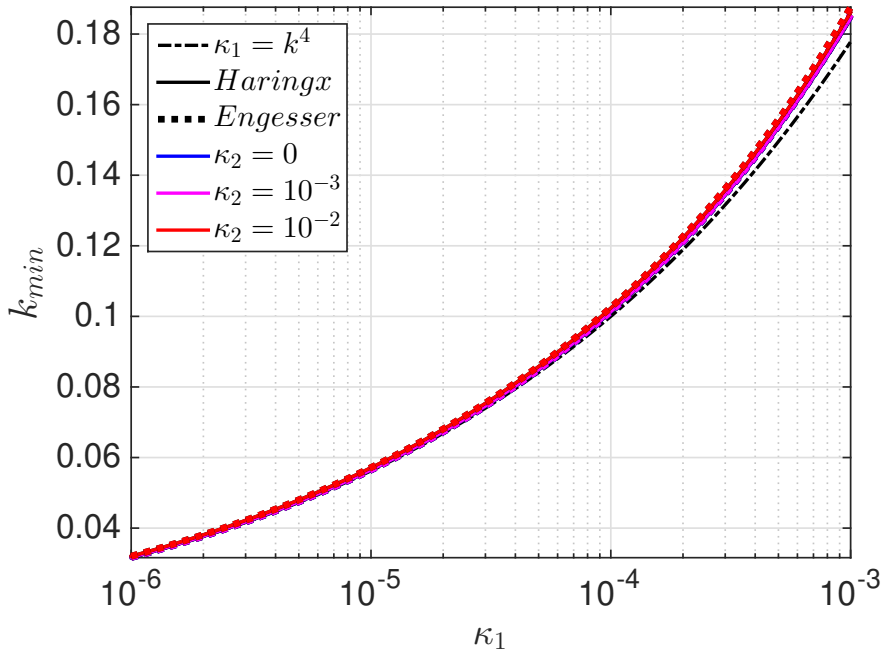

Figure 2.8 – *Solutions k_{min} of (2.57) versus κ_1 for various κ_2. Comparison between Haringx and Engesser models with $g = 5/2$.*

Euler buckling model

One can obtain the rigidity matrix, the critical strain as well as the wavenumber by applying the same procedure mentioned before to Euler beam model. A detailed analysis concerning this calculation will be given in the appendix where the relation $\kappa_1 = k^4$ is obtained for this model. This relation was presented in Figure (2.8).

Discrete analysis of the critical strain

The preceding analysis may be used to define the buckling wavenumber $k_b \in \{k_n\}$ and then ϵ_b. Practically, two cases have to be studied.

Thick beam on soft foundations

Considering first the case where $k_{min} \leq k_1$ (and $k_1 \leq 1$). Since $\epsilon(k)$ is an increasing function for $k \geq k_{min}$ then the criterion (2.55) is satisfied for $k_b = k_1$. Note that k_b could be far larger than k_{min} and the only attainable information is $k_b = \mathcal{O}(\pi/\ell) < 1$.

According to (2.58) and the discussion in the section 2.4.3, $k_{min} \leq k_1$ is satisfied only if $\kappa_1^{1/4} < \mathcal{O}(\pi/\ell)$, or in a more proper (non-dimensional or dimensional) version, if:

$$\kappa_1 \ell^4 \ll 1, \qquad \frac{K_1 L^4}{EI} \ll 1 \ .$$

Such situation appears if the foundation is soft or if the beam has a moderate slenderness ratio. This regime is called *small-regime* hereafter, as both the length and the stiffness are small numbers. From (2.45) and since $\kappa_1 \sim k_{min}^4 < k_b^4 \leq 1$ and $\kappa_2 < 1$, the buckling strains estimated by the two model are similar. It may be approached by:

$$\epsilon_b(k_b) = \frac{k_b^2}{1+gk_b^2} + \frac{\kappa_1}{k_b^2} + \frac{\kappa_2}{(1+gk_b^2)^2} \ , \tag{2.59}$$

for thick or slender beam. For thin structure, $k_b \ll 1$, allows some simplification:

$$\epsilon_b(k_b) = k_b^2 + \frac{\kappa_1}{k_b^2} + \kappa_2 \ . \tag{2.60}$$

Buckling shape is illustrated in Fig.2.10 for pinned-pinned boundary conditions.

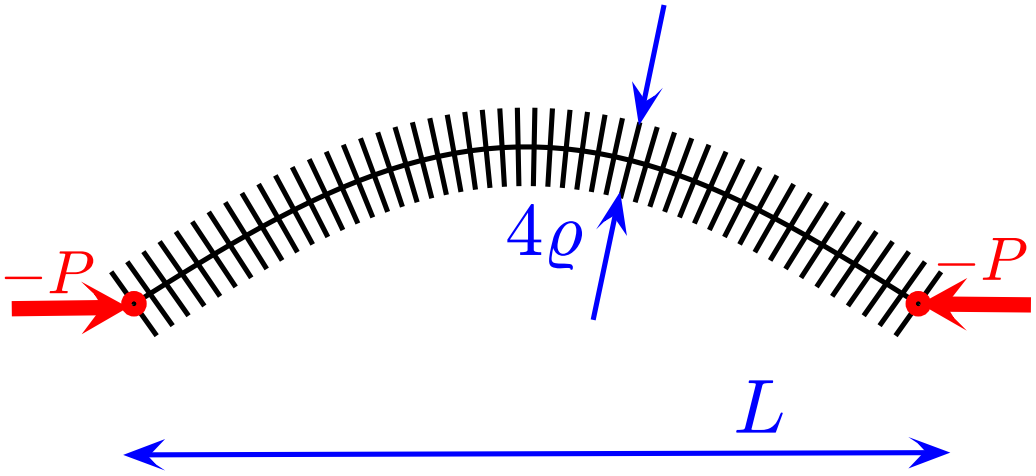

Figure 2.9 – *Shape of a pinned-pinned beam under a Winkler foundation.* $g = 5/2$, $\ell = 40$, $\kappa_1 = 10^{-8}$, $\kappa_2 = 10^{-4}$. *The buckling mode is associated to the smallest strain that is the first one:* $k_b = \pi/\ell$ *with a critical strain* $\epsilon_b = 0.0063$.

Thin beam on stiff foundations

For $k_{min} \gg k_1$, the situation is different. This regime appears for slender structure or for stiff foundations. It is called *large-regime*, and is controlled by $\kappa_1 \ell^4 \gg 1$. In that case $k_b = \mathcal{O}(k_{min})$ in order to minimize the buckling strain $\epsilon(k_b)$. Note that one observes the following hierarchy $k_b = \mathcal{O}(k_{min}) = \mathcal{O}(\kappa_1^{1/4}) \gg \mathcal{O}(1/\ell)$, however as $\kappa_1 < 1$ then $1/\ell \ll k_b \leq 1$.
The wavelength $\lambda_b = 2\pi/k_b$ of the buckling mode satisfies

$$\lambda_b \sim \frac{2\pi}{\kappa_1^{1/4}}. \tag{2.61}$$

It is controlled by $\kappa_1 = K_1 I/(EA^2)$ only, in particular it is independent of the length of the structure. The buckling appears with a pattern having several arches. The number of arches observed on a buckled structure is $N := 2\ell/\lambda_b$ (a wavelength is considered as composed of two arches). The order of magnitude of this parameter is:

$$N \sim \left\lfloor \frac{\ell}{\pi} \kappa_1^{1/4} \right\rfloor \ , \tag{2.62}$$

where $\lfloor \cdot \rfloor$ denotes the floor function.
In terms of strain criterion, since $\kappa_i \ll g\mathrm{k}$, one obtains:

$$\boxed{\epsilon_b = \mathcal{O}(2\sqrt{\kappa_1} + \kappa_2) \ ,} \tag{2.63}$$

for both models.
For pinned-pinned beam the modal amplitudes are approached by (2.49) that gives:

$$\Xi \sim \kappa_1^{1/4}(1 - g\kappa_2) \ . \tag{2.64}$$

This shows the high influence of foundation stiffness in this *large-regime*: it uniquely defines the buckling load (2.63), the modal amplitude (2.64) and the buckling's wavelength (2.61). An illustration of the buckled shape in the *large-regime* is given in Fig.2.10 for pinned-pinned boundary conditions.

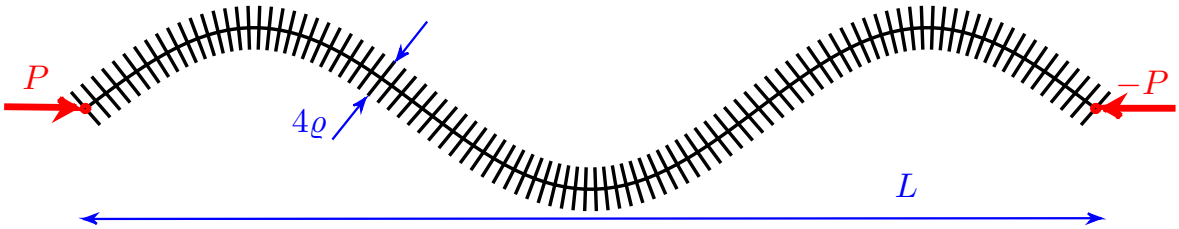

Figure 2.10 – *Shape of a pinned-pinned beam under a Winkler foundation.* $g = 5/2$, $\ell = 100$, $\kappa_1 = 10^{-4}$, $\kappa_2 = 10^{-2}$. *The buckling mode associated to the smallest strain that is the third one:* $k_b = 3\pi/\ell$ *with a critical strain* $\epsilon_b = 3 \cdot 10^{-2}$.

Remark. By examining (2.54), we remark that $\theta' \sim k\Xi(k)$, hence for buckling $\theta' \sim k_b^2 \ll 1$ and the limit $\underline{\kappa_2}(S) = \dfrac{1}{R}$ is not attained.

Discussion

The estimations of ϵ_b for *large* and *small* regimes (in (2.63) and (2.60), respectively) are given in Fig.2.11. The given approximations are clearly justified for both models. It is the occasion to highlight that the *large-regime* approximation (2.63) of ϵ_b is included in (2.60) as:

$$\lim_{k_b \to \kappa_1^{1/4}} \left(k_b^2 + \frac{\kappa_1}{k_b^2} + \kappa_2 \right) = 2\sqrt{\kappa_1} + \kappa_2 \ .$$

This fundamental equation (2.60) corresponds to the differential equation:

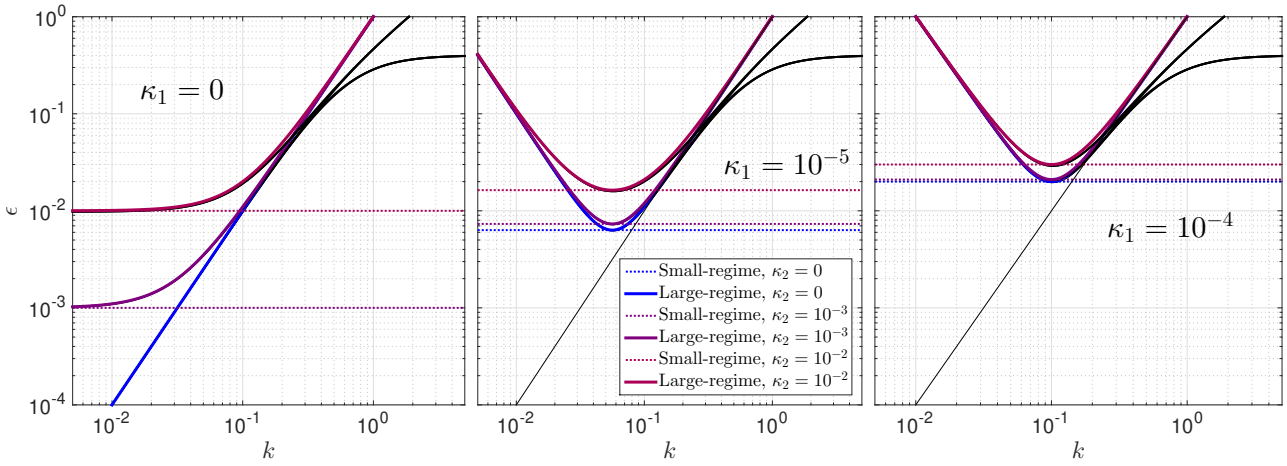

Figure 2.11 – *Report of Fig.2.7 where all previous curves are in black. The new superimposed curves are the small-regime and large-regime estimations of ϵ_b given in (2.63) and (2.60), respectively.*

$$u^{(4)} + (\epsilon_b - \kappa_2)\, u'' + \kappa_1 u = 0 \ .$$

This corresponds to the superposition of the Euler-buckling equation with the Pasternak foundation model. In the non-dimensional form used in this section, these latter are respectively:

$$u^{(4)} + \epsilon_b\, u'' = 0, \qquad u^{(4)} - \kappa_2 u'' + \kappa_1 u = 0 \ .$$

2.4.5 Yield limit

It must be recalled that the proposed models are accompanied by some physical hypotheses such as $\epsilon < \epsilon_{yield}$. For steel-like material $\epsilon_{yield} \simeq 2 \cdot 10^{-3}$ and for fiber reinforced composite $\simeq 5 \cdot 10^{-2}$. If this hypothesis is respected the Engesser and Haringx predictions of ϵ for a given wavenumber k coincide (see Fig.2.11).

Let us consider first the *small-regime* where $\kappa_1 \ell^4 \ll 1$ (*sec*-2.4.4). As (2.60) is the sum of three

positive terms, the criterion $\epsilon < \epsilon_{yield}$ implies that three constrains have to be satisfied *a minima*: $k_b^2 < \epsilon_{yield}$, $\kappa_1/k_b^2 < \epsilon_{yield}$ and $\kappa_2 < \epsilon_{yield}$. The first involves $1 < \epsilon_{yield}\ell^2$ that is already present in the Euler model without foundation: this criterion is satisfied for most of the slender structure but could be violated for thick beam. The second may be rewritten as $\kappa_1\ell^2 < \epsilon_{yield}$, however if the preceding criterion is satisfied the following hierarchy is observed $\kappa_1\ell^4 < 1 < \epsilon_{yield}\ell^2$ then $\kappa_1\ell^2 < \epsilon_{yield}$ is verified. Lastly, the third criterion $\kappa_2 < \epsilon_{yield}$ gives a constraint on κ_2 for a given material but independently of the length of the beam.
For the situation where $1 \ll \kappa_1\ell^4$ (2.63) gives two constraints on the foundation stiffness that have to be satisfied a minima :$\sqrt{\kappa_1} < \epsilon_{yield}$ and $\kappa_2 < \epsilon_{yield}$.
If the material of the structure (and then ϵ_{yield}) is known, these analyses exhibit non-trivial necessary condition on κ_i and ℓ for-which buckling may appear before irreversible transformation:

$$\kappa_2 < \epsilon_{yield}, \qquad \text{in all the cases and} \qquad \begin{array}{ll} \ell > \dfrac{1}{\sqrt{\epsilon_{yield}}} & \text{if} \quad \kappa_1\ell^4 \ll 1 \\ \kappa_1 < \epsilon_{yield}^2 & \text{if} \quad 1 \ll \kappa_1\ell^4 \end{array} \tag{2.65}$$

In the *small-regime*, combining $\ell > 1/\sqrt{\epsilon_{yield}}$ and $\kappa_1\ell^4 \ll 1$ leads to $\kappa_1 < \epsilon_{yield}^2$. Hence the preceding constraints may be easily synthesized, regardless of the regime, by:

$$\boxed{\begin{array}{lll} \ell > \dfrac{1}{\sqrt{\epsilon_{yield}}}, & \kappa_1 < \epsilon_{yield}^2, & \kappa_2 < \epsilon_{yield} \\ \text{equivalently} & \max\left(\dfrac{1}{\ell^2},\ \sqrt{\kappa_1},\ \kappa_2\right) < \epsilon_{yield} & \end{array}} \tag{2.66}$$

From the point of view of the authors, such bounds may be of particular interest for engineering design of slender structures subjected to elastic foundation.
The constraints (2.66) have motivated the choice of the values of $\kappa_1 \leq 10^{-4}$ and $\kappa_2 \leq 10^{-2}$ in Fig.2.7, Fig.2.8 and Fig.2.11 as $\epsilon_{yield} \leq 5 \cdot 10^{-2}$ for most of the standard material.
Of course, because (2.66) are *necessary* conditions, for a given problem the more restrictive *sufficient* condition $\epsilon < \epsilon_{yield}$ has to be checked even if (2.66) is respected. Hence, note that even if (2.66) are satisfied in Fig.2.11, the criterion $\epsilon < \epsilon_{yield}$ doesn't look systematically satisfied. This is particularly true if $\kappa_1 = 10^{-4}$ where ϵ_b is systematically larger than 10^{-2} while $\epsilon_{yield} > 10^{-2}$ is not necessarily obtained for large range of material. This illustrates the *non-sufficient* character of conditions (2.66). Note also that Engesser and Haringx models differ in a regime for which $\epsilon > \epsilon_{yield}$ for most of the standard material.
At last, for $\kappa_1 < 10^{-4}$, (2.61) induces $\lambda_b > 20\pi$ in the *small-regime*. In a dimensional point of view the wavelenght is $\underline{\lambda}_b > 20\pi\varrho$ (for a cylindrical beam of radius R, $\underline{\lambda}_b > 10\pi R$).
It should be mentioned that another buckling model for large transformation will be presented in chapter 3 (section (3.7.2)).

2.5 Conclusion

In this chapter, we offered an analytical study of small transformation of a planar elastic, isotropic, homogeneous Timoshenko beam with linear constitutive law and linear geometrical relations.
The problem was formulated in a non-dimensional way in order to reduce the number of independent parameters such as allowing a general statement.
We started first by examining a beam subjected to a rigid wall where exact solutions were obtained using a model decomposition method and by imposing an initial and a choc type boundary condition.
Then, we let this wall to be elastic, in this case we obtained a coupled wave equations were dispersion relations were discussed in details for different wall rigidity.
Furthermore, a study of buckling of a beam supported by foundation has been performed. The problem was stated for plane, quasi-static and infinitesimal motion of a straight and uniform Timoshenko beam superimposed to a finite longitudinal force such as Haringx and Engesser models were used. Foundations operate external densities of moment and transversal force. These densities are linearly related to rotation and transverse displacement of the beam in accordance with the two-parameters Winkler model of foundations.
For both models, buckling analysis was performed by investigating, in an analytical way, the relation between the critical buckling load and the wavenumber of buckling modes according to the foundation parameters. The explicit expression of the buckling mode and critical stress were given for pinned-pinned beam and general formulation was exhibited for general boundary conditions.
Introducing the yield stress of the material of the beam completes the discussion by introducing a criterion for which buckling prevails over irreversible transformation. The non-dimensional form of this simple criterion makes it particularly suitable for engineering design. In the buckling-regime the Engesser and Haringx model converge to the same estimation of the critical buckling stress and buckling modes have the same behaviour.
In the regime for which the effect of foundation is relevant, the equation used to determine buckling stress and eigenmodes coincides with the superposition of the Euler-buckling equation with the Pasternak foundation model. These two models were build on Euler-Bernoulli beam theory and then the Timoshenko theory proposed through the Engesser or Haringx models looked too sophisticated for the description of the problem of buckling of beam supported by two-parameter foundations. As a corollary consequence, the discussion about the meaning of the second parameter of the generalized Winkler foundations (whether it is associated to rotation θ of the section or slope u' of the centerline) is not relevant as the kinematical constraint $u' - \theta = 0$ holds for Euler-Bernoulli beam.
One can study the several approaches presented in this chapter by adapting a variational formulation (*e.g.* [DP11]). This variational approach is very powerful to solve numerically the problem using finit element methods.

Chapter 3

Explicit analysis of large transformation of a Timoshenko beam: Post-buckling solution, bifurcation and catastrophes

---

Post buckling analyses of a Timoshenko beam subjected to external loads and moments were conducted by many scientists in the last century, such as Reissner [Rei72], Humer [Hum13; HP19] and Batista [Bat13; Bat14; Bat16a] where remarkable results were obtained. We consider this chapter as an extension of these analyses by focusing on a straight Timoshenko beam supporting a large and quasi-static plane transformation with linear constitutive relation and loading that is imposed only at the boundaries. General problem under these hypotheses is presented in a dimensionless form in the first section. In order to embrace wide applications, the situations for quasi-static follower or dead load are examined and domain of variation of each dimensionless parameters is examined in the second section. In the third section, our approach leads to a Cauchy initial problem on contrary to most previously conducted studies (based on boundary value problem). This imposes a meticulous analysis (values, variation domain) of each component of the problem. Two invariants of the problem are exhibited. Existence and uniqueness of the solution for a prescribed load is addressed in the same section. The next section focuses on explicit and analytical solutions of the problem for any given load (force and moment) at one end. The problem of regularity of these solutions in regards to a smooth (and quasi-static) evolution of the load at one end is tackled through a deep analysis of the analytical expressions. After an illustrating example, the problem of a pure-shear follower load is presented and shows how asymptotic solutions can be recovered through Taylor expansion of the attainable expression. In the following section, the problem of quasi-static stability problem is addressed as a driven parametric oscillator in a general situation. At last, section seven shows how the proposed approach is able to face the problem of quasi-static instability in a more general manner than bifurcation (buckling) as catastrophe. The conclusion underlines the main points of the work.

3.1 Kinematical and dynamical variables

As seen in section (1.3.4), dimensionless kinematical variables are:

$$\begin{aligned} \text{Placement :} \qquad & \boldsymbol{\varphi} = \varphi_1 \mathbf{d}_1 + \varphi_3 \mathbf{d}_3. \\ \text{Strain :} \qquad & \boldsymbol{\varepsilon} = \varepsilon_1 \mathbf{d}_1 + \varepsilon_3 \mathbf{d}_3. \\ \text{Curvature :} \qquad & \boldsymbol{\kappa} = \kappa_2 \mathbf{d}_2 = \theta' \mathbf{d_2}. \end{aligned} \tag{3.1}$$

Dimensionless energy per unit length (1.109) becomes:

$$\Psi = \frac{1}{2}\varepsilon_1^2 + \frac{1}{2}g(\varepsilon_3 - 1)^2 + \frac{1}{2}g\kappa_2^2. \tag{3.2}$$

Hence, forces and moment:

$$\boxed{\begin{aligned} N_1 &= \varepsilon_1, \\ N_3 &= g(\varepsilon_3 - 1), \\ M_2 &= g\kappa_2. \end{aligned}} \tag{3.3}$$

3.1.1 Static equilibrium

In this chapter, we assume that $\mathbf{q} = \mathbf{m} = 0$, therefore the static dimensionless form of (1.111) becomes

$$\boxed{\begin{aligned} \mathbf{N}' &= 0, \\ \mathbf{M}' + \boldsymbol{\varepsilon} \times \mathbf{N} &= 0. \end{aligned}} \tag{3.4}$$

And the strain formulation (1.113) will be:

$$\boxed{\begin{aligned} \varepsilon_1' + g(\varepsilon_3 - 1)\kappa_2 &= 0, \\ g\varepsilon_3' - \varepsilon_1\kappa_2 &= 0, \\ g\kappa_2' + \varepsilon_1\varepsilon_3 - g\varepsilon_1(\varepsilon_3 - 1) &= 0. \end{aligned}} \tag{3.5}$$

Consitutive relation (3.3) and equilibrium relation (3.4) (or its projection (3.5)) are our starting points for the analysis of solutions of the static equilibrium problem of the beam.

Remark. Due to large transformation, a non linear geometrical relations appear, namely:

$$\begin{aligned} \varepsilon_1 &= \varphi_1' + \varphi_3\kappa_2, \\ \varepsilon_3 &= \varphi_3' - \varphi_1\kappa_2. \end{aligned} \tag{3.6}$$

So injecting (3.6) into (3.5) we obtain a second order system of differential equations with respect to the placement $\varphi_{1,3}(s)$ and the rotation $\theta(s)$. This equation is hard to solve analytically, so we will present later another way to find these variables.

3.2 Remark on the boundary conditions

The static problem is posed up to a translation and a rigid rotation. It is then natural to observe that the problem (3.4) is perfectly described thanks to dynamical (stresses or strains) quantities.

3.2.1 Parametrization of the boundary conditions

The boundary conditions are prescribed at a given end, say $s = \ell$. Then consider the known quantities

$$\mathbf{N}_\ell = \mathbf{N}(\ell), \qquad \mathbf{M}_\ell = \mathbf{M}(\ell)\,.$$

Of course, $\mathbf{M}_\ell = M_\ell \mathbf{d_2}$ is oriented along $\mathbf{e_y}$ and $\mathbf{N}_\ell$ belongs to the $(\mathbf{e_x}, \mathbf{e_z})$-plane (equivalently $(\mathbf{d_1}, \mathbf{d_3})$-plane). Hence, orientation and magnitude of $\mathbf{N}_\ell$ have to be described properly. Let us define $\phi_\ell = \widehat{\mathbf{d_3}(\ell), \mathbf{N}_\ell}$ the relative angle of the load respectively to the normal $\mathbf{d_3}(\ell)$ of the last section. By convention ϕ_ℓ is measured in a trigonometric way, such that (see fig.(3.1)):

$$N_1(\ell) = N_\ell \sin(\phi_\ell)\ , \qquad N_3(\ell) = N_\ell \cos(\phi_\ell)\ , \tag{3.7}$$

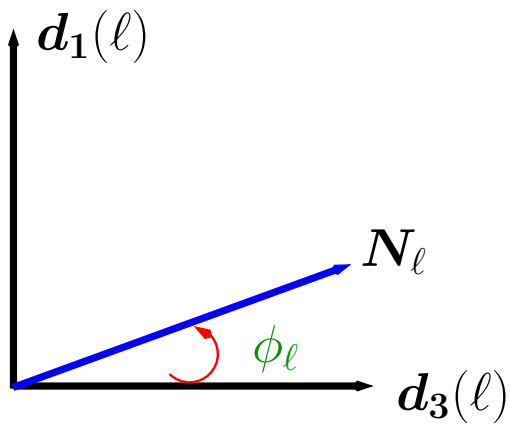

Figure 3.1 – *Variation of $N_1(\ell)$ and $N_3(\ell)$ with respect to $\phi(\ell)$ in the plan of motion.*

where $N_\ell = \|\mathbf{N}_\ell\|$ and $\phi_\ell \in]-\pi, \pi]$. This convention emphasizes the crucial role of ϕ_ℓ that prescribes the shear or normal character of the external force at this specific end. For $\phi_\ell = \pm\pi/2$ the external force is a shear, for $\phi_\ell = \pi$ it is a compression, last for $\phi_\ell = 0$ it is a traction.

Remark. [Cauchy problem] It must be stressed that under this point of view the boundary condition is the set $(N_\ell, \phi_\ell, M_\ell)$: an assignation of the variables (or their derivatives) at a specific end. In that context the problem has the structure of a Cauchy initial value problem from which the solution is known as unique [CL55]. It is clear that for most of the physical problem, distinct constraints are imposed at each end and then the problem has mainly the structure of a Cauchy boundary value problem for which the solution is not necessarily unique. The next sections are mainly related to Cauchy initial value problem associated to the set $(N_\ell, \phi_\ell, M_\ell)$. The last section would be devoted to the Cauchy boundary value problem.

3.2.2 Follower and dead load

At the end $s = \ell$, the rotation of the section $\theta(\ell)$ and the angle ϕ_ℓ between the section and the load $\mathbf{N}_\ell$ are related by

$$\phi_\ell = \hat{\phi} - \theta(\ell). \tag{3.8}$$

According to Fig.3.2, $\hat{\phi} = \widehat{\mathbf{e_z}, \mathbf{N}_\ell}$ is the angle between the external force and the normal of the last

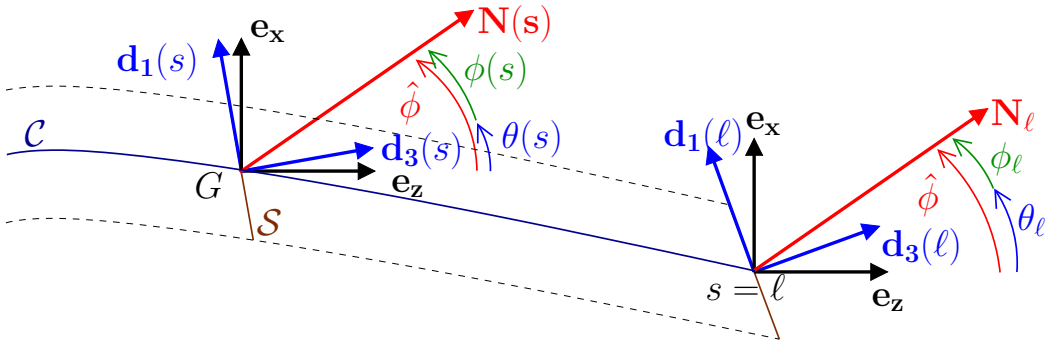

Figure 3.2 – *Parametrization of a current configuration of a Timoshenko beam. At a given curvilinear abscissa s, the center of mass G and the section $\mathcal{S}$ are given. The directors $\mathbf{d_1}(s)$ and $\mathbf{d_3}(s)$ of this section are obtained by a rotation $\theta(s)$ around $\mathbf{e_y}$. At $s = \ell$ the external force $\mathbf{N}_\ell$ has an angle $\phi(\ell) = \phi_\ell$ with the normal $\mathbf{d_3}(\ell)$ of the last section and $\hat{\phi}$ with $\mathbf{e_z}$.*

section at rest (in such a sense, it can be seen as a Lagrangian quantities).
Let us suppose that the magnitude N_ℓ and M_ℓ of the external efforts vary in a quasi-static way. A priori this may imply a possible reorientation of the last section or of the load. Indeed, prescribing the angle ϕ_ℓ during this variation has a large physical impact. More precisely, during this slow evolution, standard situations appear for such special cases:

— If ϕ_ℓ is held constant, the external force is a follower load. In particular if ϕ_ℓ is maintained equal to π the external force is a purely compressive follower load and if $\phi_\ell = \pm\pi/2$ this force acts as a pure shear follower load. Note that during this evolution the value of $\hat{\phi}$ changes in order to respect (3.8).

— If $\hat{\phi}$ is held constant, the external force is a dead load. In particular if $\hat{\phi}$ is maintained null or equal to π the external force is a pure vertical (along $\mathbf{e_z}$) dead load and if $\hat{\phi} = \pm\pi/2$, this

force acts as a pure horizontal dead load. Here ϕ_ℓ has to change during the loading process in order to respect (3.8).

3.2.3 Domain of variation

A priori, $N_\ell \geq 0$, $\phi_\ell \in [0, 2\pi[$ and $M_\ell \in \mathbb{R}$ but physical considerations may help to limit these bounds.
First of all, it can be observed that non-overlapping of the section of the beam during a large bending imposes $|\kappa_2| \lesssim 1/2$. Second, it is justified to limit the analysis to a total force lower than a certain multiple of the Euler critical load. For pinned boundary conditions this latter is physically $\underline{P}_e = EI\pi^2/L^2$, then its dimensionless form is $P_e = g\pi^2/\ell^2$. As beam model is justified for slenderness ratio $\ell \gtrsim 20$ and $2 \lesssim g \lesssim 3$, one gets $P_e \lesssim 0.1$. Hence, it is convenient to focus on the following bounds for boundary conditions variables

$$0 \leq N_\ell \leq 0.1, \qquad -0.1 \leq M_\ell \leq 0.1\ . \tag{3.9}$$

These bounds are particularly large, especially for elongated structures. It must not be considered as an indicator of the order of magnitude of these variables, but rather as a maximum bounds (physically unreachable in general). However, the bounds $N_\ell \leq 0.01$ and $|M_\ell| \leq 0.01$ are attainable in most of the cases.
These bounds may be used to prescribe some bounds for strains at $s = \ell$, and more generally at any s according to (3.3). One gets:

$$-0.1 \leq \varepsilon_1(s) \leq 0.1, \qquad 0.95 \leq \varepsilon_3(s) \leq 1.05, \qquad -0.05 \leq \kappa_2(s) \leq 0.05.$$

3.3 Problem analysis

3.3.1 First integration

The system (3.4) may be easily integrated. Considering the first line, one gets directly

$$\mathbf{N}(s) = \mathbf{N}_\ell, \qquad \forall\ s \in [0, \ell].$$

In other words, the internal load is constant along the beam. However, as the orientation of the directors $\mathbf{d_1}(s)$ and $\mathbf{d_3}(s)$ are not uniform, the shear and longitudinal component are not uniform along s, but controlled by

$$N_1(s) = \mathbf{N}_\ell \cdot \mathbf{d_1}(s), \qquad N_3(s) = \mathbf{N}_\ell \cdot \mathbf{d_3}(s). \tag{3.10}$$

Considering now the second equation of (3.4), its integration is trivial too. First as $\boldsymbol{\varepsilon} = \boldsymbol{\varphi}'$, one gets

$$\mathbf{M}' + \boldsymbol{\varphi}' \times \mathbf{N}_\ell = 0,$$

then, after integration

$$\mathbf{M}(s) - \mathbf{M}(0) + (\boldsymbol{\varphi}(s) - \boldsymbol{\varphi}(0)) \times \mathbf{N}_\ell = 0, \qquad \forall\ s \in [0, \ell]. \tag{3.11}$$

In particular, one gets a momentum relation between the bending moment at both ends:

$$\mathbf{M}(0) = \mathbf{M}_\ell + \Big(\boldsymbol{\varphi}(\ell) - \boldsymbol{\varphi}(0)\Big) \times \mathbf{N}_\ell.$$

Inspired by (3.7) and (3.10), a new variable $\phi(s)$ is introduced such that

$$\begin{array}{rcl} N_1(s) & = & N_\ell \sin\left(\phi(s)\right), \\ N_3(s) & = & N_\ell \cos\left(\phi(s)\right). \end{array} \tag{3.12}$$

Then, $\phi(s)$ is the relative angle between the normal of the section at s and the external load. Of course $\phi(\ell) = \phi_\ell$. The relation (3.8) can be extended too (see Fig.3.2):

$$\phi(s) = \hat{\phi} - \theta(s). \tag{3.13}$$

As $\theta' = -\phi'$, the internal couple $M_2 = g\theta'$ along the beam becomes

$$M_2(s) = -g\phi'(s). \tag{3.14}$$

Lastly, all strains may be written in terms of ϕ according to (3.3):

$$\boxed{\begin{array}{rcl} \varepsilon_1(s) & = & N_\ell \sin\left(\phi(s)\right), \\ \varepsilon_3(s) & = & 1 + \dfrac{N_\ell}{g} \cos\left(\phi(s)\right), \\ \kappa_2(s) & = & -\phi'(s). \end{array}} \tag{3.15}$$

To simplify further notation ϕ'_ℓ will be used instead of $\phi'(\ell)$ in the following.

3.3.2 Non-homogeneous equation

The two first equations of (3.5) are directly satisfied, the last one becomes

$$g^2\phi'' - gN_\ell \sin\left(\phi\right) + (g-1)N_\ell^2 \sin\left(\phi\right)\cos\left(\phi\right) = 0. \tag{3.16}$$

Let us consider that $\phi'' \neq 0$. By multiplying (3.16) by $2\phi'$ one obtains after integration (*e.g.* [YTM90]):

$$\boxed{(g\phi')^2 + 2gN_\ell \cos(\phi) - (g-1)N_\ell^2 \cos^2(\phi) = \mu.} \tag{3.17}$$

where μ is a constant related to set $(N_\ell, \phi_\ell, M_\ell)$ of boundary conditions

$$\boxed{\mu = M_\ell^2 + 2gN_\ell \cos(\phi_\ell) - (g-1)N_\ell^2 \cos^2(\phi_\ell)}. \tag{3.18}$$

Remark. [Invariants] The magnitude N_ℓ is the *first invariant* of the beam as, for any s:

$$N_\ell^2 = N_1(s)^2 + N_3(s)^2.$$

In the first integral (3.17) of (3.16) the parameter μ appears as *a second invariant* of the beam configuration. Indeed, in terms of internal load, as $M_2(s) = -g\phi'$ and $N_3(s) = N_\ell \cos(\phi(s))$, one gets all along the beam:

$$\mu = M_2(s)^2 + 2gN_3(s) - (g-1)N_3(s)^2.$$

These two invariants are presented graphically in Fig.3.3
Equation (3.17) is a scalar, first order and non-linear ordinary differential equation. Its coefficient is

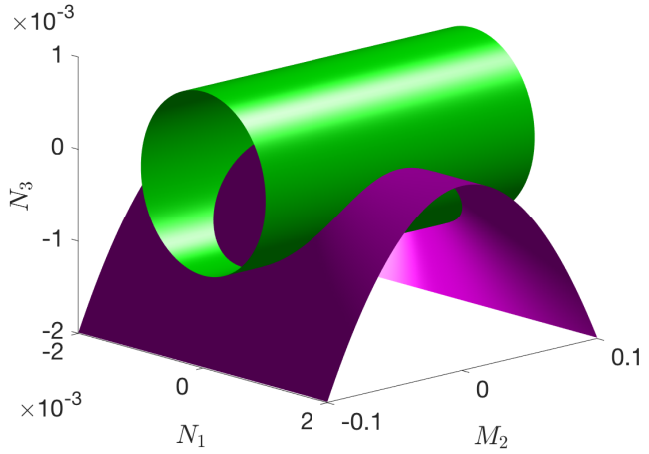

Figure 3.3 – *Representation of the two invariants (N_ℓ in green and μ in purple) in the configuration space $(N_1(s), M_2(s), N_3(s))$. The solutions $N_1(s)$, $M_2(s)$ and $N_3(s)$ of the problem is along the intersection of the two surfaces.*

written in terms of the invariants μ and N_ℓ of the problem. Its resolution can be performed thanks to some special change of variable that will be developed in the next section.

Remark. [Existence and unicity of the solution] According to Cauchy theorem, the ordinary differential equation (3.17) has a unique solution if ϕ_ℓ or ϕ'_ℓ is prescribed (*e.g.* [CL55]). Existence and unicity is then obtained if the invariants (μ, N_ℓ) are prescribed. As the load properties $(N_\ell, \phi_\ell, M_\ell)$ at $s = \ell$ defines (N_ℓ, μ, ϕ_ℓ) or $(N_\ell, \mu, \phi'_\ell)$ in a unique manner, existence and unicity of the solution are ensured by the prescription of the load at one end.

Remark. [Discussion on the regularity of the solution] As the set $(N_\ell, \phi_\ell, M_\ell)$ contributes to define both the initial condition and the coefficients μ, N_ℓ of the differential equation, the regularity of the solution may be (a prioiri) strongly affected by even a smooth change of N_ℓ, ϕ_ℓ or M_ℓ. This very special character of the problem explains (at least in a part) the attention of scientists on behaviour of beam under large transformation. This problem will be adressed more deeply in section 3.4.6.

3.3.3 Homogeneous equation

Let us consider the special case $\phi'' = 0$ for all s (then $\phi' = cste$). From (3.16) and according to the domain of variation of g, this situation appears only if $N_\ell \sin(\phi) = 0$, which corresponds to two distinct cases:

— If $N_\ell = 0$ the last end supports only a non-null couple M_ℓ. In that case $\phi(s) = as + b$ where a and b depends on boundary conditions. Since $M_\ell = -g\phi'(\ell)$, $a = -M_\ell/g$ and imposing arbitrarily $\phi(\ell) = 0$ implies $b = M_\ell \ell/g$ and by (3.8) one gets $\hat{\phi} = \theta(\ell)$, therefore, by (3.13) one obtains

$$\theta(s) = \frac{M_\ell}{g}(s - \ell) + \theta(\ell). \tag{3.19}$$

Dynamical variables are given by $N_1(s) = 0$, $N_3(s) = 0$ and $M_2(s) = M_\ell$. Using (1.108),(3.3) one gets:

$$\begin{aligned} \varphi_1(s) &= \varphi_1(0) + \frac{g}{M_\ell}(\cos(\theta(s)) - 1), \\ \varphi_3(s) &= \varphi_3(0) + \frac{g}{M_\ell}\sin(\theta(s)). \end{aligned} \tag{3.20}$$

This problem is a standard solution in Elastica theory.

— If $\sin(\phi(s)) = 0$ then $\phi(s) = 0$ or π: the load is a pure longitudinal force. Therefore, by using (3.13) one gets $N_1(s) = 0$, $N_3(s) = \pm N_\ell$ and $M_2(s) = 0$. So, kinematical variables are given for pure traction or compression by:

$$\varphi_1(s) = \varphi_1(0), \qquad \theta(s) = \theta(0), \qquad \varphi_3(s) = \varphi_3(0) + (1 \pm \frac{N_\ell}{g})s.$$

For other situations, ϕ' is necessarily not uniform and the problem consists in the resolution of (3.17).

3.3.4 Analysis of μ

As it has been observed μ plays an important role as first variable integration depending on $(N_\ell, \phi_\ell, M_\ell)$. More precisely, the shear load does not affect this parameter that is controlled by M_ℓ and the longitudinal part of the force $N_\ell \cos(\phi_\ell)$ (see (3.18)). The behaviour of μ with respect to these parameters is given in Fig.3.4.

In practice, μ is positive for a longitudinal traction or a moderate longitudinal compressive force

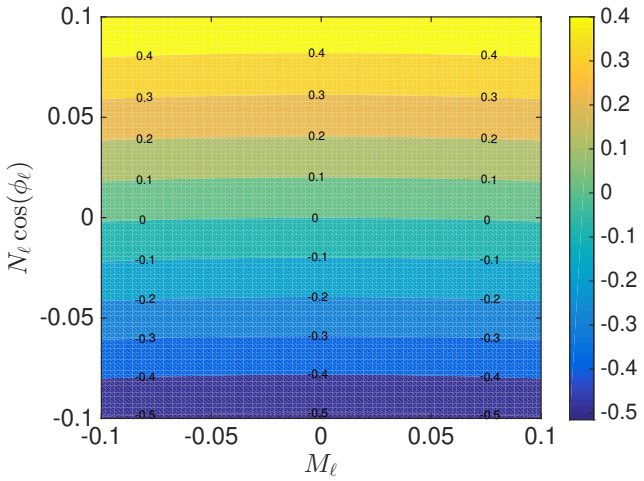

Figure 3.4 – *Variation of μ according to the parameter of the boundary conditions.*

associated to non null couple M_ℓ. The following bounds for μ are obtained

$$M_\ell^2 - 2gN_\ell - (g-1)N_\ell^2 \;\leq\; \mu \;\leq\; M_\ell^2 + 2gN_\ell - (g-1)N_\ell^2, \tag{3.21}$$

and $-0.5 \lesssim \mu \lesssim 0.5$ according to the numerical values proposed in section 3.2.3. Let us introduce

$$\mu_a = -2gN_\ell - (g-1)N_\ell^2, \qquad \mu_c = 2gN_\ell - (g-1)N_\ell^2 \ . \tag{3.22}$$

Remark that in contrary to μ, the parameters μ_a and μ_c depends only on N_ℓ. The equality $\mu = \mu_a$ is obtained only for pure compressive load. For a pure traction $\mu = \mu_c$ however, the equality $\mu = \mu_c$ may be observed for other configurations for which $\phi_\ell \neq 0$ and $M_\ell \neq 0$. There is always $\mu_a \leq \mu$ but in the special cases for which $M_\ell = 0$ the bounds are more restrictive: $\mu_a \leq \mu \leq \mu_c$.

3.4 Jacobian elliptic functions

In this section the problem (3.17) is solved using a series of transformations that leads to Jacobian elliptic functions. The study concerns non-homogeneous solutions of (3.17).

3.4.1 Problem statement

Let us first use the tangent half-angle substitution for ϕ:

$$t(s) = \tan\left(\frac{\phi(s)}{2}\right), \tag{3.23}$$

where $t(s)$ is a real valued function. Therefore,

$$\cos(\phi) = \frac{1-t^2}{1+t^2}, \qquad \sin(\phi) = \frac{2t}{1+t^2}, \qquad \phi' = \frac{2t'}{1+t^2}. \tag{3.24}$$

Injecting (3.24) into (3.17), the differential equation is written as:

$$t'^2 = a\,t^4 + b\,t^2 + c. \tag{3.25}$$

— If $a \neq 0$, the roots of the t-polynomial at the right-hand side can be computed in order to obtain:

$$t'^2 = a\,(t^2 - \alpha_-)(t^2 + \alpha_+). \tag{3.26}$$

— If $a = 0$, then

$$t'^2 = b\,t^2 + c. \tag{3.27}$$

All these formulations need a deep analysis of each parameter a, b, c and $\alpha_\pm$ that are intrinsically related to the set of boundary conditions (N_ℓ, ϕ_ℓ, M_ℓ), and more precisely to two independent coefficients μ and N_ℓ:

$$\begin{array}{rcl} a &=& \dfrac{\mu - \mu_a}{4g^2}, \\ b &=& \dfrac{2\mu + \mu_a + \mu_c}{4g^2}, \\ c &=& \dfrac{\mu - \mu_c}{4g^2}, \end{array} \qquad \text{and} \qquad \begin{array}{rcl} \alpha_+ &=& \dfrac{\frac{g+\sqrt{g^2-(g-1)\mu}}{g-1} - N_\ell}{\frac{g+\sqrt{g^2-(g-1)\mu}}{g-1} + N_\ell}, \\ \alpha_- &=& \dfrac{N_\ell - \frac{g-\sqrt{g^2-(g-1)\mu}}{g-1}}{N_\ell + \frac{g-\sqrt{g^2-(g-1)\mu}}{g-1}}. \end{array} \tag{3.28}$$

3.4.2 Parameter analysis

According to (3.3.4) $\mu_a \leq \mu$ then $a \geq 0$.

Remark. Equality $a = 0$ corresponds to a pure longitudinal compression for which an homogeneous solution has been found already. Notice that if $a = 0$, then $\mu = \mu_a$ and, as $\mu_a \leq 0 \leq \mu_c$, both b and c are strictly negative. In other words, the right hand side of (3.27) is negative and then no real non-homogeneous solutions $t(s)$ may exist. For pure compressive external force, the homogeneous solution is the only real-valued solution. It is now justified to focus hereafter on (3.26) with strictly $\mu > \mu_a$ then $a > 0$. However, sign of b and c may change according to M_ℓ, ϕ_ℓ and N_ℓ.

The roots $\alpha_\pm$ are real as $g^2 - (g-1)\mu$ is always positive. The values of α_+ according to N_ℓ and μ is presented in Fig.3.5-left (the values of α_+ are presented in a domain such that $\mu > \mu_a$). This root is strictly positive and close to 1. First order Taylor expansion gives:

$$\alpha_+ = 1 - \frac{g-1}{g} N_\ell \; + \mathcal{O}(N_\ell^2, \mu^2). \tag{3.29}$$

The values of α_- according to N_ℓ and μ are presented in Fig.3.5-right. As α_- has a large domain of variation the $\log_{10}(|\alpha_-|)$ is plotted and the sign of α_- is specified in each domain. In practice

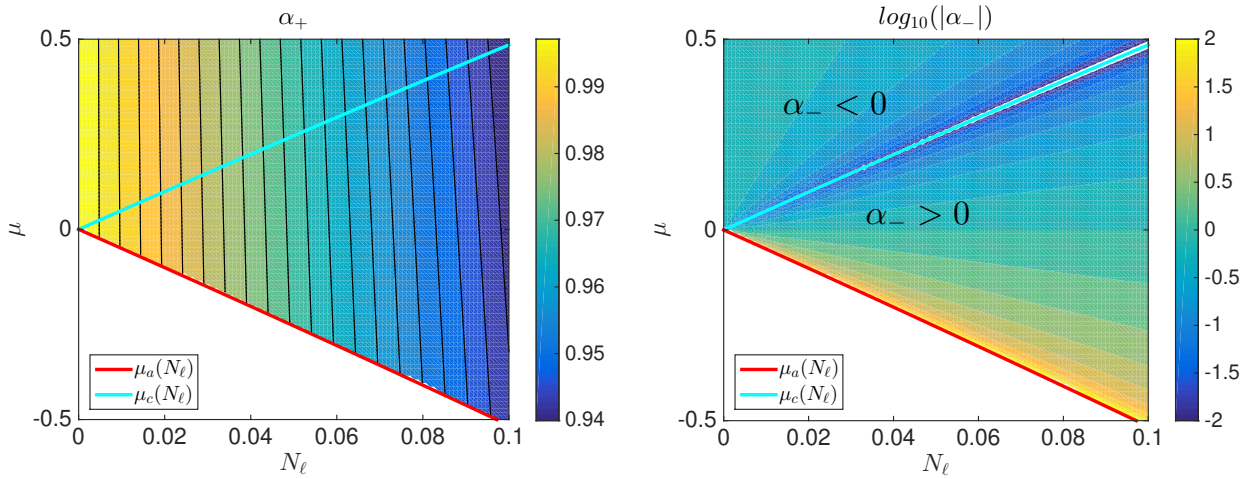

Figure 3.5 – *Variation of* α_+ *(left) and* $\log_{10}(|\alpha_-|)$ *(right) according to* N_ℓ *and* μ*. The curves* $\mu = \mu_a(N_\ell)$ *and* $\mu = \mu_a(N_\ell)$ *are presented too.*

$\alpha_- > 0$ if $\mu_a < \mu < \mu_c$ and $\alpha_- < 0$ if $\mu_c < \mu$. $\alpha_- = 0$ if $\mu = \mu_c$ and for small values of μ, N_ℓ:

$$\alpha_- = 1 - \frac{2\mu}{\mu + 2gN_\ell} + \mathcal{O}(N_\ell, \mu).$$

3.4.3 Resolution of the elliptic differential equation

As $a > 0$ and $\alpha_+ > 0$ in all the domain of variation, the following formulation of (3.26) is proposed:

$$\left(\frac{1}{\sqrt{a\alpha_+}}\frac{t'}{\sqrt{\alpha_+}}\right)^2 = \left((\frac{t}{\sqrt{\alpha_+}})^2 + 1\right)\left((\frac{t}{\sqrt{\alpha_+}})^2 - \frac{\alpha_-}{\alpha_+}\right). \tag{3.30}$$

This motivates the following change of variable associated to a rescaling of the curvilinear abscissa

$$h(\zeta) = \frac{t(s)}{\sqrt{\alpha_+}} \qquad \text{where} \qquad \zeta = \sqrt{a\alpha_+}(s + s_0), \tag{3.31}$$

where the constant s_0 will be related to the boundary conditions. As $\frac{\mathrm{d}}{\mathrm{d}s} = \sqrt{a\alpha_+}\frac{\mathrm{d}}{\mathrm{d}\zeta}$, (3.30) becomes:

$$\left(\frac{\mathrm{d}h}{\mathrm{d}\zeta}\right)^2 = (h^2 + 1)(h^2 - \frac{\alpha_-}{\alpha_+}), \tag{3.32}$$

for which solutions are a Jacobian elliptic function [Olv+10]:

$$h(\zeta) = \pm\mathrm{cs}(\zeta \,|\, m), \qquad \text{with} \qquad m = 1 + \frac{\alpha_-}{\alpha_+}. \tag{3.33}$$

3.4.4 Class of solutions

Particular attention must be drawn to the values of m presented in Fig.3.6-left. For moderate parameters μ and N_ℓ:

$$m = \frac{4gN_\ell}{\mu + 2gN_\ell} + \mathcal{O}(\mu, N_\ell). \tag{3.34}$$

This is illustrated in Fig.3.6-right, where it can be observed that this approximation is well justified.

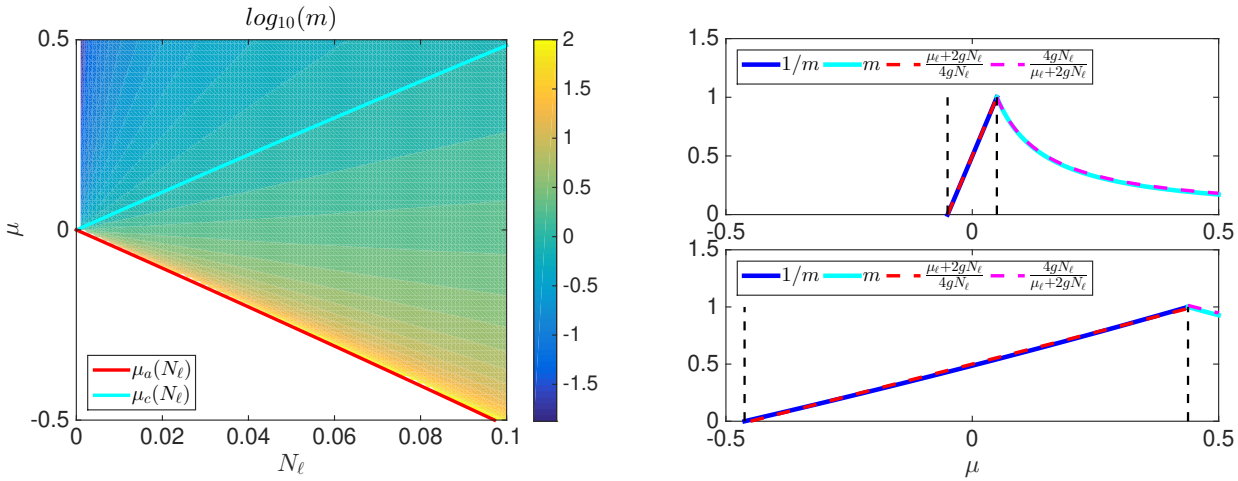

Figure 3.6 – *Left: Variation of* $\log_{10}(m)$ *according to* N_ℓ *and* μ*. The curves corresponding to* $\mu_a(N_\ell)$ *and* $\mu_c(N_\ell)$ *are presented too. Right: Variation of* m *and* $1/m$ *according to* μ *for fixed* N_ℓ*. The approximation* (3.34) *is presented too. The vertical lines depict the position of* $\mu_a(N_\ell)$ *(left) and* $\mu_c(N_\ell)$ *(right).*

In a classical formulation of Jacobian elliptic functions, the second argument m belongs in $[0, 1]$. Here, it is observed that m belongs to $]0, +\infty[$. Moreover, some analyses are given in order to link the two formulations:

— If $\mu_a < \mu < \mu_c$, we have $\alpha_- > 0$ and $\alpha_+ > 0$ then $m > 1$. For this situation, one may use [Olv+10]

$$\mathrm{cs}(\zeta \,|\, \frac{1}{m}) = \frac{1}{\sqrt{m}}\mathrm{ds}(\frac{\zeta}{\sqrt{m}} \,|\, m),$$

to obtain a more standard formulation:

$$h(\zeta) = \pm\sqrt{\frac{\alpha_+ + \alpha_-}{\alpha_+}}\mathrm{ds}(\sqrt{\frac{\alpha_+ + \alpha_-}{\alpha_+}}\zeta \,|\, \frac{\alpha_+}{\alpha_+ + \alpha_-}),$$

then

$$t(s) = \pm\sqrt{\alpha_- + \alpha_+}\ \mathrm{ds}(\sqrt{a(\alpha_- + \alpha_+)}(s + s_0) \,|\, \frac{\alpha_+}{\alpha_+ + \alpha_-}). \tag{3.35}$$

— If $\mu = \mu_c$, $\alpha_- = 0$ and $m = 1$, then

$$h(\zeta) = \pm\mathrm{cs}(\zeta \,|\, 1) = \pm\frac{1}{\sinh(\zeta)}.$$

Alternatively, this can be obtained by observing that $c = 0$, then the differential equation (3.25) becomes $t'^2 = t^2(at^2 + b)$.

— If $\mu > \mu_c$ we have $0 < m < 1$ then

$$t(s) = \pm\sqrt{\alpha_+}\ \mathrm{cs}(\sqrt{a\alpha_+}(s + s_0) \,|\, \frac{\alpha_+ + \alpha_-}{\alpha_+}). \tag{3.36}$$

This last formulation is always justified if one considers for convention $m \in \mathbb{R}$.
In Fig.3.7 the function $\mathrm{cs}(\zeta \,|\, m)$ and $\mathrm{ds}(\zeta \,|\, m)$ are presented for $m = 1/2$. These odd functions have distinct periodicity. Introducing the complete elliptic integral of the first kind $K(m)$, the periodicity is $2K$ for $\mathrm{cs}(\zeta \,|\, m)$ and $4K$ for $\mathrm{ds}(\zeta \,|\, m)$. Remark that $K(m) \to \infty$ as $m \to 1$. As m passes through 1, the transition between $\mathrm{cs}(\zeta \,|\, m)$ to $\mathrm{ds}(\zeta \,|\, m)$ through $1/\sinh(\zeta)$ is then smooth as the non-periodic function $1/\sinh(\zeta)$ is asymptotically considered as a periodic function with infinite period. This anodyne remark leads to more crucial remarks detailed in sec.3.4.6.
Lastly, it is observed that $\mathrm{ds}(\zeta \,|\, m)$ belongs to $]-\infty, -\sqrt{1-m}] \cup [\sqrt{1-m}, +\infty[$ if $0 < m < 1$. According to (3.23) and (3.35), this means that $|\phi(s)|$ does not belong to the interval $[0, 2\arctan(\sqrt{\alpha_-})[$ if $\mu_a \leq \mu \leq \mu_c$.

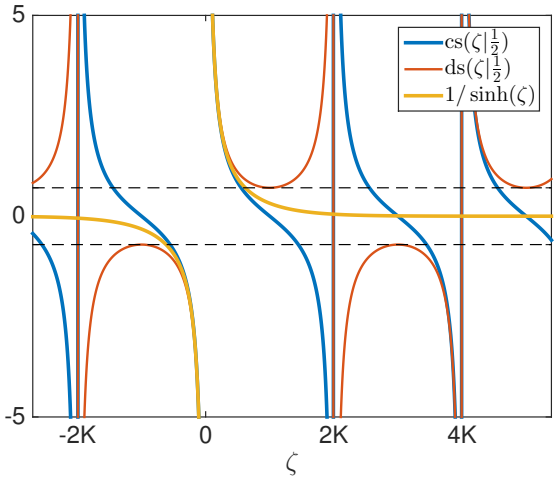

Figure 3.7 – *$\mathrm{cs}(\zeta \,|\, m)$, $\mathrm{ds}(\zeta \,|\, m)$ and $1/\sinh(\zeta)$ for $m = 1/2$. Numerically $K(m) \simeq 1.85$. The horizontal dashed lines corresponds to $\pm\sqrt{1-m} \simeq 0.71$.*

3.4.5 Determination of the unknown s_0

The shifting parameter s_0 has to be adjusted such that

$$t(\ell) = \tan\left(\frac{\phi_\ell}{2}\right), \qquad \frac{2t'(\ell)}{1+t(\ell)^2} = \phi'_\ell, \tag{3.37}$$

where ϕ'_ℓ is just determined by the bending moment according to (3.14): $M_\ell = -g\phi'_\ell$. In practice s_0 is determined numerically by an optimisation algorithm associated to the following statement

$$\text{find } s_0 \in \mathcal{D} \text{ such that} \quad \|t(\ell) - \tan(\frac{\phi_\ell}{2})\|^2 + \|\frac{2t'(\ell)}{1+t(\ell)^2} - \phi'_\ell\|^2 = 0. \tag{3.38}$$

The domain $\mathcal{D}$ and the function $t(s)$ have to be adjusted according to the boundary condition:

— If $\mu < \mu_c$, $\mathcal{D} =]0, \frac{1}{\sqrt{a(\alpha_- + \alpha_+)}} 4K(\frac{\alpha_+}{\alpha_+ + \alpha_-})[$ and $t(s) = \sqrt{\alpha_- + \alpha_+}\,\mathrm{ds}(\sqrt{a(\alpha_- + \alpha_+)}(s+s_0) \,|\, \frac{\alpha_+}{\alpha_+ + \alpha_-})$ (the sign $-$ is not necessary as $\mathrm{ds}(\zeta + 2K(m) \,|\, m) = -\mathrm{ds}(\zeta \,|\, m)$).

— If $\mu > \mu_c$ and $\phi'_\ell < 0$, then $\mathcal{D} =]0, \frac{1}{\sqrt{a\alpha_+}} 2K(\frac{\alpha_+ + \alpha_-}{\alpha_+})[$ and $t(s) = \sqrt{\alpha_+}\ \mathrm{cs}(\sqrt{a\alpha_+}(s+s_0) \,|\, \frac{\alpha_+ + \alpha_-}{\alpha_+})$

— If $\mu > \mu_c$ and $\phi'_\ell > 0$, then $\mathcal{D} =]0, \frac{1}{\sqrt{a\alpha_+}} 2K(\frac{\alpha_+ + \alpha_-}{\alpha_+})[$ too but $t(s) = -\sqrt{\alpha_+}\ \mathrm{cs}(\sqrt{a\alpha_+}(s + s_0) \,|\, \frac{\alpha_+ + \alpha_-}{\alpha_+})$

Indeed with such domain $\mathcal{D}$, the discussion associated to Fig.3.7 shows that the solution s_0 in $\mathcal{D}$ of the problem (3.38) is unique in all the cases.

3.4.6 Regularity of the solutions

The existence and unicity of the problem (3.4) have already been underlined in *rem*-3.3.2. However, regularity of the solution relatively to a smooth change of the boundary conditions parameters $N_\ell, \phi_\ell, M_\ell$ was just interrogated in rem.3.3.2.

According to the discussion of Fig.3.7 the function $t(s)$ is regularly varying according to the parameters $\alpha_\pm$, a and s_0 in all the variation domain of μ, N_ℓ and ϕ_ℓ. It is then the case for $\phi(s)$ too. In other words $\phi(s)$ is regularly dependent on the set (μ, N_ℓ, ϕ_ℓ) or $(\mu, N_\ell, \phi'_\ell)$. On one hand the map $(N_\ell, M_\ell, \phi_\ell) \to (\mu, N_\ell, \phi_\ell)$ is smooth and surjective, on the other hand $(N_1(s), N_3(s), M_2(s))$ are regular function of $\phi(s)$ thanks to (3.15). This leads to the following important result:

The solutions $N_1(s)$, $N_3(s)$, $M_2(s)$ (or equivalently $\varepsilon_1(s), \varepsilon_3(s), \kappa_2(s)$) of the problem (3.4) are regularly dependent on the boundary conditions $(N_\ell, \phi_\ell, M_\ell)$. No bifurcation may occurs if the load is completely controlled (prescription of the couple intensity, force intensity and of the orientation of the force relatively to the section) in a smooth and quasi-static way at one end of the beam. Reciprocally, some bifurcation may occur only if one of these load properties is held free (standard buckling problem of beam by a dead-load) or if a kinematical variable (position or orientation of the section) are controlled.

This result is valid for any large transformation, any shape of the beam and any isotropic and elastic material.

In term of instabilities, the preceding result shows that quasi-static instabilities cannot appear if the loads are controlled at one end in a smooth way. This is the case for follower loads. However, as this work do not invoque dynamical effect, this analysis do not allow any conjecture on dynamical-instabilities. In particular, fluttering effect is not included in the scope of the chapter.

At this stage all unknown functions and parameter are determined. It is then possible to have explicit expression of strains and shape of the beam without any approximation. This is now illustrated through a practical example.

3.5 First illustrating example

Let us consider a beam of length $\ell = 50$ and material ratio $g = 5/2$ supporting the following boundary conditions $N_\ell = 0.01$, $M_\ell = 0.05$, $\phi_\ell = 3\pi/4$. The beam is glued at $s = 0$ on the origin of

the Cartesian frame, then $\theta(0) = 0$ and $\boldsymbol{\varphi}(0) = 0$.

3.5.1 Determination of each parameters

According to the set $(N_\ell,\ M_\ell,\ \phi_\ell)$, one obtains $\mu \simeq -0.03$, $\mu_a \simeq -0.05$, $\mu_c \simeq 0.05$ and $m \simeq 5.86$ then $\mu_a < \mu < \mu_c$ and $m > 1$. The solution $t(s)$ corresponds to (3.35) but can still be written as $t(s) = \sqrt{\alpha_+}\mathrm{cs}(\sqrt{a\alpha_+}(s+s_0)\,|\,m)$, if one accepts that $m > 1$. In Fig.3.8 $t(\ell)$ is presented as a function of s_0. Intersections with the level set $\tan(\phi_\ell/2)$ respecting the constraints (3.37) are highlighted by

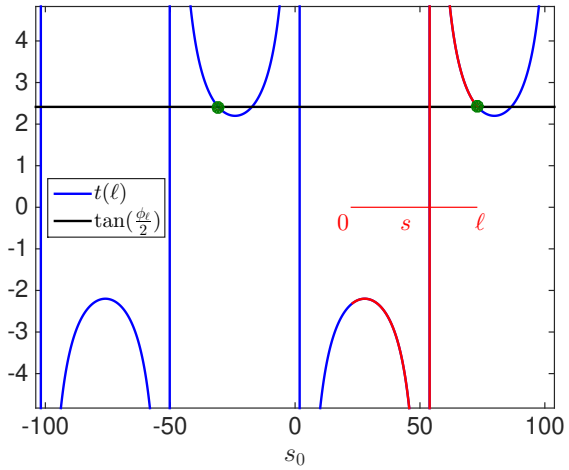

Figure 3.8 – *Graphs of $t(\ell)$ according to s_0. The level-set $\tan(\phi_\ell/2)$ is presented too. The graph of $t(s)$ for an admissible s_0 is presented in red (the corresponding abscissa is given in red too).*

a dot. The possible values of s_0 form a periodic set but any value may be chosen as position of the dot and $t(s)$ share the same periodicity. This illustrates that the definition of a restrictive domain $\mathcal{D}$ in (3.38) does not affect the generality of the resolution.

3.5.2 Determination of the internal forces and moments

According to (3.12), (3.14) and (3.24)

$$N_1(s) = N_\ell \frac{2t}{1+t^2}, \qquad N_3(s) = N_\ell \frac{1-t^2}{1+t^2}, \qquad M_2(s) = -g\frac{2t'}{1+t^2}, \tag{3.39}$$

that is easily computed as $t(s)$ is given in (3.36) and because the derivation rule $\frac{\mathrm{d}}{\mathrm{d}z}\mathrm{cs}(z|m) = -\mathrm{ns}(z|m)\mathrm{ds}(z|m)$ holds true for any $m \in \mathbb{R}$ [Olv+10]. One obtains $t'(s) = -\sqrt{a}\alpha_+\,\mathrm{ns}(\zeta\,|\,m)\mathrm{ds}(\zeta\,|\,m)$ and then:

$$\begin{aligned} N_1(s) &= N_\ell \frac{2\sqrt{\alpha_+}\mathrm{cs}(\zeta\,|\,m)}{1+\alpha_+\mathrm{cs}^2(\zeta\,|\,m)}, \\ N_3(s) &= N_\ell \frac{1-\alpha_+\mathrm{cs}^2(\zeta\,|\,m)}{1+\alpha_+\mathrm{cs}^2(\zeta\,|\,m)}, \\ M_2(s) &= \sqrt{a}g\frac{2\alpha_+\,\mathrm{ns}(\zeta\,|\,m)\mathrm{ds}(\zeta\,|\,m)}{1+\alpha_+\mathrm{cs}^2(\zeta\,|\,m)}, \end{aligned} \qquad \begin{aligned} \zeta &= \sqrt{a\alpha_+}(s+s_0), \\ m &= \frac{\alpha_+ + \alpha_-}{\alpha_+}. \end{aligned} \tag{3.40}$$

The internal forces and moment are illustrated in Fig.3.9-left.

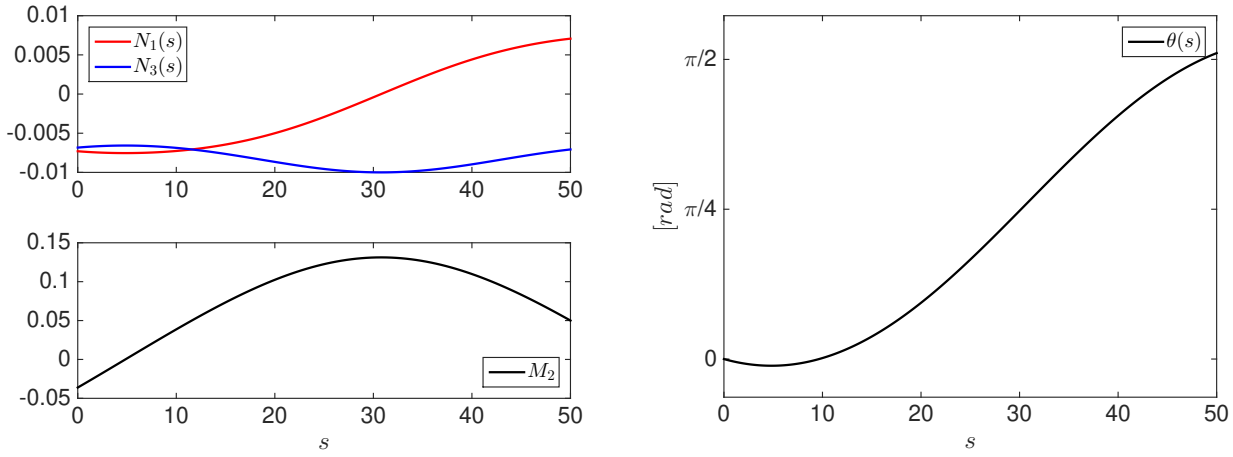

Figure 3.9 – *Left:* $N_1(s)$, $N_3(s)$ *and* $M_2(s)$ *for the example. Right:* $\theta(s)$.

3.5.3 Determination of the rotation and placement

The rotation $\theta(s)$ of the section is directely obtained by (3.13) as $\phi(s)$ is now-determined univocally by (3.23) as $\phi(s) = 2\arctan(t(s))$. Then

$$\theta(s) = \hat{\phi} - 2\arctan\Big(t(s)\Big).$$

The constant $\hat{\phi}$ can be chosen with a great liberty for a given set of boundary conditions as the static problem is unchanged up to a rigid rotation. For a quasi-static loading, details are exposed in sec.3.2.2. As the beam is glued at $s = 0$ in this example, one imposes $\theta(0) = 0$ and then $\hat{\phi} = 2\arctan(t(0))$. The result of this typical case are presented in Fig.3.9-right.

The situation is more complex for the placement function $\boldsymbol{\varphi}(s)$. The two components of this vector have to be determined. In practice $\boldsymbol{\varphi}(s)$ belongs to the $(\mathbf{e_x}, \mathbf{e_z})$-plane. The choice of a proper orthonormal basis is crucial. A Cartesian frame can be chosen such that $\boldsymbol{\varphi} = \varphi_x(s)\mathbf{e_x} + \varphi_z(s)\mathbf{e_z}$ or a mobile director frame such that $\boldsymbol{\varphi} = \varphi_1(s)\mathbf{d_1}(s) + \varphi_3(s)\mathbf{d_3}(s)$. However, another orthogonal frame is naturally introduced into the problem, let us denote it $(\mathbf{e_t}, \mathbf{e_y}, \mathbf{e_n})$, where

$$\mathbf{e_n} = \frac{\mathbf{N}_\ell}{\|\mathbf{N}_\ell\|}, \qquad \mathbf{e_t} = \mathbf{e_y} \times \mathbf{e_n}.$$

It is a fixed frame induced by the direction of the external force $\mathbf{N}_\ell = N_\ell \mathbf{e_n}$. Of course this direction is known if the external force is perfectly described. In this frame, the placement is expressed by $\boldsymbol{\varphi} = \varphi_t(s)\mathbf{e_t} + \varphi_n(s)\mathbf{e_n}$. Note that $\widehat{\mathbf{d_3}(s), \mathbf{e_n}} = \phi(s)$, then $\mathbf{e_n} \cdot \mathbf{d_3}(s) = \cos(\phi(s))$, and $\mathbf{e_n} \cdot \mathbf{d_1}(s) = \sin(\phi(s))$.

The relation (3.11) gives $\mathbf{M}(s) - \mathbf{M}(\ell) + (\boldsymbol{\varphi}(s) - \boldsymbol{\varphi}(\ell)) \times \mathbf{N}_\ell = 0$ which is written in this frame:

$M_2(s) - M_\ell - (\varphi_t(s) - \varphi_t(\ell))N_\ell = 0$, hence

$$\varphi_t(s) = \varphi_t(\ell) + \frac{M_2(s) - M_\ell}{N_\ell}.$$

Remark that $M_2(0)$ is now determined, hence the following expression holds too:

$$\varphi_t(s) = \varphi_t(0) + \frac{M_2(s) - M_2(0)}{N_\ell}. \tag{3.41}$$

and seems more appropriate, as $\boldsymbol{\varphi}(0)$ is generally imposed.
In order to determine $\varphi_n(s)$, a more tricky strategy is necessary as an integration is needed. One starts with (1.95) that is written as

$$\varphi_n' \mathbf{e_n} + \varphi_t' \mathbf{e_t} = \varepsilon_1(s)\mathbf{d_1}(s) + \varepsilon_3(s)\mathbf{d_3}(s).$$

After projection along $\mathbf{e_n}$:

$$\begin{aligned} \varphi_n' &= \varepsilon_1(s)\sin(\phi(s)) + \varepsilon_3(s)\cos(\phi(s)), \\ &= N_1(s)\sin(\phi(s)) + (\frac{1}{g}N_3 + 1)\cos(\phi(s)), \\ &= N_\ell\left(\frac{2t}{1+t^2}\right)^2 + \frac{N_\ell}{g}\left(\frac{1-t^2}{1+t^2}\right)^2 + \frac{1-t^2}{1+t^2}, \end{aligned}$$

where (3.3), (3.39) and (3.24) have been used successively. Integration is then performed as

$$\varphi_n(s) - \varphi_n(0) = \int_0^s \varphi_n'(\sigma)\,\mathrm{d}\sigma,$$

which implies

$$\varphi_n(s) = \varphi_n(0) + \int_0^s N_\ell\left(\frac{2t}{1+t^2}\right)^2 + \frac{N_\ell}{g}\left(\frac{1-t^2}{1+t^2}\right)^2 + \frac{1-t^2}{1+t^2}\,\mathrm{d}s, \tag{3.42}$$

where $t(s) = \sqrt{|\alpha_+|}\mathrm{cs}(\sqrt{a|\alpha_+|}(s+s_0)\,|\,m)$ is perfectly known. For this general case, no simple explicit formulation of a primitive of φ_n' can be obtained (a simplified expression is given in sec.3.6 for a particular case). However, the smooth behaviour of such function allows us to use a simple integration technic in order to obtain a numerical solution. In practice one uses a rectangular integration on a fine discretization of the length ($\Delta s = \ell/1\,000$).
As mentioned earlier, $\varphi_n(0) = \varphi_t(0) = 0$ is considered. The placement function is now completely determined as $\boldsymbol{\varphi}(s) = \varphi_t(s)\mathbf{e_t} + \varphi_n(s)\mathbf{e_n}$. However, if a Cartesian frame is privileged, one has of course to remind that the angle between $\mathbf{e_z}$ and $\mathbf{N}_\ell$ satisfies $\theta(\ell) + \phi_\ell = \hat{\phi}$ (see Fig.3.2). Then

$$\begin{aligned} \mathbf{e_n}\cdot\mathbf{e_z} &= \cos\hat{\phi}, & \mathbf{e_n}\cdot\mathbf{e_x} &= \sin\hat{\phi}, \\ \mathbf{e_t}\cdot\mathbf{e_z} &= -\sin\hat{\phi}, & \mathbf{e_t}\cdot\mathbf{e_x} &= \cos\hat{\phi}. \end{aligned}$$

The Cartesian components $\varphi_x = \boldsymbol{\varphi} \cdot \mathbf{e_x}$ and $\varphi_y = \boldsymbol{\varphi} \cdot \mathbf{e_y}$ become:

$$\begin{aligned} \varphi_x(s) &= \cos(\hat{\phi})\,\varphi_t(s) + \sin(\hat{\phi})\,\varphi_n(s), \\ \varphi_y(s) &= \cos(\hat{\phi})\,\varphi_n(s) - \sin(\hat{\phi})\,\varphi_t(s)\ . \end{aligned}$$

This result is plotted on Fig.3.10 where the sections (oriented along $\mathbf{d_1}(s)$) are also presented for the sake of the clarity. Knowing that the physical radius of the section is ϱ, these sections are plotted in a dimensionless way with one unit radius. Hence this picture is completely dimensionless with a respected slenderness ratio.

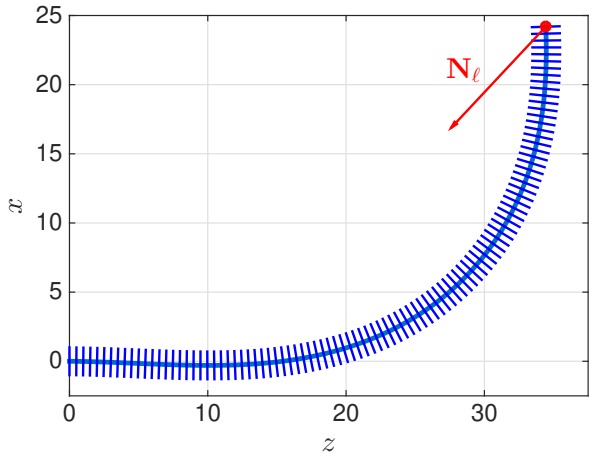

Figure 3.10 – *Dimensionless deformed shape of the beam glued at $s = 0$ and supporting a follower load $\mathbf{N}_\ell$ making an angle $\phi_\ell = 3\pi/4$ with the normal of the last section ($s = \ell$). The intensity of the force is $N_\ell = 0.01$ and a bending moment $M_\ell = 0.05$ is imposed on this last section too. The length of the beam is $\ell = 50$. No extra-amplification is used except for the force N_ℓ.*

3.6 Pure-shear follower load

The beam ($\ell = 50$, $g = 5/2$) is still glued at $s = 0$, then $\theta(0) = 0$ and support at the other end a pure shear-follower load. Then the boundary conditions at $s = \ell$ are: $N_\ell \neq 0$, $\phi_\ell = \pi/2$ and $M_\ell = 0$ (Figure (3.11)). For such type of control all the configurations presented on this section (3.6) are quasi-statically stable according to the *sec*-3.4.6.

The objective of this example is to analyze the qualitative and quantitative behaviour of the beam as N_ℓ increases. Some simplified asymptotic expressions are given in the case of moderate shear force N_ℓ.

3.6.1 Parameter analysis

In this example $\mu = 0$. In particular, according to (3.26), one gets $\alpha_- = 1$ then $\alpha_- > 0$, $t(s)$ is given by (3.35). One has explicitly $\alpha_+ = (\frac{2g}{g-1} - N_\ell)/(\frac{2g}{g-1} + N_\ell)$ but if $0 < N_\ell \ll 1$ (which is

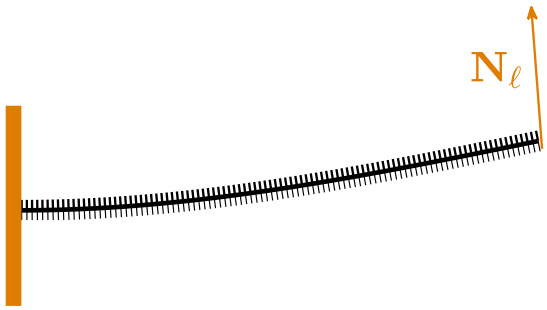

Figure 3.11 – *Beam subjected to follower load.*

almost always justified) first order Taylor (3.29) can be used. In the same spirit, Taylor expansion of $\sqrt{\alpha_- + \alpha_+}$, $\sqrt{a(\alpha_- + \alpha_+)}$ and $\frac{\alpha_+}{\alpha_+ + \alpha_-}$ in terms of N_ℓ exhibits a first order approximation:

$$t(s) = \sqrt{2}\,\mathrm{ds}(\sqrt{\frac{N_\ell}{g}}(s+s_0)\,|\,\frac{1}{2}) \;+\mathcal{O}(N_\ell).$$

Within this approximation, one obtains directly $M_2(s)$ by (3.39) and $\varphi_t(s)$ thanks to (3.41):

$$\begin{array}{rcl} M_2(s) & \simeq & \sqrt{2gN_\ell}\,\mathrm{cn}(\sqrt{\frac{N_\ell}{g}}(s+s_0)\,|\,\frac{1}{2}), \\ \varphi_t(s) & \simeq & \varphi_t(0) + \sqrt{\frac{2g}{N_\ell}}\,\mathrm{cn}(\sqrt{\frac{N_\ell}{g}}(s+s_0)\,|\,\frac{1}{2}) \end{array} .$$

The expression of φ_n is highly simplified by applying leading term approximation with respect to N_ℓ. In fact by (3.42) one gets:

$$\varphi_n(s) \;\simeq\; \varphi_n(0) + \int_0^s \frac{1-t^2}{1+t^2}\,\mathrm{d}s.$$

Integration is explicit in such a case and gives

$$\varphi_n(s) \simeq \varphi_n(0) + s - 2\sqrt{\frac{g}{N_\ell}}\mathcal{E}(\sqrt{\frac{N_\ell}{g}}(s+s_0)\,|\,\frac{1}{2}),$$

where $\mathcal{E}(x\,|\,m)$ is the Jacobian epsilon function.

3.6.2 Qualitative and quantitative analyses

Figure (3.12) represents successive configurations as the magnitude of the transverse shear load increases. These 20 simulations have been computed with the exact formulation (in particular numerical integration of (3.42)). The computation cost for these 20 simulations is $0.23\,s$ on a

2.2 GHz Intel Core i7 (without plotting curves). This analytical approach clearly allows real-time simulations.

In Fig.3.12 one observes qualitatively that the beam wrinkles with a periodicity controlled by the magnitude of the force. The asymptotic approach developed in the preceding section provides some tools in order to characterize this wrinkle.

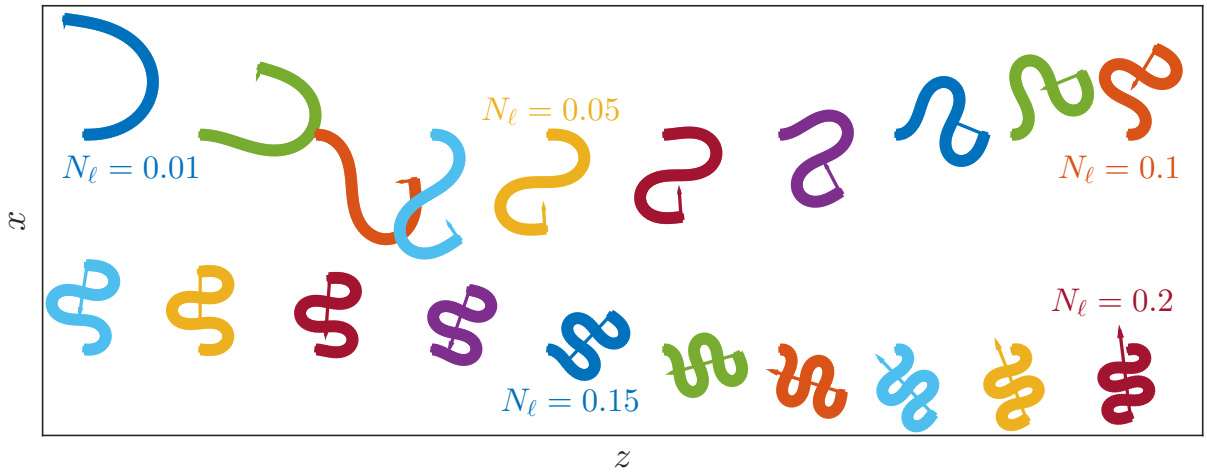

Figure 3.12 – *Dimensionless deformed shape of the beam glued at* $s = 0$ *and supporting a follower shear load* $\mathbf{N}_\ell$ *at* $s = \ell$ *(*$\phi_\ell = \pi/2$ *and* $M_\ell = 0$*). The properties of the beam are* $\ell = 50$ *and* $g = 5/2$*. The figure represents successive snap shot for* $N_\ell = [0.01, 0.2]$ *(with regular step of* 0.01*). Some values or* N_ℓ *are given and the directions of the external load are represented as well in order to help the reader.*

The periodicity P (along s) of $\boldsymbol{\varphi}$ is given by the complete elliptic integral of the first kind $K(m)$ that is the quarter period of the Jacobian elliptic functions too. According to the approximation proposed in the preceding section, the periodicity of $\boldsymbol{\varphi}$ is

$$P = 4\sqrt{\frac{g}{N_\ell}}K(\frac{1}{2}) \quad \simeq 7.41\sqrt{\frac{g}{N_\ell}}.$$

Hence the number of wrinkles along the beam is ℓ/P.

On the one hand, the size A of the wrinkle is related to the magnitude of φ_t: $A = 2\sqrt{2g/N_\ell}$. On the other hand the spatial periodicity B (indeed P is the *material* periodicity) of this wrinkle may be computed as $B = |\varphi_n(P) - \varphi_n(0)|$. Focusing on the leading terms, and detailing the computation, one obtains:

$$\begin{aligned} B &= \left|P - 2\sqrt{\frac{g}{N_\ell}}\mathcal{E}(4K(\frac{1}{2})\,|\,\frac{1}{2})\right|, \\ &= \left|4\sqrt{\frac{g}{N_\ell}}K(\frac{1}{2}) - 8\sqrt{\frac{g}{N_\ell}}E(\frac{1}{2})\right|, \\ &= 4\sqrt{\frac{g}{N_\ell}}\left(2E(\frac{1}{2}) - K(\frac{1}{2})\right), \\ &= \frac{2\pi}{K(\frac{1}{2})}\sqrt{\frac{g}{N_\ell}} \end{aligned},$$

where the complete elliptic integral E is introduced thanks to the relation $\mathcal{E}(4K(\frac{1}{2})\,|\,\frac{1}{2}) = 4E(\frac{1}{2})$ ([Olv+10]-22.16.29) and [Olv+10]-19.7.1 has been used too. Lastly, the size ratio B/A (see Fig.3.13) of the wrinkle pattern is independent of any material, geometrical or loading parameter:

$$\frac{B}{A} = \frac{\pi}{\sqrt{2}K(\frac{1}{2})} \simeq 1.2.$$

These properties of the deformed shape can been seen as a particular signature of such solicitation by a pure-shear load.

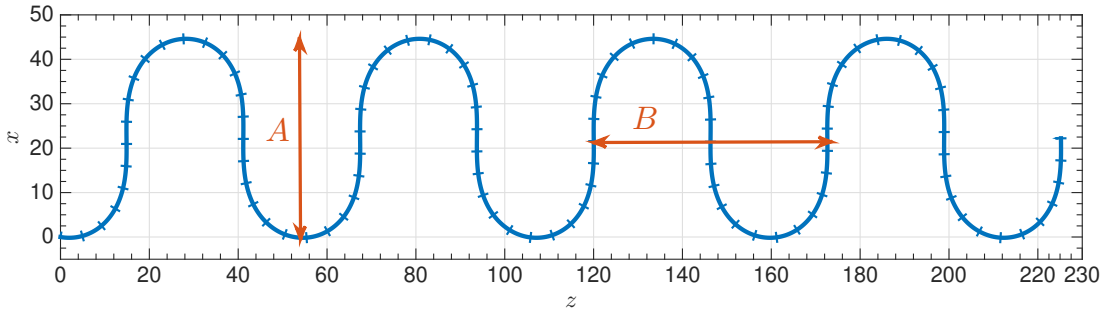

Figure 3.13 – *dimensionless deformed shape of the beam glued at* $s = 0$ *and supporting a pure shear load at* $s = \ell$ *(*$N_\ell = 0.01$, $\phi_\ell = \pi/2$ *and* $M_\ell = 0$*). The properties of the beam are* $\ell = 500$ *and* $g = 5/2$*. The wrinkles are clearly visible. For this loading* $B \simeq 53.6$ *and* $A \simeq 44.7$ *and* $P \simeq 117.3$*. There are* 4.25 *wrinkles.*

3.7 Quasi-static stability

Let us consider a given static configuration. Let us denote the associated quantities $\overline{\mathbf{V}}$ (for example $\overline{\mathbf{N}}_\ell$, $\overline{\theta}(s)$, $\overline{\mathbf{d}}_\mathbf{i}(s)$). These quantities are supposed to be known, they are solutions of the problem (3.4) for a given boundary condition. The quasi-static stability problem consists of the analysis of the behaviour of a perturbed solution $\mathbf{V} = \overline{\mathbf{V}} + \delta\mathbf{V}$ keeping invariant some boundary conditions. The perturbation $\delta\mathbf{V}$ is infinitesimal, then all quadratic terms in $\delta\mathbf{V}$ would be neglected in the following, leading to a linear analysis of the unknowns $\delta\mathbf{V}$.

3.7.1 Problem statement

Let us focus first on the vectorial quantities $\mathbf{N}(s) = \overline{\mathbf{N}}(s) + \delta\mathbf{N}(s)$, $\mathbf{M}(s) = \overline{\mathbf{M}}(s) + \delta\mathbf{M}(s)$ and $\boldsymbol{\varepsilon}(s) = \overline{\boldsymbol{\varepsilon}}(s) + \delta\boldsymbol{\varepsilon}(s)$. The prescribed initial quantities $\overline{\mathbf{V}}(s)$ satisfy (3.4). In particular $\overline{\mathbf{N}}(s) = \overline{\mathbf{N}}_\ell$ is a fixed vector. The perturbed quantities solve (3.4) too. Written as follows (linear δ-order):

$$\begin{aligned} \delta\mathbf{N}'(s) &= 0, \\ \delta\mathbf{M}'(s) + \overline{\boldsymbol{\varepsilon}}(s) \times \delta\mathbf{N}(s) + \delta\boldsymbol{\varepsilon}(s) \times \overline{\mathbf{N}}_\ell &= 0. \end{aligned} \tag{3.43}$$

According to the first line, $\delta\mathbf{N}(s)$ is a constant vector, so, let it be $\delta\mathbf{N}_\ell$ $(= \delta\mathbf{N}(s))$ where $\delta\mathbf{N}_\ell$ is indeed prescribed by boundary conditions. It is then natural to focus on

$$\boxed{\delta\mathbf{M}'(s) + \overline{\boldsymbol{\varepsilon}}(s) \times \delta\mathbf{N}_\ell + \delta\boldsymbol{\varepsilon}(s) \times \overline{\mathbf{N}}_\ell = 0}. \tag{3.44}$$

Considering now the components of vectorial quantities. Constitutive relations motivate the use of initial (respectively current) basis for the prescribed (respectively perturbed) configuration:

$$\begin{array}{rcl} \overline{\mathbf{N}}_\ell &=& \overline{N}_1(s)\,\overline{\mathbf{d}}_1(s) + \overline{N}_3(s)\,\overline{\mathbf{d}}_3(s), \\ \overline{\mathbf{M}}(s) &=& \overline{M}_2(s)\,\overline{\mathbf{d}}_2, \\ \overline{\boldsymbol{\varepsilon}}(s) &=& \overline{\varepsilon}_1(s)\,\overline{\mathbf{d}}_1(s) + \overline{\varepsilon}_3(s)\,\overline{\mathbf{d}}_3(s), \end{array} \quad \text{with} \quad \begin{array}{rcl} \overline{N}_1(s) &=& \overline{N}_\ell \sin\overline{\phi}(s), \\ \overline{N}_3(s) &=& \overline{N}_\ell \cos\overline{\phi}(s), \\ \overline{M}_2(s) &=& g\,\overline{\theta}'(s), \end{array} \tag{3.45}$$

$$\begin{array}{rcl} \mathbf{N}(s) &=& N_1(s)\,\mathbf{d}_1(s) + N_3(s)\,\mathbf{d}_3(s), \\ \mathbf{M}(s) &=& M_2(s)\,\mathbf{d}_2, \\ \boldsymbol{\varepsilon}(s) &=& \varepsilon_1(s)\,\mathbf{d}_1(s) + \varepsilon_3(s)\,\mathbf{d}_3(s), \end{array} \quad \text{with} \quad \begin{array}{rcl} N_1(s) &=& \varepsilon_1(s), \\ N_3(s) &=& g\,(\varepsilon_3(s) - 1), \\ M_2(s) &=& g\,\theta'(s). \end{array} \tag{3.46}$$

Lastly, the perturbations are arbitrary defined on the new basis:

$$\begin{array}{rcl} \delta\mathbf{N}_\ell &=& \delta N_1(s)\,\mathbf{d}_1(s) + \delta N_3(s)\,\mathbf{d}_3(s), \\ \delta\mathbf{M}(s) &=& \delta M_2(s)\,\mathbf{d}_2, \\ \delta\boldsymbol{\varepsilon}(s) &=& \delta\varepsilon_1(s)\,\mathbf{d}_1(s) + \delta\varepsilon_3(s)\,\mathbf{d}_3(s). \end{array}$$

Even if $\mathbf{d}_2 = \overline{\mathbf{d}}_2 = \mathbf{e_y}$, this is not the case for the other directors that may undergo an infinitesimal rotation: $\theta(s) = \overline{\theta}(s) + \delta\theta(s)$. Then $\mathbf{d}_1(s) = \cos(\delta\theta(s))\,\overline{\mathbf{d}}_1(s) - \sin(\delta\theta(s))\,\overline{\mathbf{d}}_3(s)$ and $\mathbf{d}_3(s) = \sin(\delta\theta(s))\,\overline{\mathbf{d}}_1(s) + \cos(\delta\theta(s))\,\overline{\mathbf{d}}_3(s)$ may be approximated in this first order approach by: $\mathbf{d_1}(s) = \overline{\mathbf{d}}_\mathbf{1}(s) - \delta\theta(s)\,\overline{\mathbf{d}}_\mathbf{3}(s)$ and $\mathbf{d_3}(s) = \overline{\mathbf{d}}_\mathbf{3}(s) + \delta\theta(s)\,\overline{\mathbf{d}}_\mathbf{1}(s)$ respectively.
The constitutive relation for the perturbation of the moment is trivial $\delta M_2(s) = g\,\delta\theta'(s)$ but this is not the case for the strains. This is obtained by considering that $N_i(s)$ may be defined by two equivalent ways:

$$\begin{array}{lll} \text{for} \quad N_1(s) & (\overline{\mathbf{N}}_\ell + \delta\mathbf{N}_\ell)\cdot\mathbf{d_1}(s) &= (\overline{\boldsymbol{\varepsilon}}(s) + \delta\boldsymbol{\varepsilon}(s))\cdot\mathbf{d_1}(s), \\ \text{for} \quad N_3(s) & (\overline{\mathbf{N}}_\ell + \delta\mathbf{N}_\ell)\cdot\mathbf{d_3}(s) &= g\,((\overline{\boldsymbol{\varepsilon}}(s) + \delta\boldsymbol{\varepsilon}(s))\cdot\mathbf{d_3}(s) - 1)\,. \end{array} \tag{3.47}$$

Expanding each side and using first δ-order approximations, one obtains, respectively:

$$\begin{array}{rcl} \overline{N}_1(s) - \delta\theta(s)\,\overline{N}_3(s) + \delta N_1(s) &=& \overline{\varepsilon}_1(s) - \delta\theta(s)\,\overline{\varepsilon}_3(s) + \delta\varepsilon_1(s), \\ \overline{N}_3(s) + \delta\theta(s)\,\overline{N}_1(s) + \delta N_3(s) &=& g\,(\overline{\varepsilon}_3(s) + \delta\theta(s)\,\overline{\varepsilon}_1(s) + \delta\varepsilon_3(s) - 1)\,. \end{array} \tag{3.48}$$

Using (3.45), a constitutive relation depending on the initial state is obtained for the perturbation:

$$\begin{aligned}\delta\varepsilon_1(s) &= \cos\left(\overline{\phi}(\ell)-\overline{\phi}(s)\right)\delta N_1(\ell)-\sin\left(\overline{\phi}(\ell)-\overline{\phi}(s)\right)\delta N_3(\ell)-\left(\tfrac{g-1}{g}\overline{N}_3(s)-1\right)\delta\theta(s),\\ \delta\varepsilon_3(s) &= \tfrac{1}{g}\Big(\sin\left(\overline{\phi}(\ell)-\overline{\phi}(s)\right)\delta N_1(\ell)+\cos\left(\overline{\phi}(\ell)-\overline{\phi}(s)\right)\delta N_3(\ell)\Big)-\tfrac{g-1}{g}\overline{N}_1(s)\,\delta\theta(s),\end{aligned} \tag{3.49}$$

where $\overline{\phi}(\ell)+\overline{\theta}(\ell)=\overline{\phi}(s)+\overline{\theta}(s)$ $(=\overline{\hat{\phi}})$ has been used. Hence strain perturbations $\delta\varepsilon_i(s)$ are all related to the field of micro-rotation $\delta\theta(s)$ and controlled by both the prescribed configuration and boundary conditions imposed on the force perturbation $\delta\mathbf{N}_\ell$ at the last section. This observation induces that (3.44) may be written merely in terms of a single degree of freedom $\delta\theta(s)$ of the perturbation with parameters controlled by the prescribed configuration and boundary conditions. Straight forward calculation gives:

$$\delta\theta''(s)+k^2(s)\,\delta\theta(s)=f(s), \tag{3.50}$$

where $k^2(s)$ and $f(s)$ are

$$\begin{aligned}k^2(s) &= -\frac{1}{g}\overline{N}_3(s)+\frac{g-1}{g^2}\Big(\overline{N}_3^2(s)-\overline{N}_1^2(s)\Big),\\ f(s) &= \frac{1}{g}\left(\frac{g-1}{g}\overline{N}_3(s)-1\right)\Big(\cos\left(\overline{\phi}(\ell)-\overline{\phi}(s)\right)\delta N_1(\ell)-\sin\left(\overline{\phi}(\ell)-\overline{\phi}(s)\right)\delta N_3(\ell)\Big)+\dots\\ &\quad\dots\quad\frac{g-1}{g^2}\overline{N}_1(s)\Big(\sin\left(\overline{\phi}(\ell)-\overline{\phi}(s)\right)\delta N_1(\ell)+\cos\left(\overline{\phi}(\ell)-\overline{\phi}(s)\right)\delta N_3(\ell)\Big).\end{aligned} \tag{3.51}$$

$\delta\theta(s)$ is a solution of a linear, non-homogeneous, second order differential equation with non-constant coefficients. This differential equation is of the class of driven parametric oscillators for which analysis is well-documented but beyond the scope of the present chapter.
Boundary conditions affect only the non-homogeneous term. Indeed, the prescription of $\delta\mathbf{N}_\ell$ is of particular physical importance. This is detailed in the next paragraph for dead and follower load cases.

3.7.2 Dead-load

For a dead-load one gets $\mathbf{N}_\ell=\overline{\mathbf{N}}_\ell$ then $\delta\mathbf{N}_\ell=0$. The equation (3.51) becomes:

$$\delta\theta''(s)+k^2(s)\,\delta\theta(s)=0. \tag{3.52}$$

Boundary conditions at $s=0$ or $s=\ell$ are either $\delta\theta(s)=0$ for constant orientation of the section or $\delta\theta'(s)=0$ if the moment kept constant.

Example for a pure longitudinal compression For this initial configuration $\overline{\phi}(s) = \pi$ and $k(s)$ is constant:

$$k^2 = \frac{N_\ell}{g} + \frac{g-1}{g^2} N_\ell^2. \tag{3.53}$$

In that case k^2 is strictly positive, hence, solutions of (3.52) are of the form

$$\delta\theta = C_1 \cos(ks) + C_2 \sin(ks), \tag{3.54}$$

for which the constants C_i depend on the boundary conditions.

— For simply supported beam, $\delta\theta'(0) = 0$ and $\delta\theta'(\ell) = 0$ (Figure (3.14) left). The trivial solution $C_i = 0$ is imposed except if $k = n\pi/\ell$ (with $n \in \mathbb{N}^*$) for which $\delta\theta(s) = C_1 \cos(ks)$ is a possible solution. A straightforward computation shows that this buckling solution occurs for

$$N_\ell = \frac{g}{2(g-1)} \left(\sqrt{1 + 4(g-1)(\frac{n\pi}{\ell})^2} - 1 \right). \tag{3.55}$$

This non-linear relation may be simplified in first approximation as $\frac{n\pi}{\ell} \ll 1$. This leads to the standard Euler critical-load $N_\ell = g(\frac{n\pi}{\ell})^2$ for buckling of simply supported beam.

— For clamped-hinged beam $\delta\theta(0) = 0$ and $\delta\theta'(\ell) = 0$ (Figure (3.14) center). Again the trivial solution is imposed except if $k = (2n+1)\pi/(2\ell)$ (with $n \in \mathbb{N}$) for which $\delta\theta(s) = C_2 \sin(ks)$ is a possible solution. In that case the critical load becomes:

$$N_\ell = \frac{g}{2(g-1)} \left(\sqrt{1 + (g-1)(\frac{(2n+1)\pi}{\ell})^2} - 1 \right), \tag{3.56}$$

which corresponds in first approximations to the standard Euler critical load $N_\ell = g(\frac{(2n+1)\pi}{2\ell})^2$ for cantilever beam.

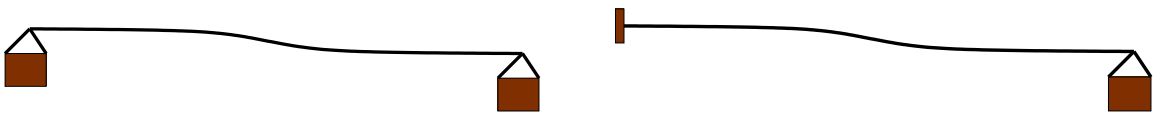

Simply supported beam. *Clamped-Hinged beam.*

Figure 3.14 – *Particular boundary conditions of a beam.*

3.7.3 Follower load

If the force acting on the last section is a follower load, then $\mathbf{N}_\ell \neq \overline{\mathbf{N}}_\ell$. However, the components of the actual force at this end are unchanged: $N_1(\ell) = \overline{N}_1(\ell)$ and $N_3(\ell) = \overline{N}_3(\ell)$. Applying (3.47) at $s = \ell$ leads to:

$$\delta N_1(\ell) = \overline{N}_3(\ell)\, \delta\theta(\ell), \qquad \delta N_3(\ell) = -\overline{N}_1(\ell)\, \delta\theta(\ell)\ . \tag{3.57}$$

Injecting these expressions in (3.51), the equation (3.50) written after rearrangement as:

$$\delta\theta''(s) + k^2(s)\Big(\delta\theta(s) - \delta\theta(\ell)\Big) = 0, \tag{3.58}$$

where $\delta\phi(s) + \delta\theta(s) = \delta\phi(\ell) + \delta\theta(\ell)$ has been used. For a follower-load, the angle between the normal of the last section and the external force is the same before and after perturbation, then $\delta\phi(\ell) = 0$. In other words: $\delta\theta(s) - \delta\theta(\ell) = -\delta\phi(s)$. According to this change of variables, the above differential equation becomes:

$$\delta\phi''(s) + k^2(s)\,\delta\phi(s) = 0, \tag{3.59}$$

where the boundary condition at $s = \ell$ is already prescribed $\delta\phi(\ell) = 0$ even if $\delta\theta(\ell)$ is unknown (note that $\delta\theta(\ell)$ may be a boundary condition prescription).

Example for a pure longitudinal compression As already mentioned k^2 is, in that case, a positive constant specified in (3.53). As $\delta\phi(\ell) = 0$, solution of (3.59) is of the form

$$\delta\phi(s) = C_1 \sin\left(k(\ell - s)\right). \tag{3.60}$$

However, the boundary conditions imposed on the beam still play an important role, as it is highlighted by the three following examples:

- If the couple remains null at the last end $\delta M_2(\ell) = 0$ then $\delta\theta'(\ell) = 0$ or equivalently $\delta\phi'(\ell) = 0$. Direct calculation shows that no solution $\delta\phi(s)$ may respect this condition except the trivial ones: $\delta\phi(s) = 0$, then $\delta\theta(s) = \delta\theta(\ell)$. Physically speaking any perturbation of the beam induced an instability in the form of a rigid rotation. Note that this observation is valid for any constraint imposed on $s = 0$. In particular if the beam is clamped at the origin $\delta\theta(s) = 0$: no transverse perturbation are possible.
- If the beam is simply supported at $s = 0$ but $\delta\theta'(\ell) \neq 0$ at the other end, the problem reads in terms of $\delta\phi$: $\delta\phi'(0) = 0$ and $\delta\phi(\ell) = 0$. These boundary conditions imposes non-trivial solution if $k = (2n+1)\pi/(2\ell)$ (with $n \in \mathbb{N}$). A buckling appears for a critical load presented in (3.56) and the mode of buckling may be written as

  $$\delta\theta(s) = \delta\theta(\ell) - C_1 \sin\left(\frac{(2n+1)\pi}{2\ell}(\ell - s)\right),$$

  where the constant C_1 is arbitrary.
- If $\delta\theta(0) = 0$ the beam is clamped at $s = 0$ then $\delta\phi(0) = \delta\theta(\ell)$ and still $\delta\phi(\ell) = 0$. According to (3.60), $C_1 \sin(k\ell) = \delta\theta(\ell)$. For moderate compression ($0 < k\ell < \pi$) solution (3.60) is always possible and reads:

  $$\delta\phi(s) = \delta\theta(\ell)\frac{\sin\left(k(\ell - s)\right)}{\sin\left(k\ell\right)}\ , \qquad \text{then} \qquad \delta\theta(s) = \delta\theta(\ell)\left(1 - \frac{\sin\left(k(\ell - s)\right)}{\sin\left(k\ell\right)}\right).$$

  Then, for any infinitesimal perturbation of the orientation of the last section (and then of the

follower load), a perturbed solution exists. No brutal bifurcation is observed. In conclusion the clamped beam is particularly unstable under the loading of a follower compressive force (even if this latter is infinitesimal).

3.8 Boundary problem

Assuming now that the same beam ($\ell = 50$, $g = 5/2$) supports a pure dead-load $\mathbf{N}_\ell = N_\ell \mathbf{e_z}$, $\mathbf{M}_\ell = 0$ (Figure (3.15)). Of course $\phi'_\ell = 0$ as $\mathbf{M}_\ell = 0$ however, ϕ_ℓ is not prescribed. Indeed, the last boundary condition is the orientation of the section at $s = 0$: $\theta_0 = \theta(0)$. Let us define in the same spirit $M_0 := M_2(0)$, $\phi_0 := \phi(0)$ and $\phi'_0 := \phi'(0)$ $(= -M_0/g)$. From (3.13) $\theta_0 = \hat{\phi} - \phi_0$ and according to the section (3.2.2) $\hat{\phi} = 0$.
The questions are the following:

What is the configuration of the beam as θ_0 varies according to a command, for a fixed pure dead-load ?
Is this solution unique ?

In order to address these questions, one must first consider the initial condition problem which has unique solution:

What is the configuration of the beam as ϕ_ℓ varies for a prescribed N_ℓ and such that $M_\ell = 0$, $\hat{\phi} = 0$?

In a second step the map of the solution associated to $\theta_0 \in \mathfrak{C} \to \phi_\ell$ is studied according to the command $\mathfrak{C}$ of the boundary condition.

3.8.1 Parameter analysis

First observe that $\mu = 2gN_\ell \cos(\phi_\ell) - (g-1)N_\ell^2 \cos^2(\phi_\ell)$ then $\mu_a \leq \mu \leq \mu_c$ and $t(s)$ is of the form (3.35). Second, as $\phi'_\ell = 0$ we have $t'(\ell) = 0$ and according to Fig.3.7 and the associated analysis:

$$\begin{array}{lll} \sqrt{a(\alpha_- + \alpha_+)}(\ell + s_0) = +K, & \text{if} & 0 \leq \phi_\ell < \pi \\ \sqrt{a(\alpha_- + \alpha_+)}(\ell + s_0) = -K, & \text{if} & \pi \leq \phi_\ell < 2\pi \end{array}, \qquad \text{where} \quad K := K(\frac{\alpha_+}{\alpha_+ + \alpha_-}).$$

Then, for a fixed ϕ_ℓ, s_0 can be determined directly. In other words, $t(s)$ is perfectly determined and then $\phi(s)$. In particular $\theta_0 := -2\arctan(t(0))$ becomes:

$$\begin{aligned} \theta_0 &= -2\arctan\Big(\sqrt{\alpha_- + \alpha_+}\ \mathrm{ds}(\sqrt{a(\alpha_- + \alpha_+)}s_0 \,|\, \frac{\alpha_+}{\alpha_+ + \alpha_-})\Big), \\ &= 2\arctan\Big(\sqrt{\alpha_- + \alpha_+}\ \mathrm{ds}(\pm K + \sqrt{a(\alpha_- + \alpha_+)}\ell \,|\, \frac{\alpha_+}{\alpha_+ + \alpha_-})\Big), \\ &= \pm 2\arctan\Big(\frac{\sqrt{\alpha_-}}{\mathrm{cn}(\sqrt{a(\alpha_- + \alpha_+)}\ell \,|\, \frac{\alpha_+}{\alpha_+ + \alpha_-})}\Big). \end{aligned}$$

Figure 3.15 – *Beam subjected to a pure dead load.*

According to the preceding results and using translation rules [Olv+10]-22.4.(iii). The sign $\pm$ is $-$ if $\phi_\ell \in [0, \pi[$ and $+$ if $\phi_\ell \in [\pi, 2\pi[$. Recall that a and $\alpha_\pm$ depend explicitly on ϕ_ℓ according to (3.28) and (3.18).

3.8.2 Catastrophic instablities

The evolution of θ_0 versus ϕ_ℓ is presented in Fig.3.16. The map $\phi_\ell \to \theta_0$ is bijective only for moderate magnitude N_ℓ of the dead-load. For moderate N_ℓ the angle ϕ_ℓ is uniquely determined for a given θ_0 hence, the associated configuration of the beam is unique. For larger N_ℓ, more than one value of ϕ_ℓ is associated to a given value of θ_0. This lack of uniqueness induces a non-uniqueness of the configurations for a fixed θ_0.
Supposing that the command $\mathfrak{C}$ is "θ_0 *increases from* 0". The initial state is then associated to the point $(\phi_\ell = 0, \theta_0 = 0)$ for which the beam supports a pure traction. Afterwards, the graph in Fig.3.16 has to be read from right to left and the first configurations are defined by the increasing branch initiated at $(0, 0)$. For large N_ℓ, this branch has an inflection point (for $\phi_\ell \simeq -\pi/3$ if $N_\ell = 0.01$ see in Fig.3.17-left). In order to respect the command imposed on θ_0, the values of ϕ_ℓ has to present a large jump (its magnitude is higher than $3\pi/2$ if $N_\ell = 0.01$). This jump corresponds to a large and brutal change of the configuration of the beam as it is observed in Fig.3.17-right. This phenomena is known as a catastrophe in instability theories ([Tho18; PS14; Gol78]).
The analytical and dimensionless approach followed along the present chapter allows to tackle this type of problem through explicit solution without *a priori* approximations or hypotheses [HLML21]. This methodology may be seen as a complementary approach to those more usually based on the internal energy.

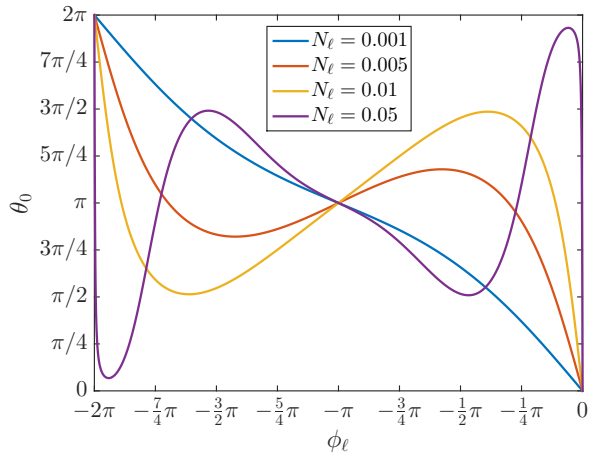

Figure 3.16 – *Evolution of θ_0 according to ϕ_ℓ for various magnitude of the dead-load ($\ell = 50$, $g = 5/2$, $\mathbf{N}_\ell = N_\ell \mathbf{e_z}$, $\mathbf{M}_\ell = 0$, $\hat{\phi} = 0$). If $\mathfrak{C}$ is θ_0 increases linearly from 0, the graph has to be read from right to left.*

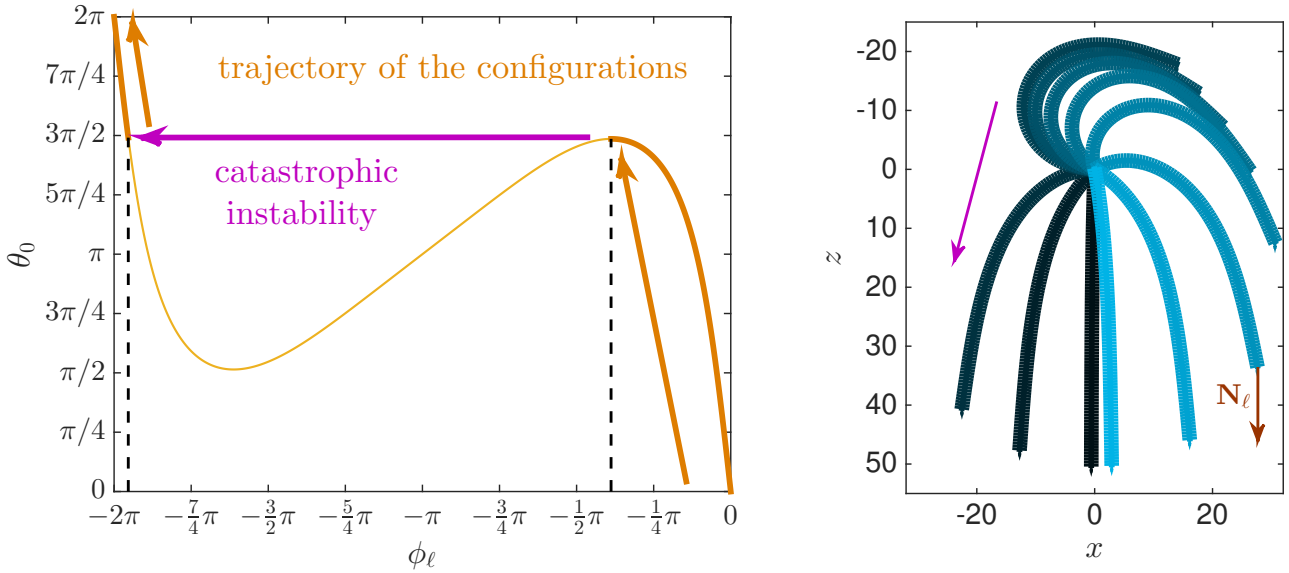

Figure 3.17 – *Left: evolution of θ_0 according to ϕ_ℓ if $N_\ell = 0.01$. In orange bold the history of the ϕ_ℓ and θ_0 for the command $\mathfrak{C}$. The arrows help to read the quasi static evolution and underline the gap associated to the catastrophe. Right: the successive configurations for various values of θ_0 respecting the command $\mathfrak{C}$. The colors of the dots in the left figure are associated to the colors of the corresponding configurations. The purple arrow highlights the brutal transition of the configurations during the catastrophe.*

Comparison between Timoshenko, Euler and Kirchhoff's model in terms of Catastrophic instabilities is given in the appendix (4.20.5).

3.9 Conclusion

We presented in this chapter, an analytical study of a large, but plane, transformation of a Timoshenko beam with linear constitutive law where non-linear geometrical relations appeared due to this transformation. Equilibrium relations in non-dimensional form were found.
The followed formulation in the present chapter chooses to emphasize a Cauchy problem formalism where all strains are prescribed at one end, in contrast to most studies in this field. More precisely, at one end, the moment and force intensities are supposed to be known as well as the orientation of the load with respect to the normal of the section.
This approach ensured existence and uniqueness of the solution. Furthermore, explicit formulation of the solution was obtained thanks to Jacobian elliptic functions for which coefficients are smoothly dependents on the invariants of the problem. This methodology allowed us to tackle several theoretical and physical problems since explicit solutions were obtained without any approximation.
Several examples were then presented to illustrate this methodology. In the case of a pure-shear follower load, force was completely prescribed at one end, and a quasi-static evolution was straightforwardly addressed. In such a case, the explicit analysis was the opportunity to exhibit a universal size ratio of a wrinkle pattern: this size-ratio is independent of the material and the geometrical properties of the beam but independent of the intensity of the load too.
For mixed boundary conditions, the perturbation of the problem was presented in a general way for any type of boundary condition, allowing us to compute the perturbed solutions under these various conditions. This general perturbed problem written as a driven parametric oscillator for which each (space-varying) parameters is explicitly available.
In the last example, the kinematic control of a beam supporting a dead-load was presented. For such a problem, the usual perturbation methodology could be used to detect eventual instability. The present chapter however, focus on an alternative nonlinear method which depicted the whole equilibrium solution. Emergence of even more critical instability than fork bifurcation (as usual buckling) was observed. Indeed such so called catastrophe remained reachable in a straightforward and explicit way.
Finally, this approach was also valid for Euler Bernoulli beam as well as Kirchhoff rod model, where comparison between these models was detailed in the appendix.

Chapter 4

Behaviour of a Kirchhoff rod under pure moments

Experience is the collecting of what is similar in different particular perceptions

Gustav Kirchhoff

4.1 Overview

Rotation of a rigid body was first introduced by Euler in the 18^{th} Century with a description based on a vectorial quasi-linear first order differential equation. This approach led to several applications. Kovaleskaya [Kow89] identified the rotation of a rigid body around a fixed point and gave the solution in terms of hyper-elliptic integrals. Then, Arnold applied Euler's method in order to find mathematical methods of classical mechanics [Arn13]. After that, Agrachev et Sachkov [AS13] used rotations of a rigid body in control theory. A while later, Van damme *et al.*. [VDMS17] examined the tennis racket effect in a three-dimensional rigid body where they described the flip of the head of the racket.

Kirchhoff filaments were first presented by Kirchhoff [Kir59] who gave a general theory of elastic filaments. This theory openend a vast application in Biology such as finding stability of DNA [TSC00], and also in Physics and Engineering, where scientists aimed to solve the problem in an analytical or numerical way. For example, Nizette and Goriely [NG99] classified the shapes of Kirchhoff filaments and gave complete description of solutions in the symmetric Rods case. Henceforth, Goriely and Tabor gave numerical solutions by applying perturbation scheme to the Kirchhoff equations [GT00].

Equilibrium equations of a thin elastic ribbon are derived by adapting the classical theory of thin elastic rods. Among others, Antman conducted the Kirchhoff's problem for nonlinearly elastic rods [Ant74]. Goriely and Nizette [GN00] linked rods and ribbons by the so-called "Kirchhoff analogy" which identifies inextensible elastic filaments with circular cross-sections. Coming after, Audoly, Clauvelin and Neukirch invested the mechanical response of elastic rods bent into open knots [ACN07]. Later on, Audoly and Seffen [AS16] tested buckling instabilities of metallic strips and related elastic Rods to Ribbons. In addition, Starostin and Heijden [SH18] proved that Forceless Sadowsky strips are spherical. Numerical modeling of inextensible elastic ribbons was suggested by

Charrondière *et al.* [Cha+20] who obtained perfect agreement between experiments for ribbon and elastica.
In this chapter, we study the static problem of a straight Timoshenko beam subjected to moments at the boundaries without external forces. Domain of variation of each dimensionless parameters is examined, furthermore, two invariants that depend on moments and energy density govern the problem, these invariants are similar to the invariants in the rotation of a rigid body problem with the only difference regarding the variables and the applications between these two different approaches. Four regimes model arise that depends on the thickness of the cross-section. Solutions are found in an analytical way (in terms of Jacobian elliptic functions). A detailed discussion is made regarding the role of the control parameters. In the last section, we implicate physical applications to give a better understanding of the problem.

4.2 Kinematics

Kinematics of the beam in this chapter are given by:

$$\begin{aligned} \text{Placement :} \qquad & \underline{\boldsymbol{\varphi}} = \underline{\varphi}_1 \mathbf{d}_1 + \underline{\varphi}_2 \mathbf{d}_2 + \underline{\varphi}_3 \mathbf{d}_3. \\ \text{Strain :} \qquad & \underline{\boldsymbol{\varepsilon}} = \underline{\varepsilon}_1 \mathbf{d}_1 + \underline{\varepsilon}_2 \mathbf{d}_2 + \underline{\varepsilon}_3 \mathbf{d}_3. \\ \text{Generalised curvatures :} \qquad & \underline{\boldsymbol{\kappa}} = \underline{\kappa}_1 \mathbf{d}_1 + \underline{\kappa}_2 \mathbf{d}_2 + \underline{\kappa}_3 \mathbf{d}_3. \end{aligned} \tag{4.1}$$

4.3 Internal energy, forces and moments

Keeping in mind that Kirchhoff-Saint Venant energy per unit length is given by:

$$\Psi = \frac{1}{2}\left(GA\,\underline{\varepsilon}_1^2 + GA\,\underline{\varepsilon}_2^2 + EA(\underline{\varepsilon}_3 - 1)^2 + EI_1\,\underline{\kappa}_1^2 + EI_2\,\underline{\kappa}_2^2 + GI_3\,\underline{\kappa}_3^2 \right). \tag{4.2}$$

Hence, the resultant stress depends linearly on the conjugate strains:

$$\begin{array}{rcll} N_1 &=& GA\,\underline{\varepsilon}_1, \qquad N_2 = GA\,\underline{\varepsilon}_2, & \text{shear forces.} \\ N_3 &=& EA\,(\underline{\varepsilon}_3 - 1), & \text{normal force.} \\ M_1 &=& EI_1\,\underline{\kappa}_1, \qquad M_2 = EI_2\,\underline{\kappa}_2, & \text{bending moments.} \\ M_3 &=& GI_3\,\underline{\kappa}_3, & \text{torsional moment.} \end{array} \tag{4.3}$$

In the directors frame, force and moment vectors are:

$$\underline{\mathbf{N}}(S) = \underline{N}_1 \mathbf{d_1} + \underline{N}_2 \mathbf{d_2} + \underline{N}_3 \mathbf{d_3}, \qquad \underline{\mathbf{M}}(S) = \underline{M}_1 \mathbf{d_1} + \underline{M}_2 \mathbf{d_2} + \underline{M}_3 \mathbf{d_3}.$$

4.4 Equilibrium relations

By imposing $\underline{\mathbf{q}} = \underline{\mathbf{m}} = 0$, static equilibrium relations will be:

$$\boxed{\begin{array}{rcl} \dfrac{d\underline{\mathbf{N}}}{dS} & = & 0, \\ \dfrac{d\underline{\mathbf{M}}}{dS} + \underline{\boldsymbol{\varepsilon}} \times \underline{\mathbf{N}} & = & 0. \end{array}} \tag{4.4}$$

Integrating the first equation of (4.4) gives $\underline{\mathbf{N}}(S) := \underline{\mathbf{N}}$ that is a constant imposed by external force imposed at one end.

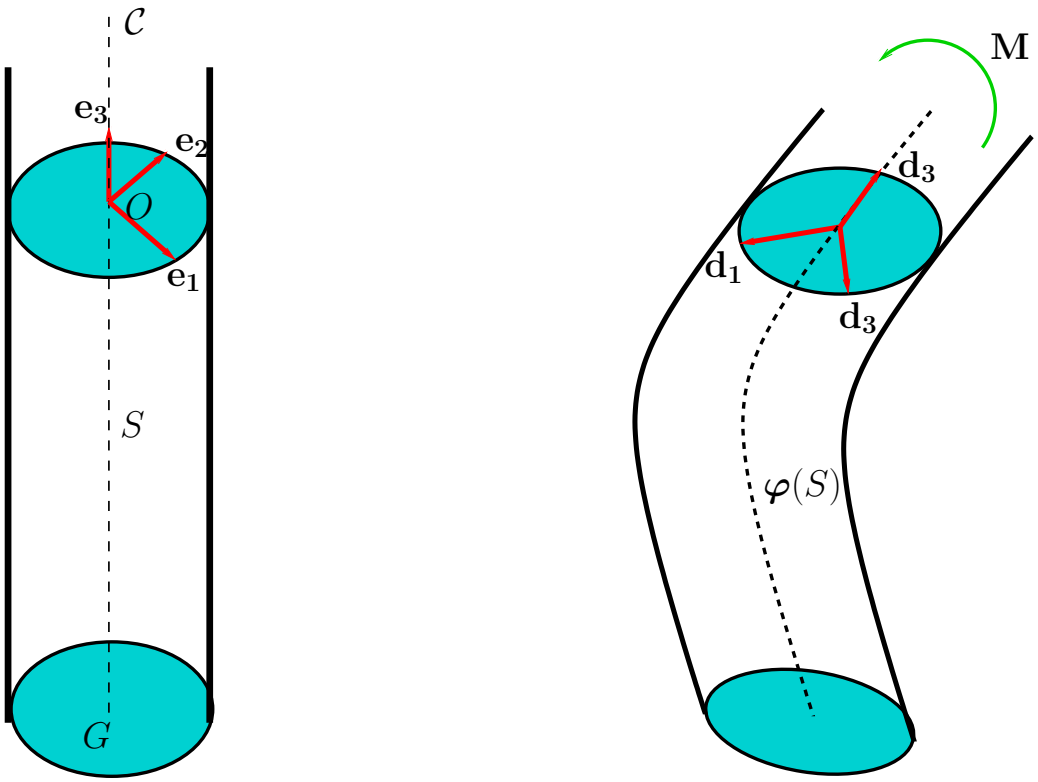

Figure 4.1 – *Reference configuration (left) and current configuration.* $\mathbf{d_3}$ *is always tangent to* $\mathcal{C}$.

All along this chapter we consider $\boxed{\underline{\mathbf{N}}=0}$ (*see fig.*(4.1)). Using stress-internal forces relation eq. (4.3) we deduce:

$$\underline{\varepsilon}_1(S) = 0, \qquad \underline{\varepsilon}_2(S) = 0, \qquad \underline{\varepsilon}_3(S) = 1. \tag{4.5}$$

As a conclusion, equation (4.4) could be written as:

$$\frac{d\underline{\mathbf{M}}}{dS} = 0. \tag{4.6}$$

Keeping in mind that we have a moving director frame, one obtains after projecting along $\mathbf{d_i}(S)$:

$$\begin{aligned} EI_1\frac{d\underline{\kappa}_1}{dS} + (GI_3 - EI_2)\underline{\kappa}_2\underline{\kappa}_3 &= 0, \\ EI_2\frac{d\underline{\kappa}_2}{dS} + (EI_1 - GI_3)\underline{\kappa}_1\underline{\kappa}_3 &= 0, \\ GI_3\frac{d\underline{\kappa}_3}{dS} + E(I_2 - I_1)\underline{\kappa}_1\underline{\kappa}_2 &= 0. \end{aligned} \tag{4.7}$$

4.5 Beam-rod relation

In this section we aim to relate our equilibrium equations to Rod equilibrium described by Kirchhoff in [Kir59]. Namely, the static Kirchhoff Rod model is given by (*e.g.*[NG99]):

$$\frac{d\underline{\mathbf{N}}}{dS} + \underline{\mathbf{q}} = 0, \tag{4.8}$$

$$\frac{d\underline{\mathbf{M}}}{dS} + \mathbf{d_3} \times \underline{\mathbf{N}} + \underline{\mathbf{m}} = 0. \tag{4.9}$$

This model doesn't impose gliding, so, we obtain the kinematical assumption:

$$\boxed{\frac{\partial \underline{\boldsymbol{\varphi}}}{\partial S} = \mathbf{d_3}}. \tag{4.10}$$

The quadratic energy density for this model is given by:

$$\mathbf{\Psi} = \frac{1}{2}\Big(EI_1\underline{\kappa}_1^2 + EI_2\underline{\kappa}_2^2 + GI_3\underline{\kappa}_3^2\Big). \tag{4.11}$$

With the linear constitutive laws with respect to moments:

$$M_1 = EI_1\underline{\kappa}_1, \qquad M_2 = EI_2\underline{\kappa}_2, \qquad M_3 = GI_3\underline{\kappa}_3. \tag{4.12}$$

And $\mathbf{N}$ could be determined from (4.8).
So, by exerting only a moment load type, a beam behaves exactly as a rod and our structure will be considered as a rod later on.

4.6 Dimensionless parameters

As mentioned before, dimensionless parameters in this case are given by:

$$\begin{aligned} &\text{Gyration radius:} && \varrho = \sqrt{\frac{I_1 + I_2}{A}}. \\ &\text{Bulk ratio:} && g := \frac{E}{G}. \\ &\text{Eccentricity:} && e = \frac{I_1}{I_2}. \end{aligned} \tag{4.13}$$

4.6.1 Non-dimensional quantities

Dimensionless kinematical variables are:

$$\varepsilon_i(s) = \underline{\varepsilon}_i(S), \qquad \kappa_i(s) = \varrho\,\underline{\kappa}_i(S), \qquad \varphi_i(s) = \frac{1}{\varrho}\underline{\varphi}_i(S). \tag{4.14}$$

It is interesting to observe that physical moment $\underline{\mathbf{M}}(S)$ has also non-dimensional form $\mathbf{M}(s)$ related by

$$\mathbf{M} = \frac{1}{\varrho}\frac{1}{GA}\underline{\mathbf{M}}.$$

In particular, in term of non-dimensional components :

$$\boxed{\begin{array}{ccc} M_1 = r_1\kappa_1, & M_2 = r_2\kappa_2, & M_3 = \kappa_3, \\ \text{with} \quad r_1 := \dfrac{eg}{1+e}, & r_2 := \dfrac{g}{1+e}. & \end{array}} \tag{4.15}$$

The non-dimensional bending stiffnesses r_i play a major role all along the analysis. They combine the material parameter g with the geometrical slenderness e of the section. Note that thanks to this non-dimensional procedure, the torsional stiffness is one.
Non dimensional energy per unit length is given by:

$$\boxed{\begin{aligned} \Psi(s) &= \frac{1}{2}\Big(M_1\kappa_1 + M_2\kappa_2 + M_3\kappa_3\Big), \\ &= \frac{1}{2}\Big(\frac{1}{r_1}M_1^2 + \frac{1}{r_2}M_2^2 + M_3^2\Big), \\ &= \frac{1}{2}\Big(r_1\,\kappa_1^2 + r_2\,\kappa_2^2 + \kappa_3^2\Big). \end{aligned}} \tag{4.16}$$

4.6.2 Domain of variation

By construction $\varrho = \mathcal{O}(R)$, where R is a typical size of the cross-section. Accordingly $\ell \gtrsim 20$ for a short beam and is even higher for a slender beam. In terms of cross-section one has by convention

$$0 < e \leq 1.$$

As $g \simeq 2(1+\nu)$ where ν is the Poisson's ratio:

$$2 \lesssim g \lesssim 3.$$

Due to non-overlapping of beam section, the curvature radius of the beam must be greater than the typical size of the section along direction of curvature, therefore:

$$|\underline{\kappa_1}(S)| < \sqrt{\frac{A}{I_1}}, \qquad |\underline{\kappa_2}(S)| < \sqrt{\frac{A}{I_2}}, \qquad |\underline{\kappa_3}(S)| < \sqrt{\frac{A}{I_1+I_2}}. \tag{4.17}$$

Written in non-dimensional form as

$$|\kappa_1(s)| < \sqrt{\frac{1+e}{e}} < +\infty, \qquad |\kappa_2(s)| < \sqrt{1+e} \leq \sqrt{2}, \qquad |\kappa_3(s)| < 1. \tag{4.18}$$

And employing (4.15) we conclude that:

$$|M_1(s)| < g\sqrt{\frac{e}{1+e}} \leq \frac{g}{\sqrt{2}}, \qquad |M_2(s)| < g\sqrt{\frac{1}{1+e}} \leq g, \qquad |M_3(s)| < 1. \tag{4.19}$$

Remark. It is worthy to mention that we adapted a material approach for which we have a moving director frame $(\mathbf{d_1}, \mathbf{d_2}, \mathbf{d_3})$ where $(\mathbf{d_1}, \mathbf{d_2})$ is attached to the rigid cross-section $\mathcal{S}$ and $\mathbf{d_3}$ is normal to $\mathcal{S}$, hence, torsional warping effect does not exist in our approach.

4.6.3 Non-dimensionnal relation

Using the fact that $\dfrac{df}{dS} = \dfrac{1}{\varrho}\dfrac{df}{ds}$ and the convention $f' := \frac{df}{ds}$ for any function $f(S)$ and injecting (4.14) into (4.7) one gets:

$$\boxed{\begin{array}{rcl} r_1\,\kappa_1'(s) - (r_2-1)\,\kappa_2(s)\kappa_3(s) &=& 0, \\ r_2\,\kappa_2'(s) + (r_1-1)\,\kappa_1(s)\kappa_3(s) &=& 0, \\ \kappa_3'(s) + (r_2-r_1)\,\kappa_1(s)\kappa_2(s) &=& 0. \end{array}} \tag{4.20}$$

Note that all coefficients in parenthesis or in front of κ_i' are related to e and g. They are positive or null expect (r_1-1) for which sign may depend on the beam. As this latter element has crucial consequences in the present work, the following definitions are introduced:

Definition 4.6.1 (Cross-section properties).

$$\begin{array}{lll} e = 1. & & \text{Symetric cross-section.} \\ 1 < r_1, \quad i.e \quad e > \dfrac{1}{g-1}. & & \text{Thick cross-section.} \\ r_1 < 1, \quad i.e \quad e < \dfrac{1}{g-1} & & \text{Thin cross-section (ribbon-like beam).} \end{array} \tag{4.21}$$

Note that these definitions involve both a geometrical parameter e and a material parameter g. It could be observed that for small Poisson parameter, *i.e.* $g \simeq 2$, the section is mainly defined as *thin* and the beam as *ribbon* even if the slenderness of the section is moderate (*i.e.* e close to unity).

4.7 Homogeneous and trivial solutions

Some trivial solutions of (4.20) may be revealed according to the domain of variation of each parameters (see Def.(4.6.1)). Hereafter, the notations $M_{i0} := M_i(0)$ and $\kappa_{i0} := \kappa_i(0)$ will be used as constant of integration satisfying the boundary conditions.

1. If $1 - e \neq 0$ and $r_1 \neq 1$:
   (a) $\kappa_1(s) = \kappa_{10}$ and $\kappa_2(s) = 0$, $\kappa_3(s) = 0$. It is a pure flexion in the $(\mathbf{e_y}, \mathbf{e_z})$-plane: elastica-1 solution.
   (b) $\kappa_2(s) = \kappa_{20}$ and $\kappa_1(s) = 0$, $\kappa_3(s) = 0$. It is a pure flexion in the $(\mathbf{e_x}, \mathbf{e_z})$-plane: elastica-2 solution.
   (c) $\kappa_3(s) = \kappa_{30}$ and $\kappa_1(s) = 0$, $\kappa_2(s) = 0$. It is a pure torsion around the axis $\mathbf{e_z}$ of the beam: torsional solution.
2. If $r_1 = r_2$ (*i.e.* $e = 1$) and $r_1 \neq 1$ then $\kappa_3(s) = \kappa_{30}$ and

$$\begin{aligned} \kappa_1(s) &= \kappa_{10} \cos\Big(\frac{g-2}{g}\kappa_{30}\, s\Big) + \kappa_{20} \sin\Big(\frac{g-2}{g}\kappa_{30}\, s\Big), \\ \kappa_2(s) &= \kappa_{20} \cos\Big(\frac{g-2}{g}\kappa_{30}\, s\Big) - \kappa_{10} \sin\Big(\frac{g-2}{g}\kappa_{30}\, s\Big). \end{aligned} \tag{4.22}$$

3. If $r_1 = 1$ and $e \neq 1$ then $\kappa_2(s) = \kappa_{20}$ and

$$\begin{aligned} \kappa_1(s) &= \kappa_{10} \cos\Big((g-2)\kappa_{20}\, s\Big) + \kappa_{30} \sin\Big((g-2)\kappa_{20}\, s\Big), \\ \kappa_3(s) &= \kappa_{30} \cos\Big((g-2)\kappa_{20}\, s\Big) - \kappa_{10} \sin\Big((g-2)\kappa_{20}\, s\Big). \end{aligned} \tag{4.23}$$

4. If $r_1 = r_2 = 1$, what implies $g = 2$ and $e = 1$, then

$$\kappa_1(s) = \kappa_{10}, \qquad \kappa_2(s) = \kappa_{20}, \qquad \kappa_3(s) = \kappa_{30}.$$

4.8 Invariants

In order to find non trivial solutions we remark that direct integration of (4.6) leads to a constant vector along the fibre $\mathbf{M}(s) = \mathbf{M}$. Its norm $M := \|\mathbf{M}\|$ is then the first invariant of the problem and according to (4.15):

$$\boxed{\begin{aligned} M^2 &= M_1(s)^2 + M_2(s)^2 + M_3(s)^2, \\ &= \Big(r_1\,\kappa_1(s)\Big)^2 + \Big(r_2\,\kappa_2(s)\Big)^2 + \kappa_3(s)^2. \end{aligned}} \tag{4.24}$$

Now by multiplying the first equation of (4.20) by κ_1, the second equation by κ_2 and the third equation by κ_3 and adding them we obtain:

$$r_1\,\kappa_1\kappa_1' + r_2\,\kappa_2\kappa_2' + \kappa_3\kappa_3' = 0 \tag{4.25}$$

According to (4.16), this relation is nothing else than $\Psi'(s) = 0$. In other words (4.25) states that the densities of strain energy is conserved along the beam: $\Psi(s) := \Psi$ that is the second invariant of the problem:

$$\boxed{\Psi = \frac{1}{2}\Big(r_1\,\kappa_1(s)^2 + r_2\,\kappa_2(s)^2 + \kappa_3(s)^2\Big),} \tag{4.26}$$

where the s dependence presents only in the right side of the equation. Note that even if the density of energy is conserved along the beam, torsion energy is converted into bending energy and vice-versa all along the beam.
These two invariants could be found also in the work of Euler and they where presented by Nizette and Goriely [NG99], as well as Kehrbaum and Maddocks [KM97].

According to (4.19):

$$M^2 \leq g^2 + 1, \qquad \Psi \leq g + \frac{1}{2}. \tag{4.27}$$

These bounds are particularly large, especially for elongated structures. It must not be considered as an indicator of the order of magnitude of these variables, but rather as a maximum bounds (physically unreachable in general).

4.8.1 Geometrical interpretation

In the configurational space (M_1, M_2, M_3), the invariants M and Ψ correspond to sphere and ellipsoid respectively. So, solutions of (4.20) belongs to their intersections. If such intersection exists, it is composed of smooth and close curves in the configurational space. As a consequence, solutions $M_1(s)$, $M_2(s)$ and $M_3(s)$ of (4.20) are expected to be described by periodic functions.
For later convenience lets introduce the positive constant μ such that:

$$\boxed{\mu^2 := 2\Psi.}$$

The second invariant is then driven by:

$$\frac{1}{r_1}M_1^2 + \frac{1}{r_2}M_2^2 + M_3^2 = \mu^2, \tag{4.28}$$

corresponding to a centered elipsoid for which semi-axis are $\sqrt{r_1}\,\mu$, $\sqrt{r_2}\,\mu$ and μ respectively along the axis M_1, M_2 and M_3 of the configurational space. As the first invariant is a centered sphere with radius M, some (non-ponctual) intersections exists if and only if

$$\min_{i=1,2}(r_i, 1) \leq \eta := \frac{M}{\mu} \leq \max_{i=1,2}(r_i, 1).$$

This criteria can be easily expanded and questioned as μ_i and M are all explicit in terms of $M_i(s)^2$, e and g. Practically, $1 < r_1 < r_2$ for *thick* section, and $r_1 < 1 < r_2$ for *thin* section. This leads to the following result:

Proposition 4.8.1 (Existence conditions). Non-trivial solutions of (4.20) exist if and only if

$$\begin{array}{rcccll} 1 & < & \eta & < & \sqrt{r_2}, & \text{when} \quad 1 < r_1. \\ \sqrt{r_1} & < & \eta & < & \sqrt{r_2}, & \text{when} \quad r_1 < 1. \end{array} \tag{4.29}$$

For a given beam, hence, given a set (e, g), this existence criteria is only controled by the loading η.

Invariants M and μ are presented in the configuration space for *thick* or *thin* cross-section in Fig.4.2. The intersections are then highlighted and define the supports of any solutions $M_1(s)$, $M_2(s)$ and $M_3(s)$ for each presented cases. These supports are systematically composed of two symmetric, close, smooth, and non-intersecting curves.

Independently to the section type, the behaviour of the solutions is highly dependent on the value of the loading-ratio η with regards to e and g.

For *thick* section, the two invariants are always intersecting in the (M_2, M_3)-plane. This intersection is obtained explicitly by solving the linear system:

$$\begin{array}{rcl} M_2^2 + M_3^2 & = & M^2, \\ \frac{1}{r_2}M_2^2 + M_3^2 & = & \mu^2, \end{array}$$

what gives some potential initial conditions for the solutions for *thick* section:

$$M_{20} = \pm\mu\sqrt{\frac{r_2(\eta^2 - 1)}{r_2 - 1}}, \qquad M_{30} = \pm\mu\sqrt{\frac{r_2 - \eta^2}{r_2 - 1}}. \tag{4.30}$$

For the *thin* section, the two invariants always intersect in the (M_1, M_2)-plane. Some potential initial conditions for the solutions for *thin* section are then:

$$M_{10} = \pm\mu\sqrt{\frac{r_1(r_2 - \eta^2)}{r_2 - r_1}}, \qquad M_{20} = \pm\mu\sqrt{\frac{r_2(r_1 - \eta^2)}{r_1 - r_2}}. \tag{4.31}$$

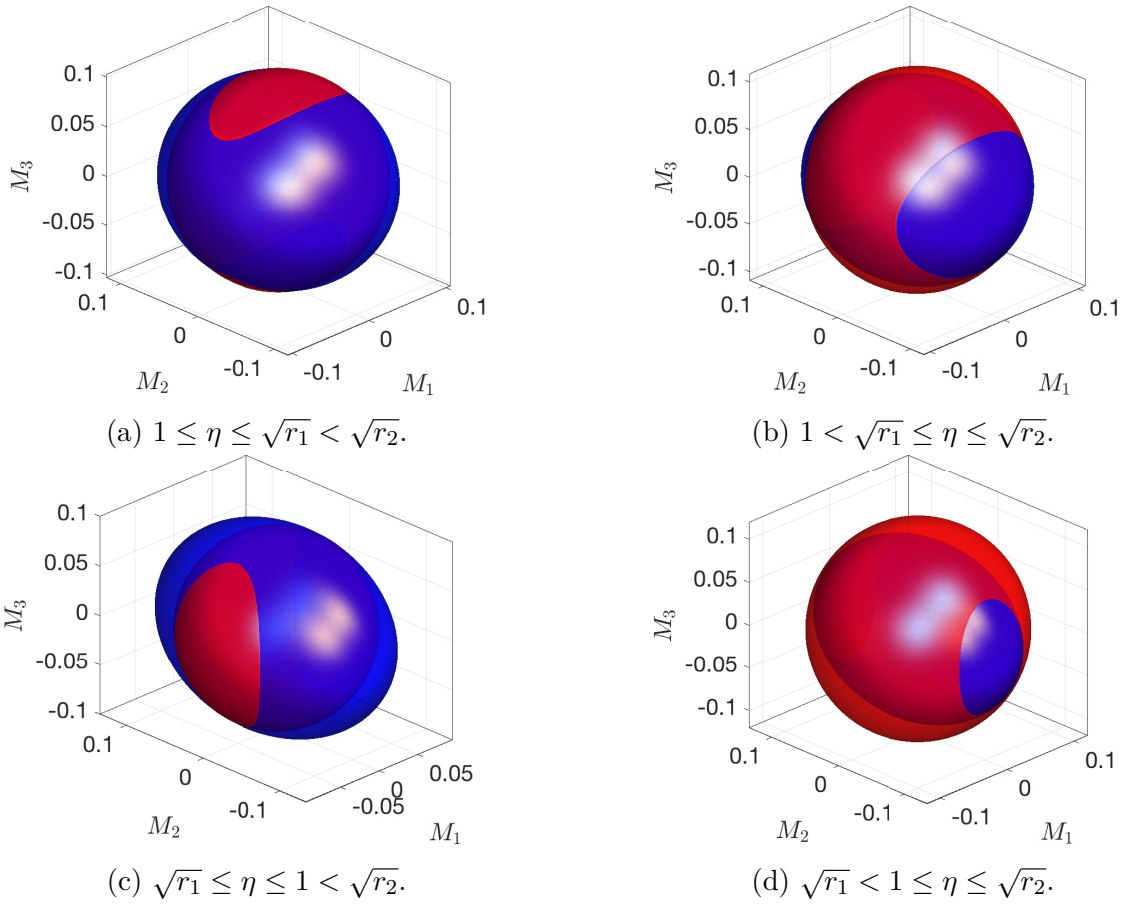

(a) $1 \leq \eta \leq \sqrt{r_1} < \sqrt{r_2}$. (b) $1 < \sqrt{r_1} \leq \eta \leq \sqrt{r_2}$.

(c) $\sqrt{r_1} \leq \eta \leq 1 < \sqrt{r_2}$. (d) $\sqrt{r_1} < 1 \leq \eta \leq \sqrt{r_2}$.

Figure 4.2 – *Invariants M (red) and μ (blue) for various section types and loading. For all the case $g = 2.5$, $\mu = 0.1$. Top: thick-section $e = 0.8$ with $\eta = 1.03$ (a) and $\eta = 1.09$ (b). Bottom: thin-section $e = 0.4$ with $\eta = 0.95$ (left) or $\eta = 1.2$ (right).*

4.9 Resolution of the elliptic differential equations

Equilibrium equations (4.20) are similar to Euler's rotation equations where solutions were found in terms of Jacobian elliptic functions (*e.g.* [LL76],[GPS80],[Cel+08],[Law13]). For thick beam, solutions are given by:

— If $1 \leq \eta \leq \sqrt{r_1} < \sqrt{r_2}$:

$$\begin{aligned}
\kappa_1(s) &= \overline{\kappa}_1 \,\mathrm{sn}\Big(\lambda(s+s_0) \mid m\Big), & \overline{\kappa}_1 &= \mu\sqrt{\frac{\eta^2-1}{r_1(r_1-1)}}, & m &= \frac{(\eta^2-1)(r_2-r_1)}{(r_1-1)(r_2-\eta^2)}.\\
\kappa_2(s) &= \overline{\kappa}_2 \,\mathrm{cn}\Big(\lambda(s+s_0) \mid m\Big), & \overline{\kappa}_2 &= \mu\sqrt{\frac{\eta^2-1}{r_2(r_2-1)}}, & \lambda &= \mu\sqrt{\frac{(r_2-\eta^2)(r_1-1)}{r_1 r_2}}.\\
\kappa_3(s) &= \pm\overline{\kappa}_3 \,\mathrm{dn}\Big(\lambda(s+s_0) \mid m\Big), & \overline{\kappa}_3 &= \mu\sqrt{\frac{r_2-\eta^2}{r_2-1}}.
\end{aligned} \tag{4.32}$$

— If $1 < \sqrt{r_1} \leq \eta \leq \sqrt{r_2}$:

$$\begin{aligned}
\kappa_1(s) &= \overline{\kappa}_1 \,\mathrm{sn}\Big(\lambda(s+s_0) \mid m\Big), & \overline{\kappa}_1 &= \mu\sqrt{\frac{r_2-\eta^2}{r_1(r_2-r_1)}}, & m &= \frac{(r_1-1)(r_2-\eta^2)}{(\eta^2-1)(r_2-r_1)}.\\
\kappa_2(s) &= \pm\overline{\kappa}_2 \,\mathrm{dn}\Big(\lambda(s+s_0) \mid m\Big), & \overline{\kappa}_2 &= \mu\sqrt{\frac{\eta^2-1}{r_2(r_2-1)}}, & \lambda &= \mu\sqrt{\frac{(r_2-r_1)(\eta^2-1)}{r_1 r_2}}.\\
\kappa_3(s) &= \overline{\kappa}_3 \,\mathrm{cn}\Big(\lambda(s+s_0) \mid m\Big), & \overline{\kappa}_3 &= \mu\sqrt{\frac{r_2-\eta^2}{r_2-1}}.
\end{aligned} \tag{4.33}$$

Similarly for thin beam, two regimes are presented:

— If $\sqrt{r_1} \leq \eta \leq 1 < \sqrt{r_2}$:

$$\begin{aligned}
\kappa_1(s) &= \pm\overline{\kappa}_1 \,\mathrm{dn}\Big(\lambda(s+s_0) \mid m\Big), & \overline{\kappa}_1 &= \mu\sqrt{\frac{r_2-\eta^2}{r_1(r_2-r_1)}}, & m &= \frac{(\eta^2-r_1)(r_2-1)}{(1-r_1)(r_2-\eta^2)}.\\
\kappa_2(s) &= \overline{\kappa}_2 \,\mathrm{cn}\Big(\lambda(s+s_0) \mid m\Big), & \overline{\kappa}_2 &= \mu\sqrt{\frac{r_1-\eta^2}{r_2(r_1-r_2)}}, & \lambda &= \mu\sqrt{\frac{(r_2-\eta^2)(1-r_1)}{r_1 r_2}}.\\
\kappa_3(s) &= \overline{\kappa}_3 \,\mathrm{sn}\Big(\lambda(s+s_0) \mid m\Big), & \overline{\kappa}_3 &= \mu\sqrt{\frac{\eta^2-r_1}{1-r_1}}.
\end{aligned} \tag{4.34}$$

— If $\sqrt{r_1} < 1 \leq \eta \leq \sqrt{r_2}$:

$$\begin{aligned}
\kappa_1(s) &= \overline{\kappa}_1 \,\mathrm{cn}\Big(\lambda(s+s_0) \mid m\Big), & \overline{\kappa}_1 &= \mu\sqrt{\frac{r_2-\eta^2}{r_1(r_2-r_1)}}, & m &= \frac{(1-r_1)(r_2-\eta^2)}{(\eta^2-r_1)(r_2-1)}.\\
\kappa_2(s) &= \pm\overline{\kappa}_2 \,\mathrm{dn}\Big(\lambda(s+s_0) \mid m\Big), & \overline{\kappa}_2 &= \mu\sqrt{\frac{r_1-\eta^2}{r_2(r_1-r_2)}}, & \lambda &= \mu\sqrt{\frac{(r_2-1)(\eta^2-r_1)}{r_1 r_2}}.\\
\kappa_3(s) &= \overline{\kappa}_3 \,\mathrm{sn}\Big(\lambda(s+s_0) \mid m\Big), & \overline{\kappa}_3 &= \mu\sqrt{\frac{r_2-\eta^2}{r_2-1}}.
\end{aligned} \tag{4.35}$$

Figure (4.3) represents the variation of the jacobian functions where it is remarkable that sn and cn are $4K(m)$ periodic where dn is $2K(m)$ periodic.

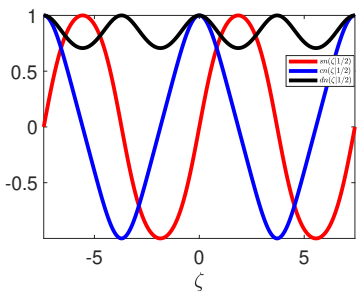

Figure 4.3 – *$sn(\zeta \mid m)$, $cn(\zeta \mid m)$ and $dn(\zeta \mid m)$ for $m = \frac{1}{2}$.*

4.10 Determination of s_0

In order to determine the translation parameter s_0, we should mention that $\overline{\kappa}_2 = \kappa_2(0)$ for thick and thin beam. This leads directly to $\mathrm{cn}\big(\lambda s_0 \mid m\big) = 1$ (or $\mathrm{dn}\big(\lambda s_0 \mid m\big) = 1$), so, referring to [Olv+10] we obtain

$$s_0 = \frac{4nK(m)}{\lambda}, \qquad n \in \mathbb{M}. \tag{4.36}$$

Remark. Without loss of generality, we assume hereafter that $s_0 = 0$ and for simplicity we abbreviate $\mathrm{pq}\big(\lambda s \mid m\big)$ by pq for any Jacobian function.

4.11 Moments

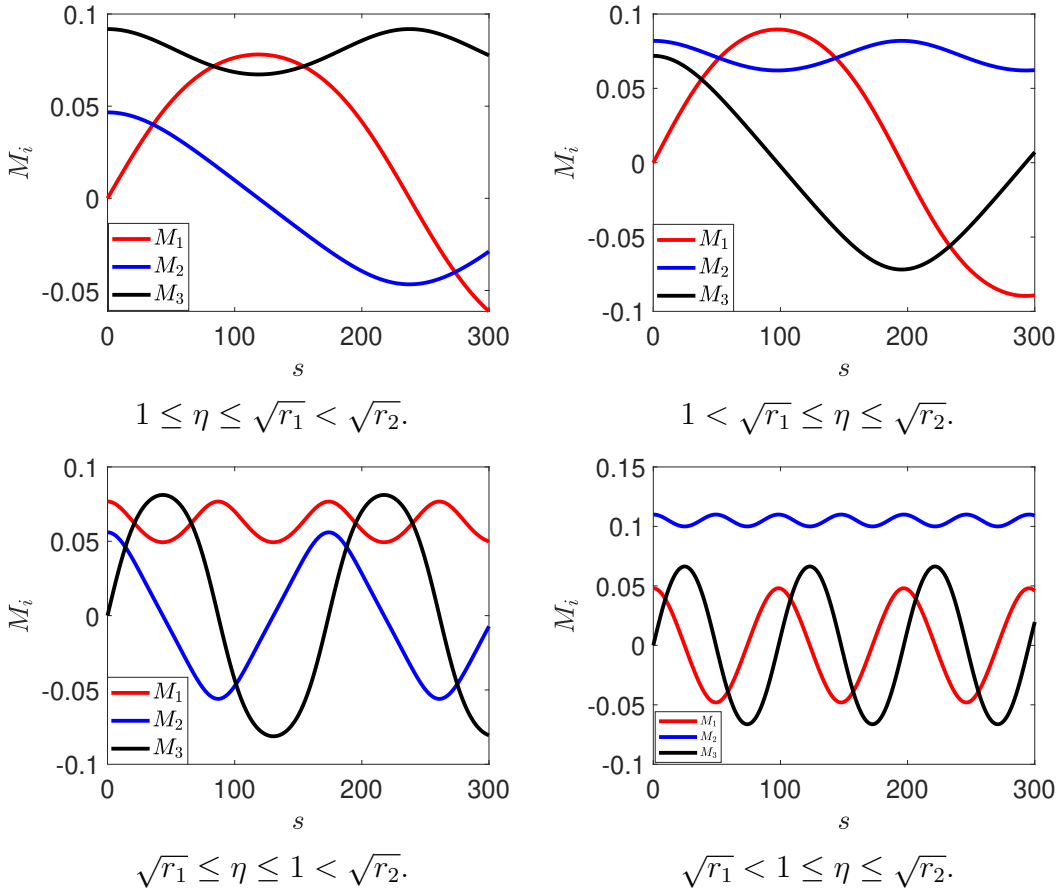

Figure 4.4 – *Moments for various section types and loading. For all the case* $g = 2.5$, $\mu = 0.1$. *Top: thick-section* $e = 0.8$ *with* $\eta = 1.03$ *(a) and* $\eta = 1.09$ *(b). Bottom: thin-section* $e = 0.4$ *with* $\eta = 0.95$ *(left) or* $\eta = 1.2$ *(right).*

Keeping in mind that

$$M_1 = r_1\kappa_1, \qquad M_2 = r_2\kappa_2, \qquad M_3 = \kappa_3. \tag{4.37}$$

Using explicit solutions presented in Sec.(4.9) we find moments. Figure (4.4) represents the variation

of moments for different regimes.

4.12 Role of η

To investigate the influence of η on the curvature, we first start by plotting the moments in (M_1, M_2, M_3) configuration. We should remark first that to move from thick regime (a) to thick regime (b) in figure (4.2) we should increase M for μ fixed, the same procedure applies to thin regimes (c) and (d). So, figure (4.5) represents the shifting between regimes for thick and thin cross-section where it is clear that this shifting is continuous. In addition, we can remark that by

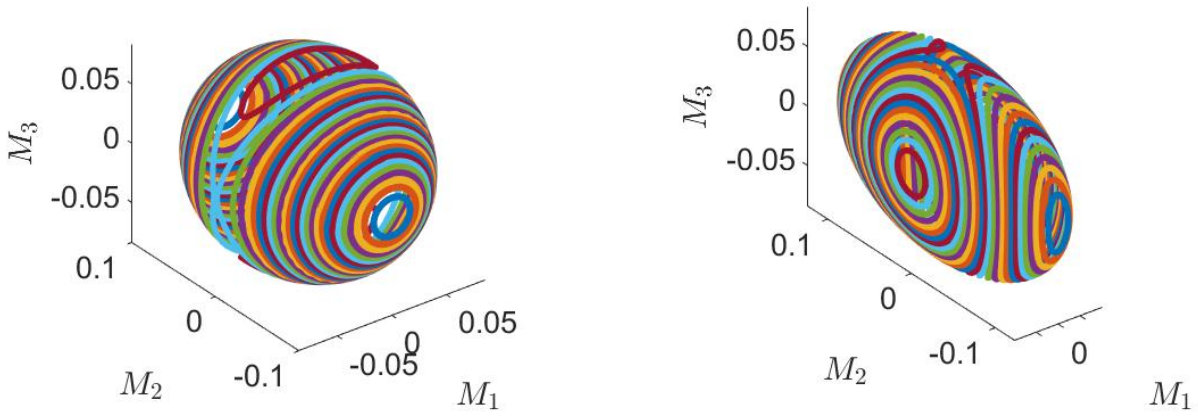

Various curvature regime for thick beam with $e = 0.8$.

Various curvature regime for thin beam with $e = 0.4$.

Figure 4.5 – *Pattern shifting with* $g = 2.5$ *and* $\mu = 0.0845$.

increasing η we obtain different curvature form so, η controls the type of the solution. Further study on rod shapes will give a better understanding of the role of η.

4.13 Impact of μ

In this section, we give the impact of μ on the curvature and shapes. To do so, we repeat exactly figure (4.5) for bigger μ. Figure (4.6) gives this approach, we can remark that by increasing μ the same pattern is repeated. Therefore, μ is a scaling parameter and it controls the size of the solution. Note that μ will be considered as constant hereafter.

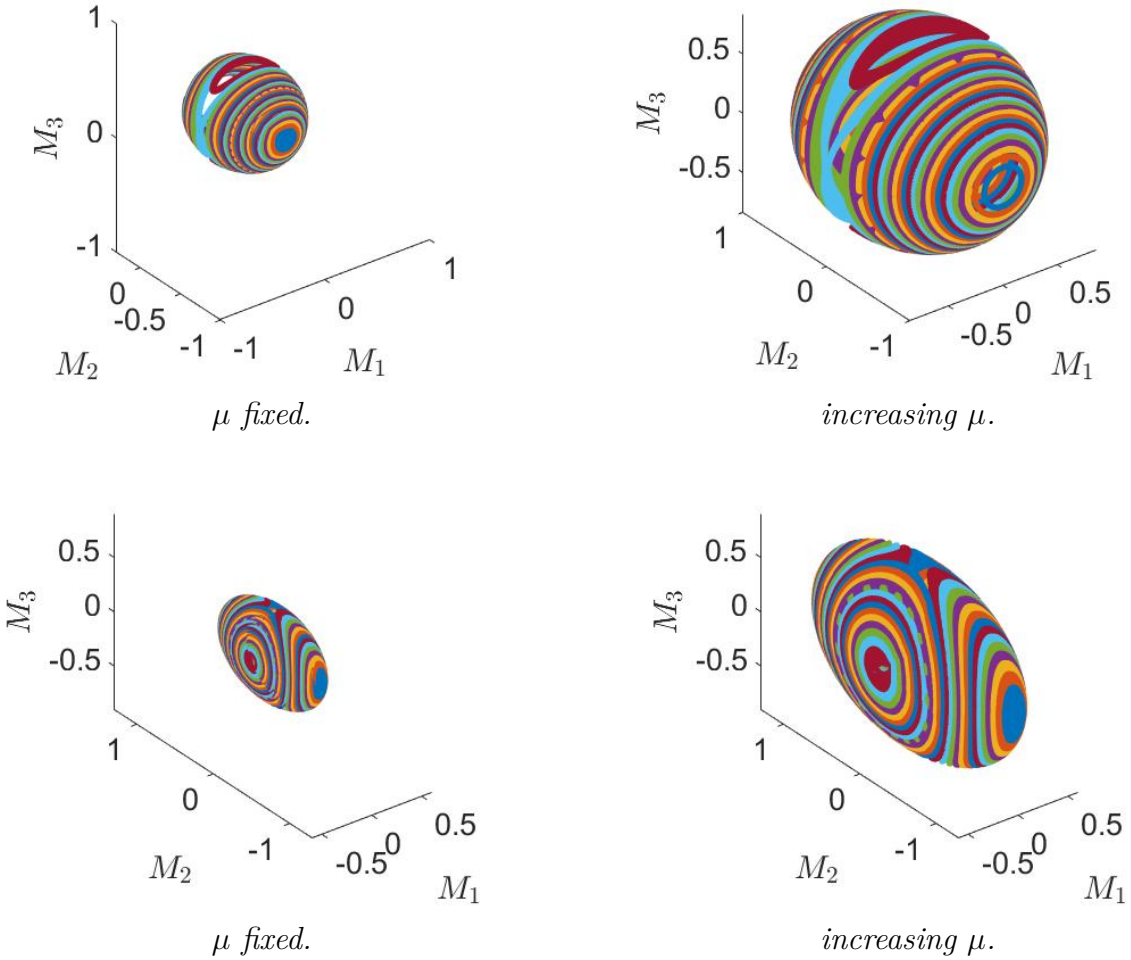

Figure 4.6 – *Pattern shifting for μ different Top: thick-section $e = 0.8$ Bottom: thin-section $e = 0.4$.*

4.14 Orientation of the section

In this section we aim to relate the moving director frame $\mathbf{d_i}$ to the Frenet frame attached to the centerline. So, reminding first Frenet-Serret relations:

$$\begin{aligned}
\mathbf{t}(s) &= \boldsymbol{\varphi}'(s) = \mathbf{d_3}(s), \\
\mathbf{n}(s) &= \frac{\mathbf{t}'(s)}{\|\mathbf{t}'(s)\|}, \\
\mathbf{b}(s) &= \mathbf{t}(s) \times \mathbf{n}(s), \\
\kappa_f(s) &= \|\mathbf{t}'(s)\|, \\
|\tau(s)| &= \|\mathbf{b}'(s)\|,
\end{aligned}
\qquad
\begin{aligned}
\mathbf{t}'(s) &= \kappa_f(s)\mathbf{n}(s) = \boldsymbol{\varphi}''(s), \\
\mathbf{n}'(s) &= -\kappa_f(s)\mathbf{t}(s) + \tau(s)\mathbf{b}(s), \\
\mathbf{b}'(s) &= -\tau(s)\mathbf{n}(s).
\end{aligned}
\tag{4.38}$$

This motivates us to introduce $\xi(s)$ that relates the moving director frame $(\mathbf{d_1}, \mathbf{d_2})$ to Frenet's triad $(\mathbf{n}, \mathbf{b})$ as follows (Figure (4.7)):

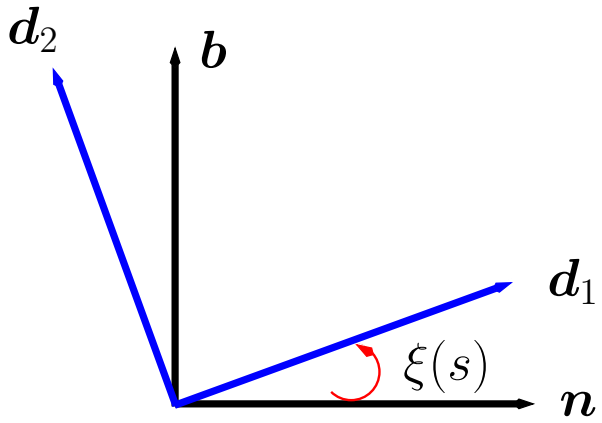

Figure 4.7 – $\mathbf{d}_i$ *with respect to Frenet's basis.*

$$\begin{aligned} \mathbf{d_1} &= \cos(\xi)\mathbf{n} + \sin(\xi)\mathbf{b}, \\ \mathbf{d_2} &= -\sin(\xi)\mathbf{n} + \cos(\xi)\mathbf{b}. \end{aligned} \tag{4.39}$$

Since

$$\mathbf{d_3}' = \boldsymbol{\kappa} \times \mathbf{d_3} = -\kappa_1 \mathbf{d_2} + \kappa_2 \mathbf{d_1}. \tag{4.40}$$

And $\mathbf{d_3}' = \kappa_f \mathbf{n}$ therefore, using the fact that $\mathbf{n} = \cos(\xi)\mathbf{d_1} - \sin(\xi)\mathbf{d_2}$ we obtain

$$\begin{aligned} \kappa_1 &= \kappa_f \sin(\xi), \\ \kappa_2 &= \kappa_f \cos(\xi). \end{aligned} \tag{4.41}$$

Since $\mathbf{b} = \sin(\xi)\mathbf{d_1} + \cos(\xi)\mathbf{d_2}$, so, using again $\mathbf{d}' = \boldsymbol{\kappa} \times \mathbf{d}$ we obtain:

$$\mathbf{b}' = ((\xi' - \kappa_3)\cos(\xi))\mathbf{d_1} + (\sin(\xi)(\kappa_3 - \xi'))\mathbf{d_2} + (\cos(\xi)\kappa_1 - \sin(\xi)\kappa_2)\mathbf{d_3}. \tag{4.42}$$

However, $\mathbf{b}' = -\tau \mathbf{n}$, therefore, we obtain the following relation:

$$\tau + \xi' = \kappa_3. \tag{4.43}$$

So, to conclude:

$$\boxed{\begin{aligned} \kappa_f^2 &= \kappa_1^2 + \kappa_2^2, \\ \theta := \tan(\xi) &= \frac{\kappa_1}{\kappa_2}, \\ \tau &= \kappa_3 - \xi'. \end{aligned}} \tag{4.44}$$

Hence, for thick beam solutions are given by:

— If $1 < \eta < \sqrt{r_1} < \sqrt{r_2}$:

$$\begin{aligned}
\kappa_f &= \mu\sqrt{(\eta^2-1)\Big(\frac{1}{r_1(r_1-1)}\mathrm{sn}^2+\frac{1}{r_2(r_2-1)}\mathrm{cn}^2\Big)},\\
\theta &= \sqrt{\frac{r_2(r_2-1)}{r_1(r_1-1)}}\mathrm{sc},\\
\tau &= \mu\sqrt{\frac{r_2-\eta^2}{r_2-1}}\mathrm{dn}-\mu(r_1-1)\frac{\sqrt{(r_2-\eta^2)(r_2-1)}\mathrm{dc}\,\mathrm{nc}}{r_1(r_1-1)+r_2(r_2-1)\mathrm{sc}^2}.
\end{aligned} \tag{4.45}$$

— If $1 < \sqrt{r_1} < \eta < \sqrt{r_2}$:

$$\begin{aligned}
\kappa_f &= \mu\sqrt{\frac{\eta^2-r_2}{r_1(r_1-r_2)}\mathrm{sn}^2+\frac{\eta^2-1}{r_2(r_2-1)}\mathrm{dn}^2},\\
\theta &= \sqrt{\frac{r_2(r_2-1)(\eta^2-r_2)}{r_1(r_1-r_2)(\eta^2-1)}}\mathrm{sd},\\
\tau &= \mu\sqrt{\frac{r_2-\eta^2}{r_2-1}}\mathrm{cn}-\mu(r_1-r_2)(\eta^2-1)\frac{\sqrt{(r_2-\eta^2)(r_2-1)}\mathrm{cd}\,\mathrm{nd}}{r_1(r_1-r_2)(\eta^2-1)+r_2(r_2-1)(\eta^2-r_2)\mathrm{sd}^2}.
\end{aligned} \tag{4.46}$$

And for thin beam:

— If $\sqrt{r_1} < \eta < 1 < \sqrt{r_2}$:

$$\begin{aligned}
\kappa_f &= \mu\sqrt{\frac{r_1-\eta^2}{r_2(r_1-r_2)}\mathrm{cn}^2+\frac{\eta^2-r_2}{r_1(r_1-r_2)}\mathrm{dn}^2},\\
\theta &= \sqrt{\frac{r_2(\eta^2-r_2)}{r_1(r_1-\eta^2)}}\mathrm{dc},\\
\tau &= \mu\sqrt{\frac{\eta^2-r_1}{1-r_1}}\mathrm{sn}-\frac{\mu(\eta^2-1)(r_1-r_2)}{\sqrt{r_1-1}}\frac{\sqrt{r_1-\eta^2}\mathrm{nc}\,\mathrm{sc}}{r_1(r_1-\eta^2)+r_2(\eta^2-r_2)\mathrm{dc}^2}.
\end{aligned} \tag{4.47}$$

— If $\sqrt{r_1} < 1 < \eta < \sqrt{r_2}$

$$\begin{aligned}
\kappa_f &= \mu\sqrt{\frac{r_1-\eta^2}{r_2(r_1-r_2)}\mathrm{dn}^2+\frac{\eta^2-r_2}{r_1(r_1-r_2)}\mathrm{cn}^2},\\
\theta &= \sqrt{\frac{r_2(\eta^2-r_2)}{r_1(r_1-\eta^2)}}\mathrm{cd},\\
\tau &= \mu\sqrt{\frac{r_2-\eta^2}{r_2-1}}\mathrm{sn}-\frac{\mu(\eta^2-1)(r_1-r_2)}{\sqrt{r_2-1}}\frac{\sqrt{r_2-\eta^2}\mathrm{nd}\,\mathrm{sd}}{r_1(r_1-\eta^2)+r_2(\eta^2-r_2)\mathrm{cd}^2}.
\end{aligned} \tag{4.48}$$

Where relation between Jacobian elliptic functions were used and will be detailed in the appendix. Furthermore, particular cases will also be provided in the appendix.

4.15 Rod shapes

In order to determine the shape of the beam we should recall first that $\boldsymbol{\varphi}' = \mathbf{d_3}$ (of course $\|\boldsymbol{\varphi}'\| = 1$ and $\int_0^\ell \|\boldsymbol{\varphi}'\|^2 \, ds = \ell$). Projecting along directors to obtain:

$$\begin{aligned} \varphi_1' - \varphi_2\kappa_3 + \varphi_3\kappa_2 &= 0, \\ \varphi_2' - \varphi_3\kappa_1 + \varphi_1\kappa_3 &= 0, \\ \varphi_3' - \varphi_1\kappa_2 + \varphi_2\kappa_1 &= 1. \end{aligned} \tag{4.49}$$

Of course directors and placement respect the following dimensionless relation:

$$\begin{aligned} \mathbf{d_1}' &= \kappa_3\mathbf{d_2} - \kappa_2\mathbf{d_3}, & \varphi_x &= \boldsymbol{\varphi}\cdot\mathbf{e}_x, \\ \mathbf{d_2}' &= \kappa_1\mathbf{d_3} - \kappa_3\mathbf{d_1}, & \varphi_y &= \boldsymbol{\varphi}\cdot\mathbf{e}_y, \\ \mathbf{d_3}' &= \kappa_2\mathbf{d_1} - \kappa_1\mathbf{d_2}, & \varphi_z &= \boldsymbol{\varphi}\cdot\mathbf{e}_z. \end{aligned} \tag{4.50}$$

In the following section, we will illustrate the general case for different loads and cross-sections, all the particular cases will be given explicitly in the appendices.

4.15.1 General case:η influence on rod shapes

In the general case curvatures are given by Jacobian functions where different regimes are represented by the four different interior area in (4.8). To find the rod shapes we should solve (4.49) and (4.50). These two equations are first order linear system with variable coefficients. Existence and uniqueness of solutions are guaranteed thanks to Picard fixed point [Jea10], however, solutions are hard to solve in an analytical way, we can solve them using a numerical method (example Runge-Kutta method).

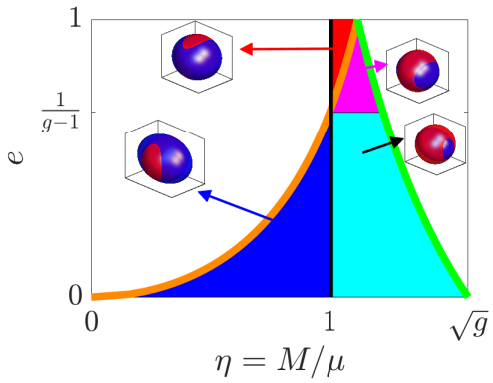

Figure 4.8 – *Illustration of Jacobian solutions in* (η, e) *plan.*

We aim to reply to the following question:

What is the behaviour of the beam by changing the load parameter η *for* μ *fixed?*

First, it should be mentioned that for μ fixed, varying η is exactly the variation of M.
In order to answer to our main question, we first represent in figure (4.9) the rod for different regimes and different values of η.
We can remark that by increasing η, we change the curvature of the rod. Therefore,

- η controls the shape of the beam.
- Increasing η switch rod shape from torsion to bending and vice versa in a continuous way.

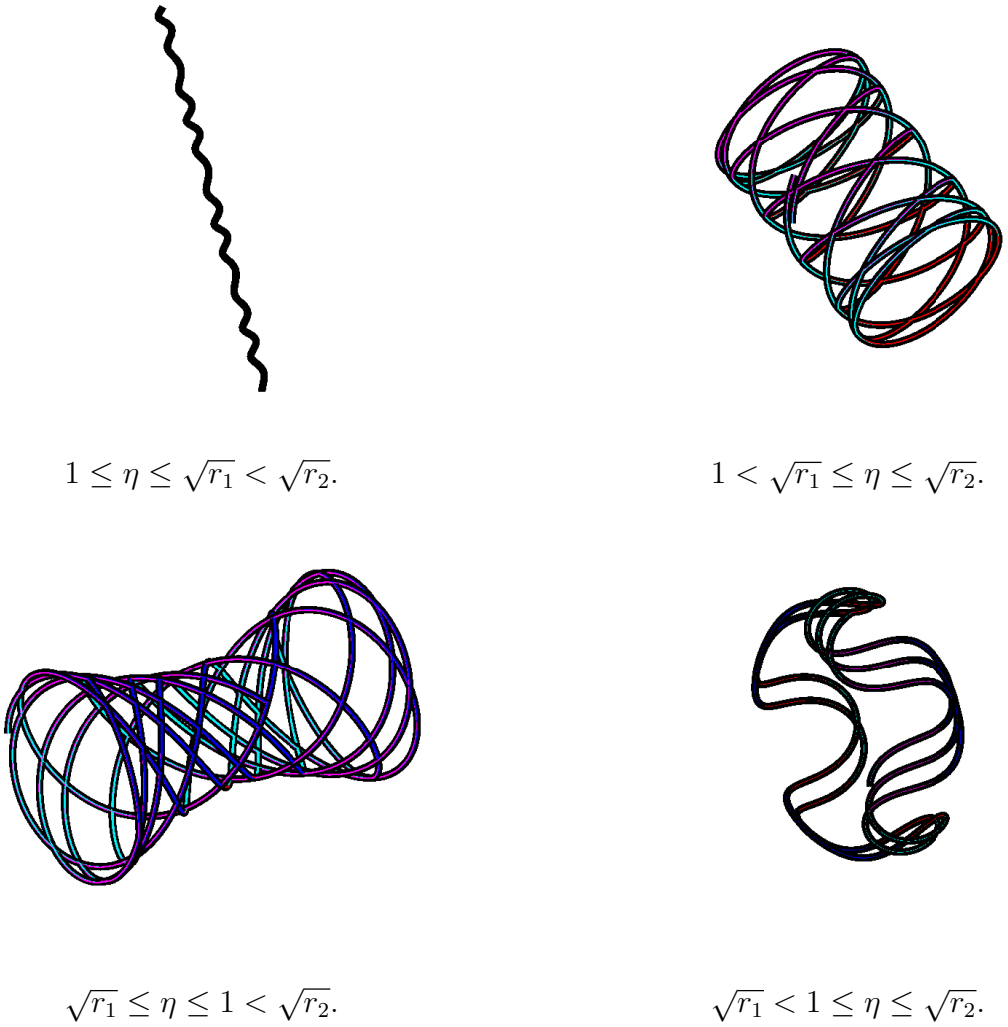

$1 \leq \eta \leq \sqrt{r_1} < \sqrt{r_2}$. $1 < \sqrt{r_1} \leq \eta \leq \sqrt{r_2}$.

$\sqrt{r_1} \leq \eta \leq 1 < \sqrt{r_2}$. $\sqrt{r_1} < 1 \leq \eta \leq \sqrt{r_2}$.

Figure 4.9 – *Beam shapes for various section types and loading. For all the case* $g = 2.5$, $\mu = 0.082$. *Top: thick-section* $e = 0.8$ *with* $\eta = 1.0268$ *(a) and* $\eta = 1.1471$ *(b). Bottom: thin-section* $e = 0.4$ *with* $\eta = 0.9218$ *(left) or* $\eta = 1.2514$ *(right).*

4.15.2 Deformed curvature parametrisation

In this section, we rewrite the deformed curvature in terms of Frenet curvature by using the invariants and the fact that $\kappa_f^2 = \kappa_1^2 + \kappa_2^2$. To do so, we first remark that invariants difference gives

$$r_1(r_1-1)\kappa_1^2 + r_2(r_2-1)\kappa_2^2 = \mu^2(\eta^2-1). \tag{4.51}$$

Using κ_f we deduce that:

$$\kappa_1^2 = \frac{\mu^2(\eta^2-1) - r_2(r_2-1)\kappa_f^2}{r_1(r_1-1) - r_2(r_2-1)}. \tag{4.52}$$

And

$$\kappa_2^2 = \frac{r_1(r_1-1)\kappa_f^2 - \mu^2(\eta^2-1)}{r_1(r_1-1) - r_2(r_2-1)}. \tag{4.53}$$

Hence, using invariants we deduce that

$$\kappa_3^2 = \frac{\mu^2(r_1+r_2-\eta^2) - r_1r_2\kappa_f^2}{r_1+r_2-1}. \tag{4.54}$$

It is clear that (4.52),(4.53) and (4.54) should not be negative. So, keeping in mind that $r_1(r_1-1) < r_2(r_2-1)$ we obtain three different cases:

- If $r_1 > 1$:

$$\frac{\mu^2(\eta^2-1)}{r_2(r_2-1)} \leq \kappa_f^2 \leq \mu^2 \min\left(\frac{\eta^2-1}{r_1(r_1-1)}, \frac{r_1+r_2-\eta^2}{r_1r_2}\right) \qquad \forall\ s \in [0,\ell]. \tag{4.55}$$

- If $r_1 < 1$ and $\eta < 1$:

$$\max\left(\frac{\mu^2(\eta^2-1)}{r_1(r_1-1)}, \frac{\mu^2(\eta^2-1)}{r_2(r_2-1)}\right) = \frac{\mu^2(\eta^2-1)}{r_2(r_2-1)} \leq \kappa_f^2 \leq \frac{\mu^2(r_1+r_2-\eta^2)}{r_1r_2} \qquad \forall\ s \in [0,\ell]. \tag{4.56}$$

- If $r_1 < 1$ and $\eta > 1$:

$$\max\left(\frac{\mu^2(\eta^2-1)}{r_1(r_1-1)}, \frac{\mu^2(\eta^2-1)}{r_2(r_2-1)}\right) = \frac{\mu^2(\eta^2-1)}{r_1(r_1-1)} \leq \kappa_f^2 \leq \frac{\mu^2(r_1+r_2-\eta^2)}{r_1r_2} \qquad \forall\ s \in [0,\ell]. \tag{4.57}$$

So Frenet's curvature is bounded, we can find explictly this bound for a given structure and load.

4.16 Möbius strip

A Möbius strip is a geometrical shape with only one side and only one boundary curve.
One of the first attempts to treat a Möbius strip as a mechanical object was made by Mahadevan and Keller [MK93] who employed an elastic rod model and found in a numerical way asymptotic solution of a Möbius band with "almost circular" centerline. A while later, Starostin and Van Der Heijden [SVDH07] used the invariant variational bicomplex formalism to derive the first equilibrium

equations for a wide developable strip undergoing large deformations and pointed of divergence of the bending energy that may serve as indicators of positions where out-of-plane tearing is likely to be initiated. Later on, Starostin *et al.* [SVDH16] deployed equilibrium shapes of a Möbius strip. Afterward, Bartels *et al.* [BH15] obtained some qualitative properties of developable Möbius strips which minimized the bending energy. Along with others, Levyakov [Lev15] tried to relate a Möbius strip to beam deformation and offered a finite element method based on kinematic-group approach to study a Möbius band obtained by exerting a moment and a rotation on a cantilever beam.

By applying our approach, we can identify a Möbius with a centerline $\boldsymbol{\varphi}$ (defined as a smooth function) and a cross-sections that verify:

$$\boldsymbol{\varphi}(0) = \boldsymbol{\varphi}(\ell), \qquad \lambda = \frac{2K(m)}{\ell}, \qquad \int_0^\ell \kappa_3(s)ds = \pi. \tag{4.58}$$

Where $\boldsymbol{\varphi(\ell) = \varphi(0)}$ implicates the reattachment condition, $\lambda = \dfrac{2K(m)}{\ell}$ gives the curvature periodicity (with $K(m)$ an elliptic integral defined in [Olv+10]) and $\displaystyle\int_0^\ell \kappa_3(s)ds = \pi$ is related to directors orientation .

4.16.1 Symmetric cross-section

In this section, we explain in details why a Möbius strip couldn't be obtained by imposing only moments at the extremity. An additional force is needed to maintain equilibrium.

To do so, we first start by imposing

$$\tau = 0, \qquad \text{and} \qquad \kappa_3 = \frac{\pi}{\ell}. \tag{4.59}$$

Direct application to equation (4.43) gives

$$\xi(s) = \frac{\pi}{\ell}s. \tag{4.60}$$

Therefore, in this case a Möbius strip (if it exists) is planar. So, a direct integration of (4.38) with the fact that $\Big(\mathbf{n}(0), \mathbf{b}(0), \mathbf{t}(0)\Big) = \Big(\mathbf{e}_x, \mathbf{e}_y, \mathbf{e}_z\Big)$ gives:

$$\mathbf{t}(s) = \Big(\sin(s\kappa_f), 0, \cos(s\kappa_f)\Big), \qquad \mathbf{n}(s) = \Big(\cos(s\kappa_f), 0, -\sin(s\kappa_f)\Big), \qquad \mathbf{b}(s) = \Big(0, 1, 0\Big). \tag{4.61}$$

Using the fact that $\boldsymbol{\varphi}' = \mathbf{t}$, we get after integration:

$$\varphi_x(s) = \frac{1-\cos(s\kappa_f)}{\kappa_f}, \qquad \varphi_y(s) = 0, \qquad \varphi_z(s) = \frac{\sin(s\kappa_f)}{\kappa_f}. \tag{4.62}$$

The reattachment condition $\boldsymbol{\varphi}(0) = \boldsymbol{\varphi}(\ell)$ is given by the fact that:

$$\kappa_f = \frac{2n\pi}{\ell}. \tag{4.63}$$

Where $n \in \mathbb{N}^*$ and we suppose that $n = 1$ hereafter.
Using (4.39) and (4.61) we obtain the directors:

$$\begin{aligned}
\mathbf{d_1}(s) &= \Big(-\cos(\frac{\pi}{\ell}s)\cos(\frac{2\pi}{\ell}s), -\sin(\frac{\pi}{\ell}s), \cos(\frac{\pi}{\ell}s)\sin(\frac{2\pi}{\ell}s)\Big), \\
\mathbf{d_2}(s) &= \Big(\sin(\frac{\pi}{\ell}s)\cos(\frac{2\pi}{\ell}s), -\cos(\frac{\pi}{\ell}s), -\sin(\frac{\pi}{\ell}s)\sin(\frac{2\pi}{\ell}s)\Big), \\
\mathbf{d_3}(s) &= \Big(\sin(\frac{2\pi}{\ell}s), 0, \cos(\frac{2\pi}{\ell}s)\Big).
\end{aligned} \tag{4.64}$$

We rewrite the deformed curvatures using (4.41):

$$\kappa_1(s) = \frac{2\pi}{\ell}\sin(\frac{\pi}{\ell}s), \qquad \kappa_2(s) = \frac{2\pi}{\ell}\cos(\frac{\pi}{\ell}s). \tag{4.65}$$

But curvature should verify the equilibrium (4.20), so injecting κ_1, κ_2 and κ_3 into (4.20), with the fact that $r_1 = r_2$, we obtain:

$$\begin{aligned}
r_1\,\kappa_1'(s) - (r_1 - 1)\,\kappa_2(s)\kappa_3(s) &= \frac{2\pi^2}{\ell^2}\cos(\frac{\pi}{\ell}s), \\
r_1\,\kappa_2'(s) + (r_1 - 1)\,\kappa_1(s)\kappa_3(s) &= -\frac{2\pi^2}{\ell^2}\sin(\frac{\pi}{\ell}s), \\
\kappa_3'(s) &= 0.
\end{aligned} \tag{4.66}$$

It is clear that the equilibrium $\mathbf{M}(s)' = 0$ is not satisfied in this case and an additional internal force exists.
We remind that for Kirchhoff rod

$$\mathbf{N}(s)' = 0, \tag{4.67}$$

$$\mathbf{M}(s)' + \mathbf{d_3} \times \mathbf{N} = 0. \tag{4.68}$$

So from the second equation we deduce that

$$\begin{aligned}
\mathbf{M}(s)' &= -\mathbf{d_3} \times (N_1\mathbf{d_1} + N_2\mathbf{d_2} + N_3\mathbf{d_3}), \\
&= -N_1\mathbf{d_2} + N_2\mathbf{d_1}.
\end{aligned} \tag{4.69}$$

We deduce by identification that

$$\begin{aligned} N_1(s) &= \frac{2\pi^2}{\ell^2}\sin\left(\frac{\pi}{\ell}s\right), \\ N_2(s) &= \frac{2\pi^2}{\ell^2}\cos\left(\frac{\pi}{\ell}s\right), \\ N_3(s) &= 0. \end{aligned} \tag{4.70}$$

Hence

$$\mathbf{N}(s) = N_1(s)\mathbf{d_1}(s) + N_2(s)\mathbf{d_2}(s) \overset{(4.64)}{=} \frac{2\pi^2}{\ell^2}\mathbf{e_2}. \tag{4.71}$$

4.16.2 Non-symmetric cross-section

For non-symmetric cross-section we should also impose an additional force in order to satisfy Möbius conditions. This idea is out of our scope in this manuscript.

4.17 Circular helices

Helix is a space curve in which the tangent at every point of the curve makes a constant angle with a fixed direction. Lancret stated that a necessary and sufficient condition to obtain a general helix is when the ratio of curvature to torsion is constant [Lan06]. Simple classification of uniform helical equilibria could be found in [CGM06]. A circular helix is a curve having non-zero constants τ and κ_f [Bar97].

In this section, we discuss circular helices for a Kirchhoff rod subjected to pure moments ($\mathbf{N} = 0$).

- If $e = 1$, by looking at (4.86), we remark that a circular helix is directly obtained since $\kappa_f = \mu\sqrt{\dfrac{(\eta^2-1)}{r_1(r_1-1)}}$ and $\tau = \pm\dfrac{\mu}{r_1}\sqrt{\dfrac{\eta^2-r_1}{1-r_1}}$.
- For $r_1 = 1$ we have

$$\begin{aligned} \kappa_2 &= \mu\sqrt{\frac{(\eta^2-1)}{r_2(r_2-1)}}, \\ \kappa_1 &= \overline{\kappa}_1\cos\Big((g-2)\kappa_2\, s\Big) + \overline{\kappa}_3\sin\Big((g-2)\kappa_2\, s\Big), \\ \kappa_3 &= \overline{\kappa}_3\cos\Big((g-2)\kappa_2\, s\Big) - \overline{\kappa}_1\sin\Big((g-2)\kappa_2\, s\Big), \\ \kappa_f &= \sqrt{\kappa_2^2 + \Big(\overline{\kappa}_1\cos\Big((g-2)s\kappa_2\Big) + \overline{\kappa}_3\sin\Big((g-2)s\kappa_2\Big)\Big)^2}, \\ \xi &= \arctan\Big(\frac{\kappa_1}{\kappa_2}\Big), \\ \tau &= \kappa_3 - \xi'. \end{aligned} \tag{4.72}$$

So, by imposing $\eta^2 = 1$, we obtain $\kappa_f = \overline{\kappa}_1$ and $\tau = \overline{\kappa}_3$ and a circular helix.

- If $r_1 = r_2 = 1$ we have a circular helix satisfied by $\kappa_f = \sqrt{\overline{\kappa}_1^2 + \overline{\kappa}_2^2}$ and $\tau = \kappa_3$.

Note that in the general case, a helix could only exist for $1 \leq \eta \leq \sqrt{r_1} < \sqrt{r_2}$ (see figure (4.9)), where curvature and torsion were given in eq.(4.45). κ_f is constant only for $\lambda = 0$ or equivalently $r_2 = \eta^2$ or $r_1 = 1$. However, these two conditions are unattainable in eq.(4.45) and a circular helix could not exist in the general case.

4.18 Torus knot

In this section, we aim to study the stability of a Torus knot.
Torus is a three dimensional shape that is parametrized by:

$$(\theta, \phi) \longrightarrow \boldsymbol{\Xi}(\theta, \phi) = (R + r\cos(\phi))\cos(\theta)\mathbf{e}_x + (R + r\cos(\phi))\sin(\theta)\mathbf{e}_y + r\sin(\phi)\mathbf{e}_z. \tag{4.73}$$

The normal vector to the surface is given by the product of both tangent directions:

$$n(\theta, \phi) = \frac{\partial \boldsymbol{\Xi}}{\partial \theta} \times \frac{\partial \boldsymbol{\Xi}}{\partial \phi} = \cos(\theta)\cos(\phi)\mathbf{e}_x + \sin(\theta)\cos(\phi)\mathbf{e}_y + \sin(\phi)\mathbf{e}_z. \tag{4.74}$$

Torus knots are closed symmetric curves that lie on the surface of a mathematical torus. A torus knot $\mathbb{T}_{p,q}$ wraps the torus p times along the longitudinal direction, and q times along the meridian direction, with p and q co-prime integers.

$\mathbb{T}_{p,q}$ torus knot is computed from (4.73) by parametrizing the curve with a single parameter. This parametrization is given by:

$$\boxed{\zeta \longrightarrow \tilde{\boldsymbol{\varphi}}(\zeta) = \Big(R + r\cos(q\zeta)\Big)\cos(p\zeta)\mathbf{e}_x + \Big(R + r\cos(q\zeta)\Big)\sin(p\zeta)\mathbf{e}_y + r\sin(q\zeta)\mathbf{e}_z}. \tag{4.75}$$

Where $\zeta \in [0, 2\pi]$. Admitting the following change of variables:

$$S = \frac{L}{2\pi}\zeta, \tag{4.76}$$

where $S \in [0, L]$. Now using dimensionless method mentioned before we obtain the dimensionless placement:

$$s \longrightarrow \boldsymbol{\varphi}(s) = R\cos(a)\Big(1 + \lambda\cos(a)\Big)\mathbf{e}_x + R\sin(a)\Big(1 + \lambda\cos(a)\Big)\mathbf{e}_y + R\lambda\sin(a)\mathbf{e}_z \tag{4.77}$$

Where $\lambda = \dfrac{r}{R}$ and $a = \dfrac{2\pi q s}{\ell}$.
Since $\mathbb{T}_{p,q}$ and $\mathbb{T}_{q,p}$ are topologically equivalent [OR16], so, from now on we suppose $p < q$.
Fig.(4.10) represent Torus knot that lies on a Torus for two different knots.
Keeping in mind that placement is given explicitly, so using Frenet's relation, curvature and torsion

Figure 4.10 – *Torus knot on a Torus with* $\ell = 50, \lambda = 0.1$ *and* $R = 10$. *Left* $(2,3)$ *Torus Knot and right* $(3,5)$ *Torus Knot.*

are given by:

$$\begin{aligned}
\kappa_f(s) &= \frac{2\pi\sqrt{\frac{2q^2(4\lambda p^2\cos(a)+\lambda^2(2p^2+q^2)+p^2)}{\lambda p^2(\lambda\cos(a)+4\cos(a))+(\lambda^2+2)p^2+2\lambda^2q^2}+\frac{4\lambda^2q^4(2\lambda p^2\cos(a)+\lambda^2(p^2+q^2)+p^2)}{(\lambda p^2(\lambda\cos(a)+4\cos(a))+(\lambda^2+2)p^2+2\lambda^2q^2)^2}+p^2-q^2}}{\ell}, \\
|\tau(s)| &= \frac{\sqrt{2}\pi}{\ell}\sqrt{\frac{4q^2(4\lambda p^2\cos(a)+\lambda^2(2p^2+q^2)+3p^2)}{\lambda p^2(\lambda\cos(2a)+4\cos(a))+(\lambda^2+2)p^2+2\lambda^2q^2}+\frac{8\lambda^2q^4(2\lambda p^2\cos(a)+\lambda^2(p^2+q^2)+p^2)}{(\lambda p^2(\lambda\cos(2a)+4\cos(a))+(\lambda^2+2)p^2+2\lambda^2q^2)^2}-p^2\cos(2a)+p^2-4q^2}.
\end{aligned} \tag{4.78}$$

We should mention that $\kappa_f(s)$ and $\tau(s)$ are periodic with $T = \dfrac{\ell}{q}$.
Now, we aim to reply to the following question:

What condition should be imposed on the knot in order to maintain the rod equilibrium?

Given the fact that

$$\kappa_f(T-s) = \kappa_f(T+s) \tag{4.79}$$

So $s = \dfrac{\ell}{2q}$ is an axis of symmetry and since κ_f is a combination of cosine functions so we can restrict our study to a domain of length $\dfrac{\ell}{2q}$. Therefore, κ_f is strictly monotonic $\in [0; \dfrac{\ell}{2q}]$ and

$$\begin{aligned}
\kappa_f(0) &= \frac{2\pi}{\ell}\sqrt{\frac{\left((\lambda+1)p^2+\lambda q^2\right)^2}{(\lambda+1)^2p^2+\lambda^2q^2}}, \\
\kappa_f(\tfrac{\ell}{2q}) &= \frac{2\pi}{\ell}\sqrt{\frac{\left((\lambda-1)p^2+\lambda q^2\right)^2}{(\lambda-1)^2p^2+\lambda^2q^2}}.
\end{aligned} \tag{4.80}$$

Therefore, $\kappa_f(0) > \kappa_f(\frac{\ell}{2q})$ and κ_f is a decreasing function. Knowing that $\kappa_f > 0$ therefore, κ_f^2 is an increasing function (and of course periodic), hence

- If $r_1 > 1$:

$$\frac{\mu^2(\eta^2-1)}{r_2(r_2-1)} \leq \frac{4\pi^2\left((\lambda+1)p^2+\lambda q^2\right)^2}{\ell^2((\lambda+1)^2p^2+\lambda^2q^2)} \leq \min\left(\frac{\mu^2(\eta^2-1)}{r_1(r_1-1)}, \frac{\mu^2(r_1+r_2-\eta^2)}{r_1r_2}\right). \tag{4.81}$$

- If $r_1 < 1$ and $\eta < 1$:

$$\frac{\mu^2(\eta^2-1)}{r_2(r_2-1)} \leq \frac{4\pi^2\left((\lambda+1)p^2+\lambda q^2\right)^2}{\ell^2((\lambda+1)^2p^2+\lambda^2q^2)} \leq \frac{\mu^2(r_1+r_2-\eta^2)}{r_1r_2}. \tag{4.82}$$

- If $r_1 < 1$ and $\eta > 1$:

$$\frac{\mu^2(\eta^2-1)}{r_1(r_1-1)} \leq \frac{4\pi^2\left((\lambda+1)p^2+\lambda q^2\right)^2}{\ell^2((\lambda+1)^2p^2+\lambda^2q^2)} \leq \frac{\mu^2(r_1+r_2-\eta^2)}{r_1r_2}. \tag{4.83}$$

Thus, for a given (p, q), we obtain a necessary condition relation between the shape of the knot λ and the external moments η and μ.

4.19 Work in progress

We are currently developping a way to determine the sufficient condition to impose on the knot in order to obtain the equilibrium, since necessary condition is chosen by invariants intersection, so one can choose one of the three equations presented in (4.20), as an example:

$$\kappa_3' + (r_2 - r_1)\kappa_1\kappa_2 = 0. \tag{4.84}$$

Note that κ_i could be found explicitly thanks to (4.52),(4.53) and (4.54) where κ_f is given by (4.78). So, the necessary condition is a value of λ that vanishes $\kappa_3' + (r_2 - r_1)\kappa_1\kappa_2$, difficulty lies in the fact that this value of lambda is hard to solve explicitly for any torus knot due to the complex form of κ_f. Of course to overcome this difficulty one can solve (4.84) numerically in order to obtain the value (or values) of λ. Asymptotic analysis is also a way to better understanding the behaviour of these knots in order to respect the equilibrium.
It should be mentioned that Once we find this condition, we can use (4.41) and (4.43) to find the deformed curvature κ_i and (4.39) to find the directors $\mathbf{d_i}$.

4.20 Conclusion

This chapter investigated the behaviour of a rod subjected to moments where in this case the structure was similar to Timoshenko beam. Two invariants governed the problems: moments and energy per unit length. These two invariants were exactly the same as invariants of Euler's rotation of a rigid body. These invariants dictated the existence of the solutions and impose four regimes depending on load parameters.
Explicit solutions for deformed curvatures and Frenet's curvature and torsion were given in terms of Jacobian elliptic functions. This is not the case for placement and directors where we obtained a nonlinear system of ordinary differential equations that is hard to solve analytically, these solutions were given by using a numerical method proposed by Matlab and rod shapes where given numer-

ically for different cases, also a detailed approach for the influence of each control parameter was introduced.
In order to validate our theoretical approach, we presented some applications, such as the classification of helical shapes, equilibrium of a circular Möbius strip and explicit analysis of the stability of a Torus knot.

APPENDICES

Appendix A: Frenet's Particular cases

First, it looks interesting to find Frenet's variables for particular cross-section geometry e and material g:

— If $r_1 = r_2$ in this case invariants are given by:

$$\begin{aligned} r_1^2\Big(\underbrace{\kappa_1^2+\kappa_2^2}_{\kappa_f^2}\Big)+\kappa_3^2 &= (\eta\mu)^2, \\ r_1\Big(\underbrace{\kappa_1^2+\kappa_2^2}_{\kappa_f^2}\Big)+\kappa_3^2 &= \mu^2. \end{aligned} \tag{4.85}$$

Hence:

$$\begin{aligned} \kappa_f &= \mu\sqrt{\frac{(\eta^2-1)}{r_1(r_1-1)}}, \\ \xi &= \frac{\kappa_3(r_1-1)}{r_1}s+n\pi, \qquad n\in\mathbb{N}, \\ \kappa_3 &= \pm\mu\sqrt{\frac{\eta^2-r_1}{1-r_1}}, \\ \tau &= \kappa_3-\xi' = \frac{\kappa_3}{r_1}. \end{aligned} \tag{4.86}$$

— If $r_1 = 1$ invariants are given by:

$$\begin{aligned} \kappa_1^2+r_2^2\kappa_2^2+\kappa_3^2 &= (\eta\mu)^2, \\ \kappa_1^2+r_2\kappa_2^2+\kappa_3^2 &= \mu^2. \end{aligned} \tag{4.87}$$

Hence:

$$\begin{aligned} \kappa_2 &= \mu\sqrt{\frac{(\eta^2-1)}{r_2(r_2-1)}}, \\ \kappa_f &= \sqrt{\kappa_2^2+\Big(\overline{\kappa}_1\cos\Big((g-2)s\kappa_2\Big)+\overline{\kappa}_3\sin\Big((g-2)s\kappa_2\Big)\Big)^2}, \\ \theta &= \frac{\overline{\kappa}_1\cos\Big((g-2)s\kappa_2\Big)+\overline{\kappa}_3\sin\Big((g-2)s\kappa_2\Big)}{\kappa_2}, \\ \tau &= \kappa_3-\xi'. \end{aligned} \tag{4.88}$$

— If $r_1 = r_2 = 1$ therefore:

$$\begin{aligned} \kappa_f &= \sqrt{\overline{\kappa}_1^2 + \overline{\kappa}_2^2}, \\ \theta &= \frac{\overline{\kappa}_1}{\overline{\kappa}_2}, \\ \tau &= \overline{\kappa}_3. \end{aligned} \tag{4.89}$$

Also it is interesting to look at these variables for extreme load η:

— If $\eta = 1 < \sqrt{r_1}$:

$$\begin{aligned} \kappa_f &= 0, \\ \theta &\text{ not defined}, \\ \tau &\text{ not defined}. \end{aligned} \tag{4.90}$$

— If $\eta = \sqrt{r_2} > \sqrt{r_1} > 1$:

$$\begin{aligned} \kappa_f &= \frac{\mu}{\sqrt{r_2}}, \\ \theta &= 0, \\ \tau &= 0. \end{aligned} \tag{4.91}$$

— If $\eta = \sqrt{r_1} < 1$:

$$\begin{aligned} \kappa_f &= \frac{\mu}{\sqrt{r_1}}, \\ \theta &= \infty, \\ \tau &= 0. \end{aligned} \tag{4.92}$$

— If $\eta = \sqrt{r_2} > 1 > \sqrt{r_1}$:

$$\begin{aligned} \kappa_f &= \frac{\mu}{\sqrt{r_2}}, \\ \theta &= 0, \\ \tau &= 0. \end{aligned} \tag{4.93}$$

Therefore, we can assume that for thick beam if $\eta = 1$ we have torsion and if $\eta = \sqrt{r_2}$, we have pure elastica. But, for thin beam if $\eta = \sqrt{r_1}$ and $\eta = \sqrt{r_2}$, we have elasticas in different planes. These ideas will be given in details in appendix **B**. Furthermore for $\eta = \sqrt{r_1}$ and thick cross-section we have $m = 1$ for the two regimes. Using the fact that $cn(z \,|\, 1) = dn(z \,|\, 1) = \dfrac{1}{\cosh z}$, for the two

regimes we have:

$$\begin{aligned}
\lambda &= \sqrt{\frac{(r_2-r_1)(r_1-1)}{r_1 r_2}},\\
\kappa_f &= \mu\sqrt{(r_1-1)\Big(\frac{1}{r_1(r_1-1)}\sin(\lambda s)^2+\frac{1}{r_2(r_2-1)}\cos(\lambda s)^2\Big)},\\
\theta &= \sqrt{\frac{r_2(r_2-1)}{r_1(r_1-1)}}\tan(\lambda s),\\
\tau &= \mu\sqrt{\frac{r_2-r_1}{r_2-1}}-\mu(r_1-1)\frac{\sqrt{(r_2-r_1)(r_2-1)}}{r_1(r_1-1)\cos(\lambda s)^2+r_2(r_2-1)\sin(\lambda s)^2}.
\end{aligned} \tag{4.94}$$

In the same spirit, for thin beam we have $m=1$ for $\eta=1$ and:

$$\begin{aligned}
\lambda &= \sqrt{\frac{(r_2-1)(1-r_1)}{r_1 r_2}},\\
\kappa_f &= \mu\sqrt{\frac{r_1-1}{r_2(r_1-r_2)}\cos(\lambda s)^2+\frac{1-r_2}{r_1(r_1-r_2)}},\\
\theta &= \sqrt{\frac{r_2(1-r_2)}{r_1(r_1-1)}},\\
\tau &= \mu\sqrt{\frac{\eta^2-r_1}{1-r_1}}\sin(\lambda s).
\end{aligned} \tag{4.95}$$

Appendix B: Particular rod shapes

Here we discuss the different rod shapes.

4.20.1 Homogeneous solutions

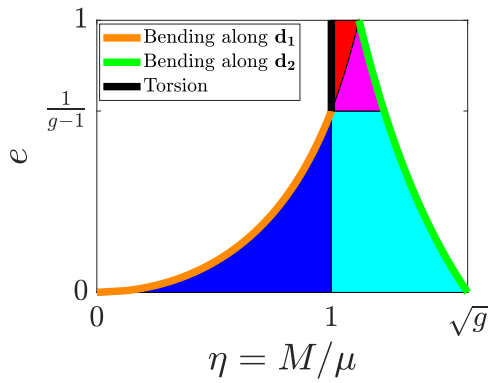

Figure 4.11 – *Illustration of homogeneous solutions in a (η, e) plan.*

$\boldsymbol{\eta = 1}$

This is a particular case of (4.32) represented by the black curve in Figure (4.11) with:

$$\kappa_1(s) = 0, \qquad \kappa_2(s) = 0, \qquad \kappa_3(s) = \mu. \tag{4.96}$$

By a straight forward calculation with the fact that $\mathbf{d_i}(0) = \mathbf{e_i}$ we obtain:

$$\begin{aligned}
\varphi_1(s) &= \varphi_1(0)\cos(s\mu) + \varphi_2(0)\sin(s\mu), & \mathbf{d_1}(s) &= \begin{pmatrix}\cos(s\mu) & \sin(s\mu) & 0\end{pmatrix},\\
\varphi_2(s) &= -\varphi_1(0)\sin(s\mu) + \varphi_2(0)\cos(s\mu), & \mathbf{d_2}(s) &= \begin{pmatrix}-\sin(s\mu) & \cos(s\mu) & 0\end{pmatrix},\\
\varphi_3(s) &= s + \varphi_3(0), & \mathbf{d_3}(s) &= \begin{pmatrix}0 & 0 & 1\end{pmatrix}.
\end{aligned} \tag{4.97}$$

Cartesian placement is given by:

$$\begin{aligned}
\varphi_x(s) &= \varphi_1(0),\\
\varphi_y(s) &= \varphi_2(0),\\
\varphi_z(s) &= s + \varphi_3(0).
\end{aligned} \tag{4.98}$$

$\boldsymbol{\eta = \sqrt{r_2}}$

This case is obtained by using (4.33) or (4.35) represented by the green curve in Figure (4.11). Curvatures are given by:

$$\kappa_1(s) = 0, \qquad \kappa_2(s) = \frac{u}{\sqrt{r_2}}, \qquad \kappa_3(s) = 0. \tag{4.99}$$

Repeating the same procedure to obtain:

$$\begin{aligned}
\varphi_1(s) &= \varphi_1(0)\cos(\frac{\mu s}{\sqrt{r_2}}) - \varphi_3(0)\sin(\frac{\mu s}{\sqrt{r_2}}) + \frac{\sqrt{r_2}}{\mu}\Big(\cos(\frac{\mu s}{\sqrt{r_2}}) - 1\Big),\\
\varphi_2(s) &= \varphi_2(0),\\
\varphi_3(s) &= \varphi_1(0)\sin(\frac{\mu s}{\sqrt{r_2}}) + \varphi_3(0)\cos(\frac{\mu s}{\sqrt{r_2}}) + \frac{\sqrt{r_2}}{\mu}\sin(\frac{\mu s}{\sqrt{r_2}}),\\
\mathbf{d_1}(s) &= \Big(\cos(\tfrac{u}{\sqrt{r_2}}s) \quad 0 \quad -\sin(\tfrac{u}{\sqrt{r_2}}s)\Big),\\
\mathbf{d_2}(s) &= \begin{pmatrix}0 & 1 & 0\end{pmatrix},\\
\mathbf{d_3}(s) &= \Big(\sin(\tfrac{u}{\sqrt{r_2}}s) \quad 0 \quad \cos(\tfrac{u}{\sqrt{r_2}}s)\Big).
\end{aligned} \tag{4.100}$$

Cartesian placement is given by:

$$\begin{aligned}\varphi_x(s) &= \varphi_1(0) - \frac{\sqrt{r_2}}{\mu}\Big(\cos(\frac{\mu s}{\sqrt{r_2}}) - 1\Big),\\ \varphi_y(s) &= \varphi_2(0),\\ \varphi_z(s) &= \varphi_3(0) + \frac{\sqrt{r_2}}{\mu}\sin(\frac{\mu s}{\sqrt{r_2}}).\end{aligned} \tag{4.101}$$

$\eta = \sqrt{r_1}$

This case is obtained by using (4.34) shown by the orange curve in Figure (4.11):

$$\kappa_1(s) = \frac{u}{\sqrt{r_1}}, \qquad \kappa_2(s) = 0, \qquad \kappa_3(s) = 0. \tag{4.102}$$

And

$$\begin{aligned}\varphi_1(s) &= \varphi_1(0),\\ \varphi_2(s) &= \varphi_2(0)\cos(\frac{\mu s}{\sqrt{r_1}}) + \varphi_3(0)\sin(\frac{\mu s}{\sqrt{r_1}}) + \frac{\sqrt{r_1}}{\mu}\Big(1 - \cos(\frac{\mu s}{\sqrt{r_1}})\Big),\\ \varphi_3(s) &= -\varphi_2(0)\sin(\frac{\mu s}{\sqrt{r_1}}) + \varphi_3(0)\cos(\frac{\mu s}{\sqrt{r_1}}) + \frac{\sqrt{r_1}}{\mu}\sin(\frac{\mu s}{\sqrt{r_2}}),\\ \mathbf{d_1}(s) &= \begin{pmatrix}1 & 0 & 0\end{pmatrix},\\ \mathbf{d_2}(s) &= \begin{pmatrix}0 & \cos(\frac{u}{\sqrt{r_1}}s) & \sin(\frac{u}{\sqrt{r_1}}s)\end{pmatrix},\\ \mathbf{d_3}(s) &= \begin{pmatrix}0 & -\sin(\frac{u}{\sqrt{r_1}}s) & \cos(\frac{u}{\sqrt{r_1}}s)\end{pmatrix}.\end{aligned} \tag{4.103}$$

Cartesian placement is given by:

$$\begin{aligned}\varphi_x(s) &= \varphi_1(0),\\ \varphi_y(s) &= \varphi_2(0) + \frac{\sqrt{r_1}}{\mu}\Big(\cos(\frac{\mu s}{\sqrt{r_1}}) - 1\Big),\\ \varphi_z(s) &= \varphi_3(0) + \frac{\sqrt{r_1}}{\mu}\sin(\frac{\mu s}{\sqrt{r_1}}).\end{aligned} \tag{4.104}$$

Figure (4.12) represent the beam for the particular loads where it is clear that $\eta = 1$ represents a torsion and $\eta = \sqrt{r_2}$ (respectively $\eta = \sqrt{r_1}$) is an elastica in $(\mathbf{d_1}, \mathbf{d_3})$ plan (respectively $(\mathbf{d_2}, \mathbf{d_3})$)

4.20.2 Trigonometric solutions

$r_1 = r_2$

This particular case is represented by the blue curve in Figure (4.13) where the curvatures are given by (4.22) and (4.86)

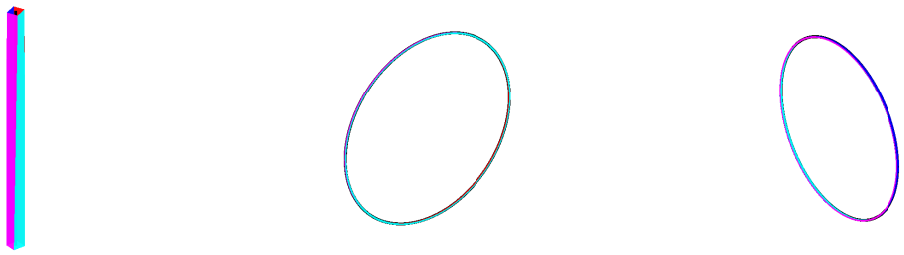

$\eta = 1.$ $\eta = \sqrt{r_2}.$ $\eta = \sqrt{r_1}.$

Figure 4.12 – *Particular beam shapes with* $g = 2.5$, $\mu = 0.082$. *Left and center: thick-section* $e = 0.8$. *Right: thin-section* $e = 0.4$.

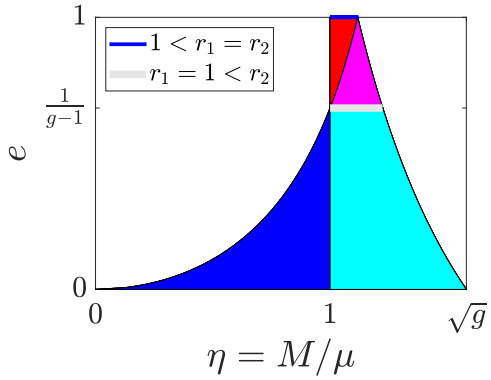

Figure 4.13 – *Illustration of trigonometric solutions in a* (η, e) *plan.*

By numerical simulations, we can present the rod shapes for different values of η.
Figure (4.14) represents rod shapes for two different values of η with fixed κ_{10} where it is clear

$\eta = 1.006$ $\eta = 1.1133$

Figure 4.14 – *Rod shapes for symmetric cross-sections* $(1 < r_1 = r_2)$ *where* $g = 2.5$ *and* $\kappa_{10} = 0.0005$.

that in this case we have helical shapes (*e.g.* [NG99]).

$r_1 = 1$

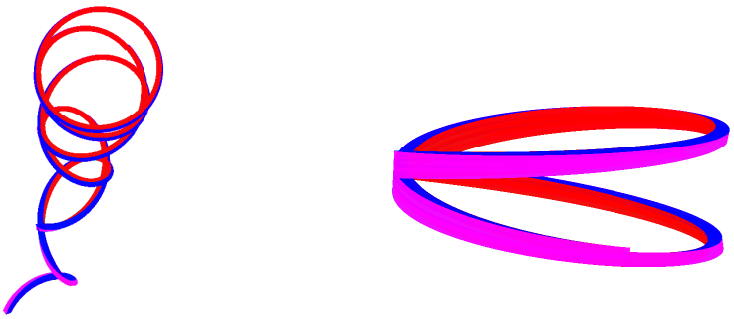

$\eta = 1.006.$ $\eta = 1.1133.$

Figure 4.15 – *Rod shapes for critical cross-sections* ($r_1 = 1$) *where* $g = 2.5$ *and* $\kappa_{10} = 0.0005$.

This is the silver line in Figure (4.13), where curvatures are given by (4.23) and (4.88).

Figure (4.15) represents rod shapes for two different values of η with fixed κ_{10} where we obtain two different rod behaviour

4.20.3 Hyperbolic solutions

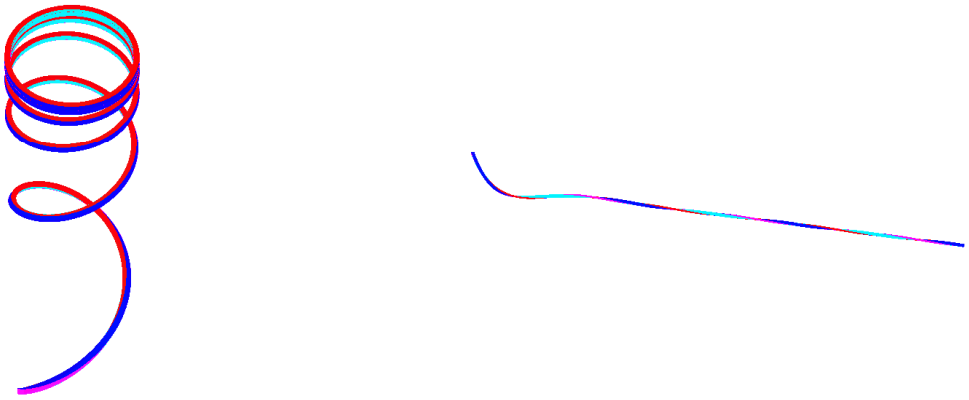

Thick section with $\eta = \sqrt{r_1}$. *Thin section with* $\eta = 1$.

Figure 4.16 – *Rod shapes for hyperbolic cross-sections.*

Hyperbolic solutions in our case are particular case of the general Jacobian solutions shown in figure (4.17) and for which $m = 1$ and frenet solutions are given in eq.(4.94) and eq.(4.95)

The left panel of figure (4.16) represents the particular thick rod that is the quasi bending orange curve in figure (4.17), whereas the right panel represents the particular thin rod that corresponds to quasi torsion black curve in figure (4.17).

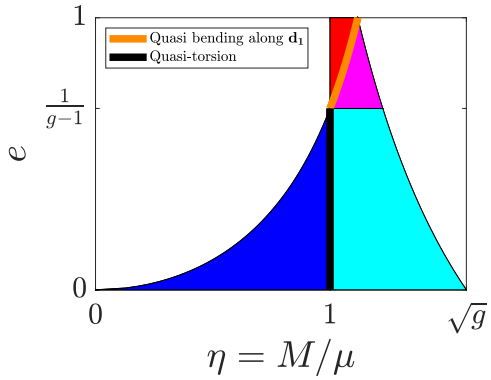

Figure 4.17 – *Illustration of hyperbolic solutions in a* (η, e) *plan.*

Appendix C: Jacobian elliptic functions

In this section we give in details the relation between Jacobian elliptic functions that have been used in the manuscript using [Olv+10].

4.20.4 Glaisher's Notation

The Jacobian functions are related in the following way. Let p,q,r be any three of the letters s, c, d, n. Then

$$\mathrm{pq} = \frac{\mathrm{pr}}{\mathrm{qr}} \tag{4.105}$$

with the convention that functions with the same two letters are replaced by unity; e.g. ss = 1.

4.20.5 Relation between the square of functions

$$\begin{aligned}
\mathrm{sn}^2 + \mathrm{cn}^2 &= m\,\mathrm{sn}^2 + \mathrm{dn}^2 &&= 1, \\
\mathrm{ns}^2 &= m + \mathrm{ds}^2 &&= 1 + \mathrm{cs}^2, \\
1 + m'\mathrm{sc}^2 &= \mathrm{dc}^2 &&= m + m'\mathrm{nc}^2, \\
m' - m'\mathrm{nd}^2 &= -m\,m'\,\mathrm{sd}^2 &&= m\mathrm{cd}^2 - m.
\end{aligned} \tag{4.106}$$

Where $m' = 1 - m$.

Appendix D: Model comparison

In this part, we compare the three models: Timoshenko model, Euler-Bernoulli beam model and Kirchhoff's rod model, for large transformation.

4.21 Equilibrium

Equilibrium equations for the three models are given by:

$$\begin{aligned} \frac{d\underline{\mathbf{N}}(S)}{dS} &= 0, \\ \frac{d\underline{\mathbf{M}}(S)}{dS} + \frac{d\underline{\boldsymbol{\varphi}}(S)}{dS} \times \underline{\mathbf{N}}(S) &= 0. \end{aligned} \tag{4.107}$$

Where,

Timoshenko	Euler	Kirchhoff
$\frac{d\underline{\boldsymbol{\varphi}}(S)}{dS} = \underline{\varepsilon}_1(S)\mathbf{d_1}(S) + \underline{\varepsilon}_3(S)\mathbf{d_3}(S)$	$\frac{d\underline{\boldsymbol{\varphi}}(S)}{dS} = \underline{\varepsilon}_3(S)\mathbf{d_3}(S)$	$\frac{d\underline{\boldsymbol{\varphi}}(S)}{dS} = \mathbf{d_3}(S)$

By projecting along directors, one obtains:

Timoshenko	Euler	Kirchhoff
$\frac{d\underline{N}_1}{dS} + \underline{N}_3(S)\underline{\kappa}_2(S) = 0,$ $\frac{d\underline{N}_3}{dS} - \underline{N}_1(S)\underline{\kappa}_2(S) = 0,$ $\frac{d\underline{M}_2}{dS} + \underline{N}_1(S)\underline{\varepsilon}_3(S) - \underline{N}_3(S)\underline{\varepsilon}_1(S) = 0.$	$\frac{d\underline{N}_1}{dS} + \underline{N}_3(S)\underline{\kappa}_2(S) = 0,$ $\frac{d\underline{N}_3}{dS} - \underline{N}_1(S)\underline{\kappa}_2(S) = 0,$ $\frac{d\underline{M}_2}{dS} + \underline{N}_1(S)\underline{\varepsilon}_3(S) = 0.$	$\frac{d\underline{N}_1}{dS} + \underline{N}_3(S)\underline{\kappa}_2(S) = 0,$ $\frac{d\underline{N}_3}{dS} - \underline{N}_1(S)\underline{\kappa}_2(S) = 0,$ $\frac{d\underline{M}_2}{dS} + \underline{N}_1(S) = 0.$

Linear constitutive laws are given by:

Timoshenko	Euler	Kirchhoff
$\underline{N}_1(S) = GA\underline{\varepsilon}_1(S),$ $\underline{N}_3(S) = EA(\underline{\varepsilon}_3(S) - 1),$ $\underline{M}_2(S) = EI\underline{\kappa}_2(S).$	$\underline{N}_3(S) = EA(\underline{\varepsilon}_3(S) - 1),$ $\underline{M}_2(S) = EI\underline{\kappa}_2(S).$	$\underline{M}_2(S) = EI\underline{\kappa}_2(S).$

4.22 Dimensionless equilibrium

We adapt a unified non-dimensional formulation thanks to the slenderness ratio $\varrho = \sqrt{\dfrac{I}{A}}$, so dimensionless curvilinear abscissa is given by :

$$s = \frac{S}{\varrho}.$$

For any physical variables $\underline{v}(S)$ previously mentioned, we can associate a non-dimensional variable $v(s)$ as follows:

$$\varepsilon_i(s) = \underline{\varepsilon}_i(S), \qquad \theta(s) = \underline{\theta}_i(S), \qquad \varphi_i(s) = \frac{1}{\varrho}\underline{\varphi}_i(S), \qquad \kappa_2(s) = \varrho\underline{\kappa_2}(S). \tag{4.108}$$

Physical force and moment $\underline{N}(S)$ and $\underline{M}(S)$ have also non-dimensional form $N(s)$ and $M(s)$ related by:

$$N(s) = \frac{\underline{N}(S)}{EA}, \qquad M(s) = \frac{\underline{M}(S)}{\varrho EA}. \tag{4.109}$$

Now using the fact that $\dfrac{d}{dS} = \dfrac{1}{\varrho}\dfrac{d}{ds}$, we re-write the equilbrium in a dimensionless form:

Timoshenko	Euler	Kirchhoff
$\dfrac{\varepsilon_1'}{g} + \Big(\varepsilon_3 - 1\Big)\kappa_2 = 0,$	$N_1' + \Big(\varepsilon_3 - 1\Big)\kappa_2 = 0,$	$N_1' + N_3\kappa_2 = 0,$
$\varepsilon_3' - \dfrac{\varepsilon_1\kappa_2}{g} = 0,$	$\varepsilon_3' - N_1\kappa_2 = 0,$	$N_3' - N_1\kappa_2 = 0,$
$\kappa_2' + \varepsilon_1 + \varepsilon_1\varepsilon_3\Big(\dfrac{1}{g} - 1\Big) = 0.$	$\kappa_2' + N_1\varepsilon_3 = 0.$	$\kappa_2' + N_1 = 0.$

Non-dimensional dynamical components are:

$$\begin{aligned} N_1(s) &= \frac{\underline{N}_1(S)}{EA} = \frac{GA\varepsilon_1(s)}{EA} = \frac{\varepsilon_1(s)}{g}, \\ N_3(s) &= \frac{\underline{N}_3(S)}{EA} = \frac{EA(\varepsilon_3(s) - 1)}{EA} = \varepsilon_3(s) - 1, \\ M_2(s) &= \frac{\underline{M}_2(S)}{\varrho EA} = \frac{EI\underline{\kappa}_2(S)}{\varrho EA} = \kappa_2(s). \end{aligned} \tag{4.110}$$

4.23 Problem analysis

The same formulation mentioned in sections (3.2) and (3.3) could be applied to the three models:

$$N_1(s) = N_\ell \sin(\phi(s)), \qquad N_3(s) = N_\ell \cos(\phi(s)), \qquad M_2(s) = -\phi'(s). \tag{4.111}$$

4.23.1 Non-homogeneous equation

Keeping in mind that

$$\varepsilon_1(s) = gN_\ell \sin(\phi(s)), \qquad \varepsilon_3(s) = 1 + N_\ell \cos(\phi(s)), \qquad \kappa_2(s) = -\phi'(s). \tag{4.112}$$

We remark that the two first equations of the equilibrium are directly satisfied, the last one becomes

Timoshenko	Euler	Kirchhoff
$-\phi'' + N_\ell \sin(\phi)\Big(1+(1-g)N_\ell \cos(\phi)\Big) = 0.$	$-\phi'' + N_\ell \sin(\phi)(1+N_\ell \cos(\phi)) = 0.$	$-\phi'' + N_\ell \sin(\phi) = 0.$

It is clear that:

- By imposing $g = 0$ in Timoshenko model we obtain Euler's model.
- By imposing $g = 1$ in Timoshenko model we obtain Kirchhoff's model.

Let us consider that $\phi'' \neq 0$. By multiplying the previous equations by $-2\phi'$ one obtains after integration:

Timoshenko	Euler	Kirchhoff
$\phi'^2 + 2N_\ell \cos(\phi) + (1-g)N_\ell^2 \cos^2(\phi) = \mu.$ Where, $\mu = M_2(\ell)^2 + 2N_3(\ell) + (1-g)N_3(\ell)^2.$	$\phi'^2 + 2N_\ell \cos(\phi) + N_\ell^2 \cos^2(\phi) = \mu.$ Where, $\mu = M_2(\ell)^2 + 2N_3(\ell) + N_3(\ell)^2.$	$\phi'^2 + 2N_\ell \cos(\phi) = \mu.$ Where, $\mu = M_2(\ell)^2 + 2N_3(\ell).$

These scalar differential equations are written as:

$$t'^2 = a\,t^4 + b\,t^2 + c. \tag{4.113}$$

Where,

Timoshenko	Euler	Kirchhoff
$a = \frac{\mu-\mu_a}{4},\ \mu_a = (1-g)N_\ell^2 - 2N_\ell$	$a = \frac{\mu-\mu_a}{4},\ \mu_a = N_\ell^2 - 2N_\ell$	$a = \frac{\mu-\mu_a}{4},\ \mu_a = -2N_\ell$
$b = \frac{2\mu+\mu_a+\mu_c}{4},$	$b = \frac{2\mu+\mu_a+\mu_c}{4},$	$b = \frac{2\mu+\mu_a+\mu_c}{4}$
$c = \frac{\mu-\mu_c}{4},\ \mu_c = (1-g)N_\ell^2 + 2N_\ell$	$c = \frac{\mu-\mu_c}{4},\ \mu_c = N_\ell^2 + 2N_\ell$	$c = \frac{\mu-\mu_c}{4},\ \mu_c = 2N_\ell$
$\alpha_+ = \frac{\frac{1+\sqrt{1+(1-g)\mu}}{1-g} + N_\ell}{\frac{1+\sqrt{1+(1-g)\mu}}{1-g} - N_\ell},$	$\alpha_+ = \frac{1+\sqrt{1+\mu}+N_\ell}{1+\sqrt{1+\mu}-N_\ell},$	$\alpha_+ = 1,$
$\alpha_- = \frac{\frac{1-\sqrt{1+(1-g)\mu}}{1-g} + N_\ell}{\frac{-1+\sqrt{1+(1-g)\mu}}{1-g} + N_\ell}.$	$\alpha_- = \frac{N_\ell+1-\sqrt{1+\mu}}{N_\ell-1+\sqrt{1+\mu}}.$	$\alpha_- = 1 - \frac{2\mu}{2N_\ell+\mu},$

It should be mentioned that all the remaining previous analysis mentioned in chapter three could be applicable on the three models. One should be aware that the Jacobian parameters vary from one model to another.

4.23.2 Placement

As seen in section (3.5.3) , to find the placement, we adapted an approach that is related to Timoshenko beam. Namely:

$$\varphi_n'\mathbf{e_n} + \varphi_t'\mathbf{e_t} = \varepsilon_1(s)\mathbf{d_1}(s) + \varepsilon_3(s)\mathbf{d_3}(s).$$

Where the relation

$$\varphi_t(s) = \varphi_t(0) + \frac{M_2(s) - M_2(0)}{N_\ell}. \tag{4.114}$$

Is true for the three models.

This is not the case for φ_n. In fact, using our first table of comparison we remark that for Euler

model we have $\varphi_n' \mathbf{e_n} + \varphi_t' \mathbf{e_t} = \varepsilon_3(s)\mathbf{d_3}(s)$. Hence after projecting along $\mathbf{e_n}$ we obtain:

$$\begin{aligned} \varphi_n' &= \varepsilon_3(s)\cos(\phi(s)), \\ &= (N_3+1)\cos(\phi(s)), \\ &= N_\ell^2\left(\frac{1-t^2}{1+t^2}\right)^2 + \frac{1-t^2}{1+t^2}, \end{aligned}$$

repeating the same procedure for Kirchhoff rod, we deduce that

$$\varphi_n' = \frac{1-t^2}{1+t^2}.$$

To illustrate these differences, we will give the following illustrating example.

4.24 Illustrating example

We wish to compare in this section, the behaviour of the three previous models when the force applied at the extremity is important. To do so, we consider:

$$\boldsymbol{\varphi}(0) = 0, \qquad \theta(0) = 0, \qquad N_\ell = 0.2, \qquad M_\ell = 0.2, \qquad \phi_\ell = \frac{2\pi}{3}, \qquad \ell = 20, \qquad g = 2.5. \tag{4.115}$$

Since we have explicit analysis for the three models. We can plot the placement with the cross section.

Looking at figure (4.18), we remark that these three models differ.

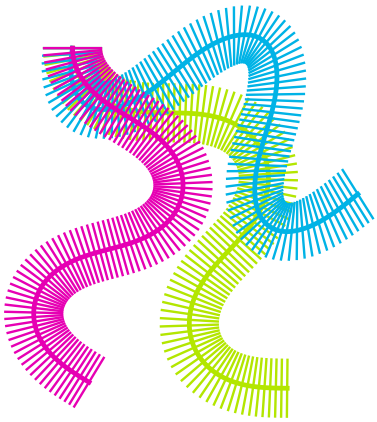

Figure 4.18 – *Dimensionless deformed shapes of a Timoshenko beam (blue curve), Euler beam (purple curve) and Kirchhoff's rod (green curve) glued at $s = 0$ and making an angle $\phi_\ell = 2\pi/3$ with the normal of the last section ($s = \ell$). The intensity of the force is $N_\ell = 0.2$ and a bending moment $M_\ell = 0.2$ is imposed on this last section too.*

4.25 Boundary problem: Comparison between models

In this section we study the difference between models in the dead load case mentioned in section (3.8). Of course the relation

$$\theta_0 = \pm 2 \arctan\left(\frac{\sqrt{\alpha_-}}{\mathrm{cn}(\sqrt{a(\alpha_- + \alpha_+)}\ell \,|\, \frac{\alpha_+}{\alpha_+ + \alpha_-})}\right).$$

holds for the three models, so, it looks interesting to compare the evolution of θ_0 according to ϕ_ℓ.

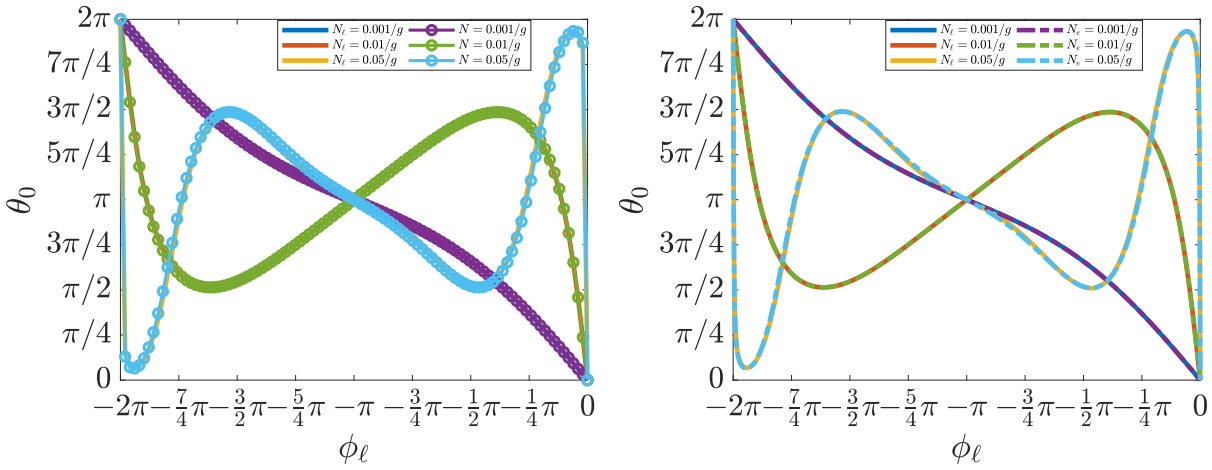

Euler model (dot curves) versus Timoshenko model (straight curves).

Kirchhoff model (dashed curves) versus Timoshenko model (straight curves).

Figure 4.19 – *Evolution of θ_0 according to ϕ_ℓ for various magnitude of the dead-load where $\ell = 50$ and $g = 2.5$.*

Figure (4.19) represent this evolution for the three different models, where it is clear that these models are similar in terms of rotation.
To complete the analysis, we will in figure (4.20) illustrate the placement for the three previous models. It is clear that these models are similar in terms of placement also. So for this example, the three models give similar results in terms of strain, stress and kinematics (placement and rotation). These results match the study stated by C. Armanini, *et.al.* in [Arm+17; Arm18].

4.26 Conclusion

In conclusion, these three models highly depend on the boundary conditions. In other terms, for some boundary conditions we obtain similar results, where for other conditions we might have different ones.

Timoshenko beam. *Euler beam.* *Kirchhoff rod.*

Figure 4.20 – *Placement for various models*

Appendix E: Buckling of Euler Timoshenko beam under two-parameters Winkler foundations

In this section we analyse the effect of a Winkler foundation on an Euler beam. Equilibrium in this case is given by:

$$\begin{aligned} \frac{\partial \underline{N}_3}{\partial S} - \frac{\partial \underline{\theta}}{\partial S}\underline{N}_1 = 0 \ , \\ \frac{\partial \underline{N}_1}{\partial S} + \frac{\partial \underline{\theta}}{\partial S}\underline{N}_3 - K_1\underline{u}_1 = 0 \ , \\ \frac{\partial \underline{M}_2}{\partial S} + (1+\widetilde{\varepsilon}_3)\underline{N}_1 - K_2\underline{\theta} = 0 \ . \end{aligned} \tag{4.116}$$

A linearised form of (4.116) will be:

$$\begin{aligned} \frac{\partial \underline{N}_1}{\partial S} - \frac{\partial \underline{\theta}}{\partial S}P - K_1\underline{u}_1 = 0, \\ EI\frac{\partial^2 \underline{\theta}}{\partial S^2} + \underline{N}_1 - K_2\underline{\theta} = 0, \end{aligned} \tag{4.117}$$

Where $\underline{M}_2 = EI\dfrac{\partial \underline{\theta}}{\partial S}$. Non-dimensional formulation of the problem is introduced thanks to the following variables:

$$\varrho = \sqrt{\frac{I}{A}}, \quad g = \frac{E}{G}, \quad \kappa_1 = \frac{K_1}{E}\frac{I}{A^2}, \quad \kappa_2 = \frac{K_2}{EA}, \quad \epsilon = \frac{P}{EA}, \quad N = \frac{\underline{N}}{EA} \tag{4.118}$$

Using the fact that $u_1' \equiv u' = \theta$ for Euler beam, (4.117) written in a dimensionless form will be:

$$\boxed{\begin{aligned} N_1' - \epsilon u'' - \kappa_1 u &= 0, \\ u^{(3)} + N_1 - \kappa_2 u' &= 0, \end{aligned}} \tag{4.119}$$

For harmonic solution $u(s) = Ue^{iks}$ and $N_1(s) = \mathcal{N}e^{iks}$, the linear differential system becomes $\mathbb{K}\boldsymbol{V} = 0$ where $\boldsymbol{V} = (U, \mathcal{N})^T$ and the rigidity matrix is:

$$\mathbb{K} = \begin{pmatrix} k^2\epsilon - \kappa_1 & ik \\ -ik(k^2 + \kappa_2) & 1 \end{pmatrix}. \tag{4.120}$$

Non-trivial solutions arise if $\det(\mathbb{K}) = 0$ what may be written as a secular equation:

$$\mathcal{P}(\epsilon, k) = k^4 + k^2(\kappa_2 - \epsilon) + \kappa_1. \tag{4.121}$$

By solving $\mathcal{P}(\epsilon) = 0$ (for a fixed k), one finds a polynomial with respect to ϵ whose real positive root is

$$\epsilon = k^2 + \frac{\kappa_1}{k^2} + \kappa_2. \tag{4.122}$$

By a direct calculation we deduce:

$$\frac{\partial \epsilon}{\partial k} = 2(k^4 - \kappa_1) \tag{4.123}$$

Hence

$$\boxed{k_{min} = \sqrt{\sqrt{\kappa_1}}.} \tag{4.124}$$

CONCLUSIONS AND PERSPECTIVES

We conclude this thesis by summarizing the main contributions and suggesting some related perspectives.

Timoshenko beam model

In this thesis, we studied in an analytical way, the behaviour of an isotropic and homogeneous straight Timoshenko beam subjected to external forces and moments, and surrounded potentially by foundations. To do so, we considered the beam as one dimensional Cosserat body where kinematical and dynamical variables depend uniquely on two variables: the curvilinear abscissa S and the time t. Thanks to the principal of virtual power, we obtained the equilibrium stated in the general form.

Another way to model our problem, is to apply intrinsic calculation on a Lie group. One could easily express the equilibrium using differential geometry of Lie groups [Ala92]. This approach helps us to investigate vibration and dynamics of curvilinear systems [Ler03; Ler05b; Ler08] as well as kinematics and dynamics of rigid body systems [CL17]. An application to acoustics could also be treated using this approach [Ben13]. This methodology is a way to tackle hard questions such as the three-dimensional aspect, large displacements and non linear elasticity.

The two-dimensional analogue of a Timoshenko beam is the Reissner–Mindlin plate theory. This theory is applied for thick plates, where the shear deformation and rotary inertia effects are included. So, Reissner–Mindlin theory does not require the cross-section to be perpendicular to the axial axes after deformation. Another plate type model used in applications is the Kirchhoff–Love theory of plates. This theory is an extension of Euler-Bernoulli beam theory and was developed in 1888 by Love using assumptions proposed by Kirchhoff. Difference between these two models is presented in [Eli20]. Furthermore, one could also study the dynamical analysis of these models [Rak09], as well as buckling and post-critical behaviour [Ced+10].

Many scientists investigated the problem of a discrete granular system that can be referred to discrete Cosserat chain, among them Massoumi *et.al.* [MCL21]. An interesting research is to investigate the asymptotical behaviour of these granular system and to compare it to our continuous Cosserat body.

One of the main assumption in this work was that the beam is homogeneous. This hypothesis does not affect the micro-structures behaviour. This hypothesis involve that no mircro-structure is taken into account. If such micro-structure exists, and additional constitutive laws is needed and the equilibrium is eventually more rich. (*e.g.* [Bar+18]).

Hyper-elasticity

The study of elastic behaviour was our main objective, so it seems reasonable to choose hyper-elastic materials for which the stress–strain relationship derives from a strain energy density function. We adapted a specific type of these materials known as Saint-Venant Kirchhoff model for which the energy is quadratic with respect to Green-Lagrange tensor $\mathbf{E}$. But, as seen in chapter one, the relation between $\mathbf{E}$ and the uni-dimensional strains was not linear, so in order to obtain analytical solutions, it appeared appropriate to take only the linear term in order to obtain linear constitutive laws with respect to the uni-dimensional strains $\boldsymbol{\kappa}$ and $\boldsymbol{\varepsilon}$.
As mentioned before, one can also consider the non-linear constitutive laws, we only gave an example of circular cross-section but the same methodology could be applied for a straight beam with general cross-section, this approach could be complementary to the study performed by Forgit *et.al.* in [For+16].
For practical applications, scientists use rubber-like material supporting large transformation. For this type of material one can apply the Neo-Hookean model. So, the study of equilibrium using this model could be important to understand more in depth the behaviour of a beam (see for example [CWD20], [dSS17]).
In addition to elastic behaviour, one can also investigate the viscosity property of a Timoshenko beam. A well known model in this case is the Kelvin–Voigt viscoelastic model [LAF13].

Statics of a Timoshenko beam

The second chapter of this thesis was dedicated to the study of a Timoshenko beam with linear constitutive laws and small transformation subjected to Winkler foundation. By imposing a longitudinal compression load, we studied the buckling where interesting results were obtained regarding wall rigidity. As seen in this chapter, elastic behaviour is limited by yield's limit, once we surpass this limit we obtain a plastic behaviour, so a more detailed study of this plastic behaviour could widen our search and our understanding of a beam subjected to this particular foundation.
One can also generalize this study by regarding the behaviour of this beam surrounded by Reissner shear-layer model wherein a shear-layer of rigidity is embedded between two spring beds as discussed in [Nob12].
In addition, one could also impose an external applied force per unit length on a Timoshenko beam such as a beam subjected to its own weight [Yok90; DC+19]. This type of load is considered as a dead load, another type of load could be applied such as follower load per unit length. One could apply numerical methods to study the behaviour of a beam subjected to these different load types.
To expand our study, we presented in the last two chapters the large transformation of a Timoshenko beam. In particular, we investigated in chapter two a planar Timoshenko beam subjected to forces and moment, we found post buckling solutions in an analytical way and we presented an example for a beam subjected to pure shear follower load. Since we obtained exact solutions, so we can

apply our approach to several real time applications. As an example, we will investigate in the near future, the explicit analysis of a clapping of a Timoshenko beam. This case could be studied in details by imposing dynamical constraints on the control parameters.
Another important aspect that was presented in this chapter is the study of instability by applying quasi-static perturbation, this approach led to a scalar equilibrium in terms of a single degree of freedom $\delta\theta(s)$:

$$\delta\theta''(s) + k^2(s)\,\delta\theta(s) = f(s). \tag{4.125}$$

This equation known as driven parametric oscillator is highly important because it is given in a general way and we can apply it to any type of boundary condition. Although this equation is hard to solve analytically in the general case, one can use simple numerical implementation to find the solutions.
A particular case of this oscillator that is widely used in mechanics is Van der Pol oscillator, a vast analysis was made in this domain, we choose to cite a recent numerical study that use the time perturbation method [Tay+21].
However, in this chapter we treated only the planar solutions of this planar problem, of course one could analyze the out-plane solutions of this problem. As an example, one can investigate the perturbation in all directions. Of course in this case (4.125) will no longer be true, it will be replaced by a coupled equation in terms of stains and curvatures.
The fourth chapter investigated a Timoshenko beam subjected to pure moment where equilibrium is given in terms of curvatures only, we presented the two invariants that control the problem and we found curvatures in an analytical way, in addition, rod shapes where found (in a numerical way) and a detailed discussion concerning the role of each control parameter was reported.
This approach helped us tackle several applications. We established a classification of circular helices and we proved that an helix (circular) could not exist by imposing only moments in the general case. One can classify helices by imposing forces and moments at the extremity [CGM06]. We also presented an explicit analysis of the equilibrium of a Torus knot, this idea will be given in details in our future research paper. Another interesting application that was detailed in this manuscript is the examination of the equilibria a Möbius strip with symmetric cross section. One can also consider a Möbius strip for any type of cross section by adding a force as a boundary condition. This addition seems difficult to investigate in an analytical way because one would obtain a system of non linear differential equations that is hard to solve, but of course a numerical approach by using a finite element method could be useful to further understand the Möbius strip [MK93]. In addition, the second invariant in this chapter was of high importance, namely, the conservation of energy. This conservation exists vastly in nature because energy is transformed from one form to another. So our approach could be applied to several real time problems such as the study of DNA helical shapes, the behaviour of the during chromatin condensation and microtubule bundles [Nov+18]. It could also be applied in Chemistry, specifically to inspect the bonds between atoms and to study the shapes of carbon nano-tubes [Sil+15].
It is worthy to mention that for the planar problem, rotation was found directly by integrating the

curvature. This is not the case for the three-dimensional problem where rotation tensor is hard to solve explicitly by simple integration. This difficulty arises by assuming a moving director frame. Furthermore, in this problem we considered a beam subjected to pure moments only, by adding additional force, we realise that the problem is hard to solve analytically. A detailed numerical approach is effective to better understand this static problem.

Dynamics of a Timoshenko beam

Dynamics in this thesis was only treated in chapter two by studying explicitly the behaviour of a Timoshenko beam with linear constitutive laws and small transformation subjected to Winkler foundation subjected to rigid wall. Solutions were found for choc type initial value problem. By letting this wall to be elastic, we obtained an eigenvalue problem where explicit analysis of dispersion curves was made. To complete our approach in chapter two, one can study the dynamical behaviour of a beam subjected to foundation. Solutions could be found by applying Fourier transformation and convolution integral theorems [KY04].
For large transformation of a planar Timoshenko beam, dynamic instabilities, such as fluttering which is one of the interesting issues that may be addressed by extending our work.
It is worthy to mention that the dynamical problem of a Timoshenko beam could be treated by applying the formalism of differential geometry and Lie groups. We can rewrite equilibrium in a simple manner rather than using complex formalism. So, we aim in the near future to study in details this intrinsic formulation for large transformation of a beam subjected to linear or non-linear constitutive laws and submitted to boundary and initial conditions.

Main results

In this section, I will remind briefly the main results obtained in my PhD thesis.
The main objective of my thesis was to give explicit/analytical analysis of a large transformation of a Timoshenko beam subjected to external loads, so I detailed in my thesis the following results:

- Explicit analysis of a static/dynamic Timoshenko beam with linear constitutive laws and small/large transformation.
- Three variables governs the problem, these variables are $(\varepsilon_1, \varepsilon_3, \kappa_2)$ in the planar deformation and $(\kappa_1, \kappa_2, \kappa_3)$ for the non-planar beam subjected to pure moments.
- Two invariants governs the problem where solution could be interpreted as intersection of these variables in the configuration space.
- General explicit solutions for Timoshenko, Euler and Kirchhoff model in the planar static problem.

BIBLIOGRAPHY

[ACN07] B Audoly, N Clauvelin, and S Neukirch, « Elastic knots », *in*: *Physical Review Letters* 99.*16* (2007), p. 164301.

[AH08] Mario M Attard and Giles W Hunt, « Column buckling with shear deformations—a hyperelastic formulation », *in*: *International Journal of Solids and Structures* 45.*14-15* (2008), pp. 4322–4339.

[Akg+16] Bekir Akgöz, Kadir Mercan, Çiğdem Demir, and Ömer Civalek, « Static analysis of beams on elastic foundation by the method of discrete singular convolution », *in*: *International Journal of Engineering and Applied Sciences* 8.*3* (2016), pp. 67–73.

[Ala92] Ibrahim Alame, « Application de la géométrie différentielle des groupes de Lie à la dynamique non linéaire des milieux curvilignes », PhD thesis, Ecole Nationale des Ponts et Chaussées, 1992.

[ALK08] Mario M Attard, Jun-Seok Lee, and Moon-Young Kim, « Dynamic stability of shear-flexible beck's columns based on Engesser's and Haringx's buckling theories », *in*: *Computers & structures* 86.*21-22* (2008), pp. 2042–2055.

[All69] HG Allen, « Analysis and Design of Structural Sandwich Panelsn Pergamon Press », *in*: *New York* (1969).

[Ant05] SS Antman, « Nonlinear Problems of Elasticity, volume 107 of Applied Mathematical Sciences, 2nd edn Springer », *in*: *New York* 1 (2005).

[Ant74] S. S. Antman, « Kirchhoff's problem for nonlinearly elastic rods », *in*: *Quarterly of Applied Mathematics* 32.*3* (1974), pp. 221–240.

[AO07] J Dario Aristizabal-Ochoa, « Static and dynamic stability of uniform shear beam-columns under generalized boundary conditions », *in*: *Journal of sound and Vibration* 307.*1-2* (2007), pp. 69–88.

[Arm+17] C Armanini, F Dal Corso, D Misseroni, and D Bigoni, « From the elastica compass to the elastica catapult: an essay on the mechanics of soft robot arm », *in*: *Proceedings of the Royal Society A: Mathematical, Physical and Engineering Sciences* 473.*2198* (2017), p. 20160870.

[Arm18] Costanza Armanini, « Instabilities and dynamics of elastic rods in the presence of movable constraints », PhD thesis, University of Trento, 2018.

[Arn13] Vladimir Igorevich Arnol'd, *Mathematical methods of classical mechanics*, vol. 60, Springer Science & Business Media, 2013.

[AS13] Andrei A Agrachev and Yuri Sachkov, *Control theory from the geometric viewpoint*, vol. 87, Springer Science & Business Media, 2013.

[AS16] Basile Audoly and Keith A Seffen, « Buckling of naturally curved elastic strips: the ribbon model makes a difference », *in*: *The Mechanics of Ribbons and Möbius Bands*, Springer, 2016, pp. 293–320.

[Att03] Mario M Attard, « Finite strain—-beam theory », *in*: *International journal of solids and structures* 40.*17* (2003), pp. 4563–4584.

[Bar+18] Emilio Barchiesi, Francesco Dell'Isola, Marco Laudato, Luca Placidi, and Pierre Seppecher, « A 1D continuum model for beams with pantographic microstructure: asymptotic micro-macro identification and numerical results », *in*: *Advances in mechanics of microstructured media and structures*, Springer, 2018, pp. 43–74.

[Bar97] Manuel Barros, « General helices and a theorem of Lancret », *in*: *Proceedings of the American Mathematical Society* 125.*5* (1997), pp. 1503–1509.

[Bat13] Milan Batista, « Large deflections of shear-deformable cantilever beam subject to a tip follower force », *in*: *International Journal of Mechanical Sciences* 75 (2013), pp. 388–395.

[Bat14] Milan Batista, « Analytical treatment of equilibrium configurations of cantilever under terminal loads using Jacobi elliptical functions », *in*: *International Journal of Solids and Structures* 51.*13* (2014), pp. 2308–2326.

[Bat16a] Milan Batista, « A closed-form solution for Reissner planar finite-strain beam using Jacobi elliptic functions », *in*: *International Journal of Solids and Structures* 87 (2016), pp. 153–166.

[Bat16b] Milan Batista, « A closed-form solution for Reissner planar finite-strain beam using Jacobi elliptic functions », *in*: *International Journal of Solids and Structures* 87 (2016), pp. 153–166.

[Baz03] Zdenek P Bazant, « Shear buckling of sandwich, fiber composite and lattice columns, bearings, and helical springs: Paradox resolved », *in*: *J. Appl. Mech.* 70.*1* (2003), pp. 75–83.

[Baz71] ZP Bazant, « A correlation study of formulations of incremental deformation and stability of continuous bodies », *in*: (1971).

[BB04] Zdeněk P Bažant and Alessandro Beghini, « Sandwich buckling formulas and applicability of standard computational algorithm for finite strain », *in*: *Composites Part B: Engineering* 35.*6-8* (2004), pp. 573–581.

[BB06] Zdeněk P Bažant and Alessandro Beghini, « Stability and finite strain of homogenized structures soft in shear: sandwich or fiber composites, and layered bodies », *in*: *International journal of solids and structures* 43.*6* (2006), pp. 1571–1593.

[BB12] Thomas E Baker and Andreas Bill, « Jacobi elliptic functions and the complete solution to the bead on the hoop problem », *in*: *American Journal of Physics* 80.*6* (2012), pp. 506–514.

[Ben13] Joël Bensoam, « Differential geometry applied to acoustics: non linear propagation in Reissner beams », *in*: *International Conference on Geometric Science of Information*, Springer, 2013, pp. 641–649.

[BH15] Sören Bartels and Peter Hornung, « Bending paper and the Möbius strip », *in*: *Journal of Elasticity* 119.*1-2* (2015), pp. 113–136.

[Big12] Davide Bigoni, *Nonlinear solid mechanics: bifurcation theory and material instability*, Cambridge University Press, 2012.

[Bla08] Johan Blaauwendraad, « Timoshenko beam–column buckling. Does Dario stand the test? », *in*: *Engineering structures* 30.*11* (2008), pp. 3389–3393.

[BW94] JR Banerjee and FW Williams, « The effect of shear deformation on the critical buckling of columns », *in*: *Journal of Sound and Vibration* 174.*5* (1994), pp. 607–616.

[CC09] Eugene Cosserat and François Cosserat, *Theorie des corps dédormables*, A. Hermann et fils, 1909.

[Ced+10] Luigi Cedolin et al., *Stability of structures: elastic, inelastic, fracture and damage theories*, World Scientific, 2010.

[Cel+08] Elena Celledoni, Francesco Fassò, Niklas Säfström, and Antonella Zanna, « The exact computation of the free rigid body motion and its use in splitting methods », *in*: *SIAM Journal on Scientific Computing* 30.*4* (2008), pp. 2084–2112.

[CGM06] Nadia Chouaieb, Alain Goriely, and John H Maddocks, « Helices », *in*: *Proceedings of the National Academy of Sciences* 103.*25* (2006), pp. 9398–9403.

[Cha+13] Noël Challamel, Ismail Mechab, Noureddine Elmeiche, Mohammed Sid Ahmed Houari, Mohammed Ameur, and Hassen Ait Atmane, « Buckling of generic higher-order shear beam/columns with elastic connections: local and nonlocal formulation », *in*: *Journal of Engineering Mechanics* 139.*8* (2013), pp. 1091–1109.

[Cha+20] Raphaël Charrondière, Florence Bertails-Descoubes, Sébastien Neukirch, and Victor Romero, « Numerical modeling of inextensible elastic ribbons with curvature-based elements », *in*: *Computer Methods in Applied Mechanics and Engineering* 364 (2020), p. 112922.

[Chu+99] S Chucheepsakul, CM Wang, XQ He, and T Monprapussorn, « Double Curvature Bending of Variable-Arc-Length Elasticas », *in*: *Journal of Applied Mechanics* 66.*1* (1999), p. 87.

[CJ99] Michael A Crisfield and Gordan Jelenić, « Objectivity of strain measures in the geometrically exact three-dimensional beam theory and its finite-element implementation », *in*: *Proceedings of the Royal Society of London. Series A: Mathematical, Physical and Engineering Sciences* 455.*1983* (1999), pp. 1125–1147.

[CL17] Dominique Paul Chevallier and Jean Lerbet, *Multi-Body Kinematics and Dynamics with Lie Groups*, Elsevier, 2017.

[CL55] Earl A Coddington and Norman Levinson, *Theory of ordinary differential equations*, Tata McGraw-Hill Education, 1955.

[CMB10] N Challamel, SA Meftah, and Fabrice Bernard, « Buckling of elastic beams on nonlocal foundation: A revisiting of Reissner model », *in*: *Mechanics Research Communications* 37.*5* (2010), pp. 472–475.

[CP88] Franklin Y Cheng and Chris P Pantelides, « Static Timoshenko beam-columns on elastic media », *in*: *Journal of Structural Engineering* 114.*5* (1988), pp. 1152–1172.

[CWD20] Wei Chen, Lin Wang, and Huliang Dai, « Nonlinear free vibration of hyperelastic beams based on neo-Hookean model », *in*: *International Journal of Structural Stability and Dynamics* 20.*01* (2020), p. 2050015.

[CY62] Stephen H Crandall and Asim Yildiz, « Random vibration of beams », *in*: (1962).

[DC+19] A Della Corte, A Battista, F Dell'Isola, and Pierre Seppecher, « Large deformations of Timoshenko and Euler beams under distributed load », *in*: *Zeitschrift für angewandte Mathematik und Physik* 70.*2* (2019), pp. 1–19.

[Del+16] Francesco Dell'Isola, Alessandro Della Corte, Leopoldo Greco, and Angelo Luongo, « Plane bias extension test for a continuum with two inextensible families of fibers: a variational treatment with Lagrange multipliers and a perturbation solution », *in*: *International Journal of Solids and Structures* 81 (2016), pp. 1–12.

[Del+19] Francesco Dell'Isola, Alessandro Della Corte, Antonio Battista, and Emilio Barchiesi, « Extensible beam models in large deformation under distributed loading: A numerical study on multiplicity of solutions », *in*: *Higher Gradient Materials and Related Generalized Continua*, Springer, 2019, pp. 19–41.

[DP11] Francesco Dell'Isola and Luca Placidi, « Variational principles are a powerful tool also for formulating field theories », *in*: *Variational models and methods in solid and fluid mechanics*, Springer, 2011, pp. 1–15.

[DR95] MA De Rosa, « Free vibrations of Timoshenko beams on two-parameter elastic foundation », *in*: *Computers & structures* 57.*1* (1995), pp. 151–156.

[dSS17] Francesco dell'Isola, Mircea Sofonea, and David Steigmann, *Mathematical Modelling in Solid Mechanics*, vol. 69, Springer, 2017.

[EG03] ME Ergüven and A Gedikli, « A mixed finite element formulation for Timoshenko beam on Winkler foundation », *in*: *Computational Mechanics* 31.*3* (2003), pp. 229–237.

[EH20] Simon R Eugster and Jonas Harsch, « A variational formulation of classical nonlinear beam theories », *in*: *Developments and Novel Approaches in Nonlinear Solid Body Mechanics*, Springer, 2020, pp. 95–121.

[Eli20] Isaac Elishakoff, *Handbook on Timoshenko-Ehrenfest beam and Uflyand-Mindlin plate theories*, World Scientific, 2020.

[Eng91] Friedrich Engesser, *Die knickfestigkeit gerader stäbe*, W. Ernst & Sohn, 1891.

[Eul44] Leonhard Euler, *Methodus inveniendi lineas curvas maximi minimive proprietate gaudentes*, apud Marcum-Michaelem Bousquet, 1744.

[Eul51] Leonhard Euler, « De motu oscillatorio corporum flexibilium », *in*: *Commentarii academiae scientiarum Petropolitanae* (1751), pp. 124–166.

[FK14] Davide Forcellini and James Marshall Kelly, « Analysis of the large deformation stability of elastomeric bearings », *in*: *Journal of Engineering Mechanics* 140.*6* (2014), p. 04014036.

[For+16] Cédric Forgit, Benoit Lemoine, Loïc Le Marrec, and Lalaonirina Rakotomanana, « A Timoshenko-like model for the study of three-dimensional vibrations of an elastic ring of general cross-section », *in*: *Acta Mechanica* 227.*9* (2016), pp. 2543–2575.

[GM15] Amin Ghannadiasl and Massood Mofid, « An analytical solution for free vibration of elastically restrained Timoshenko beam on an arbitrary variable Winkler foundation and under axial load », *in*: *Latin American Journal of Solids and Structures* 12 (2015), pp. 2417–2438.

[GN00] Alain Goriely and Michel Nizette, « Kovalevskaya rods and Kovalevskaya waves », *in*: *Regular and Chaotic Dynamics* 5.*1* (2000), pp. 95–106.

[Gol78] Martin Golubitsky, « An introduction to catastrophe theory and its applications », *in*: *Siam Review* 20.*2* (1978), pp. 352–387.

[GPS80] Herbert Goldstein, Ch Poole, and J Safko, « Classical Mechanics Addison-Wesley », *in*: *Reading, MA* (1980), p. 426.

[GS08] Oscar Gonzalez and Andrew M Stuart, *A first course in continuum mechanics*, Cambridge University Press, 2008.

[GT00] Alain Goriely and Michael Tabor, « The nonlinear dynamics of filaments », *in*: *Nonlinear Dynamics* 21.*1* (2000), pp. 101–133.

[Han+16] Bin Han, Feihao Li, Changye Ni, Qiancheng Zhang, Changqing Chen, and Tianjian Lu, « Stability and initial post-buckling of a standing sandwich beam under terminal force and self-weight », *in*: *Archive of Applied Mechanics* 86.*6* (2016), pp. 1063–1082.

[Har42] JA Haringx, « On the buckling and lateral rigidity of helical springs », *in*: *Proc. Konink. Ned. Akad. Wet* 45.*533* (1942), p. 142.

[HBW99] Seon M Han, Haym Benaroya, and Timothy Wei, « Dynamics of transversely vibrating beams using four engineering theories », *in*: *Journal of Sound and vibration* 225.*5* (1999), pp. 935–988.

[HH46] Miklós Hetényi and Miklbos Imre Hetbenyi, *Beams on elastic foundation: theory with applications in the fields of civil and mechanical engineering*, vol. 16, University of Michigan press Ann Arbor, MI, 1946.

[HLML21] Marwan Hariz, Loïc Le Marrec, and Jean Lerbet, « Explicit analysis of large transformation of a Timoshenko beam: post-buckling solution, bifurcation, and catastrophes », *in*: *Acta Mechanica* (2021), pp. 1–25.

[HP19] Alexander Humer and Astrid S Pechstein, « Exact solutions for the buckling and postbuckling of a shear-deformable cantilever subjected to a follower force », *in*: *Acta Mechanica* 230.*11* (2019), pp. 3889–3907.

[Hum13] Alexander Humer, « Exact solutions for the buckling and postbuckling of shear-deformable beams », *in*: *Acta Mechanica* 224.*7* (2013), pp. 1493–1525.

[Jea10] Frédéric Jean, « Systemes dynamiques », *in*: *Stabilité et commande. Cours AO102, ENSTA* (2010).

[Kar+02] GA Kardomateas, GJ Simitses, L Shen, and R Li, « Buckling of sandwich wide columns », *in*: *International journal of non-linear mechanics* 37.*7* (2002), pp. 1239–1247.

[Ker64] Arnold D Kerr, « Elastic and Viscoelastic Foundation Models », *in*: *Journal of Applied Mechanics* 31.*3* (1964), p. 491.

[Kir59] Gustav Kirchhoff, « Uber das Gleichgewicht und die Bewegung eines unendlich dunnen elastischen Stabes », *in*: *J. Reine Angew. Math.* 56 (1859), pp. 285–313.

[KM97] S. Kehrbaum and J. H. Maddocks, « Elastic rods, rigid bodies, quaternions and the last quadrature », *in*: *Philosophical Transactions of the Royal Society of London. Series A, Mathematical and Physical Sciences* 355.*1732* (1997), pp. 2117–2136.

[Kow89] Sophie Kowalevski, « Sur le problème de la rotation d'un corps solide autour d'un point fixe », *in*: *Acta mathematica* 12.*1* (1889), pp. 177–232.

[KY04] MH Kargarnovin and D Younesian, « Dynamics of Timoshenko beams on Pasternak foundation under moving load », *in*: *Mechanics research communications* 31.*6* (2004), pp. 713–723.

[LAF13] Y Lei, S Adhikari, and MI Friswell, « Vibration of nonlocal Kelvin–Voigt viscoelastic damped Timoshenko beams », *in*: *International Journal of Engineering Science* 66 (2013), pp. 1–13.

[Lan06] Michel-Ange Lancret, « Memoire sur les courbes ‘a double courbure », *in*: *Memoires presentes alInstitut* 1 (1806), pp. 416–454.

[Law13] Derek F Lawden, *Elliptic functions and applications*, vol. 80, Springer Science & Business Media, 2013.

[Lee98] HP Lee, « Dynamic response of a Timoshenko beam on a Winkler foundation subjected to a moving mass », *in*: *Applied Acoustics* 55.*3* (1998), pp. 203–215.

[Ler03] Jean Lerbet, « General equations of curvilinear systems: A coordinate-free approach by using Lie group theory », *in*: *Mechanics Research Communications* 30.*5* (2003), pp. 505–512.

[Ler05a] Jean Lerbet, « Intrinsic Formulation of Dynamics of Curvilinear Systems », *in*: *International Design Engineering Technical Conferences and Computers and Information in Engineering Conference*, vol. 47438, 2005, pp. 1219–1222.

[Ler05b] Jean Lerbet, « Non-linear dynamics of elastic curvilinear systems. A new coordinateless approach », *in*: *Journal of Applied Mathematics and Mechanics (PMM)* 69.*6* (2005), pp. 917–924.

[Ler08] Jean Lerbet, « About the automatic generation of equations of curvilinear systems », *in*: *Nonlinear Dynamics* 52.*1* (2008), pp. 151–158.

[Ler98] J Lerbet, « Analytic geometry and singularities of mechanisms », *in*: *ZAMM-Journal of Applied Mathematics and Mechanics/Zeitschrift für Angewandte Mathematik und Mechanik: Applied Mathematics and Mechanics* 78.*10* (1998), pp. 687–694.

[Lev15] SV Levyakov, « Formulation of a geometrically nonlinear 3D beam finite element based on kinematic-group approach », *in*: *Applied Mathematical Modelling* 39.*20* (2015), pp. 6207–6222.

[LL16] Dao-Kui Li and Xian-Fang Li, « Large deflection and rotation of Timoshenko beams with frictional end supports under three-point bending », *in*: *Comptes Rendus Mécanique* 344.*8* (2016), pp. 556–568.

[LL18] Xian-Fang Li and Kang Yong Lee, « Effects of Engesser’s and Haringx’s hypotheses on buckling of Timoshenko and higher-order shear-deformable columns », *in*: *Journal of Engineering Mechanics* 144.*1* (2018), p. 04017150.

[LL76] Lev Davidovich Landau and Evgenii Mikhailovich Lifshitz, *Mechanics: Volume 1*, vol. 1, Butterworth-Heinemann, 1976.

[LMLR18] Loïc Le Marrec, Jean Lerbet, and Lalaonirina R Rakotomanana, « Vibration of a Timoshenko beam supporting arbitrary large pre-deformation », *in*: *Acta Mechanica* 229.*1* (2018), pp. 109–132.

[LMZOS18] Loïc Le Marrec, Dansong Zhang, and Martin Ostoja-Starzewski, « Three-dimensional vibrations of a helically wound cable modeled as a Timoshenko rod », *in*: *Acta Mechanica* 229.*2* (2018), pp. 677–695.

[Lur05] AI Lurie, *Theory of Elasticity, translated by Belyaev*, 2005.

[MCL21] Sina Massoumi, Noël Challamel, and Jean Lerbet, « Exact solutions for the vibration of finite granular beam using discrete and gradient elasticity cosserat models », *in*: *Journal of Sound and Vibration* 494 (2021), p. 115839.

[Mey01] Kenneth R Meyer, « Jacobi elliptic functions from a dynamical systems point of view », *in*: *The American Mathematical Monthly* 108.*8* (2001), pp. 729–737.

[MF14] Ali Mohyeddin and Abdolhosein Fereidoon, « An analytical solution for the large deflection problem of Timoshenko beams under three-point bending », *in*: *International Journal of Mechanical Sciences* 78 (2014), pp. 135–139.

[MK93] L Mahadevan and Joseph Bishop Keller, « The shape of a Möbius band », *in*: *Proceedings of the Royal Society of London. Series A: Mathematical and Physical Sciences* 440.*1908* (1993), pp. 149–162.

[MRL01] Anders Magnusson, Matti Ristinmaa, and Christer Ljung, « Behaviour of the extensible elastica solution », *in*: *International Journal of Solids and Structures* 38.*46-47* (2001), pp. 8441–8457.

[Nak03] Mikio Nakahara, *Geometry, topology and physics*, CRC press, 2003.

[NG99] Michel Nizette and Alain Goriely, « Towards a classification of Euler–Kirchhoff filaments », *in*: *Journal of mathematical physics* 40.*6* (1999), pp. 2830–2866.

[Nob12] Andrea Nobili, « Variational approach to beams resting on two-parameter tensionless elastic foundations », *in*: *Journal of applied mechanics* 79.*2* (2012).

[Nov+18] Maja Novak, Bruno Polak, Juraj Simunić, Zvonimir Boban, Barbara Kuzmić, Andreas W Thomae, Iva M Tolić, and Nenad Pavin, « The mitotic spindle is chiral due to torques within microtubule bundles », *in*: *Nature communications* 9.*1* (2018), pp. 1–10.

[OHT86] Atsumi OHTSUKI, « An analysis of large deflection in a symmetrical three-point bending of beam », *in*: *Bulletin of JSME* 29.*253* (1986), pp. 1988–1995.

[Olv+10] Frank WJ Olver, Daniel W Lozier, Ronald F Boisvert, and Charles W Clark, *NIST handbook of mathematical functions hardback and CD-ROM*, Cambridge university press, 2010.

[OR16] Chiara Oberti and Renzo L Ricca, « On torus knots and unknots », *in*: *Journal of Knot Theory and Its Ramifications* 25.*06* (2016), p. 1650036.

[Pas54] PL Pasternak, « On a new method of an elastic foundation by means of two foundation constants », *in*: *Gosudarstvennoe Izdatelstvo Literaturi po Stroitelstuve i Arkhitekture* (1954).

[PB82] G Prathap and GR Bhashyam, « Reduced integration and the shear-flexible beam element », *in*: *International Journal for Numerical Methods in Engineering* 18.*2* (1982), pp. 195–210.

[PS14] Tim Poston and Ian Stewart, *Catastrophe theory and its applications*, Courier Corporation, 2014.

[Rak09] Lalaonirina Rakotomanana, *Eléments de dynamique des solides et structures déformables*, PPUR Presses polytechniques, 2009.

[RB07] Peter Ruge and Carolin Birk, « A comparison of infinite Timoshenko and Euler–Bernoulli beam models on Winkler foundation in the frequency-and time-domain », *in*: *Journal of Sound and Vibration* 304.*3-5* (2007), pp. 932–947.

[Rei58] E Reissner, « A note on deflections of plates on a viscoelastic foundation », *in*: *J. Appl. Mech., ASME* 25 (1958), pp. 144–145.

[Rei72] Eric Reissner, « On one-dimensional finite-strain beam theory: the plane problem », *in*: *Zeitschrift für angewandte Mathematik und Physik ZAMP* 23.*5* (1972), pp. 795–804.

[Rei82] E Reissner, « Some remarks on the problem of column buckling », *in*: *Ingenieur-Archiv* 52.*1* (1982), pp. 115–119.

[RH16] MM Rana and ASMZ Hasan, « AN EXACT SOLUTION OF POST-BUCKLED NONLINEAR BEAM ON AN ELASTIC FOUNDATION », *in*: *Proceedings of 3rd International Conference on Advances in Civil Engineering, 21-23 December 2016, CUET, Chittagong, Bangladesh* (2016).

[RS17] Korabathina Rajesh and Koppanati Meera Saheb, « Free vibrations of uniform timoshenko beams on pasternak foundation using coupled displacement field method », *in*: *Archive of Mechanical Engineering* 64.*3* (2017).

[RS91] A.Ghani Razaqpur and K.R. Shah, « Exact analysis of beams on two-parameter elastic foundations », *in*: *International Journal of Solids and Structures* 27.*4* (1991), pp. 435–454.

[SH18] E. L. Starostin and G. H. M. van der Heijden, « Forceless Sadowsky strips are spherical », *in*: *Phys. Rev. E* 97.*2* (2018), p. 023001.

[Sil+15] Hugo Santos Silva, Jacky Cresson, Agnès Rivaton, Didier Bégué, and Roger C Hiorns, « Correlating geometry of multidimensional carbon allotropes molecules and stability », *in*: *Organic Electronics* 26 (2015), pp. 395–399.

[Sim17] Pedro Dias Simão, « Influence of shear deformations on the buckling of columns using the generalized beam theory and energy principles », *in*: *European Journal of Mechanics-A/Solids* 61 (2017), pp. 216–234.

[Sim85] Juan C Simo, « A finite strain beam formulation. The three-dimensional dynamic problem. I », *in*: *Computer methods in applied mechanics and engineering* 49.*1* (1985), pp. 55–70.

[SK84] Juan C Simo and James M Kelly, « Finite element analysis of the stability of multilayer elastomeric bearings », *in*: *Engineering Structures* 6.*3* (1984), pp. 162–174.

[SVDH07] EL Starostin and GHM Van Der Heijden, « The shape of a Möbius strip », *in*: *Nature materials* 6.*8* (2007), pp. 563–567.

[SVDH16] EL Starostin and GHM Van Der Heijden, « Equilibrium shapes with stress localisation for inextensible elastic Möbius and other strips », *in*: *The Mechanics of Ribbons and Möbius Bands*, Springer, 2016, pp. 67–112.

[Tay+21] C Tayeh, G Girault, Y Guevel, and JM Cadou, « Numerical time perturbation and resummation methods for nonlinear ODE », *in*: *Nonlinear Dynamics* 103.*1* (2021), pp. 617–642.

[TG09] Stephen P Timoshenko and James M Gere, *Theory of elastic stability*, Courier Corporation, 2009.

[Tho18] René Thom, *Structural stability and morphogenesis*, CRC press, 2018.

[Tim21] Stephen P Timoshenko, « LXVI. On the correction for shear of the differential equation for transverse vibrations of prismatic bars », *in*: *The London, Edinburgh, and Dublin Philosophical Magazine and Journal of Science* 41.*245* (1921), pp. 744–746.

[Tim22] Stephan P Timoshenko, « X. On the transverse vibrations of bars of uniform cross-section », *in*: *The London, Edinburgh, and Dublin Philosophical Magazine and Journal of Science* 43.*253* (1922), pp. 125–131.

[TK05] Hsiang-Chuan Tsai and James M Kelly, « Buckling of short beams with warping effect included », *in*: *International Journal of Solids and Structures* 42.*1* (2005), pp. 239–253.

[Tru60] Clifford Truesdell, « The rational mechanics of flexible or elastic bodies: 1638-1788 », *in*: *Leonhardi Euleri Opera Omnia, Ser. 2* (1960).

[TSC00] Irwin Tobias, David Swigon, and Bernard D Coleman, « Elastic stability of DNA configurations. I. General theory », *in*: *Physical Review E* 61.*1* (2000), p. 747.

[VDMS17] Léo Van Damme, Pavao Mardešić, and Dominique Sugny, « The tennis racket effect in a three-dimensional rigid body », *in*: *Physica D: Nonlinear Phenomena* 338 (2017), pp. 17–25.

[VN71] Jürg Von Nänni, « Das Eulersche Knickproblem unter Berücksichtigung der Querkräfte », *in*: *Zeitschrift für angewandte Mathematik und Physik ZAMP* 22.*1* (1971), pp. 156–185.

[Win67] Eduard Winkler, *Die Lehre von der Elasticität und Festigkeit mit besonderer Rücksicht auf ihre Anwendung in der Technik*, 1867.

[WXK91] Chien-Ming Wang, Yang Xiang, and Sritawat Kitipornchai, « Buckling of restrained columns with shear deformation and axial shortening », *in*: *Journal of engineering mechanics* 117.*9* (1991), pp. 1973–1989.

[XZ09] GP Xia and Zhe Zhang, « A numerical method for critical buckling load for a beam supported on elastic foundation », *in*: *EJGE* 14 (2009), pp. 1–11.

[Yok90] T Yokoyama, « Vibrations of a hanging Timoshenko beam under gravity », *in*: *Journal of Sound and Vibration* 141.*2* (1990), pp. 245–258.

[YTM90] Goto Yoshiaki, Yoshimitsu Tomoo, and Obata Makoto, « Elliptic integral solutions of plane elastica with axial and shear deformations », *in*: *International Journal of Solids and Structures* 26.*4* (1990), pp. 375–390.

[Zha08] Yin Zhang, « Tensionless contact of a finite beam resting on Reissner foundation », *in*: *International Journal of Mechanical Sciences* 50.*6* (2008), pp. 1035–1041.

[Zie82] H Ziegler, « Arguments for and against Engesser's buckling formulas », *in*: *Ingenieur-Archiv* 52.*1* (1982), pp. 105–113.

[ZM05] Yin Zhang and Kevin D Murphy, « Secondary buckling and tertiary states of a beam on a non-linear elastic foundation », *in*: *International Journal of Non-Linear Mechanics* 40.*6* (2005), pp. 795–805.

DOCTORAT BRETAGNE LOIRE / MATHSTIC

UNIVERSITÉ DE RENNES 1

Titre : Étude non-linéaire d'une structure unidimensionnelle sous chargement.

Mot clés : Poutre de Timoshenko, tige de Kirchhoff, solutions exactes, bifurcation et catastrophe, grande transformation, fondation de Winkler.

Résumé : Nous discutons dans cette thèse une poutre de Timoshenko élastique, isotrope, homogène et droite avec des lois de comportements linéaires, soumise à des forces et moments extérieurs et entourée éventuellement par des fondations. Plus précisément, nous nous intéressons d'une part à l'analyse de l'effet des fondations de Winkler sur une poutre de Timoshenko. Nous donnons des solutions pour le problème dynamique, puis en imposant une force longitudinale, nous analysons le modèle de Haringx et Engesser d'une manière analytique en offrant une relation entre la rigidité de la paroi et les solutions de flambement. D'autre part, nous exposons les solutions quasi-statique d'une poutre de Timoshenko en grande déformation. Nous proposons des solutions analytiques de post-flambement pour différents régimes governés explicitement par les deux invariants du problème. Dans le cas d'une poutre plane, le problème est d'abord reformulé comme un problème de Cauchy. Nous discutons également des problèmes de bifurcation tels que le flambage et la catastrophe. Dans le cas non plan, nous imposons uniquement un moment à l'extrémité afin d'obtenir différents régimes qui dépendent de l'épaisseur de la section transversale et de la charge externe.

Title: Nonlinear study of a one-dimensional structure under loading.

Keywords: Timoshenko beam, Kirchhoff rod, exact solutions, bifurcation and catastrophe, large transformation, Winkler foundation.

Abstract: In this thesis, we discuss an elastic, isotropic and homogeneous straight Timoshenko beam with linear constitutive laws subjected to external forces and moments and surrounded eventually by foundations.
On one hand, we are interested in analysing the effect of Winkler foundation on a Timoshenko beam. We give solutions for the dynamical problem, then by imposing a longitudinal force, we analyse Haringx and Engesser model in an analytical way where relations between rigidity of the wall and buckling solutions were made.
On the other hand, we expose solutions of a quasi-static but large transformation of a Timoshenko beam. We offer analytical post-buckling solutions for different regimes driven explicitly by two invariants of the problem. In the planar case, the problem is first reformulated in the form of a Cauchy initial value problem. We discuss also bifurcation problems such as buckling and catastrophe. In the non-planar case, we impose moment only at the boundaries to obtain different regimes that depend on the thickness of the cross section and on the external load.